



Earth Resources
A Continuing
Bibliography
with Indexes

NASA SP-7041(48)
January 1986

National Aeronautics and
Space Administration



es Earth Resources
S Earth Resources
Earth Resources E
th Resources Ear
Resources Earth
Resources Earth F
resources Earth Res

(NASA-SP-7041(48)) EARTH RESOURCES: A
CONTINUING BIBLIOGRAPHY WITH INDEXES
(National Aeronautics and Space
Administration) 100 p HC A05

N86-20931

CSCL 05B

00/43

Unclas
04041

ACCESSION NUMBER RANGES

Accession numbers cited in this Supplement fall within the following ranges.

STAR (N-10000 Series)	N85-29910 – N85-36162
-----------------------	-----------------------

IAA (A-10000 Series)	A85-39961 – A85-50132
----------------------	-----------------------

EARTH RESOURCES

A CONTINUING BIBLIOGRAPHY WITH INDEXES

Issue 48

A selection of annotated references to unclassified reports and journal articles that were introduced into the NASA scientific and technical information system and announced between October 1 and December 31, 1985 in

- *Scientific and Technical Aerospace Reports (STAR)*
- *International Aerospace Abstracts (IAA).*



Scientific and Technical Information Branch
National Aeronautics and Space Administration
Washington, DC

1986

This supplement is available as NTISUB/038/093 from the National Technical Information Service (NTIS), Springfield, Virginia 22161 at the price of \$14.50 domestic; \$29.00 foreign for standing orders. Please note: Standing orders are subscriptions which do not terminate at the end of a year, as do regular subscriptions, but continue indefinitely unless specifically terminated by the subscriber.

INTRODUCTION

The technical literature described in this continuing bibliography may be helpful to researchers in numerous disciplines such as agriculture and forestry, geography and cartography, geology and mining, oceanography and fishing, environmental control, and many others. Until recently it was impossible for anyone to examine more than a minute fraction of the Earth's surface continuously. Now vast areas can be observed synoptically, and changes noted in both the Earth's lands and waters, by sensing instrumentation on orbiting spacecraft or on aircraft.

This literature survey lists 326 reports, articles, and other documents announced between October 1 and December 31, 1985 in *Scientific and Technical Aerospace Reports (STAR)*, and *International Aerospace Abstracts (IAA)*.

The coverage includes documents related to the identification and evaluation by means of sensors in spacecraft and aircraft of vegetation, minerals, and other natural resources, and the techniques and potentialities of surveying and keeping up-to-date inventories of such riches. It encompasses studies of such natural phenomena as earthquakes, volcanoes, ocean currents, and magnetic fields; and such cultural phenomena as cities, transportation networks, and irrigation systems. Descriptions of the components and use of remote sensing and geophysical instrumentation, their subsystems, observational procedures, signature and analyses and interpretive techniques for gathering data are also included. All reports generated under NASA's Earth Resources Survey Program for the time period covered in this bibliography will also be included. The bibliography does not contain citations to documents dealing mainly with satellites or satellite equipment used in navigation or communication systems, nor with instrumentation not used aboard aerospace vehicles.

The selected items are grouped in nine categories. These are listed in the Table of Contents with notes regarding the scope of each category. These categories were especially chosen for this publication, and differ from those found in *STAR* and *IAA*.

Each entry consists of a standard bibliographic citation accompanied by an abstract. The citations include the original accession numbers from the respective announcement journals.

Under each of the nine categories, the entries are presented in one of two groups that appear in the following order:

- IAA* entries identified by accession number series A85-10,000 in ascending accession number order;

- STAR* entries identified by accession number series N85-10,000 in ascending accession number order.

After the abstract section, there are seven indexes:

- subject, personal author, corporate source, foreign technology, contract number, report/ accession number, and accession number.

TABLE OF CONTENTS

	Page
Category 01 Agriculture and Forestry	1
Includes crop forecasts, crop signature analysis, soil identification, disease detection, harvest estimates, range resources, timber inventory, forest fire detection, and wildlife migration patterns.	
Category 02 Environmental Changes and Cultural Resources	6
Includes land use analysis, urban and metropolitan studies, environmental impact, air and water pollution, geographic information systems, and geographic analysis.	
Category 03 Geodesy and Cartography	7
Includes mapping and topography.	
Category 04 Geology and Mineral Resources	14
Includes mineral deposits, petroleum deposits, spectral properties of rocks, geological exploration, and lithology.	
Category 05 Oceanography and Marine Resources	24
Includes sea-surface temperature, ocean bottom surveying imagery, drift rates, sea ice and icebergs, sea state, fish location	
Category 06 Hydrology and Water Management	35
Includes snow cover and water runoff in rivers and glaciers, saline intrusion, drainage analysis, geomorphology of river basins, land uses, and estuarine studies.	
Category 07 Data Processing and Distribution Systems	37
Includes film processing, computer technology, satellite and aircraft hardware, and imagery.	
Category 08 Instrumentation and Sensors	42
Includes data acquisition and camera systems and remote sensors.	
Category 09 General	49
Includes economic analysis.	
Subject Index	A-1
Personal Author Index	B-1
Corporate Source Index	C-1
Foreign Technology Index	D-1
Contract Number Index	E-1
Report/Accession Number Index	F-1
Accession Number Index	G-1

EARTH RESOURCES

A Continuing Bibliography (Issue 48)

JANUARY 1986

01

AGRICULTURE AND FORESTRY

Includes crop forecasts, crop signature analysis, soil identification, disease detection, harvest estimates, range resources, timber inventory, forest fire detection, and wildlife migration patterns

A85-41350

THE CONTRIBUTION OF SPOT IMAGES TO SOIL MAPPING - A SPOT SIMULATION STUDY ON LAURAGAIS (1981) [CONTRIBUTION DES IMAGES SPOT A LA CARTOGRAPHIE DUE SOL - ETUDE DE SIMULATIONS SPOT SUR LE LAURAGAIS /1981/]

L. GUYOT and J.-P. POUPARD (Institut Geographique National, Departement de Teledetection, Saint-Mande, France) Societe Francaise de Photogrammetrie et de Teledetection (ISSN 0244-6014), no. 97, 1985, p. 19-40 In French. refs

A thematic simulation was made of projected soil mapping scans with the SPOT instruments under development. The study was targeted at testing the usefulness of SPOT imagery for classifying land usage, e.g., agriculture, forests, prairies, etc. The study was extended to multitemporal images. Sample images were collected using airborne instrumentation to radiometrically scan a 9 km long scene from 6 km altitude with a scan path 35 deg on either side of the vertical. Attention was given to the effects of the view angle, the level of scene illumination, and directional reflectivity. Various previously identified agricultural crops were scanned in different growth stages. Successful classifications were achieved only with multiple images, at specific times of the year, and by trained personnel who were familiar with the airborne imagery. M.S.K.

A85-42581

REMOTE SENSING INVESTIGATIONS ON SOME FRUIT ORCHARDS IN EL FAYOUM AREA, EGYPT

H. Z. ABOUL-EID, A. G. ABDEL-SAMIE, and M. A. ABDEL-HADY (Academy of Scientific Research and Technology, Cairo, Egypt) Photo Interpretation (ISSN 0031-8523), vol. 22, Nov.-Dec. 1983, 6 p. In English, French, and Spanish

Airborne multispectral photography of a region in northwestern Egypt yielded a mosaic image at 1:4000 resolution. The blue, green and red band images were taken from an altitude of 600 m in 1975. Attention was given to orchard features, i.e., total area, growth status, plant vigor, and symptoms of disease, pests, or other pathological factors. Eight ground-truth gathering forays produced data on soil type, the types and ages of fruit trees, soil moisture, irrigation, and drainage facilities, pests and diseases. The survey covered mango, apricot, orange, lemon, apple, pear, olive and palm trees and grape vines. Image features which showed high correlations with ground-measured tree health decrements are discussed. M.S.K.

A85-42650

VEGETATION PROFILES FROM COLOR-INFRARED AIRPHOTOS

W. D. HUDSON (Michigan State University, East Lansing) Michigan Academician (ISSN 0026-2005), vol. 16, Spring 1984, p. 301-313 refs

Attention is given to a method for the construction of vegetation profiles by means of color-IR aerial photography, together with such collateral material as topographic maps and soil surveys. This procedure was tested by running a transect through Antrim, Otsego, and Montgomery Counties in the northern lower peninsula of Michigan. An analysis was then conducted of the physiographic-vegetation relationships along the transect, in order to determine the usefulness of the remote sensing profile technique for vegetation distribution studies over large areas. It is concluded that the greatest utility of the method may lie in the location of specific sites in biogeographical studies. O.C.

A85-42865* Purdue Univ., West Lafayette, Ind
SPECULAR, DIFFUSE, AND POLARIZED LIGHT SCATTERED BY TWO WHEAT CANOPIES

V. C. VANDERBILT, L. GRANT, L. L. BIEHL, and B. F. ROBINSON (Purdue University, West Lafayette, IN) Applied Optics (ISSN 0003-6935), vol. 24, Aug. 1, 1985, p. 2408-2418. refs (Contract NAG5-269; NAS9-14970)

Using polarization measurements, the reflectance factor of two wheat canopies is divided into components due to specularly and diffusely reflected light. The data show that two key angles may be predicted, the angle of the polarizer for minimum flux and the angle of incidence of sunlight specularly reflected by a leaf to a sensor. The results show that specular reflection is a key aspect to radiation transfer by two canopies. Results suggest that the advent of heading in wheat may be remotely sensed from polarization measurements of the canopy reflectance. Author

A85-43114* National Aeronautics and Space Administration
Goddard Space Flight Center, Greenbelt, Md
DIRECTIONAL REFLECTANCE FACTOR DISTRIBUTIONS FOR COVER TYPES OF NORTHERN AFRICA

D. S. KIMES, W. W. NEWCOMB, C. J. TUCKER (NASA, Goddard Space Flight Center, Greenbelt, MD), I. S. ZONNEVELD, W. VAN WIJNGAARDEN (International Institute for Aerial Survey and Earth Sciences, Enschede, Netherlands) et al. Remote Sensing of Environment (ISSN 0034-4257), vol. 18, Aug. 1985, p. 1-19 refs

Directional reflectance factors that spanned the entire exitance hemisphere were collected on the ground throughout the morning period for common cover types in Tunisia, Africa. NOAA 7/8 AVHRR bands 1 (0.58-0.68 micron) and 2 (0.7301 micron) were used in data collection. The cover types reported were a plowed field, annual grassland, steppe grassland, hard wheat, salt plain, and irrigated wheat. Several of these cover types had geometric structures that are extreme as compared to those reported in the literature. Comparisons were made between the dynamics of the observed reflectance distributions and those reported in the literature. It was found that the dynamics of the measured data could be explained by a combination of soil and vegetation scattering components. The data and analysis further validated physical principles that cause the reflectance distribution dynamics as proposed by field and simulation studies in the literature. Finally, the normalized difference transformation (Band 2 - Band 1)/(Band

01 AGRICULTURE AND FORESTRY

1 + Band 2), which is useful in monitoring vegetation cover, generally decreased the variation in signal with changing view angle. However, several exceptions were noted. Author

A85-43120

VIEW AZIMUTH AND ZENITH, AND SOLAR ANGLE EFFECTS ON WHEAT CANOPY REFLECTANCE

M. SHIBAYAMA and C. L. WIEGAND (USDA, Remote Sensing Research Unit, Weslaco, TX) Remote Sensing of Environment (ISSN 0034-4257), vol. 18, Aug. 1985, p. 91-103. refs

The present study was conducted with the objective to develop a simple model to describe bidirectional characteristics of canopy reflectance. The model is needed to estimate the reflectance factor at nadir view position from off-nadir measurements. This capability would be especially helpful to handheld radiometer users when it is difficult to enter plots or fields for nadir view measurements. Spectral measurements were made at a research farm in 1984 over two canopies of hard red spring wheat. Results were obtained for the near infrared (NIR) in the range from 0.76 to 0.90 micron, and the visible region in the range from 0.63 to 0.69 micron. It was found that within experiments, at least, the simple model considered may provide an effective tool for adjusting off-nadir looking reflectance data for crop canopies. G.R.

A85-45690* California Univ., Berkeley.

EVALUATION OF THEMATIC MAPPER DATA FOR MAPPING FOREST, AGRICULTURAL AND SOIL RESOURCES

S. DEGLORIA, A. BENSON, K. DUMMER (California, University, Berkeley), and E. FAKHOURY (California, University, Davis) (COSPAR, Plenary Meeting, 25th Workshop II on the Earth's Surface Studied from Space, Graz, Austria, June 25-July 7, 1984) Advances in Space Research (ISSN 0273-1177), vol. 5, no. 5, 1985, p. 31-39. refs

(Contract NAS5-27377, NCC2-205)

Color composite TM film products which include TM5, TM4, and a visible band (TM1, TM2, or TM3) are superior to composites which exclude TM4 for discriminating most forest and agricultural cover types and estimating area proportions for inventory and sampling purposes. Clustering a subset of TM data results in a spectral class map which groups diverse forest cover types into spectrally and ecologically similar areas suitable for use as a stratification base in traditional forest inventory practices. Analysis of simulated Thematic Mapper data indicate that the location and number of TM spectral bands are suitable for detecting differences in major soil properties and characterizing soil spectral curve form and magnitude. Author

A85-45691* Maryland Univ., College Park.

SHORTWAVE INFRARED DETECTION OF VEGETATION

S. N. GOWARD (Maryland, University, College Park) (COSPAR, Plenary Meeting, 25th: Workshop II on the Earth's Surface Studied from Space, Graz, Austria, June 25-July 7, 1984) Advances in Space Research (ISSN 0273-1177), vol. 5, no. 5, 1985, p. 41-50 refs

(Contract NCC5-20; NCC5-26)

Shortwave infrared sensors were included on the Thematic Mapper (TM) to observe vegetation reflected radiance patterns related to water leaf content. Analysis of field measurements for corn and soybeans throughout the growing season showed that shortwave infrared measurements enhance discrimination between the species, particularly in midseason. A numerical model of the canopy reflectance showed that differential leaf absorptance can produce the observed patterns. Analysis of coincident studies of leaf optical properties were conducted to generalize the results to other types of vegetation. I.H.

A85-45872

EVALUATION OF SIMULATED SPOT IMAGERY FOR THE INTERPRETATION OF AGRICULTURAL RESOURCES IN CALIFORNIA

S. D. DEGLORIA (California, University, Berkeley) Photogrammetric Engineering and Remote Sensing (ISSN 0099-1112), vol. 51, Aug. 1985, p. 1103-1108 Research supported by the University of California. refs

Simulated SPOT data were acquired over a diverse agricultural site in the Central Valley of California for assessing the potential utility of these data for discriminating multiple crop types and agronomic conditions. Ground data and low altitude oblique photography were acquired coincidentally with the SPOT data acquisition. Ground data included crop type, percent crop canopy and crop residue cover, canopy and crop residue height irrigation and cultivation practices, and dominant land use for selected individual fields and tracts. The range in field size is from less than 1.0 hectare to greater than 80 hectares. Analysis of the 'P' site data set in image format has yielded the following significant results: (1) the panchromatic data sampled to 10 m IFOV pixels permit the definition of inter- and intra-field boundaries, road networks, and water distribution systems; and (2) the multispectral data sampled to 20 m IFOV pixels permit (a) the discrimination of selected crop canopies having less than 20 percent ground cover, and (b) the discrimination of within-field variability due to irrigation and fertilization practices, soil type, and type and degree of harvesting practices. Author

A85-45874

FOREST COVER TYPE MAPPING AND SPRUCE BUDWORM DEFOLIATION DETECTION USING SIMULATED SPOT IMAGERY

M. P. BUCHHEIM, A. L. MACLEAN, and T. M. LILLESAND (Wisconsin, University, Madison) Photogrammetric Engineering and Remote Sensing (ISSN 0099-1112), vol. 51, Aug. 1985, p. 1115-1122. Research supported by the University of Wisconsin. refs

A85-47806* California Univ., Berkeley.

INTERPRETATION OF LANDSAT-4 THEMATIC MAPPER AND MULTISPECTRAL SCANNER DATA FOR FOREST SURVEYS

A. S. BENSON and S. D. DEGLORIA (California, University, Berkeley) Photogrammetric Engineering and Remote Sensing (ISSN 0099-1112), vol. 51, Sept. 1985, p. 1281-1289. refs

(Contract NAS5-27377)

Landsat-4 Thematic Mapper (TM) and Multispectral Scanner (MSS) data were evaluated by interpreting film and digital products and statistical data for selected forest cover types in California. Significant results were: (1) TM color image products should contain a spectral band in the visible (bands 1, 2, or 3), near infrared (band 4), and middle infrared (band 5) regions for maximizing the interpretability of vegetation types; (2) TM color composites should contain band 4 in all cases even at the expense of excluding band 5; and (3) MSS color composites were more interpretable than all TM color composites for certain cover types and for all cover types when band 4 was excluded from the TM composite. Author

A85-49104* State Univ. of New York, Binghamton

TWO-DIMENSIONAL LEAF ORIENTATION DISTRIBUTIONS

D. E. STREBEL (Science Applications Research, Greenbelt, MD), N. S. GOEL (New York, State University, Binghamton), and K. J. RANSON (Purdue University, West Lafayette, IN) IEEE Transactions on Geoscience and Remote Sensing (ISSN 0196-2892), vol. GE-23, Sept. 1985, p. 640-647. refs

(Contract NAS9-16528)

Combined inclination/azimuth leaf angle distributions are important for accurate models of vegetation canopy reflectance. It is shown that appropriate mathematical representations can be constructed from beta distributions under most circumstances. This is illustrated by analyzing observational data on soybean leaves and balsam fir needles. There are some problems when the data is imprecise and when correlations between inclination and azimuth

angle are induced by heliotropism. Otherwise, the two-dimensional beta-type distribution appears to be a versatile tool for describing complete inclination/azimuth leaf angle distributions Author

A85-49105

REMOTE SENSING OF ANGULAR CHARACTERISTICS OF CANOPY REFLECTANCES

C. SIMMER and S. A. W. GERSTL (Los Alamos National Laboratory, NM) IEEE Transactions on Geoscience and Remote Sensing (ISSN 0196-2892), vol. GE-23, Sept. 1985, p. 648-658. refs

The effect of the atmosphere on the remotely sensed angular distribution of canopy reflectance is studied by radiative transfer calculations with a coupled atmosphere canopy model and a pure atmosphere model. The canopy in the pure atmosphere model was replaced by an equivalent bidirectional reflectance distribution function (BRDF). In the decoupled mode the canopy model was used to compute canopy equivalent BRDFs. The atmospheric perturbation of the angular reflectance pattern is computed for a Lambertian BRDF, a mixed Lambertian/specular BRDF, and the measured BRDFs of savannah and coniferous canopies using one aerosol-free and two polluted atmospheres with surface visual ranges of $V(0) = 23$ km and $V(0) = 5$ km. It is shown that the local extremes in the angular distribution of the surface reflectance were still detectable above the atmosphere and were nearly invariant to atmospheric perturbations for surface albedoes greater than 10 percent. It is suggested on the basis of the numerical results that off-nadir satellite observations may contribute additional information for crop identification. I.H.

A85-49106*

CONTRASTS AMONG BIDIRECTIONAL REFLECTANCE OF LEAVES, CANOPIES, AND SOILS

J. M. NORMAN, E. A. WALTER (Nebraska, University, Lincoln), and J. M. WELLES (Li-Cor, Inc., Lincoln, NE) IEEE Transactions on Geoscience and Remote Sensing (ISSN 0196-2892), vol. GE-23, Sept. 1985, p. 659-667. Research supported by the University of Nebraska. refs

(Contract NAG5-2777; NGT-28-004-801, NASA ORDER S-19583-D)

Simple models are presented for predicting the bidirectional reflectance distribution functions (BRDFs) for soils and plant canopies viewed from various directions. BRDFs are predicted for bare soil, individual leaves, and plant canopies, and the results are compared with measurements and a three coefficient empirical equation. BRDF measurements for corn and soybean leaves are presented to contrast with canopy and soil distributions. Estimates of the soil, canopy, and leaf BRDFs are combined into a model called Cupid to predict BRDFs for complex natural surfaces. I.H.

A85-49107*

A MONTE CARLO REFLECTANCE MODEL FOR SOIL SURFACES WITH THREE-DIMENSIONAL STRUCTURE

K. D. COOPER and J. A. SMITH (Colorado State University, Fort Collins) IEEE Transactions on Geoscience and Remote Sensing (ISSN 0196-2892), vol. GE-23, Sept. 1985, p. 668-673. refs (Contract NAG5-270)

A Monte Carlo soil reflectance model has been developed to study the effect of macroscopic surface irregularities larger than the wavelength of incident flux. The model treats incoherent multiple scattering from Lambertian facets distributed on a periodic surface. Resulting bidirectional reflectance distribution functions are non-Lambertian and compare well with experimental trends reported in the literature. Examples showing the coupling of the Monte Carlo soil model to an adding bidirectional canopy of reflectance model are also given. Author

A85-49108*

EVALUATION OF A CANOPY REFLECTANCE MODEL FOR LAI ESTIMATION THROUGH ITS INVERSION

N. S. GOEL (New York, State University, Binghamton) and D. W. DEERING (NASA, Goddard Space Flight Center, Greenbelt, MD) IEEE Transactions on Geoscience and Remote Sensing (ISSN 0196-2892), vol. GE-23, Sept. 1985, p. 674-684. NASA-supported research. refs

A technique for estimating leaf area indices (LAIs) based on bidirectional canopy reflectance (CR) data is applied to three plant canopies: a naturally growing healthy soybean canopy, and a clumped and tufted orchardgrass canopy, respectively. The CR data were collected using a PARABOLA instrument which is capable of acquiring complete sky-and-ground looking hemispheres in 11 seconds. The model fit and LAI estimates were good for the soybean and clumped orchardgrass canopies, but poor for the tufted orchardgrass canopy when the maximum zenith angle was less than 50 percent. It is shown that the biophysical parameter estimation based on CR measurements applied well to homogeneous herbaceous vegetation types, while better CR models are needed to adequately represent discontinuous plant canopies. I.H.

A85-49109*

MICROWAVE INVERSION OF LEAF AREA AND INCLINATION ANGLE DISTRIBUTIONS FROM BACKSCATTERED DATA

R. H. LANG and H. A. SALEH (George Washington University, Washington, DC) IEEE Transactions on Geoscience and Remote Sensing (ISSN 0196-2892), vol. GE-23, Sept. 1985, p. 685-694. refs

(Contract NAG5-265)

The backscattering coefficient from a slab of thin randomly oriented dielectric disks over a flat lossy ground is used to reconstruct the inclination angle and area distributions of the disks. The disks are employed to model a leafy agricultural crop, such as soybeans, in the L-band microwave region of the spectrum. The distorted Born approximation, along with a thin disk approximation, is used to obtain a relationship between the horizontal-like polarized backscattering coefficient and the joint probability density of disk inclination angle and disk radius. Assuming large skin depth reduces the relationship to a linear Fredholm integral equation of the first kind. Due to the ill-posed nature of this equation, a Phillips-Twomey regularization method with a second difference smoothing condition is used to find the inversion. Results are obtained in the presence of 1 and 10 percent noise for both leaf inclination angle and leaf radius densities. Author

A85-49110*

MODELING THE RADIANT TRANSFERS OF SPARSE VEGETATION CANOPIES

D. S. KIMES (NASA, Goddard Space Flight Center, Greenbelt, MD), J. M. NORMAN, and C. L. WALTHALL (Nebraska, University, Lincoln) IEEE Transactions on Geoscience and Remote Sensing (ISSN 0196-2892), vol. GE-23, Sept. 1985, p. 695-704. refs

The scattering dynamics of sparse vegetation canopies were studied within the framework of the three-dimensional radiative transfer model of Kimes (1984). The model was upgraded by including an algorithm for the anisotropic scattering of a soil boundary. Validation of the model was carried out using measured directional reflectance data for two canopies exhibiting typical scattering behavior with low and intermediate vegetation density. The canopies were: an orchard grass canopy; and a hard wheat canopy. A number of factors were found contributing to the final reflectance distribution of the canopies, including: (1) the strong anisotropic scattering properties of the soil; (2) the geometric effect of the vegetation probability gap function on the soil anisotropy and solar irradiance; and (3) the anisotropic scattering of vegetation which is controlled by the phase function and the layering of leaves. The application of the theoretical results to the development of earth-observing sensor systems is discussed. I.H.

01 AGRICULTURE AND FORESTRY

A85-49111* Hunter Coll., New York.

GEOMETRIC-OPTICAL MODELING OF A CONIFER FOREST CANOPY

X LI and A. H. STRAHLER (Hunter College, New York) IEEE Transactions on Geoscience and Remote Sensing (ISSN 0196-2892), vol. GE-23, Sept. 1985, p. 705-721. refs (Contract NAG5-273)

A geometric-optical model of a conifer forest canopy was constructed to describe the variance of a remotely-sensed image of a forest stand. The model is driven by interpixel variance generated from three sources: (1) the number of crowns in the pixel; (2) the size of the individual crowns; and (3) the overlapping of crowns and shadows. The illumination of a tree and its shadow is described as a cone using parallel-ray geometry. The model can also be inverted to provide estimates of the size, shape and spacing of the trees using remotely-sensed imagery and a minimum of ground measurements. The results of field tests using 10-meter and 80-meter multispectral imagery of two test conifer stands in northeastern California are presented. It is shown that the model produces reasonable estimates for the geometric parameters of the stand and appears to be sufficiently robust for application to other geometric shapes corresponding to different types of vegetation. I.H.

A85-49112* Purdue Univ., West Lafayette, Ind.

PLANT CANOPY SPECULAR REFLECTANCE MODEL

V. C. VANDERBILT and L. GRANT (Purdue University, West Lafayette, IN) IEEE Transactions on Geoscience and Remote Sensing (ISSN 0196-2892), vol. GE-23, Sept. 1985, p. 722-730. refs (Contract NAG5-269)

A model is derived for the amount of light specularly reflected and polarized by a plant canopy. The model is based on the morphological and phenological characteristics of the canopy and upon the Fresnel equations of optics. The theory demonstrates that the specular reflectance of the plant canopy is a function of the angle of incidence and potentially contains information to help discriminate between species. The theory relates the specular reflectance to botanical condition of the canopy - to factors such as development stage, plant vigor, and leaf area index (LAI).

Author

A85-49113*# Lockheed Engineering and Management Services Co., Inc., Houston, Tex.

INCLUSION OF SPECULAR REFLECTANCE IN VEGETATIVE CANOPY MODELS

E. REYNA (Lockheed Engineering and Management Services Co., Houston, TX) and G. D. BADHWAR (NASA, Johnson Space Center, Houston, TX) IEEE Transactions on Geoscience and Remote Sensing (ISSN 0196-2892), vol. GE-23, Sept. 1985, p. 731-736. NASA-supported research. refs

A detailed comparison of the observed soybeans and corn canopy reflectance with that calculated from three vegetative canopy reflectance models have shown systematic angular deviations. A likely cause of these effects is noninclusion of leaf specular reflectance. In this paper a formulation to calculate the component of canopy specular reflectance as a function of incident solar and view zenith angles, leaf area index, leaf angle distribution, and leaf specular reflectance has been developed. The SAIL model has been modified to include this component and the results are compared with an extensive observational data set on soybeans. It is shown that the systematic differences between the SAIL model and observations dependent on scattering azimuth are removed. An analysis of variance shows model improvement of 30 percent over the uncorrected SAIL model. Author

A85-49114* Kansas Univ. Center for Research, Inc., Lawrence. **SOURCES OF SCATTERING FROM VEGETATION CANOPIES AT 10 GHZ**

L.-K. WU, R. K. MOORE, and R. ZOUGHBI (University of Kansas Center for Research, Inc., Lawrence) IEEE Transactions on Geoscience and Remote Sensing (ISSN 0196-2892), vol. GE-23, Sept. 1985, p. 737-745. refs (Contract NAG5-271)

High-resolution backscatter measurements were made at X-band, with vertical polarization, and incidence angles of 30 and 50 deg, for winter wheat, soybeans, and corn during the summer of 1984. Plants were observed both under natural conditions and with partial-to-complete defoliation. The resolution volume of the measurement system is better than 20 x 20 x 11.25 cu cm within the entire range of measurements. Results are presented as a radar image, which also provides information on the spatial distribution of the (attenuated) scattering inside the canopy observed under natural conditions. Measured results indicate that: (1) for the full-grown wheat plants, heads are the dominant scatterers at the early heading stage and the ground is the dominant scatterer at the later growth stages; (2) for the soybeans, returns are mostly from the upper 30-cm portion of the plants, and leaves and stems dominate the radar signal at 30 and 50 deg incidence angles, respectively; (3) for the corn plants, leaves are the single dominant scatterers at both angles of incidence, and (4) ground returns are relatively unimportant as they are highly attenuated by the vegetation cover. Author

A85-49115

MICROWAVE ATTENUATION PROPERTIES OF VEGETATION CANOPIES

F. T. ULABY (Michigan, University, Ann Arbor) and E. A. WILSON (North Central Association of Colleges and Schools, Boulder, CO) IEEE Transactions on Geoscience and Remote Sensing (ISSN 0196-2892), vol. GE-23, Sept. 1985, p. 746-753. refs

The microwave attenuation of vegetation canopies of winter wheat and soybeans was measured during the late spring and summer of 1984 using a set of L-band, C-band, and X-band FM-CW radars mounted on a boom truck. The canopy loss factor was estimated as a function of frequency, incidence angle, and the polarization configuration at 1.55, 4.75, and 10.2 GHz, respectively. Measurements were obtained at widely separated incidence angles during different stages of growth. The relative contributions of the different canopy constituents (stalks, heads, and leaves) were examined in wheat decapitation and soybean defoliation experiments. The measured data were compared to calculations based on a model that treated the stalks as parallel elements of a uniaxial crystal and the leaves and branches as oriented disks and needles, respectively. The theoretical calculations agreed well with the measurements for the soybean canopy in both the vertical and the horizontal polarizations, and for the wheat canopy in the vertical polarization. However, the model consistently underestimated wheat attenuation in the horizontal polarization. Some possible reasons for the low estimates are discussed. I.H.

A85-49118* Texas Univ., Arlington.

A COMPARISON BETWEEN ACTIVE AND PASSIVE SENSING OF SOIL MOISTURE FROM VEGETATED TERRAINS

A. K. FUNG (Texas, University, Arlington) and H. J. EOM (Illinois, University, Chicago) IEEE Transactions on Geoscience and Remote Sensing (ISSN 0196-2892), vol. GE-23, Sept. 1985, p. 768-775. Previously announced in STAR as N85-13364. refs (Contract NAG5-268)

A comparison between active and passive sensing of soil moisture over vegetated areas is studied via scattering models. In active sensing three contributing terms to radar backscattering can be identified: (1) the ground surface scatter term; (2) the volume scatter term representing scattering from the vegetation layer, and (3) the surface volume scatter term accounting for scattering from both surface and volume. In emission three sources of contribution can also be identified: (1) surface emission; (2) upward volume emission from the vegetation layer; and (3) downward volume emission scattered upward by the ground.

surface. As ground moisture increases, terms (1) and (3) increase due to increase in permittivity in the active case. However, in passive sensing, term (1) decreases but term (3) increases for the same reason. This self compensating effect produces a loss in sensitivity to change in ground moisture. Furthermore, emission from vegetation may be larger than that from the ground. Hence, the presence of vegetation layer causes a much greater loss of sensitivity to passive than active sensing of soil moisture. M.G.

N85-30427# Joint Publications Research Service, Arlington, Va. **AEROSPACE TECHNOLOGY DETERMINES FOREST-FIRE DANGER Abstract Only**

V. VASILYEV *In its* USSR Rept. Earth Sci (JPRS-UES-85-007) p 30 8 Jul. 1985 Transl. into ENGLISH from Sov. Moldaviya (USSR), 17 Apr. 1985 p 4
Avail: NTIS HC A04/MF A01 CSDL 22B

Forest fires in the taiga can be detected and forecasted by meteorological satellites. A new method of predicting natural disasters was developed. The radiofrequency heat radiation of sectors of soil with different moisture contents differs sharply from each other. The water-content limit below which mosses, peat mosses and grasses become subject to combustion are well-known. A microwave radiometer was developed and proved suitable for determination of the moisture content of soil. This instrument is at present only installed on airplanes. Meteorological satellites will be equipped with the instrument. E.A.K.

N85-31604*# National Aeronautics and Space Administration, Washington, D. C. **INFLUENCE OF SPATIAL VARIABILITY OF HYDRAULIC CHARACTERISTICS OF SOILS ON SURFACE PARAMETERS OBTAINED FROM REMOTE SENSING DATA IN INFRARED AND MICROWAVES**

Y. BRUNET and M. VAUCLIN Jul. 1985 16 p refs Transl. into ENGLISH from INRA Colloquia (Bordeaux), no. 23, 1984 p 772-781 Transl. by The Corporate Word, Inc., Pittsburgh (Contract NASW-4006)
(NASA-TM-77902; NAS 1.15 77902) Avail: NTIS HC A02/MF A01 CSDL 08M

The correct interpretation of thermal and hydraulic soil parameters infrared from remotely sensed data (thermal infrared, microwaves) implies a good understanding of the causes of their temporal and spatial variability. Given this necessity, the sensitivity of the surface variables (temperature, moisture) to the spatial variability of hydraulic soil properties is tested with a numerical model of heat and mass transfer between bare soil and atmosphere. The spatial variability of hydraulic soil properties is taken into account in terms of the scaling factor. For a given soil, the knowledge of its frequency distribution allows a stochastic use of the model. The results are treated statistically, and the part of the variability of soil surface parameters due to that of soil hydraulic properties is evaluated quantitatively. Author

N85-33149# Joint Publications Research Service, Arlington, Va. **IMPACT OF FLUCTUATIONS IN OPTICAL PROPERTIES OF ATMOSPHERE ON THE RATIO OF SPECTRAL BRIGHTNESS FROM REMOTE SENSING OF AGRICULTURAL LAND Abstract Only**

S. A. AKHMEDOV and D. A. USIKOV *In its* USSR Rept.: Space (JPRS-USP-84-006) p 120 14 Nov. 1984 Transl. into ENGLISH from Issled. Zemli iz Kosmosa (Moscow), no. 2, Mar. - Apr. 1984 p 23-24
Avail: NTIS HC A08

The data from multiband video images made from space is distorted by the atmosphere, the optical parameters of which fluctuate around average values and are generally unknown. The mean statistical error in determining the brightness ratio of a target object at two different wavelengths is determined from measurements at 0.63 and 0.57 micrometers for the cities Krasnoyarsk, Markovo, Riga, Omsk, Pechora and Gur'yev, with the average values of the optical thickness at these wavelengths and their dispersions being taken from actinometric station data. An analytical expression is derived for calculating the dispersion

of this ratio. The maximum relative error reaches 10%, an amount which can be significant in research and practical applications

Author

N85-33152# Joint Publications Research Service, Arlington, Va. **INTERPRETATION OF MULTIBAND PHOTOGRAPHS MADE DURING TELEFOTO-80 EXPERIMENT FOR THE PURPOSE OF DISCRIMINATING AGRICULTURAL CROPS Abstract Only**

R. KACHINSKI *In its* USSR Rept.: Space (JPRS-USP-84-006) p 122 14 Nov. 1984 Transl. into ENGLISH from Issled. Zemli iz Kosmosa (Moscow), no. 2, Mar. - Apr. 1984 p 44-47
Avail: NTIS HC A08

Aerial photographs were taken from an AN-30 laboratory aircraft on July 27th, 1980 from about 2,500 m (scale of 1:20,000) with an MKF-6M camera during the Telefoto-80 experiment conducted within the framework of the Intercosmos program. The photos were interpreted to the following crops: corn, potatoes, beets, wheat, flax, meadow and pasture land, barley, oats, and rye and rape the area around the Polish villages of Kulin and Tsesazhovitse. The results of interpreting color photos of 119 fields near the former and 132 fields near the latter locations show (1) the natural colors of crops determined visually yield the same results for rye and wheat, corn and potatoes as well as meadow and pasture lands. The incorporation of an infrared analysis channel makes it possible to discriminate between corn and potatoes, and between rye and wheat. The average identification accuracy for individual agricultural crops ranged from 86 to 100% (with the exception of oats, which was only correctly identified 35% of the time, since it was incorrectly identified as flax because of the small number of fields) Author

N85-33155# Joint Publications Research Service, Arlington, Va. **CATALOGING THE SPECTRAL BRIGHTNESS COEFFICIENTS OF THE FORESTED REGION OF THE EUROPEAN TERRITORY OF THE USSR Abstract Only**

Y. K. ROSS and U. K. PETERSON *In its* USSR Rept.: Space (JPRS-USP-84-006) p 124 14 Nov. 1984 Transl. into ENGLISH from Issled. Zemli iz Kosmosa (Moscow), no. 2, Mar. - Apr. 1984 p 60-66
Avail: NTIS HC A08

Data from ground, aircraft and helicopter measurements of the spectral brightness coefficients of the Earth's surface which were obtained during 1976 to 1982 by the Institute of Astrophysics and Atmospheric Physics of the Estonian SSR Academy of Sciences, are used to compile a catalog of these brightness factors for the northwest portion of the European area of the USSR for all seasons of the year. Three wavelengths were used: 0.550, 0.675 and 0.795 micrometers. A classification system is developed for the mapping of the surface which is comparable to the land use and land cover scheme of Anderson, et al., and corresponds to the second level of this classification in terms of the degree of detail. Some 32 different classification categories were selected. The average values of the spectral brightness are summarized for these categories in tabular form for five periods of the year: winter, spring, summer, late summer and fall. The reliability of the catalog requires that the spectral brightness coefficients be supplemented with variation coefficients, however, there is still not sufficiently reliable data for this. Author

N85-33156# Joint Publications Research Service, Arlington, Va. **REGRESSION ANALYSIS OF AIRCRAFT AND GROUND MEASUREMENT DATA ON VEGETATION COVER Abstract Only**

O. Y. KLIMENKO and V. V. KOZODEROV *In its* USSR Rept.: Space (JPRS-USP-84-006) p 125 14 Nov. 1984 Transl. into ENGLISH from Issled. Zemli iz Kosmosa (Moscow), no. 2, Mar. - Apr. 1984 p 67-75
Avail: NTIS HC A08

Data from aircraft measurements using the MKF-6 multiband camera and ground measurements of the phytometric parameters of winter wheat, e.g., the height, thickness, leaf surface area, phytomass dry and moist weight by volume, vegetative soil shading and other parameters for wheat in the Kherson test area in 1981,

02 ENVIRONMENTAL CHANGES AND CULTURAL RESOURCES

were subjected to regression analysis in order to determine the relationship between the remote measurements and ground measurements for the vegetation soil system. The regression analysis consisted in calculating the coefficients of the linear step by step regression, the correlation matrices and residual dispersion of the significant parameters. The findings are: (1) the inadequate precision in relating the aircraft and ground measurements to each other for the April phenophase resulted in considerable errors in the predictive model; (2) results were much better for the June phenophase when the ground data were better tied to the aircraft measurements; (3) very low correlation coefficients are noted between the denseness and the other parameters, and the multiband brightnesses. The lack of sufficient statistical data does not now allow for an explanation; (4) a comparison of calculations based on single factor models, when the vegetation index and straight line distance was taken as the factor, showed that the results obtained for the straight line distance are substantially better. Author

02

ENVIRONMENTAL CHANGES AND CULTURAL RESOURCES

Includes land use analysis, urban and metropolitan studies, environmental impact, air and water pollution, geographic information systems, and geographic analysis.

A85-42579

ESTIMATION OF RURAL POPULATION IN KORDOFAN, SUDAN

M. STERN (Lunds Universitet, Lund, Sweden) Photo Interpretation (ISSN 0031-8523), vol. 22, Nov.-Dec. 1983, 7 p In English, French, and Spanish.

Landsat RBV images are presented of the Sudan region, with attention focusing on stable sand dunes and clay plains. The images were gathered as part of a census of settlements. The black/white images are discussed with reference to ground-truth data for, e.g., typical reflectances of human habitations, wells, land surfaces, etc. Population densities were estimated from the size of a village area within the image relative to a preset density. A 0.9 correlation was established between estimates using the Landsat data and verified census tallies. M.S.K.

A85-43375* Washington Univ., Seattle.

THE ORIGIN OF TEMPORAL VARIANCE IN LONG-LIVED TRACE CONSTITUENTS IN THE SUMMER STRATOSPHERE

P. G. HESS and J. R. HOLTON (Washington, University, Seattle) Journal of the Atmospheric Sciences (ISSN 0022-4928), vol. 42, July 1, 1985, p. 1455-1463. refs
(Contract NSF ATM-83-14111; NAGW-662)

Temporal variances in the concentrations of N₂O, CF₂Cl₂, CFCI₃ and CH₄ in the summer stratosphere at a midlatitude location have been measured by Ehhalt and others. A simple dynamical model is used to argue that these variances are created by irreversible mixing associated with the springtime final stratospheric warming. Tracer perturbations generated during the warming are advected passively in the zonal mean easterlies so that the tracer variance is effectively frozen into the summertime stratosphere. Temperature perturbations, on the other hand, are subject to radiative dissipation; the temperature variance created during the final warming relaxes quickly to an ambient value. Author

A85-45871

SPOT SIMULATION IMAGERY FOR URBAN MONITORING - A COMPARISON WITH LANDSAT TM AND MSS IMAGERY AND WITH HIGH ALTITUDE COLOR INFRARED PHOTOGRAPHY

R. N. COLWELL and C. E. POULTON Photogrammetric Engineering and Remote Sensing (ISSN 0099-1112), vol. 51, Aug. 1985, p. 1093-1101.

A85-46249

AERIAL AND SPACE-BASED REMOTE SENSING IN ECOLOGICAL PROGNOSIS [AEROKOSMICHESKIE METODY V EKOLOGICHESKOM PROGNOZE]

B. V. VINOGRADOV (AN SSSR, Institut Evoliutsionnoi Morfologii i Ekologii Zhivotnykh, Moscow, USSR) Priroda (ISSN 0032-874X), July 1985, p. 13-23. In Russian. refs

Ecological prognoses for large ecoregions can be made through the retrospective analysis of ecological tendencies in terms of coefficients of change with time and through extrapolation of the change into the future. The method depends on a comparison of periodically made photographs, obtained by aerial and space-based remote sensing equipment which permits the simultaneous monitoring of large regions. The details of the method are discussed including the optimal times between the photographing, the scale of imaging needed, and photointerpretation methods. The method is illustrated by particular examples of mathematical relationship, ranging widely in complexity. Equations are also given for finding the number of possible combinations of several ecosystems coexisting within large regions, and for the dynamics of such heterogeneous systems. The analysis described makes it possible to predict ecological catastrophes usually eight to sixteen years ahead, and thus to prepare anticipatory measures. I.S.

N85-32370* # Fort Lewis A&M Coll., Durango, Colo. Dept. of Geology

ONE APPLICATION OF MEGA-GEOMORPHOLOGY IN EDUCATION

R. W. BLAIR, JR. In NASA. Goddard Space Flight Center Global Mega-Geomorphology p 56-58 Jul. 1985 refs
Avail NTIS HC A07/MF A01 CSCL 08G

One advantage of a synoptic view displaying landform assemblages provided by imagery is that one can often identify geomorphic processes which have shaped the region and which may affect the habitability of the area over a human life time. Considering the continued growth of the world population and the resultant pressure and the exploitation of land, usually without any consideration given to geologic processes, it is imperative that we attempt to educate as large a segment of the population as we can about geologic processes and how they influence land use. Space platform imagery which exhibits regional landscapes can be used: (1) to show students the impact of geologic processes over relatively short periods of time (e.g., the Mount St. Helens lateral blast); (2) to display the effects of poor planning because of a lack of knowledge of the local geologic processes (e.g., the 1973 image of the Mississippi River flood around St. Louis, MO); and (3) to show the association of certain types of landforms with building materials and other resources (e.g., drumlins and gravel deposits). G.L.C.

N85-34563# Canada Land Data Systems, Ottawa (Ontario) Lands Directorate.

APPLIED COMPUTER GRAPHICS IN A GEOGRAPHIC INFORMATION SYSTEM: PROBLEMS AND SUCCESSES

C. L. MACDONALD and I. K. CRAIN In Canadian Information Processing Society Graphics Interface 1985 p 291-296 1985 refs

Avail: NTIS HC A19/MF A01

A geographic information system (GIS) reports and displays data which are referenced to geographic locations. As opposed to automated cartography, geographic information systems often have developed graphic output as an afterthought or secondary product. The Canada geographic information system, (CGIS) was designed with no graphic output capability, but now provides a variety of interactive and hard-copy graphics on a day-to-day basis. These graphics are applied to problems in land evaluation, land use monitoring, natural resource planning, wildlife habitat conservation, and so on. Three categories of graphic outputs in map form are required, interactive displays, working diagrams and publication quality diagrams. These were achieved by using remote interactive color and monochrome terminals, ink-jet plotters, vector-based plotting on a high quality drum plotter and the direct

production of publication quality color separates on a large format optical scanner with laser plotter capabilities. Author

N85-35459# Geological Survey, Alexandria, Va.
FEDERAL MINERAL LAND INFORMATION SYSTEM Abstract Only

R. L. KLECKNER *In its* USGS Res. on Mineral Resources, 1985 p 65-66 1985

Avail: NTIS HC A05/MF A01

The U.S. Geological Survey is developing the Federal Mineral Land Information System (FMLIS), which will allow land managers, policy makers, and others to rapidly retrieve, display, and analyze minerals information on Federal lands at regional, State, and National levels. This capability is being developed in order to input, manipulate, analyze, and output digital data through a geographic information system (GIS). A GIS is a tool for integrating and analyzing spatial data functions with a GIS allow for changes in map scale and projection, data editing, registration and overlay, selection, retrieval, and display of data tabulation of acreages; and measurement of distances. In an interactive environment, the user can rapidly analyze data, examine alternatives, and test hypotheses. Author

N85-35542# Deutsche Forschungs- und Versuchsanstalt fuer Luft- und Raumfahrt, Oberpfaffenhofen (West Germany). Inst. fuer Physik der Atmosphaere.

PROCEEDINGS OF METEOROLOGICAL MOTOR GLIDER (MEMO) WORKSHOP '84

Jan. 1985 213 p refs Partly in ENGLISH and GERMAN Proc. held at Oberpfaffenhofen, West Ger., 1-5 Oct. 1985 Report will also be announced as translation (ESA-TT-945)

(DFVLR-MITT-85-04; ISSN-0176-7739) Avail. NTIS HC A10/MF A01

Motor glider meteorology and the history of motor gliders used for meteorological flight are reviewed. Vertical wind velocity determination using aircraft motion is discussed. Meteorological data from the Falcon aircraft and the ASK 16 motor glider are compared. Atmospheric boundary layer turbulence is investigated. Environmental meteorological data in urban areas are examined. The concept of Lagrangian partitioning was applied to turbulent energy transport. Horizontal and vertical structure of the boundary layer, and the energy budgets above rural and urban areas are treated. Lee circulation in a Fohn wind is studied. Meteorological measuring campaigns with instrumented motor gliders in Poland are reviewed. A data acquisition system for meteorological measurements onboard light aircraft is developed. Accuracy and error analysis of meteorological measuring data is considered. The principles of wind velocity measurements onboard research aircraft are presented.

N85-35549# Eidgenoessisches Inst. fuer Reaktorforschung, Wuerenlingen (Switzerland)

ENVIRONMENTAL-PHYSICAL MEASUREMENTS AND DETERMINATION OF ATMOSPHERIC TURBULENCE WITH THE ASK-16 MOTOR GLIDER [UMWELTPHYSIKALISCHE MESSUNGEN UND ERFASSUNG ATMOSPHAERISCHER TURBULENZ MIT DEM MOTORSEGLER ASK-16]

M. HUTTER *In* DFVLR Proc. of Meteorol. Motor Glider (MEMO) Workshop '84 p 81-89 Jan 1985 refs In GERMAN

Avail: NTIS HC A10/MF A01

Meteorological motor glider flights are performed to determine environmental and atmospheric turbulence parameters. Temperature and humidity probes used in the project CLIMOD (climate modification) studying the effect of increasing urbanization and planned nuclear power plants with their cooling system on the climate, and the results of the measurements and model calculations are discussed. Ozone in the lower troposphere due to the existence of smog reactions in the neighborhood of Zurich is investigated in ground stations and with two captive balloons; the regional ozone distribution was measured by motor gliders, the measurements strongly point at the Zurich agglomeration as the origin of the ozone-rich air. The motions of motor gliders due to air flows are used to determine atmospheric turbulence in the

wavelength domain between 10 and 100 m; the measurements confirm previous results: agreement between the measurements and a mathematical turbulence parameterization model is found.

Author (ESA)

N85-35553# Bonn Univ. (West Germany). Inst. fuer Meteorologie

MOTOR GLIDER MEASUREMENTS DURING THE URBAN ATMOSPHERE ENERGY BUDGET EXPERIMENT (EESA 1) [MOTORSEGLERMESSUNGEN WAEREND DES EXPERIMENTES EESA 1]

J. M. HACKER *In* DFVLR Proc. of Meteorol. Motor Glider (MEMO) Workshop '84 p 135-141 Jan. 1985 refs In GERMAN

Avail: NTIS HC A10/MF A01

Meteorological measurements to compare energy budgets in rural and urban areas, and to study terms in the energy budget of sensible and latent heat are performed. The measurements of several ground stations, a radiosonde, two captive balloons, and a motor glider are combined. The model on which the investigation is based and the measuring strategy are described. The measured energy fluxes above the city and the surroundings are presented. The differences in the energy budgets of the boundary layer above the two areas are discussed. Author (ESA)

03

GEODESY AND CARTOGRAPHY

Includes mapping and topography.

A85-40003* National Aeronautics and Space Administration. Goddard Space Flight Center, Greenbelt, Md.

GEODETIC AND GEOPHYSICAL RESULTS FROM LAGEOS

D. E. SMITH, D. C. CHRISTODOULIDIS, R. KOLENKIEWICZ (NASA, Goddard Space Flight Center, Greenbelt, MD), M. H. TORRENCE, S. M. KLOSKO (EG&G Washington Analytical Services Center, Inc., Riverdale, MD) et al. (COSPAR, Workshops on Space Debris, Asteroids and Satellite Orbits, 4th and 13th, Graz, Austria, June 25-July 7, 1984) *Advances in Space Research* (ISSN 0273-1177), vol. 5, no. 2, 1985, p. 219-228. refs

Seven years of laser tracking of the Lageos spacecraft have been used to derive geodetic quantities describing the earth and its rotational motion. The dynamical motions of the solid-earth on its axis have been derived continuously since launch and changes in the length-of-day show very high correlation with variations in the atmospheric zonal winds between 1000 and 50 mbars. A significant improvement in the determination of the product of the earth's mass and the gravitational constant has been made. The high accuracy of the orbit determination of Lageos over the 7 years since launch has permitted the identification of a small deceleration in the nodal precession of the orbit. This deceleration is being caused by a small reduction in the flattening of the earth arising from the rebound of the earth after the last ice age. Measurements of the distances between the tracking stations over several years are showing changes consistent with tectonic plate motion and with general ideas of vertical movements. Author

A85-41189#

FURTHER IMPROVEMENTS OF THE ORBITAL PROGRAM SYSTEM POTSDAM-5 AND THEIR UTILIZATION IN GEODETIC-GEODYNAMIC INVESTIGATIONS

G. GENDT (Deutsche Akademie der Wissenschaften, Zentralinstitut fuer Physik der Erde, Potsdam, East Germany) *Nabludeniia Iskusstvennykh Sputnikov Zemli*, no. 23, 1984, p. 421-427. refs

The program system POTSDAM-5 had been developed in the last years on the basis of POTSDAM-4. It is implemented on the computer EC 1040 and shall provide a model accuracy of some cm. This high precision can only be achieved by improvements of the reference system, force model and parameter estimation.

03 GEODESY AND CARTOGRAPHY

Results are presented using laser data for the determination of station coordinates, baselines and polar motion. Author

A85-41195#

CALIBRATION OF DOPPLER RECEIVERS

L. BANYAI (Magyar Tudományos Akadémia, Geodéziai és Geofizikai Kutató Intézet, Sopron, Hungary) Nabludenii Iskusstvennykh Sputnikov Zemli, no 23, 1984, p 487-497. refs

A summary of different methods used for the calibration of Doppler receivers is given. Using the observations of the second Doppler calibration campaign at the Satellite Geodetic Observatory in Penc, Hungary, a new concept is presented. Consideration is given to the investigation of receiver weight, receiver delay, the phase center, and to statistics of the single-point solutions. A standard procedure for the calibration of receivers and for the optimal network determination with a multipoint solution and broadcast ephemeris is proposed. M.D.

A85-41199#

PRELIMINARY RESULTS OF FINNISH-HUNGARIAN DOPPLER OBSERVATION CAMPAIGN /FHDOP/

A. CZOBOR, J. ADAM, SZ. MIHALY, T. VASS (Satellite Geodetic Observatory, Penc, Hungary), T. PARM (Geodetic Institute, Helsinki, Finland) et al. Nabludenii Iskusstvennykh Sputnikov Zemli, no 23, 1984, p 529-548. refs

The Finnish-Hungarian Doppler Observation Campaign, carried out in Finland during 13 days in August 1983, is discussed. It is shown that three Hungarian JMR-1A receivers and one Finnish JMR-4 receiver occupied 9 stations together with the first order triangulation network points of Finland. The processing of the data, performed in SGO, Penc, using two different program systems, GEODOP III and SADOSA, is described. The observation strategy and the results obtained by the two programs, as well as the S-transformations, are given. The data are presented in tables and graphs. M.D.

A85-41203#

INTERFEROMETRIC ANALYSIS OF DOPPLER MEASUREMENTS FOR DIFFERENTIAL RECEIVER CALIBRATION

R. DIETRICH and K. LEHMANN (Deutsche Akademie der Wissenschaften, Zentralinstitut fuer Physik der Erde, Potsdam, East Germany) Nabludenii Iskusstvennykh Sputnikov Zemli, no 23, 1984, p 587-592. refs

The interferometric approach to the calibration problem which uses observation differences of two receivers instead of single observations, is examined. Doppler satellite observations from standpoints close to each other are performed for this calibration purpose. Electronic delay differences, frequency differences, and coordinate differences (baseline components in a horizontal system) in the adjustment procedure are determined by introducing the satellite positions and one receiver position as known. The numerical results are presented in tables and proposed calibration strategies for parameter determination (delay differences, antenna phase center differences) are discussed. M.D.

A85-41204#

THE RESEARCH WORK AT THE CENTRAL INSTITUTE FOR PHYSICS OF THE EARTH, POTSDAM, GDR, IN THE FIELD OF DOPPLER SATELLITE GEODESY

R. DIETRICH (Deutsche Akademie der Wissenschaften, Zentralinstitut fuer Physik der Erde, Potsdam, East Germany) Nabludenii Iskusstvennykh Sputnikov Zemli, no 23, 1984, p 593-604. refs

Since 1981 a JMR-4A Doppelp receiver is used mostly for stationary observations at the Potsdam observatory. The research activities have three main directions: (1) methodical investigations of satellite interferometry using Doppler receivers and receiver calibration, (2) computation of regional networks using the orbital program POTSDAM-5, 3. Computation of long global arcs for determination of polar motion and station coordinates. Author

A85-42451*# National Aeronautics and Space Administration, Goddard Space Flight Center, Greenbelt, Md

SATELLITE GEODYNAMICS

L. S. WALTER (NASA, Goddard Space Flight Center, Greenbelt, MD) IEEE Transactions on Geoscience and Remote Sensing (ISSN 0196-2892), vol. GE-23, July 1985, p 357-359.

The application of space technology to the study of solid-earth geophysics are reviewed. Attention is given to the major experiments in the field of space-based geodynamics research including early satellite laser ranging (SLR) measurements, the GEOS-3 satellite observations, and the installation of corner cube reflectors on the moon. The contribution of VLBI techniques to terrestrial positioning measurements is also discussed. Prospects for future advances with the development of the Global Positioning System (GPS) and observations from on board the Space Station are also assessed. I.H.

A85-42452*# National Aeronautics and Space Administration, Goddard Space Flight Center, Greenbelt, Md.

SPACE-AGE GEODESY - THE NASA CRUSTAL DYNAMICS PROJECT

R. J. COATES, H. FREY, G. D. MEAD, and J. M. BOSWORTH (NASA, Goddard Space Flight Center, Greenbelt, MD) IEEE Transactions on Geoscience and Remote Sensing (ISSN 0196-2892), vol. GE-23, July 1985, p 360-368. refs

The NASA Crustal Dynamics Project (CDP) has deployed satellite laser ranging (SLR) systems and VLBI techniques for measurements of global and regional crustal motions and earth rotation parameters. The measurement programs for the years 1984 and 1983 are described, and some preliminary results are presented. A complete list of the fixed receiving stations in the CDP network is given. I.H.

A85-42464* Jet Propulsion Lab., California Inst. of Tech., Pasadena

A WATER-VAPOR RADIOMETER ERROR MODEL

B. BECKMAN (California Institute of Technology, Jet Propulsion Laboratory, Pasadena) IEEE Transactions on Geoscience and Remote Sensing (ISSN 0196-2892), vol. GE-23, July 1985, p 474-478. NASA-supported research. refs

The water-vapor radiometer (WVR) is used to calibrate unpredictable delays in the wet component of the troposphere in geodetic microwave techniques such as very-long-baseline interferometry (VLBI) and Global Positioning System (GPS) tracking. Based on experience with Jet Propulsion Laboratory (JPL) instruments, the current level of accuracy in wet-troposphere calibration limits the accuracy of local vertical measurements to 5-10 cm. The goal for the near future is 1-3 cm. Although the WVR is currently the best calibration method, many instruments are prone to systematic error. In this paper, a treatment of WVR data is proposed and evaluated. This treatment reduces the effect of WVR systematic errors by estimating parameters that specify an assumed functional form for the error. The assumed form of the treatment is evaluated by comparing the results of two similar WVR's operating near each other. Finally, the observability of the error parameters is estimated by covariance analysis. Author

A85-42469

GEOPOTENTIAL RESEARCH MISSION - STATUS REPORT

S. M. YIONOULIS and V. L. PISACANE (Johns Hopkins University, Laurel, MD) IEEE Transactions on Geoscience and Remote Sensing (ISSN 0196-2892), vol. GE-23, July 1985, p 511-516. refs

The Geopotential Research Mission (GRM) is a NASA mission planned to produce more exact measurements of the gravitational and geomagnetic fields of the earth. A status report on the progress of the mission is presented, with emphasis given to the engineering requirements of the gravitational field measurements. The guidance and measurements instruments of the GRM spacecraft are described, including the proof-mass measurement system; the disturbance compensation system (DISCOS); and an optical interferometric system for proof-mass measurements. A schematic diagram of the GRM spacecraft is presented. I.H.

A85-42474*# National Aeronautics and Space Administration. Goddard Space Flight Center, Greenbelt, Md.
THE MAGNETIC FIELD OF THE EARTH - PERFORMANCE CONSIDERATIONS FOR SPACE-BASED OBSERVING SYSTEMS

W. J. WEBSTER, JR., P. T. TAYLOR, C. C. SCHNETZLER, and R. A. LANGE (NASA, Goddard Space Flight Center, Greenbelt, MD) IEEE Transactions on Geoscience and Remote Sensing (ISSN 0196-2892), vol. GE-23, July 1985, p. 541-551. refs

Basic problems inherent in carrying out observations of the earth magnetic field from space are reviewed. It is shown that while useful observations of the core and crustal fields are possible at the peak of the solar cycle, the greatest useful data volume is obtained during solar minimum. During the last three solar cycles, the proportion of data with a planetary disturbance index of less than 2 at solar maximum was in the range 0.4-0.8 in comparison with solar minimum. It is found that current state of the art orbit determination techniques should eliminate orbit error as a problem in gravitational field measurements from space. The spatial resolution obtained for crustal field anomalies during the major satellite observation programs of the last 30 years are compared in a table. The relationship between observing altitude and the spatial resolution of magnetic field structures is discussed. Reference is made to data obtained using the Magsat, the Polar Orbiting Geophysical Observatory (POGO), and instruments on board the Space Shuttle. I.H.

A85-43958
INTRINSIC GEODESY

A. MARUSSI (Berlin and New York, Springer-Verlag, 1985, 235 p. Translation. No individual items are abstracted in this volume. refs

Phenomenological problems in geodesy are analyzed, applying Weyl proximity theory in a three-dimensional domain, in a collection of published papers from the period 1950-1981. Topics examined include the fundamentals of intrinsic geodesy, the structure of the gravity field and Laplace's equation, the application of intrinsic-geodesy principles to the normal reference field, mapping the actual gravity field onto the normal reference field, mapping between surfaces, propagation of light in continuous isotropic refracting media, and the motion of a free particle and a spherical pendulum in the microgravitational field of a gravitationally stabilized satellite in a circular orbit in a central field. T.K.

A85-44102
ESTABLISHMENT OF THREE-DIMENSIONAL GEODETIC CONTROL BY INTERFEROMETRY WITH THE GLOBAL POSITIONING SYSTEM

Y. BOCK (USAF, Geophysics Laboratory, Bedford, MA), R. I. ABBOT, C. C. COUNSELMAN, III, S. A. GOUREVITCH, and R. W. KING (MIT, Cambridge, MA) Journal of Geophysical Research (ISSN 0148-0227), vol. 90, Aug. 10, 1985, p. 7689-7703 refs (Contract F19628-83-C-0097; F19628-82-K-0002)

The classical methods of establishing local and regional geodetic control are essentially not three dimensional, and the horizontal and the vertical problems are regarded as separate. Geodetic practices for the establishment of local and regional control have not yet been altered by the advent of the so-called extraterrestrial methods of geodesy. The reasons for this situation have been related to insufficient inaccuracy, cumbersome procedures, and cost factors. However, revolutionary changes are beginning to occur in connection with the signals provided by the Global Positioning System (GPS) satellites. An analysis of the 35-station Eifel network is discussed. It is found that radiointerferometric observations of the present, incomplete constellation of GPS satellites can yield reliable determinations of the relative position vectors between stations 10 km apart with uncertainties of 1 ppm in both horizontal coordinates. G.R.

A85-45694
APPLICATION POTENTIAL OF SPOT IMAGERY FOR TOPOGRAPHIC MAPPING

I. J. DOWMAN and D. J. GUGAN (University College, London, England) (COSPAR, Plenary Meeting, 25th Workshop II on the Earth's Surface Studied from Space, Graz, Austria, June 25-July 7, 1984) Advances in Space Research (ISSN 0273-1177), vol. 5, no. 5, 1985, p. 73-79. NERC-supported research refs

The suitability of SPOT imagery for compiling 1:100,000 scale topographical maps has been evaluated by calculating ground coordinates and pixel positions for level 1b photographic images. The use of digital image processors in the mapping procedure is described, with emphasis given to an analytical stereo plotter instrument which reconstructs the geometry of a pair of photographs on the basis of a mathematical model. The results of a mapping simulation based on SPOT imagery are presented. It is found that the geometry of SPOT imagery should be suitable for mapping most terrains on a scale of 1:100,000. I.H.

A85-45870* Georgia Univ., Athens.
CARTOGRAPHIC POTENTIAL OF SPOT IMAGE DATA

R. WELCH (Georgia, University, Athens) Photogrammetric Engineering and Remote Sensing (ISSN 0099-1112), vol. 51, Aug. 1985, p. 1085-1091 refs (Contract NAS13-190)

In late 1985, the SPOT (Système Probatoire d'Observation de la Terre) satellite is to be launched by the Ariane rocket from French Guiana. This satellite will have two High Resolution Visible (HRV) line array sensor systems which are capable of providing monoscopic and stereoscopic coverage of the earth. Cartographic applications are related to the recording of stereo image data and the acquisition of 20-m data in a multispectral mode. One of the objectives of this study involves a comparison of the suitability of SPOT and TM image data for mapping urban land use/cover. Another objective is concerned with a preliminary assessment of the potential of SPOT image data for map revision when merged with conventional map sheets converted to raster formats. G.R.

A85-46076
PROPAGATION AND DIFFRACTION OF RADIO WAVES IN THE MILLIMETER AND SUBMILLIMETER RANGES [RASPROSTRANENIE I DIFRAKTSIIA RADIOVOLN V MILLIMETROVOM I SUBMILLIMETROVOM DIAPAZONAKH]

V. P. SHESTOPALOV, ED. Kiev, Izdatel'stvo Naukova Dumka, 1984, 300 p. In Russian. For individual items see A85-46077 to A85-46112

The papers presented in this volume provide an overview of theoretical and experimental studies of the propagation and diffraction of radio waves in the ionosphere, atmospheric boundary layer, and near an interface (e.g., rough surfaces of land cover and rough sea surface). The discussion also covers various remote sensing applications of millimeter waves in studies of the atmosphere, ocean and land parameters, vegetation, and snow and ice covers. V.L.

A85-46078
BACKSCATTERING OF CENTIMETER AND MILLIMETER RADIO WAVES BY THE EARTH SURFACE AT LOW GRAZING ANGLES (REVIEW) [OBRATNOE RASSEIANIE SANTIMETROVYKH I MILLIMETROVYKH RADIOVOLN ZEMNOI POVERKHNOST'IU PRI MALYKH UGLAKH SKOL'ZENIIA /OBZOR/]

G. P. KULEMIN IN: Propagation and diffraction of radio waves in the millimeter and submillimeter ranges. Kiev, Izdatel'stvo Naukova Dumka, 1984, p. 17-28 In Russian refs

The characteristics of the backscattering of centimeter and millimeter radio waves by the earth surface at low grazing angles are examined with reference to theoretical models and experimental data. An empirical expression is proposed which relates the specific effective scattering surface to the grazing angle and the wavelength for vegetation-covered terrain. The expression is shown to provide a satisfactory approximation of experimental results in the 10-100 GHz range for grazing angles less than 30 degrees. V.L.

03 GEODESY AND CARTOGRAPHY

A85-46079

DISTRIBUTION OF THE EFFECTIVE SCATTERING AREA OF THE EARTH SURFACE AT LOW GRAZING ANGLES [O RASPREDELENII EPR ZEMNOI POVERKHNOSTI PRI MALYKH UGLAKH SKOL'ZENIIA]

G. P. KULEMIN and V. N. KHARCHENKO IN: Propagation and diffraction of radio waves in the millimeter and submillimeter ranges. Kiev, Izdatel'stvo Naukova Dumka, 1984, p. 28-37. In Russian. refs

The statistical distributions of the specific effective scattering area of the earth surface at low grazing angles are examined for the centimeter and millimeter wavelengths. A model with a variable number of scatterers in a resolution cell is proposed to explain the higher (in comparison with the Rayleigh distribution) number of 'tails'. It is shown that experimental distributions of the specific effective scattering surface allowing for the spatial-temporal structure of the reflections are adequately approximated by a lognormal function. V.L.

A85-46081

SPECIFIC EFFECTIVE SCATTERING SURFACES OF CERTAIN TERRAINS IN THE MILLIMETER WAVE BAND [UDELYNIE EPR NEKOTORYKH LANDSHAFTOV V MILLIMETROVOM DIAPAZONE RADIOVOLN]

B. D. ZAMARAEV and V. G. KOLESNIKOV IN: Propagation and diffraction of radio waves in the millimeter and submillimeter ranges. Kiev, Izdatel'stvo Naukova Dumka, 1984, p. 44-49. In Russian. refs

The existing theoretical models for randomly inhomogeneous reflecting surfaces are briefly reviewed, and their applicability to natural terrains is examined. In particular, attention is given to model selection and identification for natural terrains in the millimeter wave band with allowance for field measurements at nearly vertical angles. V.L.

A85-46131

THE EFFECT OF THE INTERFACE ALBEDO OF THE UNDERLYING SURFACE ON THE REFLECTED RADIATION [O VLIYANII GRANITS RAZDELA AL'BEDO PODSTILAIUSHCHEI POVERKHNOSTI NA OTRAZHENNOE IZLUCHEENIE]

V. I. ALEKSEEV and A. A. IOLTUKHOVSKII IN: Numerical solution of problems of atmospheric optics. Moscow, Institut Prikladnoi Matematiki AN SSSR, 1984, p. 78-87. In Russian. refs

In the interpretation of satellite imagery, the assessment of the condition of the observed areas proceeds on the basis of the reflection characteristics, i.e., the luminance factors of these areas. However, the presence of an atmospheric layer between the earth and the radiation detectors produces a change in the spectral composition of the reflected radiation. Questions arise regarding the effect of this change on the results of the interpretation process. The present study is concerned with an investigative method which is based on a consideration of the spatial-frequency characteristics of an insulated atmosphere. This method makes it possible to explore a number of significant aspects, taking into account questions concerning effects related to the distance from the interface, effects of the environment on the characteristics of the radiation above a studied homogeneous area, and the dimensions of a uniform area for which disturbing effects on the luminance can be disregarded. G.R.

A85-46132

THE DETERMINATION OF THE ALBEDO OF NATURAL COVERS OF THE EARTH ON THE BASIS OF REMOTE MEASUREMENT RESULTS [O METODIKE OPREDELEENIIA AL'BEDO PRIRODNYKH POKROVOV ZEMLI PO REZULTATAM DISTANTSIONNYKH IZMERENII]

A. A. IOLTUKHOVSKII, S. B. KOSTIUKEVICH, and T. A. SUSHKEVICH IN: Numerical solution of problems of atmospheric optics. Moscow, Institut Prikladnoi Matematiki AN SSSR, 1984, p. 88-101. In Russian. refs

A successful solution of problems involving the remote sensing of an underlying surface depends to a large extent on the possibility to consider atmospheric effects under the given conditions.

Fundamental difficulties with respect to such a consideration are related to the measurement of the optical parameters of the atmosphere and the design of a suitable transfer operator. The present investigation is concerned with the determination of the albedo of a surface for cases in which the optical atmospheric parameters are known. A conversion of spectral luminance data, measured with the aid of satellites, into values of luminance at the level of the underlying surface is feasible if the spectral transfer function of the atmosphere is known. Attention is given to the determination of the reflection characteristics in the case of natural surfaces by means of a transfer function, and suitable approaches for overcoming the arising difficulties. G.R.

A85-47804* Georgia Univ., Athens.

COMPARATIVE EVALUATIONS OF THE GEODETIC ACCURACY AND CARTOGRAPHIC POTENTIAL OF LANDSAT-4 AND LANDSAT-5 THEMATIC MAPPER IMAGE DATA

R. WELCH, T. R. JORDAN, and M. EHLERS (Georgia, University, Athens) Photogrammetric Engineering and Remote Sensing (ISSN 0099-1112), vol. 51, Sept. 1985, p. 1249-1262. refs (Contract NAS5-27383)

A Landsat Image Data Quality Analysis (LIDQA) Program is conducted by NASA. One part of this program forms studies which are being performed with the objective to evaluate the geometric fidelity of Landsat-4 and Landsat-5 Thematic Mapper (TM) data in computer tape (CCT-pt) formats. It is pointed out that the Landsat-4 and Landsat-5 systems provide image data of significantly better geometric fidelity than were obtained from the earlier Landsat missions. Attention is given to the factors which influence the geometric fidelity of the Landsat TM data, the study areas and data sets, the rectification procedures, the rectification of Landsat-4 TM data and comparisons of the Scourge and the TM Image Processing System (TIPS), the rectification of system and scene corrected Landsat-5 data processed on TIPS, and the cartographic potential of TM data. G.R.

A85-49660

GEOPHYSICS 2001

J. A. JACOBS (Cambridge University, England) Geophysical Surveys (ISSN 0046-5763), vol. 7, June 1985, p. 249-255; Comments, p. 256. refs

An attempt is made to predict the areas of study in the field of geophysics which will be most rewarding in the next one or two decades. Among the topics discussed are the history of the earth; satellite geodesy; mantle convection; and aeronomy. Topics of interest in the fields of geomagnetism and space-based geophysical observations are also discussed. I.H.

N85-30539# Stanford Linear Accelerator Center, Calif.

APPLICATION OF GPS IN A HIGH PRECISION ENGINEERING SURVEY NETWORK

R. RULAND (AFGL, Hanscom AFB, Mass.) and A. LEICK 1985 11 p refs Presented at the 1st Intern. symp. on Precise Positioning with the Global Positioning System, Rockville, Md., 15 Apr 1985 (Contract DE-AC03-76SF-00515) (DE85-010556; SU-SLAC-PUB-3620, CONF-8504111-1) Avail. NTIS HC A02/MF A01

A global positioning system (GPS) satellite survey was conducted with the Macrometer to support construction at the standard linear accelerator center (SLAC). The network consists of 16 stations of which 9 stations were part of the Macrometer network. The horizontal accuracy of the terrestrial survey, consisting of angles and distances, equals that of the GPS survey only in the loop portion of the network. All stations are part of the precise level network. The ellipsoidal heights obtained from the GPS survey and the orthometric heights of the level network are used to compute geoid undulations. The profile agreed with the observed geoid within the standard deviation of the GPS survey. Angles and distances were adjusted together (TERRA), and all terrestrial observations were combined with the GPS vector observations in a combination adjustment (COMB). A comparison of COMB and

TERRA revealed systematic errors in the terrestrial solution.

DOE

N85-31585*# Purdue Univ., West Lafayette, Ind. Dept. of Geosciences.

IMPROVING THE GEOLOGICAL INTERPRETATION OF MAGNETIC AND GRAVITY SATELLITE ANOMALIES Final Report

W. J. HINZE, L. W. BRAILE, Principal Investigators, and R. R. B. VONFRESE (Ohio State Univ., Columbus) 1985 67 p refs ERTS

(Contract NAG5-304)

(E85-10103; NASA-CR-175614; NAS 1.26.175614) Avail: NTIS HC A04/MF A01 CSCL 08G

Current limitations in the quantitative interpretation of satellite-elevation geopotential field data and magnetic anomaly data were investigated along with techniques to overcome them. A major result was the preparation of an improved scalar magnetic anomaly map of South America and adjacent marine areas directly from the original MAGSAT data. In addition, comparisons of South American and Euro-African data show a strong correlation of anomalies along the Atlantic rifted margins of the continents.

N85-31586*# Purdue Univ., West Lafayette, Ind. Dept. of Geosciences.

MAGSAT SCALAR ANOMALY MAP OF SOUTH AMERICA Abstract Only

J. R. RIDGWAY, W. J. HINZE, and L. W. BRAILE *In its* Improving the Geol. Interpretation of Magnetic and Gravity Satellite Anomalies 1 p 1985 ERTS

Avail: NTIS HC A04/MF A01 CSCL 08B

A scalar magnetic anomaly map was prepared for South America and adjacent marine areas directly from original MAGSAT orbits. The preparation of the map poses special problems, notably in the separation of external field and crustal anomalies, and in the reduction of data to a common altitude. External fields are manifested in a long-wavelength ring current effect, a medium-wavelength equatorial electrojet, and short-wavelength noise. The noise is reduced by selecting profiles from quiet periods, and since the electrojet is confined primarily to dusk profiles, its effect is minimized by drawing the data set from dawn profiles only. The ring current is corrected through the use of the standard ring current equation, augmented by further filtering with a Butterworth bandpass filter. Under the assumption that the time-variant ring current is best removed when a replication of redundant profiles is achieved, a test set of 25 groups of 3 nearly coincident orbits per group is set up for filtering with a range of long-wavelength cutoffs to determine which cutoff best replicates the residual profiles. Altitude differences are then normalized by an inversion of the profile data onto a grid of equivalent point dipoles, and recalculated at an altitude of 350 km. The resulting map, when compared to the 2 deg averaged map, shows more coherent anomalies, with notable differences in the region affected by the electrojet. M.G.

N85-31587*# Purdue Univ., West Lafayette, Ind. Dept. of Geosciences

MAGSAT SATELLITE MAGNETIC ANOMALY MAP OVER SOUTH AMERICA Abstract Only

J. R. RIDGWAY *In its* Improving the Geol. Interpretation of Magnetic and Gravity Satellite Anomalies 2 p 1985 ERTS

Avail: NTIS HC A04/MF A01 CSCL 08B

A scalar magnetic anomaly map was prepared for South America and adjacent marine areas directly from original MAGSAT orbits. Special problems associated with the separation of external field and crustal anomalies, and the reduction of data to a common altitude are addressed. External fields are manifested in a long-wavelength ring current effect, a medium-wavelength equatorial electrojet, and short-wavelength noise. The noise is reduced by selecting profiles from quiet periods (K_p or $= 3$), and the effect of the electrojet is minimized by drawing the data set from dawn profiles only. The ring current is corrected through the use of a standard equation, augmented by further digital

band-pass filtering. Profiles thus filtered differ primarily in amplitude due solely to satellite altitude differences. These differences are normalized by an inversion of the profile data onto a grid of equivalent point dipoles, and recalculated at an altitude of 350 km. The low altitudes in the study area cause instability in the inversion, necessitating separate inversions of several sub-areas which are subsequently merged. Crustal anomalies reduced-to-the-pole exhibit marked correlations to known tectonic features. M.G.

N85-31590*# Ohio State Univ., Columbus.

BINNING OF SATELLITE MAGNETIC ANOMALIES Final Report

H. K. GOYAL, R. R. B. VONFRESE, and W. J. HINZE (Purdue Univ., Lafayette, Ind.) *In* Purdue Univ. Improving the Geol. Interpretation of Magnetic and Gravity Satellite Anomalies 13 p 1985 refs ERTS

Avail: NTIS HC A04/MF A01 CSCL 08B

Crustal magnetic anomaly signals over satellite orbits were simulated to investigate numerical averaging as an anomaly estimator. Averaging as an anomaly estimator involves significant problems concerning spatial and amplitude smoothing of the satellite magnetic observations. The results of simulations suggest that the error of numerical averaging constitutes a small and relatively minor component of the total error-budget of higher orbital anomaly estimates, whereas for lower orbital estimates numerical averaging error increases substantially. As an alternative to numerical averaging, least-squares collocation was investigated and observed to produce substantially more accurate anomaly estimates, particularly as the orbital elevation of prediction was decreased towards the crustal sources. In contrast to averaging, collocation is a significantly more resource-intensive procedure to apply because of the practical, but surmountable problems related to establishing and inverting the covariance matrix for accurate anomaly prediction. However, collocation may be much more effectively used to exploit the anomaly details contained in the lower orbital satellite magnetic data for geologic analysis. M.G.

N85-31593*# Purdue Univ., West Lafayette, Ind. Dept. of Geosciences

A COMPARATIVE STUDY OF SPHERICAL AND FLAT-EARTH GEOPOTENTIAL MODELING AT SATELLITE ELEVATIONS Abstract Only

M. H. PARROTT, W. J. HINZE, L. W. BRAILE, and R. R. B. VONFRESE (Ohio State Univ., Columbus) *In its* Improving the Geol. Interpretation of Magnetic and Gravity Satellite Anomalies 1 p 1985 ERTS

Avail: NTIS HC A04/MF A01 CSCL 08N

Flat-Earth modeling is a desirable alternative to the complex spherical-Earth modeling process. These methods were compared using 2 1/2 dimensional flat-earth and spherical modeling to compute gravity and scalar magnetic anomalies along profiles perpendicular to the strike of variably dimensioned rectangular prisms at altitudes of 150, 300, and 450 km. Comparison was achieved with percent error computations (spherical-flat/spherical) at critical anomaly points. At the peak gravity anomaly value, errors are less than + or - 5% for all prisms. At 1/2 and 1/10 of the peak, errors are generally less than 10% and 40% respectively, increasing to these values with longer and wider prisms at higher altitudes. For magnetics, the errors at critical anomaly points are less than -10% for all prisms, attaining these magnitudes with longer and wider prisms at higher altitudes. In general, in both gravity and magnetic modeling, errors increase greatly for prisms wider than 500 km, although gravity modeling is more sensitive than magnetic modeling to spherical-Earth effects. Preliminary modeling of both satellite gravity and magnetic anomalies using flat-Earth assumptions is justified considering the errors caused by uncertainties in isolating anomalies. M.G.

03 GEODESY AND CARTOGRAPHY

N85-31594*# Purdue Univ., West Lafayette, Ind Dept. of Geosciences

A COMPARATIVE STUDY OF SPHERICAL AND FLAT-EARTH GEOPOTENTIAL MODELING AT SATELLITE ELEVATIONS Final Report

M. H. PARROTT, W. J. HINZE, and L. W. BRAILE (Ohio State Univ., Columbus) *In its* Improving the Geol. Interpretation of Magnetic and Gravity Satellite Anomalies 19 p 1985 refs ERTS

Avail: NTIS HC A04/MF A01 CSCL 08N

Flat-Earth and spherical-Earth geopotential modeling of crustal anomaly sources at satellite elevations are compared by computing gravity and scalar magnetic anomalies perpendicular to the strike of variably dimensioned rectangular prisms at altitudes of 150, 300, and 450 km. Results indicate that the error caused by the flat-Earth approximation is less than 10% in most geometric conditions. Generally, error increase with larger and wider anomaly sources at higher altitudes. For most crustal source modeling applications at conventional satellite altitudes, flat-Earth modeling can be justified and is numerically efficient. Author

N85-31597*# Ohio State Univ., Columbus. Dept. of Geology and Mineralogy.

LONG-WAVELENGTH MAGNETIC AND GRAVITY ANOMALY CORRELATIONS ON AFRICA AND EUROPE Abstract Only

R. R. B. VONFRESE, R. OLIVIER (Lausanne Univ., Switzerland), and W. J. HINZE (Purdue Univ., Lafayette, Ind.) *In* Purdue Univ. Improving the Geol. Interpretation of Magnetic and Gravity Satellite Anomalies 1 p 1985 Previously announced as N84-25135 ERTS

Avail: NTIS HC A04/MF A01 CSCL 08N

Preliminary MAGSAT scalar magnetic anomaly data were compiled for comparison with long-wavelength-pass filtered free-air gravity anomalies and regional heat-flow and tectonic data. To facilitate the correlation analysis at satellite elevations over a spherical-Earth, equivalent point source inversion was used to differentially reduce the magnetic satellite anomalies to the radial pole at 350 km elevation, and to upward continue the first radial derivative of the free-air gravity anomalies. Correlation patterns between these regional geopotential anomaly fields are quantitatively established by moving window linear regression based on Poisson's theorem. Prominent correlations include direct correspondences for the Baltic shield, where both anomalies are negative, and the central Mediterranean and Zaire Basin where both anomalies are positive. Inverse relationships are generally common over the Precambrian Shield in northwest Africa, the Basins and Shields in southern Africa, and the Alpine Orogenic Belt. Inverse correlations also persist over the North Sea Rifts, the Benue Rift, and more generally over the East African Rifts. The results of this quantitative correlation analysis support the general inverse relationships of gravity and magnetic anomalies observed for North American continental terrain which may be broadly related to magnetic crustal thickness variations. A.R.H.

N85-31599*# Ohio State Univ., Columbus. Dept. of Geology and Mineralogy.

CONTINENTAL MAGNETIC ANOMALY CONSTRAINTS ON CONTINENTAL RECONSTRUCTION Abstract Only

R. R. B. VONFRESE, W. J. HINZE (Purdue Univ., Lafayette, Ind.), R. OLIVIER (Lausanne Univ., Switzerland), and C. R. BENTLEY (Wisconsin Univ., Madison) *In* Purdue Univ. Improving the Geol. Interpretation of Magnetic and Gravity Satellite Anomalies 1 p 1985 ERTS

Avail: NTIS HC A04/MF A01 CSCL 08N

Crustal magnetic anomalies mapped by the MAGSAT satellite for North and South America, Europe, Africa, India, Australia and Antarctica and adjacent marine areas were adjusted to a common elevation of 400 km and differentially reduced to the radial pole of intensity 60,000 nT. These radially polarized anomalies are normalized for differential inclination, declination and intensity effects of the geomagnetic field, so that in principle they directly reflected the geometric and magnetic polarization attributes of sources which include regional petrologic variations of the crust

and upper mantle, and crustal thickness and thermal perturbations. Continental anomalies demonstrate remarkably detailed correlation of regional magnetic sources across rifted margins when plotted on a reconstruction of Pangea. Accordingly, they suggest further fundamental constraints on the geologic evolution of the continents and their reconstructions. Author

N85-31600*# Ohio State Univ., Columbus Dept. of Geology and Mineralogy

REGIONAL MAGNETIC ANOMALY CONSTRAINTS ON CONTINENTAL RIFTING Final Report

R. R. B. VONFRESE, W. J. HINZE (Purdue Univ., Lafayette, Ind.), R. OLIVIER (Lausanne Univ., Switzerland), and C. R. BENTLEY (Wisconsin Univ., Madison) *In* Purdue Univ. Improving the Geol. Interpretation of Magnetic and Gravity Satellite Anomalies 12 p 1985 refs ERTS

Avail: NTIS HC A04/MF A01 CSCL 08N

Radially polarized MAGSAT anomalies of North and South America, Europe, Africa, India, Australia and Antarctica demonstrate remarkably detailed correlation of regional magnetic lithospheric sources across rifted margins when plotted on a reconstruction of Pangea. These major magnetic features apparently preserve their integrity until a superimposed metamorphic event alters the magnitude and pattern of the anomalies. The longevity of continental scale magnetic anomalies contrasts markedly with that of regional gravity anomalies which tend to reflect predominantly isostatic adjustments associated with neo-tectonism. First observed as a result of NASA's magnetic satellite programs, these anomalies provide new and fundamental constraints on the geologic evolution and dynamics of the continents and oceans. Accordingly, satellite magnetic observations provide a further tool for investigating continental drift to complement other lines of evidence in paleoclimatology, paleontology, paleomagnetism, and studies of the radiometric ages and geometric fit of the continents M.G.

N85-31690*# National Aeronautics and Space Administration. Goddard Space Flight Center, Greenbelt, Md.

THE GLOBAL VLBI FIDUCIAL NETWORK

C. MA *In its* Geodyn. Branch Res. Program 3 p Aug. 1985

Avail: NTIS HC A09/MF A01 CSCL 08E

The NASA Crustal Dynamics Project (CDP) has been acquiring geodetic VLBI data with the Mark III system since 1979 to support studies of crustal dynamics on several scales. Both mobile and fixed stations have been used, the former to study regional deformation and the latter to study plate stability and relative motion. Data from suitably chosen fixed stations can also be used to determine the orientation of the Earth, and the National Geodetic Survey has been acquiring data through its POLARIS and IRIS programs since 1980 for this purpose. The network of fixed stations has application to regional measurements using conventional VLBI and future satellite VLBI techniques. In both cases it provides a self-consistent, precisely determined set of fiducial points to which mobile observations can be referenced. In the latter application the precise positions within the fixed network can be used to improve satellite orbits to the extent required for satisfactory regional measurements. G.L.C.

N85-31691*# National Aeronautics and Space Administration. Goddard Space Flight Center, Greenbelt, Md.

FIRST EPOCH MEASUREMENTS BY MARK III VLBI OF THE SAN ANDREAS FAULT EXPERIMENT BASELINE

J. W. RYAN *In its* Geodyn. Branch Res. Program 4 p Aug. 1985 refs

Avail: NTIS HC A09/MF A01 CSCL 08K

The 883-km-long San Andreas Fault Experiment (SAFE) baseline between Quincy in northern California and Monument Peak in southern California spans the San Andreas Fault in a way designed to measure motion between the North American and the Pacific Plates. This baseline and a closely related baseline have been measured with the satellite laser ranging techniques (SLR) for over 10 years. The baseline was measured with the very-long-baseline interferometry (VLBI) technique to confirm or reject the results already obtained from SLR. G.L.C.

N85-31694*# National Aeronautics and Space Administration. Goddard Space Flight Center, Greenbelt, Md.

SATELLITE-DETERMINED STRESSES IN THE CRUST OF EUROPE WITH PARTICULAR CONSIDERATION TO THE LIEGE EARTHQUAKE OF NOVEMBER 8, 1983

H. S. LIU *In its* Geodyn Branch Res. Program 8 p Aug. 1985 refs

Avail NTIS HC A09/MF A01 CSCL 08K

The calculated stress field in Europe as inferred from satellite gravity data predicts two important features (1) orientation of the principle stresses in the Brussels-Liege region, and (2) possible horizontal crustal block movements in central Europe. Based on these features, a seismotectonic theory was developed to derive geodynamical principles which govern the present state of stresses in the European lithosphere and predict specific seismic risk regions in central Europe. According to this theory, the lithosphere of Europe is under Northwest-Southeast compressional stress with the compression centroid located under the Brussels-Liege region in Belgium. Therefore, the Liege area in Belgium has great potential for earthquakes. Although central Europe has been seismologically stable for centuries, an earthquake did occur in the Liege area in November of 1983. G.L.C.

N85-31707*# National Aeronautics and Space Administration. Goddard Space Flight Center, Greenbelt, Md.

SPACEBORNE GRADIOMETER ERROR ANALYSIS

W. D. KAHN *In its* Geodyn. Branch Res. Program 4 p Aug. 1985 refs

Avail NTIS HC A09/MF A01 CSCL 08B

The low frequency terms of the geopotential are observable from satellite perturbations as viewed by a high orbiting satellite or satellites. To measure and map the fine structure of the Earth's gravity field could be accomplished by a Spaceborne Gravity Gradiometer Mission. Since a gradiometer measures second derivatives of the geopotential field, the gradiometer will be sensitive to the density variations of the earth's outer crust which is the source of the high frequency components of the Earth's gravity field. A gravity gradiometer mission would provide in situ measurements on a global scale of the Earth's gravity field fine structure. Covariance error analyses were performed which indicate that a spaceborne gravity gradiometer having a precision of .001 E to .0001 E in a circular/polar orbit and flown at altitudes 160 km to 200 km can determine the gravity field and geoid to accuracies of 1 to 3 mgal and 3 to 5 cm respectively, with a horizontal resolution of 50 km. The potential scientific information which could be derived from a Shuttle borne gradiometer is considered. Author

N85-31708*# National Aeronautics and Space Administration. Goddard Space Flight Center, Greenbelt, Md.

GEODYN SYSTEMS DEVELOPMENT

B. H. PUTNEY *In its* Geodyn Branch Res. Program 7 p Aug. 1985

Avail. NTIS HC A09/MF A01 CSCL 09B

The purpose of the GEODYN Orbit Determination and Parameter Estimation, the SOLVE and ERODYN computer software is to recover geodetic and geophysical parameters from satellite and other data in a state-of-the-art manner and in the most operationally efficient manner. The philosophy of the development of the software system has been maintenance of computer-efficient, well-structured software, with appropriate orbit, Earth and numerical models, using precise satellite measurement modeling and efficient numerical models, and performing careful benchmark procedures. Recent developments accomplished through the use of the three programs are noted. B.W.

N85-32316# Geological Survey, Menlo Park, Calif.

COMPARISON OF SURVEY AND PHOTOGRAMMETRY METHODS TO POSITION GRAVITY DATA, YUCCA MOUNTAIN, NEVADA

D. A. PONCE, S. S. C. WU, and J. B. SPIELMAN 1985 14 p refs

(Contract DE-AI08-78ET-44802)

(DE85-011685; USGS-OFR-85-36) Avail. NTIS HC A02/MF A01

Locations of gravity stations at Yucca Mountain, Nevada, were determined by a survey using an electronic distance-measuring device and by a photogram-metric method. The data from both methods were compared to determine if horizontal and vertical coordinates developed from photogrammetry are sufficiently accurate to position gravity data at the site. The results show that elevations from the photogrammetric data have a mean difference of 0.57 + or - 0.70 m when compared with those the surveyed data. Comparison of the horizontal control shows that the two methods agreed to within 0.01 minute. At a latitude of 45(0), an error of 0.01 minute (18m) corresponds to a gravity anomaly error of 0.015 mGal. Bouguer gravity anomalies are most sensitive to errors in elevation, thus elevation is the determining factor for use of photogrammetric or survey methods to position gravity data. Because gravity station positions are difficult to locate on aerial photographs, photogrammetric positions are not always exactly at the gravity station, therefore, large disagreements may appear when comparing electronic and photogrammetric measurements DOE

N85-32387# Air Force Geophysics Lab., Hanscom AFB, Mass. **GLOBAL GEOID AND GRAVITY ANOMALY PREDICTIONS USING THE COLLOCATION AND POINT MASS TECHNIQUES Scientific Interim Report, Jan. - Aug. 1984**

R. P. BESSETTE and G. HADGIGEORGE 6 Sep. 1984 25 p (AD-A154517, AFGL-TR-84-0236; AFGL-AFSG-446) Avail NTIS HC A02/MF A01 CSCL 08E

We previously described (14,14) spherical-harmonic global adjustments of satellite altimetry using the AFGL short-arc technique supplemented with point masses to allow incorporation of short-wavelength geoidal detail. Recently, we have also investigated another technique to enhance short-wavelength detail: least squares collocation with noise. Both methods provide a means to determine a high resolution gravity field on a local, regional or global scale. Statistical comparisons of these two methods have been made in selected areas and the results tabulated. GRA

N85-33161# Joint Publications Research Service, Arlington, Va. **DISCRIMINATION OF LINEAR CONTOUR ELEMENTS OF SPACE PHOTOGRAPHS BASED ON VISUAL PERCEPTION MODEL Abstract Only**

M. V. SMIRNOV and L. N. ROZANOV *In its* USSR Rept.: Space (JPRS-USP-84-006) p 129 14 Nov. 1984 Transl. into ENGLISH from Issled. Zemli iz Kosmosa (Moscow), no 2, Mar. - Apr. 1984 p 117-124

Avail NTIS HC A08

Formalization of the description of such objects as lineaments on space photographs in the case of visual interpretation must be based on some model of visual perception. An algorithm constructed from such a model will be heuristic. It is argued that the optimization of the heuristic algorithm is possible using the statistical properties of the images. A model using the following sequence of operations is proposed: in each iteration, the dynamic range of variation in the brightness is subjected to logarithmic transformation; after this, a filter emphasizes all density gradients and simultaneously provides isotropic smoothing; the range of values of the filtered image is then subjected to an exponential transformation. The last image into lines (ascertaining the skeletal outline). A block diagram of the proposed model, as well as the frequency response of the filters used, are given. The transition is made from the qualitative model to a statistical one for certain parameters of the heuristically developed algorithm, based on the physical characteristics of the transformed space photographs

Author

03 GEODESY AND CARTOGRAPHY

N85-33162# Joint Publications Research Service, Arlington, Va.
PHYSICO-GEOGRAPHICAL REGIONALIZATION OF CASPIAN LOWLAND BASED ON SPACE SURVEY MATERIALS Abstract Only

I. V. KOPYL and V. A. NIKOLAYEV *In its USSR Rept.: Space (JPRS-USP-84-006) p 130 14 Nov. 1984 Transl into ENGLISH from Vestn. Mosk. Univ., Ser. 5: Geografiya (Moscow), no. 1, Jan. - Feb. 1984 p 65-70*
Avail: NTIS HC A08

Imagery from Salyut-4 and Meteor and other satellites was used to establish regionalization through analysis of functional internal structures of the natural geosystems consisting of conjunctions of spatial and genetic landscape complexes. Each characteristic physico-geographical area has dominant landscapes shown in the imagery by patterns which can be analyzed according to geometry, optical density, boundaries and other features. The original sea level in the Caspian lowland, has in parts, been affected by exogenous processes such as erosion, eolianism and undermining producing Baer formations and dendritic, striated, spotted, circular-concentric and other identifiable shapes. The regional pattern is built up from textures of landscapes and their morphological subunits. The area breaks down into semi-desert and desert subregions and land use modifications such as agricultural and pasture use are visible. Large scale morphostructural and zonation lineaments as well as paleogeographical features are often visible. Regionalization is more precise and detailed and shows complex interrelations better than previous versions and can be applied for agricultural, reclamation, conservation and other purposes. Author

N85-33163# Joint Publications Research Service, Arlington, Va.
MAPPING OF DYNAMICS OF DELTAS BY SPACE PHOTOGRAPHY Abstract Only

O. N. YEFREMOVA and V. I. KRAVTSOVA *In its USSR Rept.: Space (JPRS-USP-84-006) p 130-131 14 Nov 1984 Transl into ENGLISH from Vestn. Mosk. Univ., Ser. 5: Geografiya (Moscow), no. 1, Jan. - Feb. 1984 p 70-81*
Avail: NTIS HC A08

River delta region dynamics based upon hydromorphological development processes, delta movements seawards and river flow were studied by means of space imagery deltas from Meteor-Prroda and Landsat satellite scanners with medium (240 m) and high (80 m) resolution and from Salyut orbital station photos with 30 m resolution. Delta development was shown by map series using survey mapping of present conditions as the reference. Scanner photos from earth resources and meteorological satellites were used to map seasonal variations. Photos retaken with the same technology several years later allowed representation and comparison of changes and analysis of dynamics due to hydrodynamic systems and agricultural and reclamation activities, and the identifications of delta movements, appearance of spits and bars and channel variations. Delta histories were studied over longer periods by means of topographic survey maps from the 1940 to 1950's or even 19th century military maps. Geomorphological and landscape characteristics were studied by means of space imagery mapping showing relief features; ground studies identified development stages. The practical value of space imagery for mapping was demonstrated. Author

N85-33164# Joint Publications Research Service, Arlington, Va.
COMPREHENSIVE MAPPING OF ARID TERRITORIES OF ARIZONA USING SPACE PHOTOGRAPHY Abstract Only

Y. V. GLUSHKO and T. I. KONDRATYEVA *In its USSR Rept.: Space (JPRS-USP-84-006) p 131 14 Nov. 1984 Transl. into ENGLISH from Vestn. Mosk. Univ., Ser. 5: Geografiya (Moscow), no. 3, May - Jun. 1984 p 72-77*
Avail: NTIS HC A08

Cartographic work to compile maps of the arid part of Arizona from space photographs is described. Work was done from a picture obtained from the LANDSAT 1 satellite using a multispectral scanning system. The picture was taken at a height of 915 km. at a scale of 1:3,360,000 with a spatial resolution of 70 meters and covers an area of 34 square kilometers. Decoding was done from

synthesized color images in the spectral ranges 0.5 to 0.6 micrometers (green), 0.6 to 0.7 micrometers (red), and 0.8 to 1.1 micrometers (near infrared) using a working scale of 1:1,000,000. The initial map, clearly showing the higher belt of the piedmont and the southwest edge of the Colorado Plateau, was used to compile geomorphological, soil, geobotanical and land usage maps of the same area. Features of the thematic maps are described. It is suggested that the large scale use of space photography could be useful in compiling photographic maps of the USSR at a scale of 1:1,000,000. It is asserted that the use of space methods facilitates improvements in geographical cartography, which can then also be used to compile thematic maps. Photomapping is acquiring increasing importance in monitoring the natural environment. Author

N85-33552*# National Aeronautics and Space Administration.
Goddard Space Flight Center, Greenbelt, Md.

CRUSTAL DYNAMICS PROJECT: CATALOGUE OF SITE INFORMATION

Aug. 1985 407 p refs Previously announced as N85-23258 (NASA-TM-86218; REPT-85B0413; NAS 1 15:86218; X-601-85-6)
Avail: NTIS HC A18/MF A01 CSCL 08G

This document represents a catalogue of site information for the Crustal Dynamics Project. It contains information and descriptions of those sites used by the Project as observing stations for making the precise geodetic measurements useful for studies of the Earth's crustal movements and deformation. Author

04

GEOLOGY AND MINERAL RESOURCES

Includes mineral deposits, petroleum deposits, spectral properties of rocks, geological exploration, and lithology.

A85-40612

FINE STRUCTURE OF THE PRELIMINARY IMPULSE OF A SUDDEN STORM COMMENCEMENT [O TONKOI STRUKTURE PREDVARITEL'NOGO IMPUL'SA VNEZAPNOGO NACHALA MAGNITNYKH BUR']

V. A. PARKHOMOV (Irkutskii Institut Narodnogo Khoziaistva, Irkutsk, USSR) *Geomagnetizm i Aeronomiia* (ISSN 0016-7940), vol. 25, May-June 1985, p. 420-424. In Russian. refs

The fine structure of preliminary reverse impulses is analyzed on the basis of 200 SSC events recorded during 1965-1979 at the Irkutsk station and special experiments at the meridional chain of stations; a joint analysis of ground and satellite observations of the SSC of July 29, 1977 is also performed. It is shown that the PRI fine structure has the form of a strain of damped oscillations in the Pc2-3 range with a duration not greater than approximately 2 min. The excitation of these oscillations is connected with the propagation of a fast magnetoacoustic wave, generated in the interaction between the interplanetary shock wave and the magnetosphere. B.J.

A85-41661

THE SIGNIFICANCE OF LINEAMENTS MAPPED FROM REMOTELY SENSED IMAGES OF THE 1:250,000 LAU SHEET IN BENUE TROUGH OF NIGERIA

S. A. ISIORHO (Case Western Reserve University, Cleveland, OH) *International Journal of Remote Sensing* (ISSN 0143-1161), vol. 6, June 1985, p. 911-918. refs

A85-42171

THE ANTARCTIC ICE

U. RADOK (Cooperative Institute for Research in Environmental Sciences, Boulder, CO) *Scientific American* (ISSN 0036-8733), vol. 253, Aug. 1985, p. 98-105

The data base on the physical characteristics of the Antarctic ice sheet has been increased significantly since the inception of

the International Antarctic Geological Project in 1967. Radar soundings have provided detailed maps of the geological structures beneath the ice. The ice is layered in areas and sometimes covers subglacial lakes. The movements of large areas of sublayers of the ice sheet are being tracked by satellite Doppler radar soundings. Satellite passive microwave sensors monitor the mass balance of the snow cover. A gradual mass accumulation, measured in centimeters, has been observed on some large glaciers. The ice is providing global pollution, volcanic and climatic data extending up to 20,000 yr into the past. A 3000 m deep borehole has yielded evidence of a period as warm as the present 160,000 yr ago. Finally, numerical models are becoming more accurate in simulating the growth and decay of the ice sheet. M.S.K.

A85-42476* Jet Propulsion Lab., California Inst. of Tech., Pasadena.

PRELIMINARY SPECTRAL AND GEOLOGIC ANALYSIS OF LANDSAT-4 THEMATIC MAPPER DATA, WIND RIVER BASIN AREA, WYOMING

J. E. CONEL, H. R. LANG, E. D. PAYLOR, and R. E. ALLEY (California Institute of Technology, Jet Propulsion Laboratory, Pasadena) IEEE Transactions on Geoscience and Remote Sensing (ISSN 0196-2892), vol. GE-23, July 1985, p. 562-573. NASA-supported research. refs

A Landsat-4 Thematic Mapper (TM) image of the Wind River Basin area in Wyoming is currently under analysis for stratigraphic and structural mapping and for assessment of spectral and spatial characteristics using visible, near infrared, and short wavelength infrared bands. To estimate the equivalent Lambertian surface reflectance, TM radiance data were calibrated to remove atmospheric and instrumental effects. Reflectance measurements for homogeneous natural and cultural targets were acquired about one year after data acquisition. Calibration data obtained during the analysis were used to calculate new gains and offsets to improve scanner response for earth science applications. It is shown that the principal component images calculated from the TM data were the result of linear transformations of ground reflectance. In images prepared from this transform, the separation of spectral classes was independent of systematic atmospheric and instrumental factors. Several examples of the processed images are provided. I.H.

A85-42580

GEOLOGY AND STRUCTURES STUDY OF THE NUBA MOUNTAINS, SUDAN, USING LANDSAT IMAGES

A. A. ANDRAWIS (South Dakota State University, Brookings) Photo Interpretation (ISSN 0031-8523), vol. 22, Nov.-Dec. 1983, 7 p. In English, French, and Spanish.

Digitally enhanced Landsat black/white imagery was used to generate a 1:250,000 scale map of the Nuba Mountains in the Sudan for the purposes of geological classifications. Analyses of the image resulted in mapping schists and gneisses, narva series, intrusive granites and syenites, ring intrusions, shallow surfaces and pediments, and sandy and clay-rich plains and valley alluvium. The classifications obtained will replace the existing geological maps of the area which has shown evidence of commercially exploitable oil reserves. M.S.K.

A85-42582

A SURVEY OF THE REHAMNA HERCYNIAN RANGE IN WESTERN MOROCCO USING LANDSAT COLOR COMPOSITE IMAGERY

J. J. CORNEE, J. MULLER, R. RAIS ASSA, and B. SIMON (Aix-Marseille III, Universite, Marseille, France) Photo Interpretation (ISSN 0031-8523), vol. 22, Nov.-Dec. 1983, 6 p. In English, French, and Spanish.

Landsat MSS bands 4, 5 and 7 were employed to generate 1:500,000 scale images of the Moroccan Hercynian Range in May 1979. The three bands chosen were known to provide the highest possible contrast for the identification of geological formations. Three features were most apparent: a folded Paleozoic formation, an unconformable Meso-Cenozoic formation lying over the Paleozoic formation, and agricultural plots on quarternary deposits

Granites were not easily defined by the images, which best served for identifying folded and lineament structures. M.S.K.

A85-42583

ERUPTION OF MOUNT ONTAKA IN 1979 - DETECTION OF VOLCANIC ASH FALL AREA FROM LANDSAT MSS CCT DATA

S. KISHI and S. YAZAKI (National Research Center for Disaster Prevention, Ibaraki, Japan) Photo Interpretation (ISSN 0031-8523), vol. 22, Nov.-Dec. 1983, 4 p. In English, French, and Spanish.

A85-45688

PRELIMINARY EVALUATION OF THE LANDSAT-4 THEMATIC MAPPER DATA FOR MINERAL EXPLORATION

M. H. PODWYSOCKI, M. S. POWER, and O. D. JONES (U.S. Geological Survey, Reston, VA) (COSPAR, Plenary Meeting, 25th: Workshop II on the Earth's Surface Studied from Space, Graz, Austria, June 25-July 7, 1984) Advances in Space Research (ISSN 0273-1177), vol. 5, no. 5, 1985, p. 13-17, 19, 20 refs

Landsat-4 Thematic Mapper (TM) data recorded over and terrain were analyzed in order to identify various hydrothermally altered, potentially mineralized rocks. Clays, micas, and other minerals bearing the OH anion in specific crystal lattice positions have absorption bands near 2.2 microns, and commonly lack features near 1.6 microns. Channel ratios were combined into a color-ratio-composite (CRC) image in order to distinguish hydrothermally altered rocks, unaltered rocks, and vegetation. Digital masking was used to eliminate ambiguities due to water and shadows, although some ambiguities remained in identifications of altered volcanic deposits containing clays, carbonates, and gypsum. It is shown that the TM data offer greater discrimination in mapping the mineralogical features of and terrain in comparison with Multispectral Scanner (MSS) data. I.H.

A85-45873

EVALUATION OF SPOT SIMULATOR DATA FOR THE DETECTION OF ALTERATION IN GOLDFIELD/CUPRITE, NEVADA

M. X. BORENGASSER and J. V. TARANIK (Nevada, University, Reno) Photogrammetric Engineering and Remote Sensing (ISSN 0099-1112), vol. 51, Aug. 1985, p. 1109-1114.

A85-47898#

SECULAR VARIATION, CRUSTAL CONTRIBUTIONS, AND TECTONIC ACTIVITY IN CALIFORNIA, 1976-1984

M. J. S. JOHNSTON, S. A. SILVERMAN, R. J. MUELLER, and K. S. BRECKENRIDGE (U.S. Geological Survey, Menlo Park, CA) Journal of Geophysical Research (ISSN 0148-0227), vol. 90, Sept. 10, 1985, p. 8707-8717. refs

Five to ten years of data from 34 total field magnetometers were used to define temporal and spatial characteristics of secular variations (SV) of the earth's geomagnetic field throughout central and southern California, and to compare these measurements with predictions from global SV models based on satellite and global observatory data. Least squares analysis of the magnetometer data indicates a generally linear SV decrease in southeasterly direction. However, deviations by as much as 1 nT/a occur for many neighboring locations, indicating that contributions from local induction sources and magnetization effects in the crust can contaminate SV estimates. A method is suggested for identifying and reducing these effects in data used for SV modeling. These techniques are applied to the Californian array data, and the residuals are discussed in terms of possible tectonomagnetic sources along the San Andreas fault. I.S.

04 GEOLOGY AND MINERAL RESOURCES

A85-48387

REFLECTIONS OF POSSIBLE OIL- AND GAS-BEARING STRUCTURES OF THE PRE-JURASSIC COMPLEX IN THE PRESENT-DAY TERRAIN OF WESTERN SIBERIA [OTRAZHENIYA NEFTEGAZOPERSPEKTIVNYKH STRUKTUR DOIURSKOGO KOMPLEKSA V SOVREMENNOI POVERKHNOSTI ZAPADNOI SIBIRI]

N. P. ZAPIVALOV and V. A. BELIAEVA (Proizvodstvennoe Geologicheskoe Ob'edinenie 'Novosibirskgeologiya', USSR) *Akademiya Nauk SSSR, Doklady* (ISSN 0002-3264), vol. 283, no. 4, 1985, p. 952-955. In Russian. refs

The paper is concerned with the relationship between the present-day surface structure and the tectonic elements of deeply settled crust horizons. With reference to satellite data obtained for Western Siberia, it is shown that the present-day surface structure is reflected in the most mobile components of the terrain formed as a result of exogenous geological processes associated with the activation of tectonic motions in the Holocene. It is further shown that by combining geochemical methods with satellite data it is possible to identify oil- and gas-bearing structures by analyzing natural topographic features. V.L.

A85-48873

POLAR MOTION MEASUREMENTS - SUBDECIMETER ACCURACY VERIFIED BY INTERCOMPARISON

D. S. ROBERTSON, W. E. CARTER (NOAA, National Geodetic Survey, Rockville, MD), B. D. TAPLEY, B. E. SCHUTZ, and R. J. EANES (Texas, University, Austin) *Science* (ISSN 0036-8075), vol. 229, Sept. 20, 1985, p. 1259-1261. refs

An important bound on the accuracy of modern techniques for monitoring polar motion is established by intercomparison of measurement series from two different observing techniques, very long baseline interferometry and satellite laser ranging. The root-mean-square differences between the estimates of the pole position from both techniques are shown to be only 2 milliseconds of arc (about 6 centimeters at one earth radius). In the absence of common systematic errors, these differences bound the total errors in both sets of estimates. An initial investigation did not reveal any clear signature in the pole position that seems to be associated with major earthquakes. Continued measurements at this level of accuracy hold promise for resolving long-standing arguments over such questions as the nature of the excitation mechanisms required to maintain the motion of the pole. Author

A85-49227

HIGH-LATITUDE MESOPAUSE NEUTRAL WINDS AND GEOMAGNETIC ACTIVITY - A CROSS-CORRELATION ANALYSIS

R. M. JOHNSON and J. G. LUHMANN (California, University, Los Angeles) *Journal of Geophysical Research* (ISSN 0148-0227), vol. 90, Sept. 1, 1985, p. 8501-8506. refs (Contract NSF ATM-83-12199)

A cross-correlation analysis of horizontal winds at 87 km obtained by the Poker Flat mesosphere-stratosphere-troposphere (MST) radar and College magnetometer horizontal component fluctuations has been performed on three years of summertime data. No consistent, significant peak in the average four-day estimate cross-correlation results is apparent from year to year. Individual estimates similarly do not show evidence of a peak in cross correlation at a variable time lag during geomagnetically active intervals. In addition, the one-day 24 and 12-hour wave amplitudes and phases and average zonal and meridional winds do not vary significantly and consistently with the daily averaged magnetometer horizontal component fluctuations or with the standard deviation thereof. The interval following the July 13, 1982, polar cap absorption event and geomagnetic storm, however, shows a different cross-correlation estimate behavior and is characterized by significantly more westward zonal winds and enhanced 24-hour zonal wind amplitude. Author

N85-30426# Joint Publications Research Service, Arlington, Va. DISCOVERY IN EARTHQUAKE FORECASTING AND SEISMIC ZONING RECORDED Abstract Only

R. AKHMETOV *In its USSR Rept.: Earth Sci. (JPRS-UES-85-007)* p 29 8 Jul. 1985 Transl. into ENGLISH from Bakinskiy Rabochiy (USSR), 26 Apr. 1985 p 2

Avail: NTIS HC A04/MF A01 CSCL 08K

Seismic zoning maps were compiled for a long time, however, they have not fully reflected the geological processes which determine the origins of subterranean tremors. It was established that the size of an earthquake center, is determined by the dimensions of the blocks of the Earth's crust which shift along faults. The discoveries opened the way for compiling seismic zoning maps. The zoning maps indicate zones of centers of origin of future earthquakes, and list their characteristics: the force of possible subterranean tremors, the frequency of their repetition, the size and depth of centers which affect the force of tremors at the Earth's surface. In many regions of Central Asia and India for which such maps were compiled, 23 strong earthquakes occurred during the past 40 years. All earthquakes occurred in places indicated on the maps, and their characteristics are confirmed

E.A.K

N85-30429# Joint Publications Research Service, Arlington, Va. SPACE METHODS FOR GEOLOGICAL RESEARCH Abstract Only

V. A. BUSH and V. N. BRYUKHANOV *In its USSR Rept.: Earth Sci. (JPRS-UES-85-00)* p 32 8 Jul. 1985 Transl. into ENGLISH from Sov. Geol. (Moscow), no. 3, Mar. 1985 p 6-14

Avail: NTIS HC A04/MF A01 CSCL 08G

Methods for use remote data for geological mapping, new geological data obtained by use of aerospace methods, methods for processing space information and new methods and immediate prospects for the development of remote sensing are discussed. The principal directions in the development of remote geological sensing methods are outlined. A systematic approach to use of materials from remote surveys in different stages of the geological prospecting process. Production of new types of geological maps, based on surveys from space, such as space tectonic and space photogeologic maps. Study of the nature of geological formations on the basis of their spectral characteristics, giving broad possibilities for lithological mapping by remote methods. Specialized processing of remote, geological, geophysical and geochemical data, using computers and displays. Study of the nature, geological structure and mineragenetic importance of annular structures. Use of remote survey data in the search for and prediction of mineral deposits. Interpretation of space photographs for solving major problems in regional and global geology and tectonics. Development of international scientific cooperation in application of geological remote sensing methods. These methods will advance research in the fields of geological mapping, tectonic, geodynamic and mineragenetic studies. E.A.K.

N85-30447# Joint Publications Research Service, Arlington, Va. CONDITIONS FOR FORMATION OF PARAGENESSES CONTAINING KYANITE-ORTHOCLASE IN REGION OF MOUNT PROVENDER AND PRATT PEAK (SHACKLETON RANGE, ANTARCTICA) Abstract Only

V. S. SEMENOV *In its USSR Rept.: Earth Sci. (JPRS-UES-85-007)* p 50 8 Jul. 1985 Transl. into ENGLISH from Dokl Akad Nauk SSSR (Moscow), v. 281, no. 5, Apr. 1985 p 1188-1191

Avail: NTIS HC A04/MF A01 CSCL 08G

Metamorphic formations arising under conditions of a kyanite garnet biotite orthoclase subfacies of the almandine amphibolite high pressure facies are rare throughout the world. This article describes the first finds of such metamorphic rocks in Antarctica. The gneisses and crystalline schists containing kyanite and orthoclase are regarded as of interest because they were formed under conditions of extremal pressures and temperatures and with a rather unusual composition of the fluid solutions, characterized by a high content of hydrocarbons relative to the remaining components. Three independent methods were used in ascertaining

the conditions for formation of these rocks exposed in the Shackleton Range. Three types of inclusions (melt, gas fluid and gas) in the minerals of these rocks are discussed. An analysis of the ratio of the rock minerals and their chemical composition made it possible to trace the evolution of crystallization in these parageneses and determine the nature of development of the geothermal regime of metamorphism. Author

N85-30449# Joint Publications Research Service, Arlington, Va
HIGHLY IMPORTANT FEATURES OF REGIONAL TECTONICS OF EARTH'S ARCTIC SECTOR Abstract Only

V. P. GAVRILOV *In its* USSR Rept.: Earth Sci (JPRS-UES-85-007) p 51-52 8 Jul. 1985 Transl. into ENGLISH from Izv. Vyssh. Ucheb. Zaved. Geol. i Razvedka (Moscow), no 1, Jan. 1985 p 3-7
 Avail. NTIS HC A04/MF A01 CSCL 08G

The existence of several circumarctic subconcentric tectonic zones inscribed in one another is a highly important feature of the regional tectonics of the Arctic sector. Three such zones can be discriminated outer (Precambrian), middle (Paleozoic) and inner (Cenozoic). The circum-Pacific Ocean tectonic belt in turn consists of two zones outer (Mesozoic) and inner (Cenozoic). A figure accompanying the text is a map showing these zones and such features as rift valleys, graben rifts and basement blocks. The following are the most important features characteristic of the Arctic segment with respect to the regional tectonic plan: zonal subconcentric positioning of regions of different age; presence of Baykal blocks of different age in the structure of the younger zones; and spatial overlapping of circum-Pacific Ocean zones on the circumarctic tectonic zones. The arctic sector is characterized by extensive development of fault tectonics and therefore a great fracturing of the Earth's crust. The graben-rifts are grouped into system oriented in submeridional and sublatitudinal directions

Author

N85-30455# Army Engineer Waterways Experiment Station, Vicksburg, Miss. Geotechnical Lab.
ENGINEERING GEOLOGY OF SELECTED AREAS, US ARMY ENGINEER DIVISION, LOWER MISSISSIPPI VALLEY. THE AMERICAN BOTTOM AREA, MO-IL. VOLUME 1 Technical Report, 1 Oct. 1980 - 1 Oct. 1981

L. M. SMITH and F. L. SMITH Dec 1984 41 p
 (AD-A154258; WES/TR/GL-84-14-VOL-1) Avail: NTIS HC A03/MF A01 CSCL 08M

The purpose of the report is to characterize the geotechnical parameters of the American Bottom area in the vicinity of East St. Louis, Illinois, and Missouri. The area encompassed is equivalent to 15 min of longitude and latitude, and is covered by portions of the Granite City, Monks Mound, Cahokia, and French Village 7.5-min US Geological Survey quadrangles. Geotechnical parameters of the study area were determined from existing data, including engineering and water well borings, aerial photography, soil, geologic and topographic maps, and published and unpublished reports and field notes. Geotechnical parameters selected for mapping and analysis include physiography, surface geology, subsurface geology, surficial soils, land surface slope, surface drainage, and sources of construction materials. Each parameter, or factor, is portrayed as a transparency for overlay on the map of the surface geology, enabling the simultaneous visual analysis of several geotechnical parameters. Of particular importance to engineering projects are the engineering properties of the various surficial soils, mapped by geologic environments and shown on the surface geology map. Relevant engineering properties of soils which occur in abandoned channels, point bars, chutes and bars, backswamps, alluvial fans, tributary valleys, and loessial uplands are given. The occurrence of ground water in the area and its influence on engineering projects is discussed.

GRA

N85-31588*# Ohio State Univ., Columbus Dept. of Geology and Mineralogy

GEOLOGIC ANALYSIS OF AVERAGED MAGNETIC SATELLITE ANOMALIES Abstract Only

H. K. GOYAL, R. R. B. VONFRESE, J. R. RIDGWAY (Purdue Univ., Lafayette, Ind.), and W. J. HINZE (Purdue Univ., Lafayette, Ind.) *In* Purdue Univ. Improving the Geol Interpretation of Magnetic and Gravity Satellite Anomalies 1 p 1985 ERTS
 Avail: NTIS HC A04/MF A01 CSCL 08B

To investigate relative advantages and limitations for quantitative geologic analysis of magnetic satellite scalar anomalies derived from arithmetic averaging of orbital profiles within equal-angle or equal-area parallelograms, the anomaly averaging process was simulated by orbital profiles computed from spherical-earth crustal magnetic anomaly modeling experiments using Gauss-Legendre quadrature integration. The results indicate that averaging can provide reasonable values at satellite elevations, where contributing error factors within a given parallelogram include the elevation distribution of the data, and orbital noise and geomagnetic field attributes. Various inversion schemes including the use of equivalent point dipoles are also investigated as an alternative to arithmetic averaging. Although inversion can provide improved spherical grid anomaly estimates, these procedures are problematic in practice where computer scaling difficulties frequently arise due to a combination of factors including large source-to-observation distances (400 km), high geographic latitudes, and low geomagnetic field inclinations. Author

N85-31589*# Ohio State Univ., Columbus. Dept. of Geology and Mineralogy

STATISTICAL MAGNETIC ANOMALIES FROM SATELLITE MEASUREMENTS FOR GEOLOGIC ANALYSIS Abstract Only

H. K. GOYAL, R. R. B. VONFRESE, and W. J. HINZE (Purdue Univ., Lafayette, Ind.) *In* Purdue Univ. Improving the Geol Interpretation of Magnetic and Gravity Satellite Anomalies 1 p 1985 ERTS

Avail: NTIS HC A04/MF A01 CSCL 08B

The errors of numerically averaging satellite magnetic anomaly data for geologic analysis are investigated using orbital anomaly simulations of crustal magnetic sources by Gauss-Legendre quadrature integration. These simulations suggest that numerical averaging errors constitute small and relatively minor contributions to the total error-budget of higher orbital estimates (approx. 400 km), whereas for lower orbital estimates the error of averaging may increase substantially. Least-squares collocation is also investigated as an alternative to numerical averaging and found to produce substantially more accurate anomaly estimates as the elevation of prediction is decreased towards the crustal sources.

Author

N85-31591*# Purdue Univ., West Lafayette, Ind. Dept. of Geosciences.

THE SOUTH-CENTRAL UNITED STATES MAGNETIC ANOMALY Abstract Only

P. J. STARICH, W. J. HINZE, and L. W. BRAILE *In its* Improving the Geol. Interpretation of Magnetic and Gravity Satellite Anomalies 1 p 1985 ERTS

Avail: NTIS HC A04/MF A01 CSCL 08N

A positive magnetic anomaly, which dominates the MAGSAT scalar field over the south-central United States, results from the superposition of magnetic effects from several geologic sources and tectonic structures in the crust. The highly magnetic basement rocks of this region show good correlation with increased crustal thickness, above average crustal velocity and predominantly negative free-air gravity anomalies, all of which are useful constraints for modeling the magnetic sources. The positive anomaly is composed of two primary elements. The western-most segment is related to middle Proterozoic granite intrusions, rhyolite flows and interspersed metamorphic basement rocks in the Texas panhandle and eastern New Mexico. The anomaly and the magnetic crust are bounded to the west by the north-south striking Rio Grande Rift. The anomaly extends eastward over the Grenville age basement rocks of central Texas, and is terminated to the

04 GEOLOGY AND MINERAL RESOURCES

south and east by the buried extension of the Ouachita System. The northern segment of the anomaly extends eastward across Oklahoma and Arkansas to the Mississippi Embayment. It corresponds to a general positive magnetic region associated with the Wichita Mountains igneous complex in south-central Oklahoma and 1.2 to 1.5 Ga. felsic terrane to the north. Author

N85-31592*# Purdue Univ., West Lafayette, Ind. Dept. of Geosciences.

THE SOUTH-CENTRAL UNITED STATES MAGNETIC ANOMALY Abstract Only

P. J. STARICH /In its Improving the Geol. Interpretation of Magnetic and Gravity Satellite Anomalies 1 p 1985 ERTS

Avail: NTIS HC A04/MF A01 CSCL 08N

The South-Central United States Magnetic Anomaly is the most prominent positive feature in the MAGSAT scalar magnetic field over North America. The anomaly correlates with increased crustal thickness, above average crustal velocity, negative free-air gravity anomalies and an extensive zone of Middle Proterozoic anorogenic felsic basement rocks. Spherical dipole source inversion of the MAGSAT scalar data and subsequent calculation of reduced-to-pole and derivative maps provide additional constraints for a crustal magnetic model which corresponds geographically to the extensive Middle Proterozoic felsic rocks trending northeasterly across the United States. These felsic rocks contain insufficient magnetization or volume to produce the anomaly, but are rather indicative of a crustal zone which was disturbed during a Middle Proterozoic thermal event which enriched magnetic material deep in the crust. Author

N85-31595*# Purdue Univ., West Lafayette, Ind. Dept. of Geosciences.

REDUCED TO POLE LONG-WAVELENGTH MAGNETIC ANOMALIES OF AFRICA AND EUROPE Final Report

R. OLIVIER (Lausanne Univ., Switzerland), W. J. HINZE, and R. B. VONFRESE (Ohio State Univ., Columbus) /In its Improving the Geol. Interpretation of Magnetic and Gravity Satellite Anomalies 1 p 1985 Previously announced as N84-25132 ERTS

Avail: NTIS HC A04/MF A01 CSCL 08N

To facilitate analysis of the tectonic framework for Africa, Europe and adjacent marine areas, MAGSAT scalar anomaly data are differentially reduced to the pole and compared to regional geologic information and geophysical data including surface free-air gravity anomaly data upward continued to satellite elevation (350 km) on a spherical Earth. Comparative analysis shows magnetic anomalies correspond with both ancient as well as more recent Cenozoic structural features. Anomalies associated with ancient structures are primarily caused by intra-crustal lithologic variations such as the crustal disturbance associated with the Bangui anomaly in west-central Africa. Anomalies correlative with Cenozoic tectonic elements appear to be related to Cune isotherm perturbations. A possible example of the latter is the well-defined trend of magnetic minima that characterize the Alpine orogenic belt from the Atlas mountains to Eurasia. In contrast, a well-defined magnetic satellite minimum extends across the stable craton from Finland to the Ural mountains. Prominent magnetic maxima characterize the Arabian plate, Iceland, the Kursk region of the central Russian uplift, and generally the Precambrian shields of Africa. Author

N85-31596*# Purdue Univ., West Lafayette, Ind. Dept. of Geosciences.

EURO-AFRICAN MAGSAT ANOMALY-TECTONIC OBSERVATIONS Abstract Only

W. J. HINZE, R. OLIVIER (Lausanne Univ., Switzerland), and R. B. VONFRESE (Ohio State Univ., Columbus) /In its Improving the Geol. Interpretation of Magnetic and Gravity Satellite Anomalies 2 p 1985 Previously announced as N84-25129 ERTS

Avail: NTIS HC A04/MF A01 CSCL 08N

Preliminary satellite (MAGSAT) scalar magnetic anomaly data are compiled and differentially reduced to radial polarization by equivalent point source inversion for comparison with tectonic data of Africa, Europe and adjacent marine areas. A number of associations are evident to constrain analyses of the tectonic

features and history of the region. The Precambrian shields of Africa and Europe exhibit varied magnetic signatures. All shields are not magnetic highs and, in fact, the Baltic shield is a marked minimum. The reduced-to-the-pole magnetic map shows a marked tendency for northeasterly striking anomalies in the eastern Atlantic and adjacent Africa, which is coincident to the track of several hot spots for the past 100 million years. However, there is little consistency in the sign of the magnetic anomalies and the track of the hot spots. Comparison of the radially polarized anomalies of Africa and Europe with other reduced-to-the-pole magnetic satellite anomaly maps of the Western Hemisphere support the reconstruction of the continents prior to the origin of the present-day Atlantic Ocean in the Mesozoic Era A.R.H.

N85-31605# Geological Survey, Washington, D C
PETROLEUM AND MINERAL RESOURCES OF ANTARCTICA
J C BEHRENDT, ed. 1983 78 p refs Sponsored in part by NSF

(US-GEOL-SURV-CIRC-909) Avail: NTIS HC A05/MF A01

No known petroleum or mineral resources occur in Antarctica. Economics and political consideration may change the industry's interest in the next few years. A number of countries are actively carrying out multichannel seismic reflection surveys of this region which are obviously focused on petroleum resource studies. The only types of potentially economically exploitable resources in Antarctica would be giant or supergiant fields. Some of the available information on potential petroleum resources are discussed. E.R.

N85-31608# Pacific Northwest Lab., Richland, Wash.
COMPARATIVE STUDY OF FRACTURE PLANES COMPUTED FROM TOPOGRAPHY AND LINEAMENTS FROM IMAGERY WITH STRUCTURES AND MINERALIZATION IN THE MAGNETIC BELT OF WASHINGTON STATE

J. R. ELIASON and V. L. ELIASON Apr. 1985 11 p refs Presented at the 4th Conf. on Remote Sensing for Exploration Geol., San Francisco, 1 Apr 1985

(Contract DE-AC06-76RL-01830)

(DE85-010972; PNL-SA-12666; CONF-850413-1) Avail: NTIS HC A02/MF A01

Digitally computed fracture planes for the Magnesite Belt of Washington State were obtained using a technique developed for structural geologic analysis of topography. These planes and lineaments, interpreted from aerial and satellite data sets, were compared to mapped structures and mineralization in the area. Computed fracture planes were used to develop a structural model for fracturing in the region. These planes clearly indicate that the region is dominated by normal faulting. Lineaments mapped in the area show a dominant north 30 deg east trend which correlates with mineralization in the region and the dominant computed longitudinal fracture plane trends. These predicted longitudinal fracture planes show a strong spatial correlation with the major magnesite mineralization. DOE

N85-31688*# National Aeronautics and Space Administration. Goddard Space Flight Center, Greenbelt, Md.

GEODYNAMICS BRANCH RESEARCH PROGRAM Annual Report, 1984

W. D. KAHN, ed. and S. C. COHEN, ed. Aug. 1985 177 p refs Submitted for publication

(NASA-TM-86223; NAS 1.15:86223; AR-3) Avail: NTIS HC A09/MF A01 CSCL 08E

Current topics in earth geodynamics are discussed. Among the topics presented are: (1) crustal movements and solid earth dynamics; (2) gravity field modeling and sensing techniques; and (3) sea surface topography.

N85-31689*# National Aeronautics and Space Administration. Goddard Space Flight Center, Greenbelt, Md.

CONTEMPORARY PLATE MOTIONS FROM LAGEOS

D. CHRISTODOULIDIS and D. E. SMITH *In its* Geodyn. Branch Res. Program 4 p Aug. 1985 refs

Avail: NTIS HC A09/MF A01 CSCL 08K

The objective of Dynamic Satellite Geodesy is to relate points on the surface of the Earth with the satellite's orbital ephemeris through the observed ranges and times. Laser data taken on Lageos continue to be analyzed in this dynamical mode to yield precise positions of the Earth-based systems in a geocentric reference system. Definition of the laser network has been assessed through simultaneous solutions of station coordinates and Earth orientation parameters on an annual basis. These annual solutions have been intercompared and have yielded preliminary observations of tectonic motions.

N85-31692*# National Aeronautics and Space Administration. Goddard Space Flight Center, Greenbelt, Md.

GEOPHYSICAL INTERPRETATION OF SATELLITE LASER RANGING MEASUREMENTS

S. C. COHEN *In its* Geodyn. Branch Res. Program 5 p Aug. 1985 refs

Avail: NTIS HC A09/MF A01 CSCL 08K

Since 1972 satellite laser ranging (SLR) measurements were made in California at two sites whose 900 km intersite baseline spans the San Andreas Fault. The research reported compares the SLR measurements with ground-based geodetic surveys and information derived from seismological and geological studies. The objective is to determine whether the various data are consistent with one another and to determine the distribution of crustal deformation over the extent of the SLR baseline G.L.C.

N85-31719# Geological Survey, Washington, D.C.

THE U.S. GEOLOGICAL SURVEY IN ALASKA: ACCOMPLISHMENTS DURING 1982

K. M. REED, ed. and S. BARTSCH-WINKLER, ed. 1984 165 p refs

(US-GEOL-SURV-CIRC-939, LC-76-608093) Avail NTIS HC A08/MF A01

The results of 1982 geologic studies on a wide range of subjects of economic and scientific interest are summarized. Included are lists of references cited for each article and a compilation of reports about Alaska written by the U.S. Geological Survey and published by the geological survey and other organizations. Many aspects of the land and water in Alaska were investigated. Basic data are provided and the results and significance of Geological Survey studies are described. The results of some Alaskan studies in 1982 are discussed. The articles are arranged by geographic area, with a section for offshore topics. E.A.K.

N85-32357*# National Aeronautics and Space Administration. Goddard Space Flight Center, Greenbelt, Md.

GLOBAL MEGA-GEOMORPHOLOGY

R. S. HAYDEN, ed. (George Mason Univ., Fairfax, Va.) Jul. 1985 130 p refs Workshop held in Oracle, Ariz., 14-16 Jan. 1985; sponsored by NASA and the International Union of Geological Sciences

(NASA-CP-2312; REPT-85B0472; NAS 1.55:2312) Avail: NTIS HC A07/MF A01 CSCL 08G

The extension of space exploration to the Moon and to other planets has broadened the scope of geomorphology by providing information on landforms which have developed in environments that differ significantly in fundamental factors such as temperature, pressure and gravity from the environments in which Earth's landforms have been shaped. In some cases the landforming processes themselves appear to be significantly different than any found in the terrestrial environment. Some investigators have suggested that features observed on other planets, such as chaos terrain and labyrinths on Mars, can help us understand Earth's early history better because they may have been formed by processes which were important in the early ages of Earth but have long ceased to be active here. Corresponding terrestrial

landforms would have long since been altered or obliterated by subsequent activity.

N85-32358*# Arizona Univ., Tucson. Dept. of Geosciences.

A NEW GLOBAL GEOMORPHOLOGY? Abstract Only

V. R. BAKER *In* NASA. Goddard Space Flight Center Global Mega-Geomorphology p 9 Jul. 1985

Avail: NTIS HC A07/MF A01 CSCL 08G

Geomorphology is entering a new era of discovery and scientific excitement centered on expanding scales of concern in both time and space. The catalysts for this development include technological advances in global remote sensing systems, mathematical modeling, and the dating of geomorphic surfaces and processes. Even more important are new scientific questions centered on comparative planetary geomorphology, the interaction of tectonism with landscapes, the dynamics of late Cenozoic climatic changes, the influence of cataclysmic processes, the recognition of extremely ancient landforms, and the history of the world's hydrologic systems. These questions all involve feedback relationships with allied sciences that have recently yielded profound developments. G.L.C.

N85-32361*# George Mason Univ., Fairfax, Va. Dept. of Public Affairs (Geography).

GEOMORPHOLOGICAL SIMILARITY AND UNIQUENESS

R. S. HAYDEN *In* NASA. Goddard Space Flight Center Global Mega-Geomorphology p 21-22 Jul. 1985

Avail: NTIS HC A07/MF A01 CSCL 08G

Remote sensing technology, particularly the development of satellite imagery, has given geomorphology a valuable tool for the study of large area, regional landscapes. The small scale large area format of LANDSAT and other satellite imagery reduces the amount of detailed information provided for a given region. This can be an advantage for regional study as much of the local information that is filtered out tends to be detail which, while significant in small area studies, could mask regional patterns. G.L.C.

N85-32362*# University of Southern Illinois, Carbondale. Dept. of Geology

REGIONAL LANDFORM THRESHOLDS

D. F. RITTER *In* NASA. Goddard Space Flight Center Global Mega-Geomorphology p 23-26 Jul. 1985

Avail: NTIS HC A07/MF A01 CSCL 08B

Remote sensing technology allows us to recognize manifestations of regional thresholds, especially in the spatial characteristics of process agents. For example, a change in river channel pattern over a short distance reflects a threshold alteration in the physical controls of discharge and/or sediment. It is, therefore, a valuable indication of conditions as they exist. However, we probably will have difficulty determining whether the systemic parameters are now close to threshold conditions at which a different change will occur. This, of course, is a temporal and magnitude problem which is difficult to solve from the spatial characteristics. G.L.C.

N85-32365*# Chevron Oil Field Research Co., La Habra, Calif. **GEOMORPHOLOGY, TECTONICS, AND EXPLORATION Abstract Only**

F. F. SABINS, JR. *In* NASA. Goddard Space Flight Center Global Mega-Geomorphology p 41 Jul. 1985

Avail: NTIS HC A07/MF A01 CSCL 08G

Explorationists interpret satellite images for tectonic features and patterns that may be clues to mineral and energy deposits. The tectonic features of interest range in scale from regional (sedimentary basins, fold belts) to local (faults, fractures) and are generally expressed as geomorphic features in remote sensing images. Explorationists typically employ classic concepts of geomorphology and landform analysis for their interpretations, which leads to the question - Are there new and evolving concepts in geomorphology that may be applicable to tectonic analyses of images? G.L.C.

04 GEOLOGY AND MINERAL RESOURCES

N85-32366*# New Mexico Inst. of Mining and Technology, Socorro.

MEGA-GEOMORPHOLOGY AND NEOTECTONICS

L. H. LATTMAN /in NASA. Goddard Space Flight Center Global Mega-Geomorphology p 42-43 Jul. 1985

Avail: NTIS HC A07/MF A01 CSCL 08G

For several decades, subtle neotectonic effects involving several square kilometers have been studied in detail using remote sensing, primarily various types of stereo-aerial photographs at scales of 1:10,000 to 1:80,000. These subtle effects, especially local uplifts associated with growing structures of differential compaction, have been detected by the effect on drainage patterns, changes in hydraulic geometry of individual channels or groups of channels, tonal halos (soil) and fracture patterns. The studies were extended with the advent of thermal IR imagery particularly in tonal analysis, and SLAR primarily in fracture pattern studies. Lately, quantitative efforts have begun attempting to link measured uplift over known structures with measured changes in hydraulic geometry and alluvial deposition. Thus, efforts are now underway attempting to quantify the relationship between neo- (micro-) tectonic changes and geomorphic parameters of drainage systems. G.L.C.

N85-32367*# Cornell Univ., Ithaca, N.Y. Dept. of Geological Sciences.

ANDREAN EXAMPLES OF MEGA-GEOMORPHOLOGY THEMES

A. L. BLOOM /in NASA. Goddard Space Flight Center Global Mega-Geomorphology p 44-45 Jul. 1985

Avail: NTIS HC A07/MF A01 CSCL 08G

Geomorphic (or physiographic) provinces have been a well known and useful method of regional landform classification for a century. Every earth scientist will recognize a phrase such as Appalachian Plateau or Southern Rocky Mountains as defining a discrete region of consistent geologic structure that has experienced a similar interval of erosion by a similar process or set of processes. The geomorphic provinces formalized in the United States by Fenneman in the 1920's continue to be highly satisfactory even though some boundaries were only vaguely drawn. Mosaics of LANDSAT images illustrate better than any earlier maps the validity and coherence of Fenneman's provinces. The concept of geomorphic provinces has been used subconsciously or intuitively, to describe the relief of the ocean floor and the topography of the Moon and other planets. G.L.C.

N85-32368*# Purdue Univ., West Lafayette, Ind. Dept. of Geosciences.

SPACE IMAGERY AND SOME GEOMORPHOLOGICAL PROBLEMS OF THE GUIANA SHIELD, SOUTH AMERICA

W. N. MELHORN /in NASA. Goddard Space Flight Center Global Mega-Geomorphology p 46-53 Jul. 1985 refs

Avail: NTIS HC A07/MF A01 CSCL 08B

Some ongoing involvement in regional geomorphologic research in South America is described. Because of association with LARS at Purdue University, there has been engagement, vicarious or advisory, in projects which led to LANDSAT 1-2 mapping of the natural resources of Bolivia (1:8,000,000 scale), and preparation of a geographic information system which mapped the general hydrology, geology, soils, and vegetation of Ecuador (1:4,000,000 scale). Currently we are involved more specifically in geological-geomorphological mapping of the Venezuelan portion of the Guiana shield, and because of manuscript limitations only questions pertinent to this region are posed in the ensuing discussion. G.L.C.

N85-32371*# Geological Survey, Flagstaff, Ariz.

USE OF THE SYNOPTIC VIEW: EXAMPLES FROM EARTH AND OTHER PLANETS

B. K. LUCCHITTA /in NASA. Goddard Space Flight Center Global Mega-Geomorphology p 59-61 Jul. 1985 refs

Avail: NTIS HC A07/MF A01 CSCL 08B

Space technology has added the synoptic view to other techniques used in geomorphology. Synoptic views are provided

by spacecraft images or by application of space technology to time-honored information systems. Examples of spacecraft images of Earth are LANDSAT, SEASAT, and the SIR (Shuttle Imaging Radar) series. Examples of applied space technologies include the digital conversion of topographic maps to shaded relief maps and digital correlation methods. From the study of other planets we have learned that synoptic views enable the deciphering of a planet's history: large features are identified and mapped before small ones; studies proceed from the general to the specific. On Earth, we generally recognize smaller features and study specific processes first, then extrapolate toward larger features and a general synthesis. With the advent of space images of Earth, perhaps the time is ripe to employ the methods used for other planets to the study of terrestrial geology and geomorphology. The following examples illustrate the use of regional-scale studies on Earth: the application of synoptic-view images in Antarctica, the use of digital methods and correlations of multiple data sets in regional studies, and some benefits to our understanding of terrestrial geology that have been obtained from analyses of other planets. G.L.C.

N85-32372*# Geological Survey, Reston, Va.

GEOMORPHIC CLASSIFICATION OF ICELANDIC AND MARTIAN VOLCANOES: LIMITATIONS OF COMPARATIVE PLANETOLOGY RESEARCH FROM LANDSAT AND VIKING ORBITER IMAGES

R. S. WILLIAMS, JR. /in NASA. Goddard Space Flight Center Global Mega-Geomorphology p 62-63 Jul. 1985

Avail: NTIS HC A07/MF A01 CSCL 08K

Some limitations in using orbital images of planetary surfaces for comparative landform analyses are discussed. The principal orbital images used were LANDSAT MSS images of Earth and nominal Viking Orbiter images of Mars. Both are roughly comparable in having a pixel size which corresponds to about 100 m on the planetary surface. A volcanic landform on either planet must have a horizontal dimension of at least 200 m to be discernible on orbital images. A twofold bias is directly introduced into any comparative analysis of volcanic landforms on Mars versus those in Iceland because of this scale limitation. First, the 200-m cutoff of landforms may delete more types of volcanic landforms on Earth than on Mars or vice versa. Second, volcanic landforms in Iceland, too small to be resolved on orbital images, may be represented by larger counterparts on Mars or vice versa. R.J.F.

N85-32374*# State Univ. of New York, Binghamton Dept. of Geological Sciences

GEOMORPHIC ANALYSES FROM SPACE IMAGERY

M. MORISAWA /in NASA. Goddard Space Flight Center Global Mega-Geomorphology p 68-75 Jul. 1985 refs

Avail: NTIS HC A07/MF A01 CSCL 08B

One of the most obvious applications of space imagery to geomorphological analyses is in the study of drainage patterns and channel networks. LANDSAT, high altitude photography and other types of remote sensing imagery are excellent for depicting stream networks on a regional scale because of their broad coverage in a single image. They offer a valuable tool for comparing and analyzing drainage patterns and channel networks all over the world. Three aspects considered in this geomorphological study are: (1) the origin, evolution and rates of development of drainage systems; (2) the topological studies of network and channel arrangements; and (3) the adjustment of streams to tectonic events and geologic structure (i.e., the mode and rate of adjustment). R.J.F.

N85-32377*# Jet Propulsion Lab., California Inst. of Tech., Pasadena.

USE OF SPACEBORNE IMAGING RADAR IN REGIONAL GEOMORPHIC STUDIES

J. P. FORD /in NASA. Goddard Space Flight Center Global Mega-Geomorphology p 81-83 Jul. 1985 refs

Avail: NTIS HC A07/MF A01 CSCL 171

In the past two decades, the use of both photographic and non-photographic remote sensing from satellite platforms has

provided a unique capability for the observation and study of Earth and planetary surfaces. A wide range of imaging sensors that operate in different portions of the electromagnetic spectrum have yielded images of large areas that formerly were unknown or that had not previously been observed at a simultaneous instant in time. In addition, remote sensors equipped with multispectral or multiband capabilities are capable of taking data at different wavelengths simultaneously. Notable examples include the LANDSAT series of multispectral scanners, thematic mappers, and return beam vidicons. Synthetic aperture radar and LANDSAT imagery are discussed R.J.F.

N85-32378*# London Univ. (England). Faculty of Science (Geography).

TECHNIQUES, PROBLEMS AND USES OF MEGA-GEOMORPHOLOGICAL MAPPING

C. EMBLETON *In* NASA Goddard Space Flight Center Global Mega-Geomorphology p 84-88 Jul. 1985 refs
Avail: NTIS HC A07/MF A01 CSCL 08B

A plea for a program of global geomorphological mapping based on remote sensing data is presented. It is argued that the program is a necessary step in bringing together the rapidly evolving concepts of plate tectonics with the science of geomorphology. Geomorphologists are urged to bring temporal scales into their subject and to abandon their recent isolation from tectonics and geological history. It is suggested that a start be made with a new geomorphological map of Europe, utilizing the latest space technology. R.J.F.

N85-32380*# Geological Survey, Reston, Va.
QUANTITATIVE ANALYSIS OF GEOMORPHIC PROCESSES USING SATELLITE IMAGE DATA AT DIFFERENT SCALES

R. S. WILLIAMS, JR. *In* NASA Goddard Space Flight Center Global Mega-Geomorphology p 91-93 Jul 1985
Avail: NTIS HC A07/MF A01 CSCL 08B

When aerial and satellite photographs and images are used in the quantitative analysis of geomorphic processes, either through direct observation of active processes or by analysis of landforms resulting from inferred active or dormant processes, a number of limitations in the use of such data must be considered. Active geomorphic processes work at different scales and rates. Therefore, the capability of imaging an active or dormant process depends primarily on the scale of the process and the spatial-resolution characteristic of the imaging system. Scale is an important factor in recording continuous and discontinuous active geomorphic processes, because what is not recorded will not be considered or even suspected in the analysis of orbital images. If the geomorphic process of landform change caused by the process is less than 200 m in x to y dimension, then it will not be recorded. Although the scale factor is critical, in the recording of discontinuous active geomorphic processes, the repeat interval of orbital-image acquisition of a planetary surface also is a consideration in order to capture a recurring short-lived geomorphic process or to record changes caused by either a continuous or a discontinuous geomorphic process R.J.F.

N85-32381*# Geological Survey, Reston, Va.
QUANTITATIVE GEOMORPHOLOGIC STUDIES FROM SPACEBORNE PLATFORMS

R. S. WILLIAMS, JR. *In* NASA Goddard Space Flight Center Global Mega-Geomorphology p 94-97 Jul. 1985
Avail: NTIS HC A07/MF A01 CSCL 08B

Although LANDSAT images of our planet represent a quantum improvement in the availability of a global image-data set for independent or comparative regional geomorphic studies of landforms, such images have several limitations which restrict their suitability for quantitative geomorphic investigations. The three most serious deficiencies are: (1) photogrammetric inaccuracies, (2) two-dimensional nature of the data, and (3) spatial resolution. These deficiencies are discussed, as well as the use of stereoscopic images and laser altimeter data R.J.F.

N85-32382*# National Aeronautics and Space Administration. Goddard Space Flight Center, Greenbelt, Md.

GLOBAL GEOMORPHOLOGY: REPORT OF WORKING GROUP NUMBER 1

I. DOUGLAS (Manchester Univ., England) *In* its Global Mega-Geomorphology p 101-104 Jul. 1985
Avail: NTIS HC A07/MF A01 CSCL 08G

Remote sensing was considered invaluable for seeing landforms in their regional context and in relationship to each other. Sequential images, such as those available from LANDSAT orbits provide a means of detecting landform change and the operation of large scale processes, such as major floods in semiarid regions. The use of remote sensing falls into two broad stages (1) the characterization or accurate description of the features of the Earth's surface; and (2) the study of landform evolution. Recommendations for future research are made R.J.F.

N85-32383*# National Aeronautics and Space Administration. Goddard Space Flight Center, Greenbelt, Md.

LANDSCAPE INHERITANCE: REPORT OF WORKING GROUP NUMBER 2

C. R. TWIDALE (Adelaide Univ., Australia) *In* its Global Mega-Geomorphology p 105 Jul. 1985
Avail: NTIS HC A07/MF A01 CSCL 08B

The conventional wisdom is, or until recently has been, that the earth's scenery is essentially youthful, much of it being of pleistocene age. The validity of this assertion was questioned, surfaces and forms of much greater antiquity being cited from several cratonic regions, and also from the older orogens. Exhumed forms, some of them of great age (one inselberg landscape of Archaean age was noted), are more common and extensive than has previously been supposed. Epigene forms of Mesozoic age are increasingly being demonstrated from the world's cratons and orogens. Etch features also are more widely developed than has been realized. It was recommended that studies of denudation chronology be undertaken, possible in relation to contrasted cratonic regions. The nature and age range of surfaces that make up the shields ought to be analysed, the processes responsible for shaping the surfaces, and, in the case of the ancient epigene forms, the reasons for their survival. R.J.F.

N85-32384*# National Aeronautics and Space Administration. Goddard Space Flight Center, Greenbelt, Md.

PROCESS THRESHOLDS: REPORT OF WORKING GROUP NUMBER 3

R. S. WILLIAMS, JR. (Geological Survey, Reston, Va.) *In* its Global Mega-Geomorphology p 106-108 Jul. 1985
Avail: NTIS HC A07/MF A01 CSCL 08B

The Process Thresholds Working Group concerned itself with whether a geomorphic process to be monitored on satellite imagery must be global, regional, or local in its effect on the landscape. It was pointed out that major changes in types and magnitudes of processes operating in an area are needed to be detectable on a global scale. It was concluded from a review of geomorphic studies which used satellite images that they do record change in landscape over time (on a time-lapse basis) as a result of one or more processes. In fact, this may be one of the most important attributes of space imagery, in that one can document land form changes in the form of a permanent historical record. The group also discussed the important subject of the acquisition of basic data sets by different satellite imaging systems. Geomorphologists already have available one near-global basis data set resulting from the early LANDSAT program, especially images acquired by LANDSATs 1 and 2. Such historic basic data sets can serve as a benchmark for comparison with landscape changes that take place in the future. They can also serve as a benchmark for comparison with landscape changes that have occurred in the past (as recorded) by images, photography and maps. R J F

04 GEOLOGY AND MINERAL RESOURCES

N85-32385*# National Aeronautics and Space Administration. Goddard Space Flight Center, Greenbelt, Md
PLANETARY PERSPECTIVE. REPORT OF WORKING GROUP NUMBER 4

L. A. ROSSBACHER (California State Polytechnic Univ., Pomona)
In its Global Mega-Geomorphology p 109-110 Jul. 1985
Avail: NTIS HC A07/MF A01 CSDL 03B

The study of global megageomorphology from a planetary perspective requires that, philosophically, we view the Earth as a planet like any other; one among a number of bodies of varied size and composition which, together with the Sun, form the Solar System. A first step in the study of the Earth from the planetary perspective is the development of global distribution maps of surface factors as landforms, tectonics, and of key processes operating on Earth. Data of other types, such as gravity and magnetism, should also be included and, so far as possible, multiple data sets should be developed. The compilation of maps would serve as a catalyst for research and a basis for interpretation. They could be used scientifically to document changes such as glacial variations and their relationships to climate, volcanic eruptions and their effects, and coastal alterations. Slow and rapid changes should be studied together with the relationships between scale and the rapidity of change. A study of the relationship of geomorphology (i.e., surficial processes) to lithology and structure is needed. The planetary perspective can also help in the identification and investigation of exotic features such as suspect terrains.
R.J.F.

N85-33147# Joint Publications Research Service, Arlington, Va.
SPACECRAFT-AIDED RESEARCH DISCUSSED AT GEOLOGY CONGRESS Abstract Only

N. KONSTANTINOV and Y. SHCHEVYAKOV *In its* USSR Rept.: Space (JPRS-USP-84-006) p 118 14 Nov. 1984 Transl into ENGLISH from *Turkmenskaya Iskra* (Ashkhabad, USSR), 10 Aug. 1984 p 3
Avail: NTIS HC A08

A presentation of the Space Geological Map of the USSR turned out to be one of the highlights of the 27th International Geological Congress. A discussion of problems of satellite aided geology and comparative planetology was included in the program. B. N. Mozhayev, general director of the Aerogeologiya association, discussed achievements in this field. He said that structures whose existence could only be suspected by geologists in the past become visible on the Earth's surface from the altitude of an orbital flight. This pertains primarily to ring shaped structures hundreds of kilometers in diameter, and to linear transcontinental faults of the Earth's crust which are thousands of kilometers long. More than 4,000 structures have been detected from space on the territory of the USSR and entered on maps. Soviet orbiting stations, Soyuz spaceships and satellites of the Meteor and Kosmos series are equipped with photographic and scanning instruments. MKF-6 cameras, for example, are capable not only of distinguishing details only 15 kilometers in size in a locality; they also can determine the chemical composition of rocks on the basis of remote spectrograms.
Author

N85-33151# Joint Publications Research Service, Arlington, Va.
LANDSCAPE INTERPRETATION CAPABILITIES USING SPACE PHOTOGRAPHS OF REGIONS OF A MULTISTAGE PLATFORM MANTLE STRUCTURE Abstract Only

O. S. OBRYADCHIKOV and S. Y. PETROV *In its* USSR Rept.: Space (JPRS-USP-84-006) p 121-122 14 Nov. 1984 Transl. into ENGLISH from *Issled Zemli iz Kosmosa* (Moscow), no. 2, Mar. - Apr. 1984 p 35-43
Avail: NTIS HC A08

Space photographs of such regions as the sub-Urals plateau (a semi arid plain practically devoid of vegetation) exhibit a uniform, washed out shading with little contrast. This paper analyzes the information content of such local regional space photos for the eastern part of the Caspian basin, an area with a complex structure of the lower strata of the platform mantle (down to the lower Permian inclusively) and extensively developed salt dome tectonic systems. Using the deviation of the plan view position of the

lineaments from the projection onto the ground surface of the fracture faults corresponding to the lineaments revealed by deep seismic prospecting, one can determine the inclination angles of the planes of their displacements. For the Emba and Temir river faults, these angles average 45 deg and 55 deg, respectively. While local space photos can be of practical importance in terrain interpretation when studying the deep structure and developmental history of the most complexly structured ancient platforms with a multistage mantle, careful combined analysis of space and geophysical data is still required. When geophysical data are inadequate, unambiguous interpretation of space photographs is impossible, but they will be of definite value in assisting with the planning of further ground studies.
Author

N85-33153# Joint Publications Research Service, Arlington, Va.
USE OF SPACE PHOTOGRAPHS FOR ANALYSIS OF STRUCTURAL AND DYNAMIC CONDITIONS OF FORMATION OF ANCIENT PHLOGOPITE AND APATITE DEPOSITS Abstract Only

K. G. ZINATOV and R. F. VAFIN *In its* USSR Rept.: Space (JPRS-USP-84-006) p 123 14 Nov. 1984 Transl. into ENGLISH from *Issled. Zemli iz Kosmosa* (Moscow), no. 2, Mar. - Apr. 1984 p 48-54 Original language document previously announced in IAA as A84-34781
Avail: NTIS HC A08

From a tectonophysical analysis of satellite photos, the mechanism by which systems of diagonal fractures were formed in the central part of the Aldan shield is established. Reasons are also suggested to explain why the pattern has been preserved and why Precambrian fractures survived into the Phanerozoic. Attention is given to the role played by stress fields in forming structures which in the Precambrian were able to accumulate phlogopite and apatite and in the Phanerozoic ensured that these deposits were preserved. The method is shown to be applicable in regional analyses for other minerals.
C.R.

N85-33154# Joint Publications Research Service, Arlington, Va.
USING REMOTE PHOTOGRAPHS IN PROSPECTING FOR HYDROCARBONS ON THE KERCH PENINSULA Abstract Only

V. I. KHNYKIN and N. V. KOLODIY *In its* USSR Rept.: Space (JPRS-USP-84-006) p 124 14 Nov. 1984 Transl. into ENGLISH from *Issled Zemli iz Kosmosa* (Moscow), no. 2, Mar. - Apr. 1984 p 55-59 Original language document previously announced in IAA as A84-34782
Avail: NTIS HC A08

Satellite TV images, photographs from manned spacecraft and aerial photographs were interpreted to ascertain the configuration of lineaments in the Indolo-Kuban trough on the Kerch Peninsula. The lineaments are grouped into two systems: the first, which is the most extensive and pronounced in photographs with the greatest generalization, contains lineaments running parallel to the large tectonic structures and emphasizes individual structural elements in some cases; the second group is a system of lineaments running primarily transverse to the strike of the local folds, and can usually be traced intermittently over long distances. The latter can serve as tectonic shields for pools of hydrocarbons. Prospecting for such pools in the Nizimemaykopsky deposits is underway on the Kerch Peninsula at the present time. It has been shown that there are no reservoirs in the crests of the structures in the southwest plain. Considering the presence of transverse fractures here, local folds in this area can be treated as consisting of individual blocks of pools. The prospecting is to be started in these blocks from the periclinal portions of the folds, considering them to be independent prospecting targets from the central portions of the structures
Author

N85-34468# Geological Survey, Washington, D.C.
THE UNITED STATES GEOLOGICAL SURVEY IN ALASKA: ACCOMPLISHMENTS DURING 1983

S. BARTSCH-WINKLER, ed. and K. M. REED, ed. 1985 118 p refs

(USGS-CIRC-945) Avail NTIS HC A06/MF A01

Geologic studies carried out in Alaska during 1983 are reported. Various geological aspects of the onshore and offshore areas of Alaska are investigated. Topics cover a wide range in scientific and economic interest. E.A.K.

N85-35437# Geological Survey, Alexandria, Va.
AEROMAGNETIC AND RADIOMETRIC SIGNATURES OF A POSSIBLE PORPHYRY SYSTEM IN THE WESTERN TUSHAR MOUNTAINS, UTAH Abstract Only

D. L. CAMPBELL, J. A. PITKIN, J. S. DUVAL, T. A. STEVEN, C. G. CUNNINGHAM, and C. W. NAESER *In its* USGS Res. on Mineral Resources, 1985 p 3-4 1985

Avail: NTIS HC A05/MF A01

Geologic mapping, petrologic analysis, isotopic dating, geochemical sampling, and geophysical studies have identified several areas in the western Tushar Mountains, Utah, that may be underlain by mineralized intrusive systems containing molybdenum, uranium, and other valuable metals. One of these areas is near Indian Creek, 18 km north of Beaver, Utah, where there may be a multiple intruded mineralized stock. Several lines of evidence were pulled together to make this interpretation, providing a good example of synergism in geological research. The geophysical component of these studies is focused upon.

R.J.F.

N85-35442# Geological Survey, Alexandria, Va.
AEROMAGNETIC AND GRAVITY MODELS OF THE PLUTON BELOW THE LAKE CITY CALDERA, COLORADO Abstract Only

V. J. S. GRAUCH *In its* USGS Res. on Mineral Resources, 1985 p 15-16 1985

Avail: NTIS HC A05/MF A01

Aeromagnetic and gravity data collected over the Lake City caldera, San Juan Mountains, Colorado, were used to calculate models of the pluton below the caldera. Magnetic data are from a draped airborne survey and are in digital form. Gravity data were assembled from the Department of Defense files and were combined with more recent data collected across the caldera. Both data sets were gridded and contoured in map form and also examined in profile form. Regional trends were removed where necessary and data were continued upward mathematically, to enhance the effect of the subsurface pluton over the effects of shallow sources. Geologic mapping revealed isolated outcrops of quartz syenite inside the caldera. It was inferred that these rocks were intruded at the time of resurgence of the caldera. R.J.F.

N85-35445# Geological Survey, Alexandria, Va.
NEW SILVER RESOURCE MAP OF THE UNITED STATES: POTENTIAL FOR INCREASED DOMESTIC SILVER PRODUCTION Abstract Only

A. V. HEYL and R. B. HALL *In its* USGS Res. on Mineral Resources, 1985 p 24-25 1985

Avail: NTIS HC A05/MF A01

A new silver resource map of the United States was compiled in 1984 to replace the out of print U.S. Geological Survey Map MR-34 published in 1962. Estimated past production (in troy ounces) plus estimated resources of each district are indicated on the new map by the size of the dot representing the district. The text includes brief summaries of mining history, geologic setting and character of the ores for each district, an improvement over the one line descriptions of districts that accompanied the 1962 map. Many locations have been added, especially in the Eastern United States. R.J.F.

N85-35451# Geological Survey, Alexandria, Va.
APPLICATIONS OF THE MINERAL RESOURCES DATA SYSTEM AND THE INTERNATIONAL STRATEGIC MINERALS INVENTORY IN MINERAL-RESOURCE ASSESSMENTS BY REGION AND COMMODITY Abstract Only

A. L. MEDLIN, D. M. SUTPHIN, and J. H. DEYOUNG, JR. *In its* USGS Res. on Mineral Resources, 1985 p 32-33 1985

Avail: NTIS HC A05/MF A01

From 1972 to 1982, the USGS developed the Computerized Resources Information Bank (CRIB). CRIB, a centralized data base, was initiated to meet the growing need for rapid access to data on mineral deposits and occurrences. Regional and commodity information was collected from geologists and commodity specialists at the USGS, other Federal agencies, and State geological agencies. In 1982, CRIB was used as the basis for establishing the Mineral Resources Data System (MRDS), which applies computerized data to mineral resource assessments. MRDS includes the capability of storing data on mineral deposits and occurrences for use in deposit type studies. Another of the goals of the MRDS is to have data coverage by area and commodity for the major domestic and foreign deposits. Author

N85-35452# Geological Survey, Alexandria, Va.
A COMPARISON OF LANDSAT THEMATIC MAPPER, MULTISPECTRAL SCANNER AND AIRBORNE SENSORS FOR MAPPING THE DISTRIBUTION OF ALTERATION MINERALS: EXAMPLES FROM THE SOUTHWESTERN UNITED STATES Abstract Only

M. H. PODWYSOCKI, M. S. POWER, O. D. JONES, M. H. KOSLOW, and W. E. COLLINS *In its* USGS Res. on Mineral Resources, 1985 p 43 1985

Avail: NTIS HC A05/MF A01

Spaceborne geologic remote sensing capabilities have progressed over the years from the relatively simple four channel LANDSAT Multispectral Scanner (MSS), which operates in the visible and near infrared region and is capable of few mineralogic distinctions, to the present seven channel LANDSAT Thematic Mapper (TM), which has additional channels in the near and mid infrared regions, allowing further mineralogic distinctions. Airborne spectroradiometers, precursors to future spaceborne systems, contain 64 or more narrow channels that can be used to identify individual species in some mineral groups. Data from these instruments are compared to determine their effectiveness for mapping hydrothermally altered rocks in Nevada and Utah.

Author

N85-35453# Geological Survey, Alexandria, Va.
SOME RECENT DEPOSIT MODELING EFFORTS Abstract Only

D. A. SINGER and D. P. COX *In its* USGS Res. on Mineral Resources, 1985 p 52 1985

Avail: NTIS HC A05/MF A01

A compilation of 62 descriptive and 37 gradetonnage models, which was published in 1983, provides a starting point for a larger deposit modeling effort useful for resource assessment and exploration. The classification of deposits is empirical rather than genetic and is based on a study of well known deposits. Use of data from many deposits increases the robustness of the models, and emphasis on lithologic-tectonic associations allows the use of geology to indicate which resources are possible in a region. The deposit models make possible effective project design for assessments and exploration and provide a basis for quantitative assessments. Author

N85-35455# Geological Survey, Alexandria, Va.
PROCESSING OF LANDSAT IMAGERY TO MAP SURFACE MINERAL ALTERATION ON THE ALASKA PENINSULA, ALASKA Abstract Only

F. H. WILSON and J. E. YORK *In its* USGS Res. on Mineral Resources, 1985 p 56-57 1985

Avail: NTIS HC A05/MF A01

LANDSAT images are digitally processed to facilitate assessment of the mineral resources of the Port Moller, Stepovak Bay, and Simeonof Island (Alaska) areas. Field mapping and

04 GEOLOGY AND MINERAL RESOURCES

assessment of these quadrangles were begun in 1983 as part of the Alaska Mineral Resource Assessment Program (AMRAP). It was realized that time and budget constraints would limit mapping coverage. Therefore existing LANDSAT multispectral scanner imagery was used to aid in locating surface alteration, which could be field checked or related to stream sediment or hand sample geochemical data. Author

N85-35456# Geological Survey, Alexandria, Va.
MINERAL RESOURCES PROGRAMS Abstract Only
In its USGS Res. on Mineral Resources, 1985 p 58 1985
Avail. NTIS HC A05/MF A01

A series of extended abstracts is presented that briefly explain the various Mineral Resource Programs of the U.S. Geological Survey (U.S.G.S.) The programs have the following goals: to assess the mineral resource potential of specific areas in the United States (particularly Federal lands) for resource management and Congressional action, to provide timely assessments of the Nation's mineral resources, to identify new areas for exploration and develop new concepts of ore formation and distribution to increase our known mineral resources, particularly the strategic and critical minerals; to improve current methodology and develop new techniques for identifying and evaluating mineral resources and analyzing resource data more efficiently and more precisely. Author

N85-35457# Geological Survey, Alexandria, Va.
THE DEVELOPMENT OF ASSESSMENT TECHNIQUES PROGRAM Abstract Only
C G CUNNINGHAM *In its* USGS Res. on Mineral Resources, 1985 p 60 1985
Avail. NTIS HC A05/MF A01

The Development of Assessment Techniques (DAT) Program is a program of basic and applied research on the origin and the geological geochemical, and geophysical expression of mineral deposit systems. The objectives are to develop concepts and techniques to improve the capability of identifying and evaluating mineral resources. To achieve these objectives, the program supports multidisciplinary field and laboratory studies directed toward understanding the processes by which mineral deposits form and developing new technology and models to assess the mineral resource potential in areas of concealed deposits. The studies are organized under the following major categories: ore deposit models, geophysical exploration techniques; district and deposit studies; and laboratory studies. Author

N85-35458# Geological Survey, Alexandria, Va.
THE CONTERMINOUS UNITED STATES MINERAL ASSESSMENT PROGRAM Abstract Only
G C. CURTIN *In its* USGS Res. on Mineral Resources, 1985 p 61-63 1985
Avail. NTIS HC A05/MF A01

Regional assessments of the mineral and energy potential of the conterminous United States are being made under the Conterminous United States Mineral Assessment Program (CUSMAP). This program is providing up to date, systematic assessments of areas that have identified resources or are thought to have potential for mineral occurrences, especially strategic and critical minerals. Areas are assessed for their mineral and energy potential by integrating existing information, reevaluating known mineral occurrences and acquiring new data through coordinated geologic, geochemical, geophysical, and related studies. The results are published in format tailored to meet the needs of existing and potential users such as industry, the public, Congress, other Federal agencies, and State and local governments. Author

N85-35460# Geological Survey, Alexandria, Va.
THE ALASKA MINERAL RESOURCES ASSESSMENT PROGRAM Abstract Only
G. R. WINKLER *In its* USGS Res. on Mineral Resources, 1985 p 66-68 1985
Avail: NTIS HC A05/MF A01

AMRAP (Alaska Mineral Resources Assessment Program), the prototype U.S. Geological Survey regional resource assessment program, enters its second decade with the continuing goal to provide comprehensive information on the mineral and energy resource endowment of Alaska to the public, the private sector the academic community and those who are concerned with national mineral policy. The program is designed: (1) to provide information to land management agencies for decisions regarding the classification and allocation of Alaska's Federal lands; (2) to produce systematic, state of the art geoscience information to the mineral and energy industries, Alaska natives, and other public and private interests; and (3) to expand the general knowledge of Alaska's complex geological setting, much of which is known presently only in reconnaissance. Author

N85-35470# Dennett, Muessing, Ryan and Associates Ltd., Iowa City, Iowa.
EVALUATION: CLOSE-RANGE PHOTOGRAMMETRY FOR SLOPE INVENTORY AND MONITORING Final Report
H. MUESSIG Sep. 1984 43 p refs Sponsored by Pennsylvania Dept. of Transportation
(PB85-192755; FHWA/PA-84-012) Avail: NTIS HC A03/MF A01 CSCL 13B

The use of close-range photogrammetry as a rock slope inventory procedure for the inspection, identification, and classification of slope stability was studied. A geotechnical description and evaluation form is supplemented by photogrammetric measurements and a contour map and profiles of the slope are illustrated which were prepared from a single stereopair using an analytical stereoplotter. Slope stability monitoring, using close-range photogrammetry, is discussed and compared with other measurement procedures and several metric camera systems and analytical stereoplotters are compared. Implementation of a close-range photogrammetric inventory and monitoring program is recommended. GRA

05

OCEANOGRAPHY AND MARINE RESOURCES

Includes sea-surface temperature, ocean bottom surveying imagery, drift rates, sea ice and icebergs, sea state, fish location.

A85-40237
THE IMPACT OF HIGHER-ORDER BRAGG TERMS ON RADAR SEA RETURN
B FISCELLA, P. P. LOMBARDINI, and P. TRIVERO (Torino, Università, CNR, Istituto di Cosmogeofisica, Turin, Italy) *Nuovo Cimento C, Serie 1* (ISSN 0390-5551), vol. 8, Mar.-Apr. 1985, p 118-124. refs

The possibility that radar sea return observed using a Ku band fan beam Doppler airborne scatterometer flown over crude oil artificial spills might have been back-scattered via the second-order Bragg interaction is surmised. An attempt is made to justify the absence of the first-order Bragg term. Author

A85-40644

INVESTIGATION OF ICE COVER FROM PLATFORMS IN THE AIR AND IN SPACE USING RADAR EQUIPMENT [ISLEDOVANIE LEDOVYKH POKROVOV RADIOFIZICHESKIMI SREDSTVAMI S AEROKOSMICHESKIKH NOSITELI]

V. B. EFIMOV, A. I. KALMYKOV, V. A. KOMIAK, A. S. KUREKIN, A. S. LEVDA (AN USSR, Institut Radiofiziki i Elektroniki, Kharkov, Ukrainian SSR) et al. *Akademiia Nauk SSSR, Izvestia, Fizika Atmosfery i Okeana* (ISSN 0002-3515), vol. 21, May 1985, p. 512-519. In Russian. refs

The possibility of using space platforms to study sea-ice cover is discussed. Data obtained using both side-looking radar and microwave radiometer instruments mounted on the Cosmos-1500 satellite and various airborne platforms are evaluated in terms of their information content concerning ice thickness and general morphological features. A Legendre polynomial expansion for Cosmos-1500 data is proposed, which is applicable to the identification of sea-ice types. A series of Cosmos-1500 images of sea-ice formations in the Karsk Sea is provided. I. H.

A85-41662

THERMAL SATELLITE IMAGERY APPLIED TO A LITTORAL MACROBENTHOS INVESTIGATION IN THE GULF OF MAINE

P. F. LARSEN (Bigelow Laboratory for Ocean Sciences, West Boothbay Harbor, ME) *International Journal of Remote Sensing* (ISSN 0143-1161), vol. 6, June 1985, p. 919-926. refs (Contract NOAA-NA-80FAC0008)

The application of satellite imagery to oceanographic problems has grown in recent years. Its use in biological oceanography, however, has been largely limited to studies of primary productivity. The ability of thermal satellite imagery to identify coastal oceanic fronts suggests that there may be an application to macrobenthos investigations. This communication describes how thermal satellite imagery was applied to the study of sand-beach community distribution in the Gulf of Maine. Author

A85-41752

RADAR SENSING OF THE OCEAN

R. K. MOORE (Kansas, University, Lawrence) *IEEE Journal of Oceanic Engineering* (ISSN 0364-9059), vol. OE-10, April 1985, p. 84-113. refs

A discussion is conducted concerning the principles of radar scattering from the sea that form the bases for such diverse techniques as spaceborne radar altimetry and scatterometry, and of synthetic aperture radars (SARs). Attention is given to the principle of wind vector scatterometry and to unresolved questions that have emerged in the course of its development. It is noted that the theory of SAR wave imaging (for ocean surfaces) is the focus of controversy; nevertheless, SAR imaging is expected to furnish important future advancements in the detection of the presence of internal waves, eddies, and currents, and in the acquisition of information about bottom topography in shallow waters. SAR of this type will require a theory for bathymetric imaging. O.C.

A85-41753

METHODS OF OBTAINING OFFSHORE WIND DIRECTION AND SEA-STATE DATA FROM X-BAND AIRCRAFT SAR IMAGERY OF COASTAL WATERS

G. A. MASTIN (Sandia National Laboratories, Albuquerque, NM), C. A. HARLOW, O. K. HUH, and S. A. HSU (Louisiana State University, Baton Rouge) *IEEE Journal of Oceanic Engineering* (ISSN 0364-9059), vol. OE-10, April 1985, p. 159-174. Navy-supported research. refs

X-band synthetic aperture radar (SAR) imagery of the Goto Islands of Japan was digitally analyzed to extract air-sea interaction parameters and to assess the potential of texture measures in analysis of SAR ocean imagery. Wind direction is extracted from wind rows, wind streaks, and random turbulence patterns observed in the SAR imagery. Sea-state parameters are either extracted directly from the imagery or estimated using the extracted information in previously established empirical formulas. A convenient method of digitally presenting imagery, local power

spectra, and the extracted/estimated parameters is presented. Texture analysis based on gray-level co-occurrence (GLC) matrices is applied to SAR ocean imagery. The inertia measure is shown to extract similar information to the power spectrum. The cluster-shade measure is shown to be sensitive to image phase. Author

A85-41961

WAVE-INDUCED PRECIPITATION AS A LOSS PROCESS FOR RADIATION BELT PARTICLES

U. S. INAN, H. C. CHANG, R. A. HELLIWELL, J. P. KATSUFRAKIS (Stanford University, CA), W. L. IMHOF (Lockheed Research Laboratories, Palo Alto, CA) et al. (COSPAR, SCOSTEP, IAGA, and URSI, Symposium, 9th, and Topical Meeting on Magnetospheric and Ionospheric Plasmas, Graz, Austria, June 25-July 7, 1984) *Advances in Space Research* (ISSN 0273-1177), vol. 5, no. 4, 1985, p. 243-245 (Contract N00014-82-K-0489; N00014-79-C-0824)

Precipitation of radiation belt electrons by VLF waves injected from ground based transmitters was achieved during the Stimulated Emission of Energetic Particles (SEEP) experiments (Imhof et al., 1983), the first direct satellite based observation of modulated precipitation of electrons in the bounce loss cone. This paper considers the temporal and spectral shape as well as the absolute flux level of the observed precipitation pulses. In order to model these results, both the pitch angle dependence of the particle distribution near the edge of the loss cone and atmospheric backscatter which leads to multiple interactions of the particles with the wave are considered. Based on a comparison of theory with observations, the leverage of the precipitation process is estimated. Crude estimates of the percentage depletion of the radiation belt population due to the observed transmitter induced precipitation are also made. Author

A85-41993#

SATELLITE MEASUREMENT OF SEA SURFACE TEMPERATURE IN THE PRESENCE OF VOLCANIC AEROSOLS

C. WALTON (NOAA, National Environmental Satellite, Data, and Information Service, Washington, DC) *Journal of Climate and Applied Meteorology* (ISSN 0733-3021), vol. 24, June 1985, p. 501-507. refs

A procedure is described for including aerosol effects in atmospheric transmittance models. It is then shown that two-window correction algorithms produce errors up to 3°C in the presence of a realistic aerosol concentration. An alternative triple-window algorithm is developed which provides accurate corrections for atmospheric absorption and is essentially impervious to the aerosols simulated in this study. The results are verified by using actual satellite measurements made after the eruption of El Chicon in April 1982, which are compared with buoy measurements near Mauna Loa, Hawaii and in the Gulf of Mexico. V.L.

A85-41994

TRANSMISSION MODEL AND GROUND-TRUTH INVESTIGATION OF SATELLITE-DERIVED SEA SURFACE TEMPERATURES

I. J. BARTON (CSIRO, Div. of Atmospheric Research, Mordialloc, Australia) *Journal of Climate and Applied Meteorology* (ISSN 0733-3021), vol. 24, June 1985, p. 508-516. refs

Multichannel sea surface temperature algorithms from ground-truth regression analyses are compared with theoretical algorithms obtained by using a band model of atmospheric transmission. Good agreement in calculated sea surface temperatures is found between the theoretical and regression algorithms. Ground-truth data are used to investigate further the performance of these algorithms, and it is found that the effect of atmospheric absorption as calculated by the model is too small. The model is also used to derive algorithms for the AVHRR and VAS radiometers that are used on the operational NOAA and GOES satellites, respectively. Results indicate that in some cases different algorithms should be used for different view angles. V.L.

A85-42050

SATELLITE PROPAGATION IN THE SOUTH PACIFIC REGION
E. BACHMANN (Overseas Telecommunications Commission of Australia, Sydney, Australia) ATR/Australian Telecommunication Research (ISSN 0001-2777), vol. 19, no. 1, 1985, p. 3-11. refs

Attention is given to the propagation impairments associated with those frequency bands that are useful in a South Pacific satellite system, with emphasis on the satellite signal attenuation effects of rainfall. On the basis of the climatological regional commonality of eastern (tropical) Australia, Papua New Guinea, and the South Pacific islands, reliable long term rain intensity measurements have been obtained and converted to rain attenuation values by means of an empirical formula. System margins are proposed for trunk and concentrated subscriber telephone circuits, and transmission margins are calculated for 25 representative earth stations in the South Pacific region for 11 and 14 GHz operation. O.C.

A85-42134

OPTICAL-PHYSICAL METHODS FOR THE STUDY OF THE OCEAN [OPTIKO-FIZICHESKIE SREDSTVA ISSLEDOVANIYA OKEANA]

V. N. GULKOV, V. A. ZAITSEV, M. A. KROPOTKIN, E. G. PASHCHENKO, and V. V. TIKHONOV Leningrad, Izdatel'stvo Sudostroenie, 1984, 264 p. In Russian. refs

Current trends in the investigation of the ocean by physical-optical methods are reviewed. Theoretical principles are given for recent experimental studies of the oil pollution of the world ocean, the radiation balance of the ocean surface and water mass, the electromagnetic fields of the ocean, and sea roughness. Various devices are described, and test results are presented. Particular attention is given to the design of thermoelectric radiation detectors; instruments for measuring the underwater field of solar radiation; the determination of the statistical characteristics of the three-dimensional wave roughness field on the ocean, roughness studies using self-orienting buoys; and instruments for measuring the characteristics of underwater electromagnetic fields B.J.

A85-42177#

GEOPOTENTIAL HEIGHTS AND THICKNESSES AS PREDICTORS OF ATLANTIC TROPICAL CYCLONE MOTION AND INTENSITY

A. C. PIKE (NOAA, National Hurricane Center, Coral Gables, FL) Monthly Weather Review (ISSN 0027-0644), vol. 113, June 1985, p. 931-939. refs

In response to the increasing availability of satellite and aircraft temperature observations on the periphery of tropical cyclones, archived thickness and geopotential height data from National Meteorological Center analyses are compared as Atlantic cyclone predictors. For maximum use in motion prediction, thicknesses must be converted into deep-layer-mean or midtropospheric heights using an accurate reference-level height analysis. The 1000-700 mb thickness in the vicinity of cyclones in the poleward and eastward quadrant is a significant predictor of 24 h intensity change, even when combined with climatology and persistence. Author

A85-42222

SATELLITE OCEANOGRAPHY

I. S. ROBINSON (Southampton, University, England) Chichester, England/New York, Ellis Horwood, Ltd./Halsted Press, 1985, 455 p. refs

The acquisition of terrestrial remote-sensing data from satellites and the applications of these data in oceanography are examined in an introductory text intended for graduate or senior undergraduate students. Individual chapters are devoted to space hardware and data transmission, the oceanographic possibilities of satellite sensors, the principles of remote sensing of the sea, image processing, visible-wavelength ocean-color sensors, sea-surface temperatures from IR scanning radiometers, passive microwave radiometers, satellite altimetry of sea-surface topography, active microwave sensing of surface roughness, the altimeter as a roughness sensor, SAR, microwave scatterometers, and advanced sensors currently being developed. Graphs,

diagrams, maps, tables of numerical data, and sample images are provided. T.K

A85-42254

WAVE REFRACTION BY WARM CORE RINGS

G. R. MAPP, C. S. WELCH, and J. C. MUNDAY (College of William and Mary, Gloucester Point, VA) Journal of Geophysical Research (ISSN 0148-0227), vol. 90, July 20, 1985, p. 7153-7162. refs (Contract NOAA-NA-79SAC00775)

A numerical model for refraction of ocean swell by currents associated with a warm core ring was developed and tested with Seasat synthetic aperture radar (SAR) data. The wave field of SAR orbit 1232 was measured using optical Fourier transforms. The wave refraction model produced rays by simultaneous, numerical integration of the Hamiltonian ray equations applied to a moving medium. Wave orthogonals were constructed from wave number vectors calculated at each incremental time step. The flow field used by the model to simulate a warm ring was a steady, circular jet, with the radial profile of tangential velocity composed of a power function joined to a Gaussian. Initial wave conditions for simulation of refraction by the SAR-imaged ring were determined from measurements outside the ring. No data were available from which to determine the current field of the SAR-imaged ring, so the current field input to the model was adjusted until the output wave field most nearly resembled the SAR observations. The relative locations of convergence and divergence of rays were as observed on the SAR image, and the relative energy density in crossed seas was correctly predicted. However, predicted patterns of wavelength variation (presuming that incident waves were uniform in wavelength) were not observed. Author

A85-42255

SOME FEATURES OF THE ALGERIAN CURRENT

C. MILLOT (Laboratoire d'Océanographie Physique, La-Seyne-sur-Mer, France) Journal of Geophysical Research (ISSN 0148-0227), vol. 90, July 20, 1985, p. 7169-7176. refs

The dynamics of the Algerian Current and flow of the Atlantic Water in the Algerian Basin are investigated on the basis of thermal satellite images. An analysis of hydrological and infrared data indicates that the Algerian Basin is characterized by a large mesoscale variability mainly due to the instability of the Algerian Current. The Basin looks like a reservoir in which the Atlantic Water is amassed, it forms a buffer zone which partially disconnects the flux coming in at Gibraltar from the fluxes going out toward the Ligurian Sea and through the Strait of Sardinia V.L.

A85-42257

DISPERSION OF SEA ICE IN THE BERING SEA

S. MARTIN (Washington, University, Seattle) and A. S. THORNDIKE (University of Puget Sound, Tacoma, WA) Journal of Geophysical Research (ISSN 0148-0227), vol. 90, July 20, 1985, p. 7223-7226. refs

(Contract NR PROJECT 083-012, N00014-84-C-0111; NSF DPP-82-17594)

The dispersion of sea ice in the Bering Sea is analyzed in terms of the changes in separation between pairs of ice floes. The statistics of these changes depend on the separation itself and on the time interval over which the changes are measured. Rather than being constant, as in the case of molecular or Fickian diffusion, the diffusivity increases according to the 1.8 power of the separation. For short times the diffusivity is proportional to time. For times greater than three days the diffusivity appears to approach a constant value for any particular separation. Comparison with other data shows that the ice floe diffusivity is about an order of magnitude smaller than the diffusivity at the surface of the temperate ocean and about an order greater than the diffusivity of sea ice in the Beaufort Sea. Author

A85-42259

ALBEDO OF A WATER SURFACE, SPECTRAL VARIATION, EFFECTS OF ATMOSPHERIC TRANSMITTANCE, SUN ANGLE AND WIND SPEED

K. B. KATSAROS, L. A. MCMURDIE, R. J. LIND, and J. E. DEVAULT (Washington, University, Seattle) *Journal of Geophysical Research* (ISSN 0148-0227), vol. 90, July 20, 1985, p. 7313-7321. refs

(Contract N00014-75-C-0502-P00015, N00014-80-C-0252-P00015)

The albedo's dependence on transmittance (cloudiness) and solar altitude is examined using observations obtained from aircraft and a ship in the Joint Air-Sea Interaction experiment, from a ship in the GARP Atlantic Tropical Experiment, and from an instrumented mast located in Lake Washington (Seattle, WA). For short solar wavelengths (0.28-0.53 micron), surface albedo shows little dependence on transmittance, while for longer solar wavelengths (0.53-2.8 microns), albedo increases with decreasing transmittance. The results obtained are in general agreement with those of Payne (1972), but some deviations are indicated at high solar altitudes with low transmittance and for solar altitudes below 20 deg.

V. L.

A85-42512#

VISIBLE FLUORESCENCE FROM ULTRAVIOLET EXCITED CRUDE OIL

J. S. KNOLL (NOAA, National Environmental Satellite, Data, and Information Service, Washington, DC) *Applied Optics* (ISSN 0003-6935), vol. 24, July 15, 1985, p. 2121-2123. refs

Radiant fluorescent intensity, from a UV irradiated sample of crude oil in the visible spectral region, was measured as a function of exposure time of the crude oil to the atmosphere. The intensity of the laboratory source of UV irradiation (300-400 nm) was calibrated and compared with the intensity of the sun at sea level through 1 atm. The maximum intensity of the sun excited fluorescence was estimated to be 5 times less than that required to be detected by presently available satellite mounted visible spectrum detectors and 500 times less than that required to differentiate one crude oil type from another.

Author

A85-43117

SATELLITE OBSERVATIONS OF THE CIRCULATION EAST OF THE MISSISSIPPI DELTA - COLD-AIR OUTBREAK CONDITIONS

W. W. SCHROEDER (Alabama, University, Dauphin Island), O. K. HUH, L. J. ROUSE, JR., and W. J. WISEMAN, JR. (Louisiana, State University, Baton Rouge) *Remote Sensing of Environment* (ISSN 0034-4257), vol. 18, Aug. 1985, p. 49-58. Research supported by the University of Alabama, Dauphin Island Sea Laboratory, and NOAA. refs

Examination of 12 years of Landsat multispectral scanner images shows a recurrent pattern of westward flow immediately south of the Mississippi-Alabama barrier islands under northerly winds. Such flow patterns are also seen under similar conditions in imagery from the Advanced Very High Resolution Radiometer (AVHRR) of the NOAA-series satellites. The flow enters Chandeleur Sound between Ship Island and the northern end of the Chandeleur Islands. It appears to be driven by northerly winds, which force water south through the Chandeleur-Breton Sound, drawing water in from the shelf region south of the Mississippi-Alabama barrier islands. These observations on circulation can be simply explained assuming linear dynamics. These two operational satellite systems are accumulating valuable records of coastal circulation patterns under clear-sky conditions.

Author

A85-43373*# National Aeronautics and Space Administration, Langley Research Center, Hampton, Va.

THE ALBEDO FIELD AND CLOUD RADIATIVE FORCING PRODUCED BY A GENERAL CIRCULATION MODEL WITH INTERNALLY GENERATED CLOUD OPTICS

T. P. CHARLOCK and V. RAMANATHAN (NASA, Langley Research Center, Hampton, VA) *Journal of the Atmospheric Sciences* (ISSN 0022-4928), vol. 42, July 1, 1985, p. 1408-1429. NASA-supported research. refs

A general circulation model (GCM) study is presented in which cloud radiative properties are computed from cloud liquid water content inferred from the GCM hydrological cycle. Model-generated and satellite albedos are in rough agreement. Analysis of the cloud radiative forcing indicates that cloud albedo effects overcome cloud infrared opacity effects in most regions. Both computed and observed albedo of clouds decrease from low to high altitudes. The model with variable cloud optics produces significantly different regional albedos from the same one with fixed cloud optics, especially over the tropics. The cloud droplet size distribution also has a significant impact on the model albedos. The temperature of the tropical upper troposphere is somewhat sensitive to the microphysical characteristics of the model cirrus clouds.

C.D.

A85-44925

THERMAL ISOSTASY IN THE SOUTH ATLANTIC OCEAN FROM GEIOD ANOMALIES

M. G. KOGAN (AN SSSR, Institut Fiziki Zemli, Moscow, USSR), M. DIAMENT, A. BULOT (Paris XI, Universite, Orsay, France), and G. BALMINO (Bureau Gravimetrique International, CNES, Groupe de Recherches de Geodesie Spatiale, Toulouse, France) *Earth and Planetary Science Letters* (ISSN 0012-821X), vol. 74, no. 2-3, July 1985, p. 280-290. refs

Transfer functions (admittances) were computed for the main tectonic units of the South Atlantic Ocean using the detailed Seasat geoid Ensemble averaging in the two-dimensional wavenumber domain was applied. The topography of the Walvis Ridge and Rio Grande Rise visually correlates with the local geoid, i.e., the difference between the total Seasat geoid and first ten harmonics of the GRIM 3 model. The mid-Atlantic geoid visually correlates with the total geoid. Sea-gravimetry was used to evaluate the contribution of mechanical isostasy to the geoid. Admittances computed from the geoid and from gravimetry data agree well in the short waveband (wavelengths shorter than 300 km). A deviation at longer wavelengths is found between the observed admittance and the one due to mechanical isostasy for the southwestern Walvis Ridge. It is explained with a density perturbation at about 20 km deep. The admittance for the Mid-Atlantic Ridge is interpreted in terms of a boundary layer model and an average thickness of 30 km for the thermal lithosphere is obtained.

Author

A85-45875

A COMPARISON OF SPOT SIMULATOR DATA WITH LANDSAT MSS IMAGERY FOR DELINEATING WATER MASSES IN DELAWARE BAY, BROADKILL RIVER, AND ADJACENT WETLANDS

S. G. ACKLESON, V. KLEMAS (Delaware, University, Newark), H. L. MCKIM, and C. J. MERRY (U.S. Army, Cold Regions Research and Engineering Laboratory, Hanover, NH) *Photogrammetric Engineering and Remote Sensing* (ISSN 0099-1112), vol. 51, Aug. 1985, p. 1123-1129. refs

A85-46251

PROGRAM OF EXPERIMENTS ON THE COSMOS-1500 SATELLITE [PROGRAMMA EKSPERIMENTOV NA ISZ 'KOSMOS-1500']

IU. A. AFANASEV, B. A. NELEPO, A. S. SELIVANOV, B. E. KHYMYROV, G. M. TAMKOVICH (GNI Tsentr Izucheniiia Prirodnykh Resursov, AN SSSR, IR i E and IKI, Moscow, USSR, AN USSR, MGU, Sevastopol; AN USSR, IR i E, Kharkov; Dnepropetrovskii Gosudarstvennyi Universitet, Dnepropetrovsk, Ukrainian SSR) et al. Issledovanie Zemli iz Kosmosa (ISSN 0205-9614), May-June 1985, p. 3-8. In Russian. refs

The main objectives and results of experiments involving the remote sensing of the ocean from the Cosmos-1500 satellite are summarized. The features of the scientific instrumentation are described along with details of subsatellite measurements. In addition, programs for the support and control of the measurements are discussed, and the planning of satellite operations and the distribution of data to users are considered. As an example, attention is given to the application of ice-radar-survey data to the analysis of the ice situation in the Eastern Arctic during the winter of 1983. B.J

A85-46252

INTERPRETATION OF SEA ICE ON SATELLITE RADAR IMAGES [DESHIFIROVANIE MORSKIKH L'DOV NA RADIOLOKATSIONNYKH SPUTNIKOVYKH SNIMKAKH]

A. V. BUSHUEV, V. D. GRISHCHENKO, and A. D. MASANOV (Arkticheskii i Antarkhticheskii Nauchno-Issledovatel'skii Institut, Leningrad, USSR) Issledovanie Zemli iz Kosmosa (ISSN 0205-9614), May-June 1985, p. 9-15. In Russian.

The information content of radar images of Arctic sea ice obtained from the Cosmos-1500 satellite during December 1983 is analyzed on the basis of subsatellite reference data. Features characterizing the interpretation of sea ice on these images are examined. It is concluded that such interpretation can provide information of navigational significance, including data on channels in massive old ice, the location and configuration of giant ice fields, and the drift velocity and direction of ice over the entire Arctic Ocean. B.J.

A85-46253

DETERMINATION OF THE ICE-COVER CHARACTERISTICS OF THE SEA OF OKHOTSK IN THE WINTER OF 1983-1984 ON THE BASIS OF RADAR-SOUNDING DATA [OPREDELENIE KHARAKTERISTIK LEDIANOGA POKROVA OKHOTSKOGO MORIA ZIMOI 1983-1984 GG. PO DANNYM RADIOLOKATSIONNOGO ZONDIROVANIYA]

L. M. MITNIK (AN SSSR, Tikhookeanskii Okeanologicheskii Institut, Vladivostok, USSR), G. I. DESIATOVA (Dal'nevostochnyi Regionalnyi Tsentri Priema i Obrabotki Sputnikovykh Danykh, Khabarovsk, USSR), and V. V. KOVBASIUK (Kamchatskoe Territorial'noe Upravlenie po Gidrometeorologii i Kontroliu Prirodnoi Sredy, Petropavlovsk-Kamchatskii, USSR) Issledovanie Zemli iz Kosmosa (ISSN 0205-9614), May-June 1985, p. 16-22. In Russian. refs

Cosmos-1500 radar images of the Sea of Okhotsk during the winter of 1983-1984 are analyzed. A comparison of these images with ice maps obtained through aerial reconnaissance made it possible to determine the features of the formation and development of new, nilas, and young ice which have not been obtained through satellite measurements in various spectral bands. B.J

A85-46254

THE USE OF RADAR IMAGES OBTAINED WITH THE COSMOS-1500 SATELLITE TO STUDY THE DISTRIBUTION AND DYNAMICS OF SEA ICE [ISPOL'ZOVANIE RADIOLOKATSIONNYKH SNIMKOV ISZ 'KOSMOS-1500' DLIYA ISSLEDOVANIYA RASPREDELENIYA I DINAMIKH MORSKIKH L'DOV]

A. V. BUSHUEV and IU. D. BYCHENKOV (Arkticheskii i Antarkhticheskii Nauchno-Issledovatel'skii Institut, Leningrad, USSR) Issledovanie Zemli iz Kosmosa (ISSN 0205-9614), May-June 1985, p. 23-27. In Russian.

A85-46255

QUANTITATIVE INTERPRETATION OF SATELLITE RADAR IMAGES OF SEA ICE USING A PRIORI DATA [KOLICHESTVENNAIA INTERPRETATSIIA SPUTNIKOVYKH RADIOLOKATSIONNYKH IZOBRAZHENII MORSKIKH L'DOV S ISPOL'ZOVANIEM APRIORNYKH DANNYKH]

V. IU. ALEKSANDROV and V. S. LOSHCHILOV (Arkticheskii i Antarkhticheskii Nauchno-Issledovatel'skii Institut, Leningrad, USSR) Issledovanie Zemli iz Kosmosa (ISSN 0205-9614), May-June 1985, p. 28-31. In Russian.

A85-46256

IDENTIFICATION OF EDDY FORMATIONS IN A RADAR IMAGE OF THE OCEAN SURFACE [OB IDENTIFIKATSII VIKHREVYKH OBRAZOVANII V RADIOLOKATSIONNOM IZOBRAZHENII POVERKHNOSTI OKEANA]

V. A. DULOV, G. K. KOROTAEV, V. N. KUDRIAVTSEV, V. S. SUETIN, and IU. V. TEREKHIN (AN USSR, Morskoi Gidrofizicheskii Institut, Sevastopol, Ukrainian SSR) Issledovanie Zemli iz Kosmosa (ISSN 0205-9614), May-June 1985, p. 32-40. In Russian. refs

A model for the formation of the radar image of a synoptic eddy is proposed with reference to Cosmos-1500 radar data on the ocean surface near Newfoundland. The model is based on the dependence of the radar backscattering on the breaking intensity of wind-generated waves. This dependence results from the covering of the ocean surface by foam (which absorbs the radio waves) and the smoothing of the scattering ripples in foci of small-scale near-surface turbulence generated by wave breaking. The breaking intensity is defined by the parameters of the wind-generated waves. B.J.

A85-46257

ORDERED MESOSCALE STRUCTURES ON THE OCEAN SURFACE IDENTIFIED FROM SATELLITE RADAR DATA [OB UPORIADOCHENNYKH MEZOMASSHTABNYKH STRUKTURAKH NA POVERKHNOSTI OKEANA, VYIAVLENNYKH PO DANNYM RADIOLOKATSIONNYKH S'EMOK IZ KOSMOSA]

A. I. KALMYKOV, M. NAZIROV, P. A. NIKITIN, A. P. PICHUGIN, and IU. G. SPIRIDONOV (AN USSR, Institut Radiofiziki i Elektroniki, Kharkov, Ukrainian SSR; Gosudarstvennyi Nauchno-Issledovatel'skii Tsentri Izucheniiia Prirodnykh Resursov, Moscow, USSR) Issledovanie Zemli iz Kosmosa (ISSN 0205-9614), May-June 1985, p. 41-47. In Russian. refs

Synchronous radar and optical surveys of the ocean from the Cosmos-1500 satellite revealed the existence of a mesoscale cellular and linearly periodic quasi-homogeneous spatial organization of near-surface hydrophysical fields (wind-generated waves and related temperature fields, currents, and dissolved and suspended substances) connected with convective and wave processes in the atmospheric surface layer. The mechanism for this phenomenon consists in the fact that these structures are adapted to the spatial distribution of elements of convective and wave perturbations in the atmospheric surface layer as the result of nonuniform molecular, turbulent, and convective energy transfer between ocean and atmosphere. Empirical rules are established for determining the direction of general air transfer over the ocean in accordance with a physical interpretation of ordered structures observed on radar images. B.J.

A85-46258

COMBINED ANALYSIS OF RADAR AND OPTICAL IMAGES OF THE NORTHWEST PACIFIC ON DECEMBER 6, 1983 [KOMPLEKSNYI ANALIZ RADIOLOKATSIONNOGO I OPTICHESKOGO IZOBRAZHENII SEVERO-ZAPADNOI CHASTI TIKHOGO OKEANA ZA 6 DEKABRIA 1983 G.]

L. M. MITNIK, G. I. DESIATOVA, and V. V. KOVBASIUK (AN SSSR, TOI, Vladivostok, USSR; Dal'nevostochnyi Regional'nyi Tsentr Priema i Obrabotki Sputnikovykh Danykh, Khabarovsk, USSR; Kamchatskoe Territorial'noe Upravlenie po Gidrometeorologii i KPS, Petropavlovsk-Kamchatskii, USSR) Issledovanie Zemli iz Kosmosa (ISSN 0205-9614), May-June 1985, p. 48-53. In Russian. refs

A85-46259

RADAR MAPS OF THE ARCTIC AND ANTARCTIC COMPILED ON THE BASIS OF COSMOS-1500 SATELLITE DATA, AND PRELIMINARY RESULTS OF THEIR ANALYSIS [RADIOLOKATSIONNYE KARTY ARKTIKI I ANTARKTIDY PO DANNYM ISZ 'KOSMOS-1500' I PREDVARITEL'NYE REZUL'TATY IKH ANALIZA]

A. I. BURTSEV, V. A. KROVOTYNTSEV, M. NAZIROV, P. A. NIKITIN, and I. U. G. SPIRIDONOV (Gosudarstvennyi Nauchno-Issledovatel'skii Tsentr Izucheniia Prirodnykh Resursov, Moscow, USSR) Issledovanie Zemli iz Kosmosa (ISSN 0205-9614), May-June 1985, p. 54-63. In Russian. refs

Theoretical aspects of the formation of radar signals reflected from land and sea ice are examined. Radar maps of the Arctic and Antarctic basins obtained with the Cosmos-1500 sidelooking radar are presented. Ice-cover features of the maps are analyzed

B.J.

A85-46260

THE DATA ACQUISITION SYSTEM ON THE COSMOS-1500 SATELLITE [BORTOVOI INFORMATSIONNYI KOMPLEKS SPUTNIKA 'KOSMOS-1500']

S. S. KAVELIN, E. I. BUSHUEV, V. I. DRANOVSKII, V. V. PUSTOVOITENKO, I. U. D. SALTIKOV (Dnepropetrovskii Gosudarstvennyi Universitet, Dnepropetrovsk, AN USSR, Morskoi Gidrofizicheskii Institut, Sevastopol', Ukrainian SSR) et al. Issledovanie Zemli iz Kosmosa (ISSN 0205-9614), May-June 1985, p. 64-69. In Russian. refs

The data acquisition system (DAS) of the Cosmos-1500 oceanographic satellite includes a sidelooking radar, an 0.8-cm-wavelength scanning microwave radiometer, a three-frequency microwave spectrometer, a radio-TV system, and a system for the acquisition of data from buoy stations. The design features and specifications of this DAS are described. Attention is given to differences between this DAS and those of the Cosmos-1076, Cosmos-1151, and Meteor-Priroda oceanographic satellites

B.J.

A85-46261

INVESTIGATION OF THE OCEAN WITH LOW-RESOLUTION MULTISPECTRAL SCANNERS [ISSEDOVANIIE OKEANA S POMOSHCH'U MNOGOSPEKTRAL'NYKH SKANIRUIUSHCHIKH USTROISTV MALOGO RAZRESHENIIA]

A. S. SELIVANOV, I. U. M. GEKIN, M. K. NARAEVA, A. S. PANFILOV, and V. P. CHEMODANOV Issledovanie Zemli iz Kosmosa (ISSN 0205-9614), May-June 1985, p. 70-75. In Russian. refs

Trends in the remote sensing of the ocean by optomechanical multispectral scanners are reviewed. The design features of the low-resolution multispectral scanner system on the Cosmos-1500 satellite are examined, and features characterizing the joint use of the MSS and sidelooking radar on this satellite are described. Results of the survey of the ocean surface by a low-resolution multispectral scanner system in the optical range are presented.

B.J.

A85-46262

THE SIDELOOKING RADAR ON THE COSMOS-1500 SATELLITE [RADIOLOKATOR BOKOVOGO OBZORA ISZ 'KOSMOS-1500']

A. I. KALMYKOV, A. S. KUREKIN, V. B. EFIMOV, A. B. FETISOV, V. V. IGOLKIN (AN USSR, Institut Radiofiziki i Elektroniki, Kharkov, Ukrainian SSR) et al. Issledovanie Zemli iz Kosmosa (ISSN 0205-9614), May-June 1985, p. 76-83. In Russian. refs

The choice of the main specifications of the sidelooking radar (SLR) of the Cosmos-1500 oceanographic satellite is justified. These specifications include the wavelength of the sounding signal, the surface irradiation angles, the polarization of the radiation, and the mean power of the transmitter. The main components of the SLR are described, and the overall system design is examined. It is concluded that results of full-scale experiments confirm the correctness of the theoretical principles and design solutions underlying the development of the SLR

B.J.

A85-46263

INFORMATIONAL POTENTIAL OF THE SIDELOOKING RADAR OF THE COSMOS-1500 SATELLITE [INFORMATSIONNYE VOZMOZHNOСТИ RADIOLOKATSIONNOI SISTEMY BOKOVOGO OBZORA ISZ 'KOSMOS-1500']

V. N. TSYMBAL, A. I. KALMYKOV, A. S. KUREKIN, A. P. PICHUGIN, A. B. FETISOV (AN USSR, Institut Radiofiziki i Elektroniki, Kharkov, USSR) et al. Issledovanie Zemli iz Kosmosa (ISSN 0205-9614), May-June 1985, p. 84-92. In Russian. refs

An assessment of the informational potential of the Cosmos-1500 sidelooking radar (SLR) shows that this system can efficiently solve various problems of oceanographic research and ice survey. The system is characterized by a wide survey band (450-500 km), a sufficiently high resolution (1-2 km), efficient onboard data processing, and data transmission on standard transmission lines. The SLR is particularly suitable for the study of the wind velocity field near the ocean surface and the rough ocean surface.

B.J.

A85-46265

AUTOMATED PROCESSING OF REMOTE-SENSING DATA OBTAINED WITH THE MICROWAVE RADIOMETER OF THE COSMOS-1500 SATELLITE [AVTOMATIZIROVANNIA OBRABOTKA DANNYKH DISTANTSIONNYKH IZMERENII SVCH-RADIOMETROM ISZ 'KOSMOS-1500']

V. S. SUETIN, V. D. MASLOV, V. V. MAKOVKIN, A. N. NEDOVESOV, V. V. MIROSHNICHENKO (AN USSR, Morskoi Gidrofizicheskii Institut, Sevastopol', Ukrainian SSR; AN SSSR, Institut Kosmicheskikh Issledovani, Moscow, USSR) et al. Issledovanie Zemli iz Kosmosa (ISSN 0205-9614), May-June 1985, p. 103-106. In Russian. refs

A block diagram of the system for the processing of remote-sensing data obtained with the multichannel microwave radiometer of the Cosmos-1500 oceanographic satellite is presented. The processing is carried out using the Es computer and a special software package. The various steps of processing are described in some detail.

B.J.

A85-46266

DIGITAL PROCESSING OF RADAR IMAGES OBTAINED WITH THE COSMOS-1500 SATELLITE [TSIFROVAIA OBRABOTKA RADIOLOKATSIONNYKH IZOBRAZHENII, POLUCHENNYKH SO SPUTNIKA 'KOSMOS-1500']

V. G. ASMUS, P. A. NIKITIN, A. E. POPOV, V. I. POPOV, and I. U. G. SPIRIDONOV (Gosudarstvennyi Nauchno-Issledovatel'skii Tsentr Izucheniia Prirodnykh Resursov, Moscow, USSR) Issledovanie Zemli iz Kosmosa (ISSN 0205-9614), May-June 1985, p. 107-114. In Russian. refs

The method for the digital processing of radar images obtained with the sidelooking radar of the Cosmos-1500 oceanographic satellite is described, and a block diagram of the processing is presented. The functional groups of the software modules are described, and preliminary processing results are presented. It is concluded that the processing method described here can be used to determine wind velocity over the ocean and other

05 OCEANOGRAPHY AND MARINE RESOURCES

characteristics of the state of the ocean and atmosphere, as well as to classify types of ice cover. B.J.

A85-46267

THE EXPERIMENTAL OCEANOGRAPHIC SATELLITE COSMOS-1500 [EKSPERIMENTAL'NYI OKEANOGRAFICHESKII SPUTNIK 'KOSMOS-1500']

S. S. KAVELIN, D. G. BELOV, V. S. GLADILIN, V. F. ZUBENKO, I. S. IGDALOVA (Dnepropetrovskii Gosudarstvennyi Universitet, Dnepropetrovsk, Ukrainian SSR) et al. *Issledovanie Zemli iz Kosmosa* (ISSN 0205-9614), May-June 1985, p 115-122 in Russian.

After a discussion of requirements on the design and operation of oceanographic remote-sensing satellites, the paper describes the design of the Cosmos-1500 satellites. The basic structural-design features are considered, and the principles of satellite control are described. B.J.

A85-47921* National Aeronautics and Space Administration. Goddard Space Flight Center, Greenbelt, Md.

LIDAR OBSERVATIONS OF VERTICALLY ORGANIZED CONVECTION IN THE PLANETARY BOUNDARY LAYER OVER THE OCEAN

S. H. MELFI, J. D. SPINHIRNE, S.-H. CHOU (NASA, Goddard Space Flight Center, Greenbelt, MD), and S. P. PALM (Science Systems and Applications, Inc., Greenbelt, MD) *Journal of Climate and Applied Meteorology* (ISSN 0733-3021), vol. 24, Aug. 1985, p. 806-821. refs

Observations of a convective planetary boundary layer (PBL) were made with an airborne, downward-looking lidar system over the Atlantic Ocean during a cold air outbreak. The lidar data revealed well-organized, regularly spaced cellular convection with dominant spacial scales between two and four times the height of the boundary layer. It is demonstrated that the lidar can accurately measure the structure of the PBL with high vertical and horizontal resolution. Parameters important for PBL modeling such as entrainment zone thickness, entrainment rate, PBL height and relative heat flux can be inferred from the lidar data. It is suggested that wind shear at the PBL top may influence both entrainment and convective cell size. Author

A85-48670* University of South Florida, St. Petersburg. **SOLID-STATE SPECTRAL TRANSMISSOMETER AND RADIOMETER**

K. L. CARDER, R. G. STEWARD (South Florida, University, St. Petersburg), and P. R. PAYNE (Aztec Computer Engineering, Pinellas Park, FL) *Optical Engineering* (ISSN 0091-3286), vol. 24, Sept.-Oct 1985, p. 863-868. refs (Contract NAGW-465)

An in situ instrument designed to measure the spectral attenuation coefficient of seawater and the ocean remote-sensing reflectance from 400 to 750 nm is in the test and development stage. It employs a 256 channel, charge-coupled type of linear array measuring the spectral intensities diffracted by a grating. Examples of the types of data delivered by this instrument have been simulated using a breadboard laboratory instrument and an above-water, solid-state radiometer. Algorithms developed using data from these instruments provide measures of chlorophyll *a* plus phaeophytin concentrations from less than 0.1 to 77.0 mg/cu m, gelbstoff spectral absorption coefficients, and detrital spectral backscattering coefficients for waters of the west Florida shelf. Author

A85-48970

INVERSE METHODS FOR OCEAN WAVE IMAGING BY SAR

S. ROTHERAM and J. T. MACKLIN (General Electric Co., PLC, Marconi Research Centre, Chelmsford, England) IN: *Inverse methods in electromagnetic imaging: Proceedings of the NATO Advanced Research Workshop, Bad Windsheim, West Germany, September 18-24, 1983. Part 2*. Dordrecht, D. Reidel Publishing Co., 1985, p. 907-930. ESA-supported research. refs

A Synthetic Aperture Radar (SAR) can form high resolution images of the sea surface. The direct problem for such an imaging

system is now reasonably well understood and is summarized here for both the SAR image and its power spectrum. The inverse problem has only recently been explored and some simple approaches based on linear demodulation and speckle removal are described. These are applied to a number of Seasat images.

Author

A85-49477

MODELING OF RADIO-WAVE SCATTERING BY ICE COVER [MODELIROVANIE PROTSESSOV RASSEIANIIA RADIOVOLN LEDOVYMI POKROVAMI]

A. I. TIMCHENKO, I. A. SINITSYN, and V. B. EFIMOV (AN USSR, Institut Radiofiziki i Elektroniki, Kharkov, Ukrainian SSR) *Radiofizika* (ISSN 0021-3462), vol. 28, no. 7, 1985, p. 816-822 in Russian. refs

The use of numerical modeling to study scattering characteristics in the radar sounding of ice cover, with the aim of determining ice age and thickness, is examined. Radiation-transfer theory is used to investigate radio-wave reflection from a dielectric layer with rough boundaries for different values of the bulk absorption coefficient. Results of numerical calculations are compared with experimental data, and analytical solutions of the transfer equations are discussed. Particular attention is given to the formation of the scattering indicatrix. B.J.

A85-49855* Washington Univ., Seattle.

SMALL-SCALE CYCLONES ON THE PERIPHERY OF A GULF STREAM WARM-CORE RING

M. A. KENNELLY (Washington, University, Seattle), R. H. EVANS (Miami, University, FL), and T. M. JOYCE (Woods Hole Oceanographic Institution, MA) *Journal of Geophysical Research* (ISSN 0148-0227), vol. 90, Sept. 20, 1985, p. 8845-8857. refs (Contract NSF OCE-80-16983; NSF OCE-80-169919; NAGW-272; NAGW-273)

Small-scale cyclones found around Gulf Stream warm-core ring 82B are investigated by using infrared satellite images and current information obtained with an acoustic-Doppler velocimeter. Currents in these cyclones reveal speeds ranging from 20 to 80 cm/s. One small cyclone or 'ringlet' found in June 1982 was studied extensively by removing the basic rotational velocities of 82B. The azimuthal velocity field for this ringlet was used with the gradient current equation to calculate the absolute dynamic topography at 100 dbar. It was found that the ringlet was 13 dyn-cm lower than its surroundings. In addition, neglect of the centrifugal term would have changed the dynamic topography of the ringlet by 30 percent. From a comparison with CTD data the absolute reference level was determined, and a vertical profile of horizontal currents was calculated for the ringlet. Other cyclones were found throughout the slope water region around warm-core ring 82B with observable lifetimes of 1 to 2 weeks. The northeast quadrant of 82B was a favored generation site for ringlets. Two cyclones were observed to form in this region and were advected anticyclonically around 82B. Typically, at any one time, six cyclones with diameters of approximately 40 to 50 km can be detected north of the Gulf Stream by using satellite images. Author

A85-49863

A WIND-INDUCED MESOSCALE EDDY OVER THE VANCOUVER ISLAND CONTINENTAL SLOPE

R. E. THOMSON and J. F. R. GOWER (Institute of Ocean Sciences, Sidney, Canada) *Journal of Geophysical Research* (ISSN 0148-0227), vol. 90, Sept. 20, 1985, p. 8981-8993. refs

Nimbus 7 satellite coastal zone color scanner imagery and direct oceanic measurements are used to investigate the mesoscale circulation pattern formed off the coast of Vancouver Island, British Columbia, in July, 1979. Attention is given to a well defined cyclonic eddy that formed in 1000 m of water over the central portion of the continental slope. The eddy and its attendant mesoscale circulation pattern are suggested to have evolved through mixed barotropic-baroclinic instability of a poleward-flowing coastal 'jet' that had been generated during a one-week period of strong southeast winds. O.C.

A85-49872

COMMENT ON 'MEASUREMENT OF HIGH-FREQUENCY WAVES USING A WAVE FOLLOWER' BY S. TANG AND O. H. SHEMDIN

F. DOBSON (Bedford Institute of Oceanography, Dartmouth, Canada) Journal of Geophysical Research (ISSN 0148-0227), vol. 90, Sept. 20, 1985, p. 9203, 9204; Reply, p. 9205.

A85-49933

THE EFFECT OF EL CHICHON ON WIND VARIABILITY IN THE TROPOSPHERE, STRATOSPHERE, AND MESOSPHERE OVER ALASKA

B. B. BALSLEY and R. GARELLO (NOAA, Aeronomy Laboratory, Boulder, CO) Geophysical Research Letters (ISSN 0094-8276), vol. 12, Sept. 1985, p. 581-584 NSF-supported research. refs

Data from the Poker Flat, Alaska MST radar combined with standard NWS balloon observations at Fairbanks, Alaska show that low-frequency (3-11 day) wind fluctuations within the troposphere and lower stratosphere for the period January-March 1983 were noticeably weaker than those for other similar periods between 1979-1984. Similar effects can be detected in the higher-frequency (1-6 hr and 8-48 hr) wind fluctuations obtained from the radar data alone. In contrast to these decreases in the troposphere and lower stratosphere wind variations, the magnitude of the tidal period (8-48 hr) atmospheric wind fluctuations observed by radar in the mesosphere during June-July were significantly increased in 1983 relative to surrounding years. All of these variations appear to be reasonably well associated with the presence of enhanced aerosol concentrations in the lower stratosphere following the explosion of El Chichon volcano in April 1982.

Author

N85-30411# Joint Publications Research Service, Arlington, Va. MODEL COMPUTATIONS OF LIGHT REFLECTION FROM SEA SURFACE Abstract Only

K. S. SHIFRIN and R. G. GARDASHOV In its USSR Rept.: Earth Sci. (JPRS-UES-85-007) p 17 8 Jul. 1985 Transl into ENGLISH from Izv. Akad. Nauk SSSR: Fiz. Atm. i Okeana (Moscow), v. 21, no. 2, Feb. 1985 p 162-169 Original language document was announced in IAA as A85-28945
Avail NTIS HC A04/MF A01 CSCL 20F

The method of stochastically distributed surfaces is used extensively in marine optics in computing the reflection of light from the wave covered sea surface; surface brightness is determined through the Fresnel reflection coefficient for which there is a mirror observation direction relative to the direction of incidence. This method cannot be used for other angles because then shadow effects and multiple reflection of light from roughness elements which are not taken into account in the stochastically distributed surfaces method become important. This problem has been solved in the example of a very simple model which makes it possible to obtain important estimates. In this model it is possible to trace the fate of each ray incident on the surface separately; both the shadow effect and multiple reflection are taken into account. Refracted beams are neglected in order to study the characteristics of the phenomenon related only to reflection from the surface.

Author

N85-30451*# National Aeronautics and Space Administration. Goddard Space Flight Center, Greenbelt, Md

MIZEX, 1984, NASA CV-990 FLIGHT REPORT

May 1985 155 p refs Submitted for publication (NASA-TM-86216; NAS 1.15:86216) Avail: NTIS HC A08/MF A01 CSCL 08L

During June/July 1984, the NASA CV-990 Airborne Laboratory was utilized in a mission to overfly the Fram Strait/East Greenland Sea marginal ice zone (MIZ) during the main summer marginal ice zone experiment (MIZEX '84). The eight data flights were coordinated where possible with overpasses of the Nimbus-7 satellite, and with measurement of sea ice, open ocean, and atmospheric properties at the surface. The surface research teams were based on seven research vessels, some with helicopters: (1) M/V Kvibjorn, (2) M/V Polarqueen, (3) M/S Haakon Mosby;

(4) a M/S H.U. Sverdrup, all from Norway; (5) F/S Polarstern from the Federal Republic of Germany; and (6) the USNS Lynch from the USA. There were also coordinated flights with the NRL P3, NOAA P3, Canadian CV580, and the French B-17 during the overlap portions of their respective missions. Analysis of the real-time data acquired during the mission and uncalibrated data stored on tape has served to indicate the mission was over 90% successful.

Author

N85-30452*# National Aeronautics and Space Administration. Goddard Space Flight Center, Greenbelt, Md.

NIMBUS 7 COASTAL ZONE COLOR SCANNER (CZCS). LEVEL 2 DATA PRODUCT USERS' GUIDE

S. P. WILLIAMS (Systems and Applied Sciences Corp., Vienna, Va.), E. F. SZAJNA, and W. A. HOVIS Jul 1985 61 p (NASA-TM-86202; REPT-85B0302; NAS 1.15:86202) Avail: NTIS HC A04/MF A01 CSCL 08C

The coastal zone color scanner (CZCS) is a scanning multispectral radiometer designed for the remote sensing of ocean color parameters from an earth orbiting space platform. A Technical Manual was designed for users of NIMBUS 7 CZCS Level 2 data products. It contains information which describes how the Level 1 data was processed to obtain the Level 2 (derived) product. It contains information needed to operate on the data using digital computers and related equipment.

E.A.K

N85-30453*# National Aeronautics and Space Administration. Goddard Space Flight Center, Greenbelt, Md.

NIMBUS 7 COASTAL ZONE COLOR SCANNER (CZCS). LEVEL 1 DATA PRODUCT USERS' GUIDE

S. P. WILLIAMS (Systems and Applied Sciences Corp., Vienna, Va.), E. F. SZAJNA, and W. A. HOVIS Jul. 1985 53 p (NASA-TM-86203; REPT-85B0358, NAS 1.15:86203) Avail: NTIS HC A04/MF A01 CSCL 08C

The coastal zone color scanner (CZCS) is a scanning multispectral radiometer designed specifically for the remote sensing of Ocean Color parameters from an Earth orbiting space platform. A technical manual which is intended for users of NIMBUS 7 CZCS Level 1 data products is presented. It contains information needed by investigators and data processing personnel to operate on the data using digital computers and related equipment.

E.A.K

N85-30459# Massachusetts Inst of Tech, Cambridge. Research Lab of Electronics.

ACTIVE AND PASSIVE REMOTE SENSING OF ICE Semiannual Report, 1 Feb. - 31 Jul. 1984

J. A. KONG Sep. 1984 29 p (Contract N00014-83-K-0258)

(AD-A154406) Avail: NTIS HC A03/MF A01 CSCL 08L

This is a report on the progress that has been made in the study of active and passive remote sensing of ice during the period of February 1, 1984. During this period we have: (1) calculated the emissivity of a two-layer anisotropic random medium; and (2) participated in the microwave sea ice measurement program at the Cold Regions Research and Engineering Laboratory (CRREL). The emissivity of a two-layer anisotropic random medium has been calculated using the dyadic Green's function for a two-layer anisotropic medium and the first-order Born approximation. The emissivity is calculated by obtaining coherent and incoherent reflectivities and by making use of the relationship $\epsilon = 1 - r$. The incoherent reflectivity is obtained by integrating over the upper hemisphere the bistatic scattering coefficients obtained under the Born approximation. The theoretical results are illustrated by plotting the emissivities as functions of viewing angles and polarizations. They are used to interpret the passive microwave remote sensing data from vegetation canopy which also show strong anisotropic dependencies. Data obtained from the field measurements with corn stalks arranged in various configurations with preferred azimuthal directions are successfully interpreted with this model. It is expected that the radiometric data from CRREL measurements will also be successfully interpreted with this

05 OCEANOGRAPHY AND MARINE RESOURCES

theoretical model. A manuscript has been prepared for submission to a journal for publication. GRA

N85-30556# Science Applications International Corp., La Jolla, Calif.

SATELLITE MEASUREMENTS OF ATMOSPHERIC AEROSOLS **Final Report, 1 Dec. 1983 - 18 Nov. 1984**

M GRIGGS 29 Mar. 1985 28 p

(Contract N00014-77-C-0489)

(AD-A153807; SAIC-85/1606) Avail: NTIS HC A03/MF A01
CSCL 04B

An error analysis of the two-channel techniques has shown that the AVHRR noise will result in root-mean-square errors of about 0.40 in the size distribution parameter, and about 0.08N in aerosol content, N. These errors are increased due to the effects of undetected clouds in the field of view and variations in the ocean surface reflectance. Based on an analysis of the Barbados and USNS Hayes data, these environmental errors could be of the same magnitude for, and larger for N. However, because of uncertainties in the data set there is uncertainty in these estimates of the environmental errors GRA

N85-31598# Ohio State Univ., Columbus. Dept of Geology and Mineralogy.

CONTINENTAL AND OCEANIC MAGNETIC ANOMALIES: **ENHANCEMENT THROUGH GRM Abstract Only**

R. R. B. VONFRESE and W. J. HINZE (Purdue Univ., Lafayette, Ind.) *In* Purdue Univ. Improving the Geol. Interpretation of Magnetic and Gravity Satellite Anomalies 4 p 1985 ERTS

Avail: NTIS HC A04/MF A01 CSCL 08N

In contrast to the POGO and MAGSAT satellites, the Geopotential Research Mission (GRM) satellite system will orbit at a minimum elevation to provide significantly better resolved lithospheric magnetic anomalies for more detailed and improved geologic analysis. In addition, GRM will measure corresponding gravity anomalies to enhance our understanding of the gravity field for vast regions of the Earth which are largely inaccessible to more conventional surface mapping. Crustal studies will greatly benefit from the dual data sets as modeling has shown that lithospheric sources of long-wavelength magnetic anomalies frequently involve density variations which may produce detectable gravity anomalies at satellite elevations. Furthermore, GRM will provide an important replication of lithospheric magnetic anomalies as an aid to identifying and extracting these anomalies from satellite magnetic measurements. The potential benefits to the study of the origin and characterization of the continents and oceans, that may result from the increased GRM resolution are examined.

M G.

N85-31609# Centre National d'Etudes Spatiales, Toulouse (France). Centre Spatial.

RESULTS OF THE MIZEX PRELIMINARY CAMPAIGN: 29 JUNE TO 19 JULY 1983 [RESULTATS DE LA CAMPAGNE PRELIMINAIRE MIZEX, 29 JUIN 1983 - 19 JUILLET 1983]

E. CHAPUIS, C. SCHGOUNN, and N. LANNELONGUE 20 Feb 1984 76 p refs *In* FRENCH; ENGLISH summary Sponsored by CNES and CNRS

(CNES-84/142/T/CT/DRT/TIT/RL) Avail: NTIS HC A05/MF A01

A frequency modulated scatterometer mounted on an icebreaker was used to study microwave interactions with sea-ice and water. The frequency, polarization and incidence of radar signals were studied to identify ice types and ice-snow surface characteristics. The most significant results are obtained with a polarized signal that at 13.66 Hz allows the identification of 4 types of surfaces

Author (ESA)

N85-31710*# National Aeronautics and Space Administration. Goddard Space Flight Center, Greenbelt, Md.

GLOBAL MEAN SEA SURFACE BASED UPON A COMBINATION OF THE GEOS-3 AND SEASAT ALTIMETER DATA

J. G. MARSH *In* its Geodyn. Branch Res Program 5 p Aug 1985 refs

Avail: NTIS HC A09/MF A01 CSCL 08C

A global mean sea surface based upon a combination of the total set of GEOS-3 and SEASAT altimeter data was computed. In order to minimize the effects of radial orbit error, a combination of accurate SEASAT reference orbits and crossing-arc techniques was used in the computation process. The mean sea surface provides a reference surface for the detection of mesoscale ocean circulation features, global ocean circulation patterns and detailed information over the oceans on the internal structure of the Earth.

B.W.

N85-31712*# National Aeronautics and Space Administration. Goddard Space Flight Center, Greenbelt, Md.

OCEAN CIRCULATION STUDIES

C. J. KOBLINSKY *In* its Geodyn. Branch Res Program 4 p Aug. 1985 refs

Avail: NTIS HC A09/MF A01 CSCL 08C

Studies were carried out to utilize remotely-sensed signatures of ocean surface characteristics from active and passive satellite-borne radiometers. The large scale low frequency circulation of the world's oceans was examined. Direct observations of low frequency deep-ocean currents have now been made that demonstrate the ocean's response to wind forcing. Low frequency wind-driven deep-ocean currents are thought to provide a background level of eddy kinetic energy and drive the general circulation.

B.W.

N85-31714*# National Aeronautics and Space Administration. Goddard Space Flight Center, Greenbelt, Md.

SEASAT ALTIMETRY FOR SURFACE HEIGHT OF INLAND SEAS

J. E. WELKER *In* its Geodyn. Branch Res. Program 7 p Aug. 1985 refs

Avail: NTIS HC A09/MF A01 CSCL 08C

A pilot study has been conducted to determine a proof of concept analysis for the use of altimetry data in earth resources studies. For the geodynamic studies, the principal interest was centered in the determination of the height, or change in height of inland seas and lakes. The principal target objectives were to determine the type of coverage available for four bodies of water in the Soviet Union, the Caspian, Black, and Aral Seas, and Lake Baikal in Siberia, along with a few bodies of water in the United States, Canada and the People's Republic of China. From the preliminary proof of concept, two major determinations were made for the bodies of water tested. First, an altimetry track from northeast to southwest across the Caspian Sea revealed a profile that dropped approximately 13 meters at its lowest point over a 330 km track path. Secondly, contours also appeared possible for three of the five Great Lakes, and from an initial assessment, a small geoid oscillation was visible over the larger lakes.

B.W.

N85-31716*# National Aeronautics and Space Administration. Goddard Space Flight Center, Greenbelt, Md.

OCEAN TIDAL PARAMETERS FROM LAGEOS

D. CHRISTODOULIDIS and D. E. SMITH *In* its Geodyn. Branch Res. Program 5 p Aug. 1985 refs

Avail: NTIS HC A09/MF A01 CSCL 08C

The LAGEOS satellite is so clearly perturbed by gravitational forces and little else, that it has provided the means of improving the gravity model and models of Earth and ocean tides. A description of the ocean tidal constituents at long wavelength has been obtained in a simultaneous solution from 4 years of laser tracking data. The computed values are compared to those obtained by oceanographic analyses

Author

N85-31735# World Meteorological Organization, Geneva (Switzerland).

COMMISSION FOR MARINE METEOROLOGY Abridged Final Report

1985 126 p Proc. of 9th Session, Geneva, 1-12 Oct 1984 (WMO-640; ISBN-92-63-10640-1) Avail: NTIS MF A01, print copy available at WMO, Geneva

World Meteorological Organization projects in marine observation and data collection, marine climatology, and sea ice were discussed. Technical, administrative, and legal aspects of the Organization's work were covered Author (ESA)

N85-31738*# Jet Propulsion Lab., California Inst of Tech, Pasadena.

TROPICAL OCEAN AND GLOBAL ATMOSPHERE (TOGA) HEAT EXCHANGE PROJECT: A SUMMARY REPORT

W. T. LIU and P. P. NILLER 1 Jun. 1985 16 p refs (Contract NAS7-918)

(NASA-CR-176038; JPL-PUB-85-49; NAS 1.26:176038) Avail. NTIS HC A02/MF A01 CSDL 08J

A pilot data center to compute ocean atmosphere heat exchange over the tropical ocean is proposed at the Jet Propulsion Laboratory (JPL) in response to the scientific needs of the Tropical Ocean and Global Atmosphere (TOGA) Program. Optimal methods will be used to estimate sea surface temperature (SET), surface wind speed, and humidity from spaceborne observations. A monthly summary of these parameters will be used to compute ocean atmosphere latent heat exchanges. Monthly fields of surface heat flux over tropical oceans will be constructed using estimations of latent heat exchanges and short wave radiation from satellite data. Verification of all satellite data sets with in situ measurements at a few locations will be provided. The data center will be an experimental active archive where the quality and quantity of data required for TOGA flux computation are managed. The center is essential to facilitate the construction of composite data sets from global measurements taken from different sensors on various satellites. It will provide efficient utilization and easy access to the large volume of satellite data available for studies of ocean atmosphere energy exchanges. Author

N85-32223# Naval Ocean Systems Center, San Diego, Calif.
USING SHIP WAKE PATTERNS TO EVALUATE SAR (SYNTHETIC APERTURE RADAR) OCEAN WAVE IMAGING MECHANISMS. JOINT US-CANADIAN OCEAN WAVE INVESTIGATION PROJECT Interim Technical Report, FY83 - FY84

R. R. HAMMOND, R. R. BUNTZEN, and E. E. FLOREN Feb 1985 68 p (Contract NR PROJ ZR0-3103, NR PROJ. ZR0-0001) (AD-A154633; NOSC/TR-978) Avail NTIS HC A04/MF A01 CSDL 17I

The Joint Ocean Wave Investigation Project (JOWIP) was conducted to evaluate the detectability of ocean wave structures on imaging synthetic aperture radar (SAR). This project used Kelvin surface ship wake patterns generated under controlled and well documented surface environmental conditions to isolate SAR image parameters. Use of waves of known wavelength and direction provide the opportunity to evaluate the SAR contribution to ocean wave forecasting. SEASAT-like images made with L-band SAR are presented: (1) to suggest how ship-generated surface roughness combines with the velocity-bunching mechanism in calm ocean areas to produce the unusually narrow wakes observed for azimuth-traveling ships on SEASAT images; and (2) to estimate conditions under which SAR image modulation mechanisms can be expected to produce wake images. A method is described for using the Kelvin transverse ship wake wave component to quantitatively evaluate the contributions of various SAR ocean wave imaging mechanisms. It makes use of the narrow sector of surface roughness generated by a ship along its track to produce SAR images of the longest waves in its wake system on flat calm water. GRA

N85-32310# Emory Univ., Atlanta, Ga Dept. of Chemistry.

A MICROPROCESSOR-CONTROLLED, MULTICHANNEL FLUORIMETER FOR ANALYSIS OF SEA WATER

P. B. OLDHAM, G. PATONAY, and I. M. WARNER 30 Apr 1985 29 p

(Contract N00014-83-K-0026)

(AD-A154986; EMORY/DC/TR/6) Avail: NTIS HC A03/MF A01 CSDL 08J

The multichannel fluorimeter described provides good sensitivity and rapid data acquisition. The advantages of multichannel fluorescence detection are discussed with special reference to the continuous monitoring of in vivo chlorophyll fluorescence in sea waters. Experiments on chlorophyll a determinations indicate a detection limit of 5 times 10 to the minus 12th power M with a linear range over at least three orders of magnitudes of concentration. GRA

N85-32369*# Woods Hole Oceanographic Institution, Mass Dept of Geology and Geophysics

DEEP SEA MEGA-GEOMORPHOLOGY: PROGRESS AND PROBLEMS

W. B. BRYAN /in NASA Goddard Space Flight Center Global Mega-Geomorphology p 54-55 Jul. 1985

Avail: NTIS HC A07/MF A01 CSDL 08C

Historically, marine geologists have always worked with mega-scale morphology. This is a consequence both of the scale of the ocean basins and of the low resolution of the observational remote sensing tools available until very recently. In fact, studies of deep sea morphology have suffered from a serious gap in observational scale. Traditional wide-beam echo sounding gave images on a scale of miles, while deep sea photography has been limited to scales of a few tens of meters. Recent development of modern narrow-beam echo sounding coupled with computer-controlled swath mapping systems, and development of high-resolution deep-towed side-scan sonar, are rapidly filling in the scale gap. These technologies also can resolve morphologic detail on a scale of a few meters or less. As has also been true in planetary imaging projects, the ability to observe phenomena over a range of scales has proved very effective in both defining processes and in placing them in proper context. G.L.C

N85-32388# Army Engineer Waterways Experiment Station, Vicksburg, Miss. Environmental Lab.

HANDBOOK FOR OBTAINING AND USING AERIAL PHOTOGRAPHY TO MAP AQUATIC PLANT DISTRIBUTION Final Report

J. M. LEONARD Nov. 1984 42 p

(AD-A154584; WES-IR-A-84-2) Avail. NTIS HC A03/MF A01 CSDL 06C

Stepwise procedures are given for the tasks required in using low-altitude aerial photography to map aquatic plants. The tasks include problem identification, photomission design, acquisition of ground truth data, and photointerpretation and data presentation. The sources of existing aerial photographs and the general and technical requirements for aerial photography are given in Appendixes A and B, respectively. Author (GRA)

N85-32584# Naval Postgraduate School, Monterey, Calif.

MESOSCALE FEATURES AND ATMOSPHERIC REFRACTION CONDITIONS OF THE ARCTIC MARGINAL ICE ZONE M.S. Thesis

J. A. MCNITT Dec. 1984 129 p

(AD-A155139; AD-F630645) Avail NTIS HC A07/MF A01 CSDL 04A

This thesis summarizes the Marginal Ice Zone Experiment (MIZEX-83) conducted in the Arctic during the summer of 1983 and describes the mesoscale features and atmospheric refraction conditions. The three case studies examined are: warm air advection over dense pack ice causing strong elevated ducting and subrefraction; cold air advection over relatively open water causing shallow convection and normal refraction conditions; and large scale subsidence in the western quadrants of an anticyclone leading to super-refraction and weak ducting. Developing synoptic

05 OCEANOGRAPHY AND MARINE RESOURCES

scale cyclones adjacent to the MIZEX-83 area often determined the airflow over the region. The observed large horizontal sea surface temperature gradients were the dominant forcing mechanisms on surface layer stability. Trapping layers associated with subsidence inversions can be located on satellite imagery by assuming that stratiform clouds form immediately below the inversion. Uniform cloud and refraction layers were not common during MIZEX-83 due to strong mesoscale variability. Factors affecting inversion height include subsidence and entrainment mixing. Bulk Richardson number value for locations over the open water and pack ice show significant variability in stability conditions across the MIZ. GRA

N85-32622# Colorado State Univ., Fort Collins. Dept. of Atmospheric Science.

PROPERTIES OF AEROSOL PARTICLES DETECTED BY SATELLITES IN COASTAL REGIONS

E. E. HINDMAN, P. A. DURKEE, and W. KEUNNING *In Intern. Comm. for Cloud Phys. 11th Intern. Conf. on Atmosphere Aerosols, Condensation and Ice Nuclei, Vol 2 p 148-154 1984 refs (Contract N00014-79-C-0793)*

Avail: NTIS HC A09/MF A01

The particles detected in the marine boundary layer were primarily spherical, 1 to 6 microns in diameter and of oceanic origin. Optical depths 0.04 to 0.10 were resolved. The particles detected above the boundary layer were primarily submicron, partially hygroscopic and a mixture of rural, oceanic and possibly urban particles. These particles could mask radiation scattered by boundary layer particles. Near-simultaneous satellite radiometric measurements and airborne aerosol measurements have shown particles of oceanic origin are responsible for a majority of the scattered energy in cloud-free regions except when significant upper-level haze layers are present R.J.F.

N85-32660# Institute of Experimental Meteorology (USSR).

THE VARIABILITY OF AEROSOL MICROSTRUCTURE IN CONTINENTAL AND OCEANIC SURFACE LAYERS OF THE ATMOSPHERE IN ANTICYCLONES

N. V. GONCHAROV, O. A. LIPSKAYA, V. V. SMIRNOV, and A. D. UVAROV *In International Commission for Cloud Physics 11th Intern. Conf. on Atmospheric Aerosols, Condensation and Ice Nuclei, Vol 1 p 154-158 1984 refs*

Avail: NTIS HC A14/MF A01

Data on the atmospheric $D=0.01-20$ micron aerosol dispersive composition and variability, generalized for summer and winter anticyclones typical of the center of the European territory of the USSR and the Southern Hemisphere oceans are presented.

Author

N85-32707# Naval Postgraduate School, Monterey, Calif.

COASTAL EROSION ALONG MONTEREY BAY M.S. Thesis

A. I. SKLAVIDIS and W. R. LIMABLANCO Mar. 1985 108 p (AD-A155610) Avail: NTIS HC A06/MF A01 CSCL 08C

Permanent beach erosion in Southern Monterey Bay, CA, is episodic, occurring infrequently when high tides coincide with stormy weather which allows wave action to erode the toe of the cliffs. This thesis uses precise aerial photogrammetric techniques to measure cliff recession from 1946 through 1984. Maximum erosion occurs in the vicinity of Fort Ord (7.3 ft yr) and decreases to the south. A model is developed to predict cliff erosion based on the hypothesis that erosion occurs only when the water level due to combined tides, wave set-up and run-up exceeds the cliff elevation. The model combines predicted tidal elevations and wave heights. Shallow water wave heights at various locations are calculated by transforming deep-water directional wave spectra provided by the Fleet Numerical Oceanography Center. Refraction of the wave energy is responsible for the variability of erosion rates along the shore. The bathymetry of Monterey Bay is such that the refracted wave energy is greater in the Fort Ord area than to the south. The erosion model was calibrated using the spectral wave climatology and aerial photographs covering an 18-year period. The model qualitatively replicates the temporal variability of the measured recession rates and gives a reasonable

prediction of the spatial variation of the mean recession rates.

GRA

N85-33384# Joint Publications Research Service, Arlington, Va. **BASIC PROPERTIES AND INTERPRETATION OF SYNTHESIZED RADAR IMAGES OF SEA WAVES WITH LONG SYNTHETIZATION TIME Abstract Only**

A. V. IVANOV *In its USSR Rept. Electron. and Elec. Eng. (JPRS-UEE-84-003) p 3 21 Mar 1984 Transl. into ENGLISH from Izv. Vysshikh Uchebn. Zavedeniy. Radiofiz (Gorkiy), v. 26, no 5, May 1983 p 540-550 Previously announced in IAA as A83-41793*

Avail: NTIS HC A05/MF A01

The synthetic-aperture-radar (SAR) imaging of sea waves is considered as a process of measuring the correlation between values of backscattered radiation of the SAR for different azimuthal positions of the SAR platform. A relatively simple description is proposed for the focusing effect peculiar to the SAR imaging of sea waves, and it is shown that the wave image contrast does not degrade with increasing synthesis time. The same results are obtained by the direct analysis of the transformation of the radar input signal (calculated in accordance with the two-scale model of scattering) into an image for the case of a sinusoidal wave without limits on the synthesis time. B.J.

N85-33651*# SeaSpace, San Diego, Calif.

LARGE-SCALE SEA SURFACE TEMPERATURE VARIABILITY FROM SATELLITE AND SHIPBOARD MEASUREMENTS

R. L. BERNSTEIN and D. B. CHELTON (Oregon State Univ., Corvallis) 30 Apr. 1985 40 p refs Prepared in cooperation with JPL, Pasadena, Calif. Original contains color illustrations (NASA-CR-176123, JPL-9950-1142; NAS 1.26:176123) Avail: NTIS HC A03/MF A01 CSCL 08J

A series of satellite sea surface temperature intercomparison workshops were conducted under NASA sponsorship at the Jet Propulsion Laboratory. Three different satellite data sets were compared with each other, with routinely collected ship data, and with climatology, for the months of November 1979, December 1981, March 1982, and July 1982. The satellite and ship data were differenced against an accepted climatology to produce anomalies, which in turn were spatially and temporally averaged into two-degree latitude-longitude, one-month bins. Monthly statistics on the satellite and ship bin average temperatures yielded rms differences ranging from 0.58 to 1.37 C, and mean differences ranging from -0.48 to 0.72 C, varying substantially from month to month, and sensor to sensor. Author

N85-33653# Department of Energy, Morgantown, W. Va. Energy Technology Center

ARCTIC AND OFFSHORE RESEARCH Technology Status Report

Oct. 1984 32 p

(DE85-001995; DOE/METC/85-0219) Avail: NTIS HC A03/MF A01

The DOE Arctic and Offshore Research (AOR) effort is designed to meet the needs for a centralized, high quality, Arctic energy related data base and for long term, high risk research. The ultimate purpose of the DOE effort is to promote extensive private use of the evolving AOR technology data base in order to accelerate development of Arctic oil and gas resources. Current activities included determining the Arctic bibliographic data base and initiating most pieces of the research described above (except multiyear ice properties and pipeline research). Some of the FY 1984 major accomplishments are: four to five ice islands 1 to 2 miles in length drifting off the Ellesmere ice shelves north of Ellesmere Island were aerially surveyed. A report was completed on the location of the ice shelf edge, breakup, and regrowth of the Ellesmere ice shelves over the past two decades. Ice ridging shear zone studies have shown that the 6 to 10 feet high shoals usually under the shear zone are not totally destroyed from ice gouging from one year to the next, but that the ice gouging may be instrumental in initiating and maintaining the shoals, which may protect Arctic offshore structures. Airborne radar sensing techniques were used

to determine the electromagnetic properties of sea ice and physical properties. DOE

N85-34327* National Aeronautics and Space Administration. Pasadena Office, Calif.
METHOD AND APPARATUS FOR DELTA KAPPA SYNTHETIC APERTURE RADAR MEASUREMENT OF OCEAN CURRENT Patent

A. JAIN, inventor (to NASA) (JPL, Pasadena, Calif.) 2 Apr. 1985 8 p Filed 18 Mar. 1982 Supersedes N82-28502 (20 - 19, p 2673)
 (NASA-CASE-NPO-15704-1; US-PATENT-4,509,048; US-PATENT-APPL-SN-359382; US-PATENT-CLASS-343-5-CM, US-PATENT-CLASS-343-5-W, US-PATENT-CLASS-343-17 2-PC)
 Avail: US Patent and Trademark Office CSCL 171

A synthetic aperture radar (SAR) employed for delta k measurement of ocean current from a spacecraft without the need for a narrow beam and long observation times. The SAR signal is compressed to provide image data for different sections of the chirp band width, equivalent to frequencies and a common area for the separate image fields is selected. The image for the selected area at each frequency is deconvolved to obtain the image signals for the different frequencies and the same area. A product of pairs of signals is formed, Fourier transformed and squared. The spectrum thus obtained from different areas for the same pair of frequencies are added to provide an improved signal to noise ratio. The shift of the peak from the center of the spectrum is measured and compared to the expected shift due to the phase velocity of the Bragg scattering wave. Any difference is a measure of current velocity $v \sin \theta$ (delta k).

Official Gazette of the U.S. Patent and Trademark Office

N85-35322*# Jet Propulsion Lab., California Inst. of Tech., Pasadena.

MICROWAVE PROPERTIES OF A QUIET SEA

J. STACEY 15 May 1985 74 p refs
 (Contract NAS7-918)

(NASA-CR-176199; NAS 1.26 176199; JPL-PUB-85-33) Avail: NTIS HC A04/MF A01 CSCL 20N

The microwave flux responses of a quiet sea are observed at five microwave frequencies and with both horizontal and vertical polarizations at each frequency--a simultaneous 10 channel receiving system. The measurements are taken from Earth orbit with an articulating antenna. The 10 channel responses are taken simultaneously since they share a common articulating collector with a multifrequency feed. The plotted flux responses show: (1) the effects of the relative, on-axis-gain of the collecting aperture for each frequency; (2) the effects of polarization rotation in the output responses of the receive when the collecting aperture mechanically rotates about a feed that is fixed; (3) the difference between the flux magnitudes for the horizontal and vertical channels, at each of the five frequencies, and for each pointing position, over a 44 degree scan angle; and (4) the RMS value of the clutter--as reckoned over the interval of a full swath for each of the 10 channels. The clutter is derived from the standard error of estimate of the plotted swath response for each channel. The expected value of the background temperature is computed for each of the three quiet seas. The background temperature includes contributions from the cosmic background, the downwelling path, the sea surface, and the upwelling path. Author

N85-35439# Geological Survey, Alexandria, Va.
MARINE PHOSPHORITE DEPOSITS MODEL FOR EXPLORATION, WITH EMPHASIS ON DEPOSITS IN THE US ATLANTIC COASTAL PLAIN Abstract Only

J. B. CATHCART In *its* USGS Res on Mineral Resources, 1985 p 7 1985
 Avail: NTIS HC A05/MF A01

Phosphorus is an essential element for growth in plants and animals; its principal source is deposits of phosphate rock. Onshore deposits of phosphorite, a marine sedimentary rock, constitute about 80 percent of the world's phosphate resources and are the source for about 80 percent of world production. Identified

resources (reserve base) of phosphorite in the world are estimated to be about 69 billion metric tons containing at least 25 percent P₂O₅, and resources in deposits that may become economic are thought to be about double the identified resources. Deposits on the sea floor form an additional, probably enormous, resource. R.J.F.

N85-35465# Geological Survey, Washington, D.C.
USGS COASTAL RESEARCH, STUDIES AND MAPS: A SOURCE OF INFORMATION FOR COASTAL DECISION MAKING

J. T. SUN, ed. 1985 84 p
 (USGS-CIRC-883) Avail: NTIS HC A05/MF A01

The tasks of the U.S. Geological Survey (USGS) coastal research, an information resource for coastal decision making, are outlined. The different projects include: coastal zone management, national mapping, geologic and water resources investigation and research, and activities applicable to coastal states. E.A.K.

06

HYDROLOGY AND WATER MANAGEMENT

Includes snow cover and water runoff in rivers and glaciers, saline intrusion, drainage analysis, geomorphology of river basins, land uses, and estuarine studies

A85-40098#
PROFILE STATISTICS OF RAIN IN SLANT PATH AS MEASURED WITH A RADAR

C. CAPSONI, E. MATRICCIANI, and M. MAURI (Milano, Politecnico, Milan, Italy) Alta Frequenza (English Edition) (ISSN 0002-6557), vol 54, Mar.-Apr. 1985, p. 50-57. refs

Rain rate profile statistics along a slant path have been derived with the use of an S band meteorological radar, calibrated with the satellite SIRIO beacon. The results may be used as physical inputs to models for the prediction of rain attenuation in satellite-earth radiolinks operating at frequencies above 10 GHz. Information is given about absolute and conditional rain rate, space autocorrelation functions and correlation distances. Also distributions of point rain rate versus slant distance are given: these latter present two regions of 'apparent stationarity', discussed in the paper. Joint and marginal distributions among the above variables have been computed showing high correlation between the parameters related to rain rate, while no significant correlation exists between rain rate and path length. Also average and standard deviation curves of profiles normalized to their maximum values versus slant distance are given. Author

A85-41320#
HYDROLOGIC AND LAND SCIENCES APPLICATIONS OF NOAA POLAR-ORBITING SATELLITE DATA

M. MATSON and F. PARMENTER-HOLT Washington, DC, U.S. Department of Commerce, 1985. 20 p refs
 (Contract NOAA-NA-83SAC00650)

The National Environmental Satellite, Data, and Information Service (NESDIS) of the National Oceanic and Atmospheric Administration (NOAA) operates the civil polar-orbiting satellite system for the collection of environmental data. This program began in 1960 with the launch of Tiros-1. Successive satellites in the Improved Tiros Operational Satellite (ITOS) program include concurrent multiple-channel sensing on a daily basis. The data obtained with the sensors of the NOAA satellites are used for hydrology and land sciences. In a discussion of hydrologic applications, attention is given to the continental snow cover, a regional snow cover assessment, river basin snow mapping, river flood monitoring, and soil moisture analysis. A description is provided of studies related to renewable resources, taking into account monitoring vegetation progress, seasonal vegetation changes, fire fuels monitoring, fire detection, and fire monitoring.

06 HYDROLOGY AND WATER MANAGEMENT

Urban effects are also considered along with dust and sandstorm monitoring, volcanoes, and a geologic assessment. G.R.

A85-45693

EVALUATION OF SPOT HRV SIMULATION DATA FOR CORPS OF ENGINEERS APPLICATIONS

H. L. MCKIM and C. J. MERRY (U.S. Army, Cold Regions Research and Engineering Laboratory, Hanover, NH) (COSPAR, Plenary Meeting, 25th Workshop II on the Earth's Surface Studied from Space, Graz, Austria, June 25-July 7, 1984) *Advances in Space Research* (ISSN 0273-1177), vol. 5, no. 5, 1985, p. 61-71. Army-sponsored research. refs

Land cover classifications and water quality assessments were carried out for three different aquatic regions of the U.S., based on simulated data of the High Resolution Visible (HRV) radiometer instrument onboard SPOT. The three sites were: Chesapeake Bay, MD; Berlin Lake, OH, and Lac Qui Parle, MN. Multispectral imagery data of 20-meter resolution were obtained for each of the sites in three spectral bands: 0.50-0.59 microns; 0.61-0.68 microns; and 0.79-0.89 microns. The data were analyzed for use in dredging; recreational resource management; and wildlife habitat monitoring. In situ water quality measurements in the Lac Qui Parle site were compared with the simulated SPOT data, and the results are discussed. I.H.

A85-47923* Wisconsin Univ., Madison

MEASURING THE GLOBAL DISTRIBUTION OF INTENSE CONVECTION OVER LAND WITH PASSIVE MICROWAVE RADIOMETRY

R. W. SPENCER and D. A. SANTEK (Space Science and Engineering Center, Madison, WI) *Journal of Climate and Applied Meteorology* (ISSN 0733-3021), vol. 24, Aug. 1985, p. 860-864. refs

(Contract NAG5-391)

The global distribution of intense convective activity over land is shown to be measurable with satellite passive-microwave methods through a comparison of an empirical rain rate algorithm with a climatology of thunderstorm days for the months of June-August. With the 18 and 37 GHz channels of the Nimbus-7 Scanning Multichannel Microwave Radiometer (SMMR), the strong volume scattering effects of precipitation can be measured. Even though a single frequency (37 GHz) is responsive to the scattering signature, two frequencies are needed to remove most of the effect that variations in thermometric temperatures and soil moisture have on the brightness temperatures. Because snow cover is also a volume scatterer of microwave energy at these microwavelengths, a discrimination procedure involving four of the SMMR channels is employed to separate the rain and snow classes, based upon their differences in average thermometric temperature. Author

A85-49116* Atmospheric and Environmental Research, Inc., Cambridge, Mass.

STRONG FLUCTUATION THEORY FOR SCATTERING, ATTENUATION, AND TRANSMISSION OF MICROWAVES THROUGH SNOWFALL

Y.-Q. JIN (Atmospheric and Environmental Research, Inc., Cambridge, MA) and J. A. KONG (MIT, Cambridge, MA) *IEEE Transactions on Geoscience and Remote Sensing* (ISSN 0196-2892), vol. GE-23, Sept. 1985, p. 754-760. refs

(Contract NAG5-270; NSF ECS-82-03390; N00014-83-K-0528)

The strong fluctuation theory is applied to the study of the atmospheric snowfall which is modeled as a layer of random discrete-scatterers medium. As functions of size distribution, fractional volume, and radius of scatterers, the relationship is illustrated between the reflectivity factor and precipitation rate, the attenuation of the centimeter and millimeter waves, and the line-of-sight transmission of coherent and incoherent wave components. The theoretical results are shown to match favorably with experimental data. Author

N85-31603* Jet Propulsion Lab., California Inst of Tech., Pasadena.

MICROWAVE HYDROLOGY: A TRILOGY

J. M. STACEY, E. J. JOHNSTON, M. A. GIRARD, and H. A. REGUSTERS 1 Apr. 1985 48 p

(Contract NAS7-918)

(NASA-CR-176042; JPL-PUB-85-21; NAS 1.26:176042) Avail:

NTIS HC A03/MF A01 CSCL 08H

Microwave hydrology, as the term is construed in this trilogy, deals with the investigation of important hydrological features on the Earth's surface as they are remotely, and passively, sensed by orbiting microwave receivers. Microwave wavelengths penetrate clouds, foliage, ground cover, and soil, in varying degrees, and reveal the occurrence of standing liquid water on and beneath the surface. The manifestation of liquid water appearing on or near the surface is reported by a microwave receiver as a signal with a low flux level, or, equivalently, a cold temperature. Actually, the surface of the liquid water reflects the low flux level from the cosmic background into the input terminals of the receiver. This trilogy describes and shows by microwave flux images: the hydrological features that sustain Lake Baykal as an extraordinary freshwater resource; manifestations of subsurface water in Iran; and the major water features of the Congo Basin, a rain forest.

Author

N85-32570* South Dakota School of Mines and Technology, Rapid City.

RAIN VOLUME ESTIMATION OVER AREAS USING SATELLITE AND RADAR DATA Semiannual Report, 1 Jan. - 30 Jun. 1985

A. A. DONEAUD and T. H. VONDERHAAR 30 Jun. 1985 22 p refs

Prepared in cooperation with Colorado State Univ., Fort Collins

(Contract NAG5-386)

(NASA-CR-176050; NAS 1.26:176050) Avail: NTIS HC A02/MF

A01 CSCL 04B

The feasibility of rain volume estimation over fixed and floating areas was investigated using rapid scan satellite data following a technique recently developed with radar data, called the Area Time Integral (ATI) technique. The radar and rapid scan GOES satellite data were collected during the Cooperative Convective Precipitation Experiment (CCOPE) and North Dakota Cloud Modification Project (NDCMP). Six multicell clusters and cells were analyzed to the present time. A two-cycle oscillation emphasizing the multicell character of the clusters is demonstrated. Three clusters were selected on each day, 12 June and 2 July. The 12 June clusters occurred during the daytime, while the 2 July clusters during the nighttime. A total of 86 time steps of radar and 79 time steps of satellite images were analyzed. There were approximately 12-min time intervals between radar scans on the average. B.W.

N85-35466 Texas Univ., Austin.

HYDROGEOLOGY OF THE LOWER GLEN ROSE AQUIFER, SOUTH-CENTRAL TEXAS Ph.D. Thesis

W. W. HAMMOND, JR. 1984 344 p

Avail. Univ. Microfilms Order No. DA8508274

The lower member of the Glen Rose Formation contains one of the most productive and laterally extensive aquifers in the region. The lower member is divided into an upper and lower unit on the basis of lithologic and hydrologic differences. Ground water in the Lower Glen Rose aquifer is under confined and unconfined conditions. Two types of systems of groundwater flow are present, a regional system dominated by syndepositional permeability and porosity, and many local systems produced by later solutional activity. Isotopic dating of samples of ground water from the Lower Glen Rose aquifer by C yields modern apparent ages for ground water of the local systems and old apparent ages (8,490 to 28,980 years) for ground water of the regional system. Velocity of ground water movement in the regional system as determined by C analyses ranges from 4.2 to 4.9 m/year. Velocities obtained from hydrologic parameters compare favorably with these values. A similar range of velocity of ground water movement was determined for the Floridan aquifer of Florida and the Pahasapa Limestone of South Dakota and Wyoming. Dissert. Abstr.

N85-35467# Pennsylvania State Univ., University Park. Office of Remote Sensing of Earth Resources.

REMOTE SENSING OF HYDROLOGIC TRANSPORT PROCESSES USING SPOT SIMULATION DATA Final Report, 1 Aug. 1983 - 30 Apr. 1985

T. W. GARDNER, G. W. PETERSEN, K. F. CONNORS, and G. M. BAUMER Apr. 1985 125 p refs
(Contract DE-AC02-83ER-60182)
(DE85-012412; DOE/ER-60182/1) Avail: NTIS HC A06/MF A01

The utility of the next generation of high resolution, digital satellite imagery was evaluated to characterize surface hydrology and geomorphology in both arid and humid regions. The simulated data have three multispectral (MS) bands. Resolution of the SPOT system allows for landscape classification at level three and occasionally level four across distinctly different climatic zones and in areas disturbed by different types of energy exploitation. Given the SPOT feature recognition and the extensive data base on Quaternary history and rates of surficial geomorphic processes for the two study sites, it was possible to recognize and classify critical components of the hydrologic system and landscape stability. These component maps include (1) infiltration/ potential runoff rate maps; (2) groundwater recharge/discharge site maps; (3) landscape stability maps, and (4) fluvial erosion intensity maps. Eight analytic techniques, including manual interpretation of four analog imagery and statistical analyses of digital imagery are evaluated. E A K.

07

DATA PROCESSING AND DISTRIBUTION SYSTEMS

Includes film processing, computer technology, satellite and aircraft hardware, and imagery.

A85-41396

A FAST FOURIER TRANSFORM METHOD FOR COMPUTING TERRAIN CORRECTIONS

M G SIDERIS (Calgary, University, Canada) Manuscripta Geodetica (ISSN 0340-8825), vol. 10, no. 1, 1985, p. 66-73. NSERC-supported research. refs

The paper presents a method of evaluating the terrain correction integral using the Fast Fourier Transform. The method requires height data on a regular grid and produces terrain corrections on all grid points. For a 1 km grid spacing, the accuracy is generally better than 1.5 mgal for typically rough areas and is rather insensitive to errors in the data. The required CPU time is proportional to $N \log N$, where N is the number of grid points. This paper also discusses the covariance function computation by Fourier techniques. The method is most suitable for application in the solution of geodetic boundary value problems, but it can also be used for other types of geodetic or geophysical problems involving terrain corrections. Author

A85-41658

CONTEXTUAL CLASSIFICATION POST-PROCESSING OF LANDSAT DATA USING A PROBABILISTIC RELAXATION MODEL

R. HARRIS (Durham, University, England) International Journal of Remote Sensing (ISSN 0143-1161), vol. 6, June 1985, p. 847-866 refs

A85-41659

THE GENERATION AND INTERPRETATION OF FALSE-COLOUR COMPOSITE PRINCIPAL COMPONENT IMAGES

A. A. D. CANAS and M. E. BARNETT (Imperial College of Science and Technology, London, England) International Journal of Remote Sensing (ISSN 0143-1161), vol. 6, June 1985, p. 867-881. refs

Following the observation that the presentation of multichannel image information as a false color composite is achievable with minimum sacrifice of data if the three leading image components are used, rather than the three conventional 'raw' channels, a hard wired electronic system has been developed which implements principal components analysis on a 256×256 four-channel array of pixels in a few seconds. The system is controlled by a microcomputer, and can generate color hard copy outputs in the form of composites of the principal component images. The system's use is illustrated by a Landsat MSS subframe of southern Spain. The necessity of contrast stretching the minor principal component images, in order to generate a visually effective color composite, is demonstrated. O.C.

A85-41660

STANDARDIZED PRINCIPAL COMPONENTS

A. SINGH (Reading, University, England) and A. HARRISON (NERC, Thematic Information Services, Swindon, England) International Journal of Remote Sensing (ISSN 0143-1161), vol. 6, June 1985, p. 883-896 Research supported by the Forest Department of Manipur refs

In remote sensing, principal components analysis is usually performed using unstandardized variables. However, the use of standardized variables yields significantly different results. In this paper principal components of two Landsat MSS subscenes were separately calculated using both methods. The results indicate substantial improvement in signal-to-noise ratio and image enhancement by using standardized variables in the principal components analysis. Author

A85-41664

IMPROVING THEMATIC MAPPER LAND COVER CLASSIFICATION USING FILTERED DATA

P. ATKINSON, J. L. CUSHNIE, J. R. G. TOWNSHEND (Reading, University, England), and A. WILSON (NERC, Thematic Information Services, Swindon, England) International Journal of Remote Sensing (ISSN 0143-1161), vol. 6, June 1985, p. 955-961. refs
(Contract NERC-F60/G6/03)

In an attempt to alleviate the classification problems introduced by the higher spatial resolution of the Thematic Mapper in comparison to the Multispectral Scanner, classifications were performed on two to six band combinations, first using Thematic Mapper bands only, and subsequently replacing band 5 by its mean-filtered and median-filtered counterpart. The combination of filtered data with non-filtered data smooths out scene noise while retaining some of the boundary detail. Author

A85-42511

MEASUREMENT AND ANALYSIS OF 2-D INFRARED NATURAL BACKGROUND

N. BEN-YOSEF, K. WILNER, S. SIMHONY, and G. FEIGIN (Jerusalem, Hebrew University, Israel) Applied Optics (ISSN 0003-6935), vol. 24, July 15, 1985, p. 2109-2113. refs

Natural background was recorded in the 8-12-micron band using an airborne IR camera. The results were analyzed and the statistical and spatial features of the radiance in this band were found. The statistical distribution approaches the normal distribution inside the two standard deviation regions but deviates slightly outside. The spatial autocorrelation function fits to a high degree a 2-D exponent. Author

A85-42584

MODELING MANUAL EXTRACTION OF TEXTURAL ELEMENTS BY MATHEMATICAL MORPHOLOGY

G. FLOUZAT and Y. MERGHOU (Centre d'Etude Spatiale des Rayonnements, Toulouse, France) Photo Interpretation (ISSN 0031-8523), vol. 22, Nov.-Dec. 1983, 6 p. In English, French, and Spanish.

The results of attempts to mathematically perform photointerpretation tasks of remotely sensed imagery are illustrated in terms of the analysis of a Landsat image. Textural features are preserved by one- or multi-dimensional classifications in the first thematic examination of pixels, then construction and extraction of textural elements by the laws of mathematical morphology (MM). The MM technique joins neighboring pixels of similar signatures and generates the features numerically. Erosion and expansion operators combined to form opening and closing operations permit the classification of sets of pixels representing agricultural, village, forest and water areas and surface minerals. Although some errors are observed, the resulting binary filter is concluded useful for an overall analysis requiring discriminations among villages and other structures. M.S.K.

A85-42853* New York State Univ., Syracuse.

COMMENTS ON THE INTERCALIBRATION OF MULTISENSOR, MULTITEMPORAL, MULTICHANNEL DIGITAL RADIANCE DATA

M. J. DUGGIN (New York, State University, Syracuse) Applied Optics (ISSN 0003-6935), vol. 24, Aug. 1, 1985, p. 2292-2294. refs

(Contract USDA-58-319T-40238X; NAS5-27595)

When comparing the recorded radiance data obtained on a given date by means of different sensors or on different dates using the same sensor, the values in question must be referred to some common datum. It is presently noted that more data are required for remote sensing instruments, and that these should consist of gain, offset, spectral response and point spread function for each bandpass. Such information will be the bases for studies of sensor intercalibration procedure. O.C.

A85-43118

ON THE ANALYSIS OF THERMAL INFRARED IMAGERY - THE LIMITED UTILITY OF APPARENT THERMAL INERTIA

J. C. PRICE (USDA, Plant Physiology Institute, Beltsville, MD) Remote Sensing of Environment (ISSN 0034-4257), vol. 18, Aug. 1985, p. 59-73. refs

A spectral window in the thermal infrared permits observations of surface temperature by satellite radiometry. The Heat Capacity Mapping Mission (HCMM) acquired 10-12 micron data at times of day favorable for estimation of surface thermal properties and the surface energy budget. Two variables, surface wetness, which controls evaporation and hence mean surface temperature, and thermal inertia, which relates the diurnal excursion of surface temperature to ground heat flux, are responsible for most observed temperature variability. These variables may be estimated from the midnight (2:30 a.m.) and early afternoon (1:30 p.m.) data from the HCMM or from the afternoon NOAA satellites. However, the HCMM data product, 'apparent thermal inertia,' is potentially misleading in agricultural areas because surface evaporation reduces the amplitude of the soil heat flux compared to the amplitude in dry areas. Thus apparent thermal inertia should not be used in regions having variability in surface moisture. Author

A85-44864

CARTOGRAPHIC-PHOTOGRAMMETRIC ANALYSIS AND ANALYTICAL CORRECTION OF SPACE SCANNER IMAGES [KARTOGRAFO-FOTOGRAFMETRICHESKII ANALIZ I ANALITICHESKOE ISPRAVLENIE SKANERNYKH KOSMICHESKIKH IZOBRAZHENII]

B. A. NOVAKOVSKII and P. V. PETROV Geodeziia i Kartografiia (ISSN 0016-7126), June 1985, p. 39-41. In Russian refs

It is demonstrated, on the example of multispectral scanner images obtained with the Meteor-satellite Fragment system, that the analytical correction of space scanner images makes possible

a significant improvement in the accuracy with which coordinates on the earth surface can be determined from such images. This leads to an improvement in the accuracy and efficiency with which cartographic information can be obtained. B.J

A85-45687* Santa Barbara Research Center, Goleta, Calif.

LANDSAT IMAGE DATA QUALITY STUDIES

C. F. SCHUELER (Santa Barbara Research Center, Goleta, CA) and V. V. SALOMONSON (NASA, Goddard Space Flight Center, Greenbelt, MD) (COSPAR, Plenary Meeting, 25th: Workshop II on the Earth's Surface Studied from Space, Graz, Austria, June 25-July 7, 1984) Advances in Space Research (ISSN 0273-1177), vol. 5, no. 5, 1985, p. 1-11 refs

Preliminary results of the Landsat-4 Image Data Quality Analysis (LIDQA) program to characterize the data obtained using the Thematic Mapper (TM) instrument on board the Landsat-4 and Landsat-5 satellites are reported. TM design specifications were compared to the obtained data with respect to four criteria, including spatial resolution; geometric fidelity; information content; and image reliability to Multispectral Scanner (MSS) data. The overall performance of the TM was rated excellent despite minor instabilities and radiometric anomalies in the data. Spatial performance of the TM exceeded design specifications in terms of both image sharpness and geometric accuracy, and the image utility of the TM data was at least twice as high as MSS data. The separability of alfalfa and sugar beet fields in a TM image is demonstrated. I.H.

A85-45692

SPOT IMAGE QUALITY AND POST-LAUNCH ASSESSMENT

G. BEGNI, B. BOISSIN, and J. PERBOS (CNES, Toulouse, France) (COSPAR, Plenary Meeting, 25th Workshop II on the Earth's Surface Studied from Space, Graz, Austria, June 25-July 7, 1984) Advances in Space Research (ISSN 0273-1177), vol. 5, no. 5, 1985, p. 51-60. refs

The image quality specifications of the SPOT are presented, and the methods used to evaluate SPOT performance are described. Consideration is given to two separate categories of evaluation techniques: pre-launch ground testing, and post-launch assessment during the first two months in orbit. Specifications are described with respect to image location accuracy; length distortion; multi-data and multispectral recording; and local coherence. Radiometric specifications are presented with respect to: SNR; detector equalization, distortion due to high radiances (blooming); and the modulation transfer function (MTF). Plans for post-launch assessment following the launching of the SPOT in August 1985 are described. I.H.

A85-45695

MULTIPLE SENSOR GEOCODED DATA

F. E. GUERTIN, R. SIMARD, R. J. BROWN, P. M. TEILLET (Canada Centre for Remote Sensing, Ottawa), and D. FRIEDMANN (MacDonald Dettwiler and Associates, Ltd., Richmond, Canada) (COSPAR, Plenary Meeting, 25th Workshop II on the Earth's Surface Studied from Space, Graz, Austria, June 25-July 7, 1984) Advances in Space Research (ISSN 0273-1177), vol. 5, no. 5, 1985, p. 81-90. refs

A general description is given of the design of the Multi-Observational Satellite Image Correction (MOSAICS) system for integrating remotely sensed images from satellites into a reference projection. The MOSAICS system is currently being developed for use with the Canadian National Topographic System for resource management applications. The main processing functions of MOSAICS include: data transcription; data correction; manual and digital control point marking, and geocoding to a national standard map base. The geocoded data are formatted to film and CCT products. MOSAICS will offer bulk scene and geocoded subscene projections of Landsat MSS and TM data, together with data from the HRV and PLA sensors of SPOT. The hardware and software requirements of MOSAICS are considered, with emphasis given to its high functionality and throughput rate. The digital stereo processing procedure of MOSAICS was used

to derive a Digital Evaluation Model (DEM) from Landsat-4 TM data. Contour plots of the DEM are presented in a table. I H

A85-47807

INVESTIGATION OF LANDSAT-4 THEMATIC MAPPER LINE-TO-LINE AND BAND-TO-BAND REGISTRATION AND RELATIVE DETECTOR CALIBRATION

J. DESACHY (Toulouse III, Université, France), G. BEGNI, B. BOISSIN, and J. PERBOS (CNES, Toulouse, France) Photogrammetric Engineering and Remote Sensing (ISSN 0099-1112), vol. 51, Sept. 1985, p. 1291-1298 refs

It has been found that image quality parameters can have an important influence on the results of users' investigations. An evaluation of the scanners delivering the images is, therefore, of the first importance. The defaults linked to the scanner itself can be partially corrected by a ground preprocessing. A study of the raw image quality is needed to optimize the ground segment algorithms. The present study is concerned with the Thematic Mapper (TM). Aspects of line-to-line and band-to-band registration are discussed, taking into account the use of a method based on automatic correlation techniques, intraband misregistrations, and misregistrations between different bands. Attention is also given to the general problem of detector calibration and the related bright target saturation. G R

A85-47809* Environmental Research Inst. of Michigan, Ann Arbor.

CHARACTERIZATION AND COMPARISON OF LANDSAT-4 AND LANDSAT-5 THEMATIC MAPPER DATA

M. D. METZLER and W. A. MALILA (Michigan, Environmental Research Institute, Ann Arbor) Photogrammetric Engineering and Remote Sensing (ISSN 0099-1112), vol. 51, Sept. 1985, p. 1315-1330. refs
(Contract NAS5-27346)

Engineering analyses of Thematic Mapper (TM) image data have been conducted, giving particular attention to the radiometric characterization of the sensor. While the data in general were found to be excellent, anomalies do exist in the data from both Landsat-4 and Landsat-5 TM. A summary is provided of the Landsat-4 TM image data. The present paper concentrates, however, on recent analyses of Landsat-5 TM data and comparisons of the radiometry of the two sensors. One of the specific topics covered is within-line droop, a phenomenon whereby the signal levels of the sensor change systematically during the active scan. Attention is also given to scan-correlated level shifts, an effect which raises or lowers the signal level of all pixels in a scan line or set of scan lines. A comparison of Landsat-4 and Landsat-5 radiometric corrections is also discussed. G.R.

A85-47810

INTRABAND RADIOMETRIC PERFORMANCE OF THE LANDSAT THEMATIC MAPPERS

H. H. KIEFFER, D. A. COOK, E. M. ELIASON, and P. T. ELIASON (U.S. Geological Survey, Flagstaff, AZ) Photogrammetric Engineering and Remote Sensing (ISSN 0099-1112), vol. 51, Sept. 1985, p. 1331-1350. refs

The present report is concerned with several intrinsic radiometric characteristics of the Landsat-4 and Landsat-5 Thematic Mappers (TMs). The approach employed is based on an examination of internal consistency within natural scenes rather than depending on calibration data. It is pointed out that the overall behavior of the TMs is excellent; imperfect behavior is barely discernible in a typical image. The reported study is part of the Landsat Image Data Quality Analysis Program conducted by NASA. Attention is given to the Landsat scenes used in this report, the width of the digital levels, aspects of level shift, droop, overshoot, delay in bright-target recovery, noise, and a comparison of Landsat-4 and Landsat-5 responses. G.R.

A85-47812

ASSESSMENT OF RADIOMETRIC ACCURACY OF LANDSAT-4 AND LANDSAT-5 THEMATIC MAPPER DATA PRODUCTS FROM CANADIAN PRODUCTION SYSTEMS

J. M. MURPHY, F. J. AHERN, P. F. DUFF (Canada Centre for Remote Sensing, Ottawa), and A. J. FITZGERALD (Roy Ball Associates, Ottawa, Canada) Photogrammetric Engineering and Remote Sensing (ISSN 0099-1112), vol. 51, Sept. 1985, p. 1359-1369. refs

A85-47813* General Electric Co., Lanham, Md.

METHODS FOR DESTRIPIING LANDSAT THEMATIC MAPPER IMAGES - A FEASIBILITY STUDY FOR AN ONLINE DESTRIPIING PROCESS IN THE THEMATIC MAPPER IMAGE PROCESSING SYSTEM (TIPS)

D. J. POROS and C. J. PETERSON (General Electric Co., Space Div., Lanham, MD) Photogrammetric Engineering and Remote Sensing (ISSN 0099-1112), vol. 51, Sept. 1985, p. 1371-1378. refs

(Contract NAS5-25300)

Methods for destripping TM images and results of the application of these methods to selected TM scenes with sensor and scan striping, which was not removed by the radiometric correction during the TM Archive Generation Phase in TIPS, are presented. These methods correct only for gain and offset differences between detectors over many image lines and do not consider within-line effects. The feasibility of implementing a destripping process online in TIPS is also described. Author

A85-47817* Arizona Univ., Tucson.

LANDSAT THEMATIC MAPPER IMAGE-DERIVED MTF

R. A. SCHOWENGERDT (Arizona Remote Sensing Center; Arizona, University, Tucson), C. ARCHWAMETY (Arizona, University, Tucson), and R. C. WRIGLEY (NASA, Ames Research Center, Moffett Field, CA) Photogrammetric Engineering and Remote Sensing (ISSN 0099-1112), vol. 51, Sept. 1985, p. 1395-1406 refs

(Contract NCC2-234)

The Landsat Image Data Quality Analysis (LIDQA) Program conducted by NASA has the objective to quantify the performance of the Thematic Mapper (TM) on the Landsat-4 and Landsat-5 spacecraft. The interest in the spatial resolution performance of the TM is partly related to the decrease of the instantaneous field of view (IFOV) from 80 m for the MSS to 30 m for the TM. Studies related to the preflight line spread function (LSF), square wave response (SWR), and theoretical component modeling of the TM system modulation transfer function (MTF) have been conducted. However, the need remains to estimate the MTF of the complete system. The present paper is concerned with investigations related to this task. Attention is given to three approaches for measuring the MTF of the TM system from imagery. G.R.

A85-47818

LANDSAT-4 AND LANDSAT-5 THEMATIC MAPPER DATA QUALITY ANALYSIS

E. MALARET, L. A. BARTOLUCCI, D. F. LOZANO, P. E. ANUTA, and C. D. MCGILLEM (Purdue University, West Lafayette, IN) Photogrammetric Engineering and Remote Sensing (ISSN 0099-1112), vol. 51, Sept. 1985, p. 1407-1416. refs

The analysis of Landsat-5 Thematic Mapper (TM-5) data described in this paper was undertaken to evaluate geometric and radiometric quality. Anuta et al. (1984) had analyzed Landsat-4 Thematic Mapper (TM-4) and Multispectral Scanner (MSS) data for the geometric and radiometric quality and information content. The results of the studies related to Landsat-5 are compared with the results of the Landsat-4 study. Attention is given to aspects of band-to-band misregistration, striping effects, a coherent noise analysis, the resolution estimation in TM data, the calibration of Landsat-5 TM thermal IR data, and system response curves for the Landsat-4 and Landsat-5 thermal IR band detectors. G.R.

07 DATA PROCESSING AND DISTRIBUTION SYSTEMS

A85-47820* State Univ. of New York, Syracuse
SYSTEMATIC AND RANDOM VARIATIONS IN THEMATIC MAPPER DIGITAL RADIANCE DATA

M. J. DUGGIN, H. SAKHAVAT (New York, State University, Syracuse), and J. LINDSAY (Systems and Applied Sciences Corp., Vienna, VA) Photogrammetric Engineering and Remote Sensing (ISSN 0099-1112), vol 51, Sept. 1985, p. 1427-1434. refs (Contract NAS5-27595)

Studies are reported of the systematic and random variations in digital radiance data obtained by the Landsat-4 and Landsat-5 Thematic Mappers over an agricultural crop area which was apparently uniform and cloud-free. Systematic variations appeared to be time-dependent and bandpass-dependent. The predominant effect seemed to be random variations, which appeared to be in keeping with those expected from prior investigations. It is suggested that uncorrected variations will provide a limitation on the nonphotointerpretative analysis of images. Author

A85-47821* Jet Propulsion Lab., California Inst of Tech., Pasadena.

AN ANALYSIS OF LANDSAT THEMATIC MAPPER P-PRODUCT INTERNAL GEOMETRY AND CONFORMITY TO EARTH SURFACE GEOMETRY

N. A. BRYANT, A. L. ZOBRIST, R. E. WALKER, and B. GOKHMAN (California Institute of Technology, Jet Propulsion Laboratory, Pasadena) Photogrammetric Engineering and Remote Sensing (ISSN 0099-1112), vol 51, Sept. 1985, p. 1435-1447. refs

Performance requirements regarding geometric accuracy have been defined in terms of end product goals, but until recently no precise details have been given concerning the conditions under which that accuracy is to be achieved. In order to achieve higher spatial and spectral resolutions, the Thematic Mapper (TM) sensor was designed to image in both forward and reverse mirror sweeps in two separate focal planes. Both hardware and software have been augmented and changed during the course of the Landsat TM developments to achieve improved geometric accuracy. An investigation has been conducted to determine if the TM meets the National Map Accuracy Standards for geometric accuracy at larger scales. It was found that TM imagery, in terms of geometry, has come close to, and in some cases exceeded, its stringent specifications. G R

A85-47822* Environmental Research Inst. of Michigan, Ann Arbor.

COMPARISON OF THE INFORMATION CONTENTS OF LANDSAT TM AND MSS DATA

W. A. MALILA (Michigan, Environmental Research Institute, Ann Arbor) Photogrammetric Engineering and Remote Sensing (ISSN 0099-1112), vol 51, Sept. 1985, p. 1449-1457. refs (Contract NAS5-27346)

A communications-theory approach is taken to analyze the dispersion and concentration of signal values in various data spaces, irrespective of specific class membership. Entropy is used to quantify information, and mutual information is used to measure the information represented by subsets of spectral variables. Several different comparisons of information content are made. These include comparisons of system design capacities, of data volumes occupied by agricultural data in the spaces defined by original bands and by transformed spectral (Tasseled Cap) variables, of the information contents of original bands and Tasseled Cap variables, and of the information contents of TM and MSS for the given agricultural data sets. Also, the effects of sample size, scene content, and quantization level are examined. Author

A85-47823* National Aeronautics and Space Administration. Goddard Space Flight Center, Greenbelt, Md.

PERFORMANCE COMPARISONS BETWEEN INFORMATION EXTRACTION TECHNIQUES USING VARIABLE SPATIAL RESOLUTION DATA

R. S. LATTY, R. NELSON, B. MARKHAM, D. WILLIAMS, D. TOLL (NASA, Goddard Space Flight Center, Greenbelt, MD) et al. Photogrammetric Engineering and Remote Sensing (ISSN 0099-1112), vol. 51, Sept. 1985, p. 1459-1470. NASA-supported research refs

The decreased instantaneous field of view (IFOV) is one of the principal advances noted for the Thematic Mapper (TM) sensor. The 42.5 microradian IFOV of TM and the 710 km nominal orbit altitude result in a 30 m nominal spatial resolution at the earth surface. This is a considerable decrease in the projected pixel area when compared to the 79 m nominal spatial resolution of the Landsat Multispectral Scanner (MSS). An experiment was conducted which allowed a rigorous test of the influence of classifier design, with data spatial resolution of TM (30 m) and approximately that of the Landsat MSS (90 m), on classification performance for a particular TM scene. The experiment involved evaluation of the results for the per-point Gaussian maximum likelihood (GML) classifier and the supervised ECHO (Extraction and Classification of Homogeneous Objects) classifier. G.R.

A85-47824* National Aeronautics and Space Administration. Goddard Space Flight Center, Greenbelt, Md.

LANDSAT-4 THEMATIC MAPPER SCENE CHARACTERISTICS OF A SUBURBAN AND RURAL AREA

D. L. TOLL (NASA, Goddard Space Flight Center, Greenbelt, MD) Photogrammetric Engineering and Remote Sensing (ISSN 0099-1112), vol. 51, Sept. 1985, p. 1471-1482. refs

The Thematic Mapper (TM) sensor, which is carried by the Landsat-4 and Landsat-5 satellites, represents the latest generation of an earth resource scanner system. TM applications range from determining the extent and changes of land cover to estimating agricultural yields. The TM has improvements over the Multispectral Scanner (MSS) with respect to spatial resolution, spectral regions, and radiometry. The present paper is concerned with two major objectives related to the analysis of the Landsat TM. One of these objectives is related to an evaluation of the utility of TM in the discrimination of surface cover. In connection with the second objective, an evaluation was conducted of the utility of selected image processing procedures to enhance the capability of Landsat TM to map land cover. It was found that TM data may be used for discriminating smaller targets, such as agricultural fields and city blocks, than previously obtainable with MSS data. G.R.

A85-47825
EFFECT OF SPATIAL FILTERING ON SCENE NOISE AND BOUNDARY DETAIL IN THEMATIC MAPPER IMAGERY

J. L. CUSHNIE and P. ATKINSON (Reading University, England) Photogrammetric Engineering and Remote Sensing (ISSN 0099-1112), vol. 51, Sept. 1985, p. 1483-1493. refs (Contract NERC-F60/G6/03)

The improvement in spatial resolution provided by the Thematic Mapper (TM) of the Landsat-4 and Landsat-5 satellites has resulted in visually more interpretable images. However, computer interpretations using the standard per-point classifiers have in some cases been less than satisfactory. In an investigation of the effects of increasingly fine spatial resolution on per-point classification, it was found that the internal variation (or scene noise) within cover classes is increased. Thus, the presence of trees, roads, and lawns in residential areas may lead to classification difficulties. On the other hand, a reduction in the proportion of mixed or boundary pixels leads to a corresponding reduction in the number of misclassified or rejected pixels. The present study is concerned with reducing the scene noise effects within land cover categories where this is necessary, without significantly increasing the proportion of boundary pixels between the categories. G.R.

N85-30450*# National Aeronautics and Space Administration Langley Research Center, Hampton, Va.
SPECTRAL REFLECTANCES OF NATURAL TARGETS FOR USE IN REMOTE SENSING STUDIES

D. E. BOWKER, R. E. DAVIS, D. L. MYRICK, K. STACY, and W. T. JONES Jun 1985 185 p refs Prepared in cooperation with Computer Sciences Corp.
 (NASA-RP-1139, L-15920; NAS 1.61:1139) Avail. NTIS HC A09/MF A01 CSCL 20F

A collection of spectral reflectances of 156 natural targets is presented in a uniform format. For each target both a graphical plot and a digital tabulation of reflectance is given. The data were taken from the literature and include laboratory, field, and aircraft measurements. A discussion of the different measurements of reflectance is given, along with the changes in apparent reflectance when targets are viewed through the atmosphere. The salient features of the reflectance curves of common target types are presented and discussed. Author

N85-33158# Joint Publications Research Service, Arlington, Va.
INTERACTIVE PROCEDURES FOR DISCRIMINATING AND RESTORING CONTOUR LINE NETWORKS Abstract Only

R. I. ELMAN *In its* USSR Rept.: Space (JPRS-USP-84-006) p 126-127 14 Nov. 1984 Transl. into ENGLISH from Issled. Zemli iz Kosmosa (Moscow), no. 2, Mar - Apr. 1984 p 87-97 Avail. NTIS HC A08

In computer aided topical mapping using data derived from aerial and space photographs the contour lines comprising the structural outlines of a map can be fed into the computer in various ways (encoder, TV or optomechanical input unit). A series of interactive procedures are analyzed which allow an operator controlling a display to discriminate the sketched outline on a photograph and reproduce it on the screen of the display within the precision allowed by computer digitization errors. It is assumed that the contour outlines are sketched on the photos by the person interpreting them with white gouache paint. The discrimination of the contour lines is accomplished by either an indistinct mask or a logic mask. Following the discrimination procedures, the contour outlines in the marker display memory are in binary form. The recovery procedures are based on the use of a domain with dimensions of 3x3 store locations. The techniques and decision making rules for the reproduction of the contours are discussed in depth and illustrated with sample maps, showing the intermediate stages. Author

N85-33165# Joint Publications Research Service, Arlington, Va.
REPETITION OF DENSE CLOUD COVER ABOVE INDIAN OCEAN FROM GENERALIZED SATELLITE DATA Abstract Only

R V ABRAMOV *In its* USSR Rept.: Space (JPRS-USP-84-006) p 132 14 Nov. 1984 Transl. into ENGLISH from Izv. Vsesoyuznogo Geograficheskogo Obshchestva (Leningrad), v. 116, no. 2, Mar - Apr 1984 p 138-144 Avail. NTIS HC A08

Using as a data base information contained in the USSR Hydrometeorological Center maps compiled during the period 1967 to 1971 (produced from pictures obtained by Soviet and U.S. satellites for the purpose of petroleum analysis) an attempt was made to determine patterns of repetition in dense cloud cover above the Indian Ocean (latitude 30 deg south to 30 deg north, longitude 30 deg east to 150 deg east) and the association (if any) between cloud type and cloud cover. It was found that the cloud cover repetition patterns during the survey period (1967 to 1971) was most marked in the region of the equator, reaching 25 to 26% between 92 deg east and 96 deg east. In the median field cloud cover repetition reached approximately 10.6%. Patterns over the Indian Ocean are compared with similar patterns over the Atlantic and Pacific oceans, and the significance of cloud cover patterns on global thermal flows is discussed. Cloud types were analyzed. It was found that the dominant type overall above the Indian Ocean is cumuliform, which does not usually form dense cloud covers. Dense covers of cumulus dominate in the east equatorial and Arabian Sea zones. Stratiform and cirrus frequently

accompany cumulus. It is concluded that most of the dense cloud cover in the Southern Hemisphere occurs in the equatorial region and that the Southern Hemisphere is still the major recipient of solar heat Author

N85-34547# Perception Computing, Inc., Downsview (Ontario).
THE SCIENTIFIC AND TECHNICAL ISSUES IN INTEGRATING REMOTELY SENSED IMAGERY WITH GEOCODED DATA BASES

W. M. STROME and B. GRUSH *In* Canadian Information Processing Society Graphics Interface 1985 p 171-177 1985 refs

Avail: NTIS HC A19/MF A01

Digital analysis techniques of remote sensed data are discussed. The decreasing cost of computer equipment, especially both on-line and off-line memory, has led to an explosion in the use of digital mapping techniques. It is recognized that the full potential benefits of satellite remote sensing can not be realized until digital analysis of satellite image data and automated cartography/geocoded information systems are more compatible and integrated. The difficulties associated with this integration are explored. E.A K

N85-34548# National Research Council of Canada, Ottawa (Ontario).

SELECTION OF SEGMENT SIMILARITY MEASURES FOR HIERARCHICAL PICTURE SEGMENTATION

J M. BEAULIER and M. GOLDBERG (Ottawa Univ) *In* Canadian Information Processing Society Graphics Interface 1985 p 179-186 1985 refs

Avail: NTIS HC A19/MF A01

The problem of defining appropriate segments similarity measures for picture segmentation was examined. In agglomerative hierarchical segmentation, two segments are compared and merged if found similar. The approximation error resulting from merging two segments. Similarity measures derived from constant approximations and planar approximations are applied to a LANDSAT picture, and the results are presented. The advantages of combining similarity measures are stressed. Different picture areas require different measures which must be combined to obtain good overall results. In hierarchical segmentation, simple measures are used for the first merging steps, while, at a higher level of the segment hierarchy, more complex measures are employed.

E.A.K.

N85-35463*# Purdue Univ., West Lafayette, Ind. Lab. for Application of Remote Sensing.

LANDSAT-4/5 IMAGE DATA QUALITY ANALYSIS Final Report, 9 Aug. 1982 - 8 Dec. 1984

E. MALARET, L. A. BARTOLUCCI, D. F. LOZANO, P. E. ANUTA, and C. D. MCGILLEM 8 Dec. 1984 80 p refs Original contains imagery. Original photography may be purchased from the EROS Data Center, Sioux Falls, S.D. 57198 ERTS (Contract NAS5-26859)

(E85-10105; NASA-CR-176264; NAS 1.26:176264;

LARS-CR-060185) Avail: NTIS HC A05/MF A01 CSCL 05B

A LANDSAT Thematic Mapper (TM) quality evaluation study was conducted to identify geometric and radiometric sensor errors in the post-launch environment. The study began with the launch of LANDSAT-4. Several error conditions were found, including band-to-band misregistration and detector-to-detector radiometric calibration errors. Similar analysis was made for the LANDSAT-5 Thematic Mapper and compared with results for LANDSAT-4. Remaining band-to-band misregistration was found to be within tolerances and detector-to-detector calibration errors were not severe. More coherent noise signals were observed in TM-5 than in TM-4, although the amplitude was generally less. The scan direction differences observed in TM-4 were still evident in TM-5. The largest effect was in Band 4 where nearly a one digital count difference was observed. Resolution estimation was carried out using roads in TM-5 for the primary focal plane bands rather than field edges as in TM-4. Estimates using roads gave better resolution. Thermal IR band calibration studies were conducted and new nonlinear calibration procedures were defined for TM-5.

07 DATA PROCESSING AND DISTRIBUTION SYSTEMS

The overall conclusion is that there are no first order errors in TM-5 and any remaining problems are second or third order.

Author

N85-35464* Environmental Research Inst. of Michigan, Ann Arbor Infrared and Optics Div.

STUDY OF SPECTRAL/RADIOMETRIC CHARACTERISTICS OF THE THEMATIC MAPPER FOR LAND USE APPLICATIONS Quarterly Status Technical Progress Report, 21 Dec. 1984 - 20 Mar. 1985

W. A. MALILA and M. D. METZLER, Principal Investigators May 1985 74 p refs ERTS

(Contract NAS5-27346)

(E85-10106; NASA-CR-175317; NAS 1.26.175317;

ERIM-164000-18-P) Avail: NTIS HC A04/MF A01 CSCL 08B

Progress during ERIM's tenth quarter of effort under the LANDSAT-4 and 5 Image Data Quality Assessment program for the Thematic Mapper is described. Coincident LANDSAT-4 and 5 fully corrected (CCT-PT) TM data are analyzed in more detail and revised band-by-band relationships between the two sensors derived. An analysis technique employing the matching of cumulative distributions is developed and used and is believed to offer advantages over the histogram matching procedure currently used to produce LANDSAT data. Multiplicative factors ranging from 0.987 to 1.145 and offsets ranging from -2.7 to -6.2 video quantum levels are required to cause LANDSAT-5 data to match LANDSAT-4 data values. Evidence of low level clipping is found in TM Bands 5 and 7 of LANDSAT-5 but not LANDSAT-4. Analysis of the information content of LANDSAT TM and MSS data is continued. Components of information loss are identified and quantified and the effects of coarsened quantization are explored

Author

N85-35566# National Oceanic and Atmospheric Administration, Washington, D. C. National Environmental Satellite, Data and Information Service.

SURFACE CYCLOGENESIS AS INDICATED BY SATELLITE IMAGERY

F. J. SMIGIELSKI and G. P. ELLROD Mar 1985 37 p refs (PB85-191815; NOAA/TM-NESDIS-9) Avail: NTIS HC A03/MF A01 CSCL 04B

Indications of extratropical cyclogenesis which can be observed in infrared, visible or 6.7 micrometers moisture channel satellite imagery are summarized. These include semi-quantitative techniques for estimating the minimum central pressure and the location and strength of maximum surface winds accompanying the low. Satellite analysis of extratropical storm systems is invaluable over oceanic regions where conventional data is limited.

GRA

08

INSTRUMENTATION AND SENSORS

Includes data acquisition and camera systems and remote sensors.

A85-40792* Washington Univ., Seattle.

THEORY OF MICROWAVE REMOTE SENSING

L. TSANG (Washington, University, Seattle), J. A. KONG, and R. T. SHIN (MIT, Cambridge, MA) Research supported by the Schlumberger-Doll Research Center, NSF, NASA, Navy, et al. New York, Wiley-Interscience, 1985, 627 p. refs

Active and passive microwave remote sensing of earth terrains is studied. Electromagnetic wave scattering and emission from stratified media and rough surfaces are considered with particular application to the remote sensing of soil moisture. Radiative transfer theory for both the random and discrete scatterer models is examined. Vector radiative transfer equations for nonspherical particles are developed for both active and passive remote sensing. Single and multiple scattering solutions are illustrated with

applications to remote sensing problems. Analytical wave theory using the Dyson and Bethe-Salpeter equations is employed to treat scattering by random media. The backscattering enhancement effects, strong permittivity fluctuation theory, and modified radiative transfer equations are addressed. The electromagnetic wave scattering from a dense distribution of discrete scatterers is studied. The effective propagation constants and backscattering coefficients are calculated and illustrated for dense media

C.D.

A85-41089* Wisconsin Univ., Madison.

RESTORATION OF MULTICHANNEL MICROWAVE RADIOMETRIC IMAGES

R. T. CHIN, C.-L. YEH (Wisconsin, University, Madison), and W. S. OLSON (Eastman Kodak Research Laboratories, Rochester, NY) IEEE Transactions on Pattern Analysis and Machine Intelligence (ISSN 0162-8828), vol. PAMI-7, July 1985, p. 475-484. Research supported by the University of Wisconsin refs (Contract NAGW-380)

A constrained iterative image restoration method is applied to multichannel diffraction-limited imagery. This method is based on the Gerchberg-Papoulis algorithm utilizing incomplete information and partial constraints. The procedure is described using the orthogonal projection operators which project onto two prescribed subspaces iteratively. Its properties and limitations are presented. The effect of noise was investigated and a better understanding of the performance of the algorithm with noisy data has been achieved. The restoration scheme with the selection of appropriate constraints was applied to a practical problem. The 6.6, 10.7, 18, and 21 GHz satellite images obtained by the scanning multichannel microwave radiometer (SMMR), each having different spatial resolution, were restored to a common, high resolution (that of the 37 GHz channels) to demonstrate the effectiveness of the method. Both simulated data and real data were used in this study. The restored multichannel images may be utilized to retrieve rainfall distributions.

Author

A85-41362#

ON OBSERVATION OF MIDDLE ATMOSPHERE WITH LAS (LIMB-ATMOSPHERIC INFRARED SPECTROMETER) ON BOARD OF SATELLITE 'OHZORA' (EXOS-C)

A. MATSUZAKI, T. ITOH, and Y. NAKAMURA (Tokyo, University, Japan) (Japan-U.S. Seminar on Review of Work Related to Sensing of Stratospheric Aerosol and Gas Components, Fukuoka, Japan, June 12-14, 1984) Meteorological Society of Japan, Journal (ISSN 0026-1165), vol. 63, April 1985, p. 328-333. refs

An IR spectrometer on board the satellite Ohzora for taking atmospheric limb absorption spectra is described, together with observational results. The instrument analyzes sunlight passing through the limb and permits identification of various atmospheric species. Spectra are recorded in the 1.6-2.4, 2.8-4.8 and 8.8-10.2 microns intervals by 32- and 64-element self-scanning pyroelectric arrays. Sample data from April 1984 observations are discussed, noting distinctions between water vapor and aerosol signatures. A variation of aerosol scattering extinction was noted to be a function of altitude

M.S.K.

A85-41570#

PROBABILITIES, PROBLEMS, AND PERSPECTIVES OF MICROWAVE LONG-RANGE RECONNAISSANCE [MOEGELICHKEITEN, PROBLEME UND PERSPEKTIVEN DER MIKROWELLENFERNERKUNDUNG]

W. KEYDEL (DFVLR, Institut fuer Hochfrequenztechnik, Oberpfaffenhofen, West Germany) (International Union of Radio Science and Nachrichtentechnische Gesellschaft, Gemeinsame Tagung, Kleinheubach, West Germany, Oct. 1-5, 1984) Kleinheubacher Berichte (ISSN 0343-5725), vol. 28, 1985, p. 385-398. In German. refs

The present state of the art in the use of radar and microwave remote sensing of land and sea is discussed in terms of technology and areas of application. The problems and potential of long-range reconnaissance are highlighted, in particular those pertaining to the use of microwave sensors in aircraft and satellites. Different methods of remote sensing are compared in terms of their

parameters, such as radial and tangential velocity, distance, bandwidth, integration time, and all-weather capability. C.D.

A85-41571#
SIGNATURE MEASUREMENTS USING COOLED MICROWAVE RADIOMETERS AT FREQUENCIES FROM 90 GHZ TO 140 GHZ [SIGNATURMESSUNGEN MIT GEKUEHLTEN MIKROWELLENRADIOMETERN BEI FREQUENZEN VON 90 GHZ UND 140 GHZ]

H. SUESS (DFVLR, Institut fuer Hochfrequenztechnik, Oberpfaffenhofen, West Germany) (International Union of Radio Science and Nachrichtentechnische Gesellschaft, Gemeinsame Tagung, Kleinheubach, West Germany, Oct. 1-5, 1984) Kleinheubacher Berichte (ISSN 03430-5725), vol. 28, 1985, p. 399-408. In German. refs

A passive, modular 90-140 GHz microwave imaging system is described, and the multiplicity of signatures from objects in the environment is demonstrated using selected characteristic measurement results. The physical background of the system is examined, including the Rayleigh-Jeans law, the radiation temperature, and the contributions of eigenemission and background emission to the radiation temperature of a natural object. The structure of the imaging system is described, as is the preparation and presentation of the data. Images and derived histograms and temperature profiles are presented for flights over water- and vegetation-covered surfaces, over a built-up island, and over a parking place. C.D.

A85-42292#
REMOTE SENSING OF TEMPERATURE PROFILES FROM A COMBINATION OF OBSERVATIONS FROM THE SATELLITE-BASED MICROWAVE SOUNDING UNIT AND THE GROUND-BASED PROFILER

E. R. WESTWATER, Z. WANG (NOAA, Wave Propagation Laboratory, Boulder, CO), N. C. GRODY, and L. M. MCMILLIN (NOAA, National Environmental Satellite, Data, and Information Service, Washington, DC) Journal of Atmospheric and Oceanic Technology (ISSN 0739-0572), vol. 2, June 1985, p. 97-109. refs

Temperature profiles are derived from ground- and satellite-based microwave radiometric observations. Data taken by the NOAA Profiler during December 1981 to December 1982, at Stapleton International Airport, Denver, CO, are combined with NOAA 6/7 Microwave Sounding Unit (MSU) observations over Denver. The results of 460 retrievals by the Profiler, the MSU, and the Profiler + MSU are compared with soundings by National Weather Service radiosondes (RAOBs). From the surface to 300 mb, maximum rms differences between the combined retrievals and RAOBs are less than about 2 K. For 17 cases in March 1981, radiometric data from the Profiler and MSU were combined with tropopause height measurements obtained from a VHF radar. The combined retrievals using the tropopause height information were improved in the vicinity of the tropopause by about 2 K rms relative to the pure passive ones. Author

A85-42475
CRYOGENIC MAGNETIC GRADIOMETERS FOR SPACE APPLICATIONS

R. HASTINGS, R. P. S. MAHLER, R. SCHNEIDER, JR., and J. H. ERAKER (Sperry Corp., Eagan, MN) IEEE Transactions on Geoscience and Remote Sensing (ISSN 0196-2892), vol. GE-23, July 1985, p. 552-561. refs

This article proposes the use of superconducting magnetic gradiometer, magnetometer sensors based on SQUID technology as sensors for space-borne magnetic investigations. The existing state of the art of such sensors is described. Estimates of their performance as space sensors is made; in particular, it is shown that they will provide magnetic data of improved sensitivity and accuracy over conventional magnetic sensors. It is also found that gradiometers of the sensitivity proposed here will aid in the analytic continuation of field data, will allow separation of magnetic field temporal variations from field changes due to flight past fixed magnetic sources, will provide the ability to make meaningful

measurements of fixed anomalies on magnetospherically active days, and will allow increased spatial resolution of magnetic sources. The requirements for a high-performance space gradiometer sensor are described as well as current progress aimed at achieving such a sensor. Satellite system requirements are also addressed. Particular attention is given to magnetic noise sources in the sensor environment and to the problems associated with reducing this noise to the desired sensor noise levels. Author

A85-42484#
THE SELECTION OF OPTIMUM SPECTRAL CHANNELS FOR MULTISPECTRAL REMOTE SENSING

C.-S. WANG Chinese Journal of Space Sciences, vol. 5, Jan. 1985, p. 45-52. In Chinese, with abstract in English.

A technique based on statistically determined maximum-information criteria is developed to facilitate the selection of multispectral remote-sensing channels. The information value of each possible combination of channels is estimated by calculating the determinants of a correlation matrix constructed using data on the spectral properties of the objects of interest. Since for large numbers of channels this procedure is complex and time-consuming, a quasi-optimum selection procedure is considered. Numerical results for a typical remote-sensing problem involving channels in the 450-1650-nm range are presented in tables and graphs and compared with experimental data. T.K.

A85-42576* Jet Propulsion Lab., California Inst. of Tech., Pasadena.

LASERS IN SPACE

E. D. HINKLEY, J. R. LESH, and R. T. MENZIES (California Institute of Technology, Jet Propulsion Laboratory, Pasadena) Laser Focus (ISSN 0023-8589), Feb. 1985, 6 p. NASA-supported research. refs

Hinkley and Herring (1984) have considered the differences between active (laser) and passive remote sensing from space. The conclusion was reached that spaceborne lasers will eventually complement passive sensors in providing information on the distributions of key atmospheric species and meteorological parameters. Precise information can also be obtained of ice sheet and crustal dynamics for geological and mapping applications. NASA initiated recently an airborne measurement program directed toward some of these objectives. The program employs optical radar (laser radar) systems onboard the NASA advanced ER-2 high-flying aircraft. The results of the experiments are to provide important information with respect to the potential utility of spaceborne laser remote sensing. A study indicated that a spaceborne pulsed carbon dioxide laser could measure tropospheric winds. Attention is also given to measurements of atmospheric gases by spaceborne lasers, solid-state lasers for spaceborne remote sensing, and laser communication in space. G.R.

A85-43074
DATA ACQUISITION AND PROCESSING SYSTEM BASED ON A MICROPROCESSOR SET FOR THE STUDY OF EARTH RESOURCES [СИСТЕМА СБОРА І ОБРАБОТКИ ДАНИЙ НА МІКРОПРОЦЕСОРНИХ НАБОРАХ ДЛІА ІСЛІДОВАНІЯ ПРІРОДНИХ РЕСУРСІВ]

O. I. A. GUMETSKII, V. I. RAKOV, and I. A. IATSUN Kosmicheskie Issledovaniia na Ukraine (ISSN 0321-4508), no. 18, 1984, p. 57-62. In Russian

Problems in the design of multichannel data acquisition and processing systems for the remote sensing of earth resources are examined. The functional diagram, description, and specifications of a system of this type based on the K589-series microprocessor set are presented. B.J.

A85-43115* Maryland Univ., Baltimore.

THE ATMOSPHERIC EFFECT ON THE SEPARABILITY OF FIELD CLASSES MEASURED FROM SATELLITES

Y. J. KAUFMAN (NASA, Goddard Space Flight Center, Greenbelt; Maryland, University, Baltimore) Remote Sensing of Environment (ISSN 0034-4257), vol. 18, Aug. 1985, p. 21-34. refs

The atmospheric effect on the upward radiance emerging from the atmosphere above a nonuniform surface results in a reduction of the separability between the surface classes by broadening the radiance probability distribution of each class, while narrowing the total radiance range. The atmospheric modulation transfer function (MTF) is used in Fourier transform analyses to simulate the atmospheric effect on the imagery of a nonuniform surface and to demonstrate the atmospheric effect on separability of field classes. Author

A85-43116* National Aeronautics and Space Administration. Goddard Space Flight Center, Greenbelt, Md.

SENSOR-INDUCED TEMPORAL VARIABILITY OF LANDSAT MSS DATA

R. F. NELSON (NASA, Goddard Space Flight Center, Greenbelt, MD) Remote Sensing of Environment (ISSN 0034-4257), vol. 18, Aug. 1985, p. 35-48. refs

Landsat-1 and Landsat-2 multispectral scanner (MSS) data were studied to determine the consistency of the calculated reflectance values over time. Data from six spectrally stable targets were collected over a 3-year period (1975-1977). Reflectance values calculated from the digital numbers were regressed against time to note any long term changes. Results indicate that, over a 1000-day period beginning 1 January 1975, MSS 2 reflectances were stable. MSS 1 reflectances over that same period decreased approximately 25-32 percent. The observed decreases are most likely due to a deterioration of the transmissive qualities of the Landsat-1 scanner's internal optical path. Although MSS temporal variation may be unique to MSS 1, time (days in orbit) should be considered as an independent variable when intersatellite calibration equations are computed. A case is made for a stable, monitored calibration system which would permit the calculation of true top-of-the-atmosphere reflectance measures. Author

A85-43691

TO FLY ON THE WINGS OF THE SUN - A STUDY OF SOLAR-POWERED AIRCRAFT

D. W. HALL (Lockheed Missiles and Space Co., Inc., Sunnyvale, CA) Lockheed Horizons, June 1985, p. 60-68.

Solar High Altitude Powered Platform (Solar HAP) aircraft are unmanned remote sensing vehicles designed for cruises lasting up to one year at 20-km altitude, while carrying up to 250 pounds of cameras and electrooptic sensors in an underslung payload pod. It is anticipated that real time IR and UV images of earth features may be more inexpensively and accurately obtained by this means than by the conventional geosynchronous earth resources satellites. Solar HAPs, with wing spans of over 300 ft and weights of only 2000 lb, require ultralight composite structures with external wire bracing. Solar cells will cover both sides of the vertical wing stabilizers and wing tips, which hinge up in daytime to capture the maximum amount of sunlight. A 15-hp electric propulsion unit drives a low-rpm, large diameter propeller; power will be derived from the solar cells diurnally, and from hydrogen-oxygen fuel cells nocturnally. The fuel gases will be generated in a water electrolyzer during the day by excess solar cell output. O.C.

A85-43944

TECHNIQUES OF RADAR REFLECTIVITY MEASUREMENT

N. C. CURRIE, ED. (Georgia Institute of Technology, Atlanta) Dedham, MA, Artech House, Inc., 1984, 539 p. No individual items are abstracted in this volume.

The experimental determination of radar reflectivities (RRs) is examined in an introductory and reference text comprising review chapters contributed by leading experts. Chapters are devoted to the fundamentals of RR measurement, the radar cross section (RCS), basic RCS measurement concepts and systems, RR

calibration procedures, data-acquisition and recording systems, data-analysis procedures, bistatic RCS measurements, far-field RCS measurement ranges, organization of test programs, ground-truth measurements, statistical properties of RR data, radar angle measurements, and radiometric measurements. Graphs, diagrams, and photographs are provided. T.K.

A85-44015

METHODS FOR THE PREDICTION OF THE ATTENUATION STATISTICS OF RADIO WAVES IN THE 10-100 GHZ RANGE IN RAIN - INCLINED PATHS [O METODAKH PROGNOZA STATISTIKI OSLABLENIIA V DOZHDIKHI RADIOVOLN DIAPAZONA 10-100 GGTS - NAKLONNYE TRASSY]

V. B. ERMAKOV, M. A. KOLOSOV, and V. N. POZHIDAIEV Radiotekhnika i Elektronika (ISSN 0033-8494), vol. 30, June 1985, p. 1071-1079. In Russian refs

Available data on methods and computational models for the prediction of the mean statistical probability of radio-wave attenuation at 10-100 GHz in rain on inclined space-ground paths are examined. Existing prediction methods are compared, and the method of Misme and Waldteufel (1980) is found to yield the best agreement between calculations and experimental results. A computational algorithm is developed with the aim of extending the applicability of the Misme-Waldteufel method to higher frequencies. B.J.

A85-45235* National Aeronautics and Space Administration. Goddard Space Flight Center, Greenbelt, Md.

A GLOBAL CLIMATOLOGY OF TOTAL OZONE FROM THE NIMBUS 7 TOTAL OZONE MAPPING SPECTROMETER

K. P. BOWMAN and A. J. KRUEGER (NASA, Goddard Space Flight Center, Greenbelt, MD) Journal of Geophysical Research (ISSN 0148-0227), vol. 90, Aug. 20, 1985, p. 7967-7976. refs

A global climatology of total column ozone has been computed from 4 years of daily observations by the total ozone mapping spectrometer aboard the Nimbus 7 polar-orbiting satellite. Observations were made at local noon, no observations are available in polar regions during the polar night. The orbital data have been area averaged onto a regular 5 deg by 5 deg latitude-longitude grid. The global coverage is more than 90 percent complete during the last 3 observing years (October 1979 to September 1982) and approximately 70 percent complete during the first year (October 1978 to September 1979). Global maps of the temporal mean and rms variance and the amplitude and phase of the annual and semiannual harmonics are presented. Similar analyses of the zonal mean values are given along with a time-latitude section of the zonal-mean total ozone. This climatology should be useful both for validating numerical models and for inspiring theoretical analyses. Author

A85-45696

VERIFICATION STUDIES OF MOS-1 SENSORS

K. TSUCHIYA (Chiba University, Japan) (COSPAR, Plenary Meeting, 25th: Workshop II on the Earth's Surface Studied from Space, Graz, Austria, June 25-July 7, 1984) Advances in Space Research (ISSN 0273-1177), vol. 5, no. 5, 1985, p. 101-110. Translation. refs

Verification experiments with a breadboard model of the Microwave Scanning Radiometer (MSR) instrument to be installed on the Manne Observation Satellite (MOS-1) are described. The accuracy of MSR measurements was determined with respect to: observed brightness temperature (Tb); Tb corrected for contributions other than the target; Tb content of the vertical polarization component of the 23.8 GHz channel; and the observed Tb of the horizontal polarization component of the 23.8 GHz channel of the MSR. Correlation coefficients are obtained between the vertical Tb component at 23.8 GHz and the horizontal component at 23.8 GHz, and Tb values are obtained for observations over fresh water targets and ocean targets in various meteorological conditions. On the basis of the obtained MSR measurements, it is concluded that the MSR will be an effective tool for observing the correlations between the physical properties of snow and atmospheric water content in different regions of the

World Ocean A diagram of the antenna pattern of the MSR is given I.H

A85-45697

UTILITY OF PROPOSED SENSORS FOR COASTAL ENGINEERING STUDIES

I. V. MURALIKRISHNA (National Remote Sensing Agency, Marine Applications Div., Hyderabad, India) (COSPAR, Plenary Meeting, 25th: Workshop II on the Earth's Surface Studied from Space, Graz, Austria, June 25-July 7, 1984) *Advances in Space Research* (ISSN 0273-1177), vol. 5, no. 5, 1985, p. 111-114. refs

The utility of satellite-based sensors for coastal engineering applications is discussed. The spatial resolution of several instruments is evaluated with respect to 20-meter resolution requirements of studies of fisheries potential; erosion of shore contours; and littoral drift. Among the current instruments considered are: the NOAA AVHRR radiometer, and the Landsat Multispectral Scanner (MSS). The utility of sensors proposed for future satellite missions is discussed, with emphasis given to the Thematic Mapper (TM) instrument of Landsat-4 and Landsat-5; the High-Resolution Visible (HRV) radiometer of the SPOT satellite; and the Multispectral Electronic Self-Scanning Radiometer (MESSR) of the Marine Observation Satellite (MOS-1). A map showing the movement in the position of a shoreline from 1980 to 1981 is constructed in order to demonstrate the utility of MSS data. I.H

A85-46297

SCATTERING IN PRECIPITATION DURING MICROWAVE-BEAM POWER TRANSMISSION [O RASSEIANII V OSADKAKH PRI PEREDACHE ENERGII PUCHKOM SVCH-RADIOVOLN]

A. N. KOCHUBEI Radiotekhnika i Elektronika (ISSN 0033-8494), vol. 30, July 1985, p. 1434-1436. In Russian. refs

Consideration is given to the effect of precipitation on microwave energy beamed down toward earth from a satellite solar power station in geostationary orbit. The level of microwave radiation scattered by rain at distances up to 200 km from the center of the receiving antenna is calculated. The results indicate that the scattered-signal level in intense rain is sufficiently high to overload the input circuits of the radio receiver, thus making necessary special means of protection. B.J.

A85-46424* Institute for Atmospheric Optics and Remote Sensing, Hampton, Va.

VARIATION IN THE STRATOSPHERIC AEROSOL ASSOCIATED WITH THE NORTH CYCLONIC POLAR VORTEX AS MEASURED BY THE SAM II SATELLITE SENSOR

G. S. KENT, U. O. FARRUKH (Institute for Atmospheric Optics and Remote Sensing, Hampton, VA), C. R. TREPTE (SASC Technologies, Inc., Hampton, VA), and M. P. MCCORMICK (NASA, Langley Research Center, Hampton, VA) *Journal of the Atmospheric Sciences* (ISSN 0022-4928), vol. 42, July 15, 1985, p. 1536-1551. refs
(Contract NAS1-17032, NAS1-17165)

Optical depth data gathered by the stratospheric aerosol measurement (SAM II) satellite during the 1979-80 winter season are analyzed to study mean atmospheric motions. The spacecraft photometer yielded extinction rates over the Northern Hemisphere in the 8-30 km altitude interval. Filtering was performed to remove the effects of high clouds and polar stratospheric clouds. Free horizontal mixing was prevalent below 14 km, as was a systematic difference across the polar jet stream above that altitude. The aerosol declined in altitude as the winter progressed. The polar vortex is concluded to have a base at the 14 km altitude and an outer boundary which coincides with the jet stream axis. The model accords with atmospheric tracer measurements made during the open-air nuclear testing programs in the 1950s. M.S.K.

A85-46849

THE ERS-1 SYNTHETIC APERTURE RADAR AND SCATTEROMETER

S. R. BROOKS, D. J. SMITH (General Electric Co., PLC, Marconi Research Centre, Chelmsford, England), H. JOYCE (Marconi Space and Defence Systems, Ltd., Stanmore, England), and F. G. SAWYER (Marconi Space and Defence Systems, Ltd., Portsmouth, England) *GEC Journal of Research* (ISSN 0264-9187), vol. 3, no. 2, 1985, p. 124-136. refs

The synthetic aperture radar (SAR) and scatterometer instruments on board the European Remote Sensing satellite (ERS-1) are described. SAR performance requirements are presented with respect to: impulse response function measures; radiometric resolution, and antenna geometry. The radar frequency and polarization requirements of the scatterometer instrument are given in a table. In addition to the SAR and scatterometer instruments, consideration is given to the Active Microwave Instrument (AMI) on board ERS-1. The On-Board Data Handling System (OBDHS) for receiving instrument commands and transmitting instrument status data to a ground station is also described. I.H

A85-47244#

APPLICATION OF PATTERN-RECOGNITION AND EXTRAPOLATION TECHNIQUES TO FORECASTING

G. L. AUSTIN (McGill Radar Weather Observatory, Sainte-Anne-de-Bellevue, Canada) (IAMAP, WMO, and ESA, International Symposium on Nowcasting, 3rd, Honolulu, HI, Aug. 5-16, 1985) *ESA Journal* (ISSN 0379-2285), vol. 9, no. 2, 1985, p. 147-155. refs

The indirect inference of fields of user-important phenomena from remote-sensed data and synoptic analyses is discussed as a problem of pattern recognition. The general procedures are illustrated by a review of the skills of objective procedures for forecasting rainfall, severe weather and aircraft-icing conditions from radar, satellite, and synoptic data. Work done in the last 20 years on nowcasting these phenomena by extrapolation and advection is described. Author

A85-47245#

CONCEPTUAL MODELS OF PRECIPITATION SYSTEMS

K. A. BROWNING (Meteorological Office, Bracknell, England) (IAMAP, WMO, and ESA, International Symposium on Nowcasting, 3rd, Honolulu, HI, Aug. 5-16, 1985) *ESA Journal* (ISSN 0379-2285), vol. 9, no. 2, 1985, p. 157-180. refs

Nowcasting of precipitation systems using radar and satellite imagery is discussed, noting imagery interpretation in terms of synoptic and mesoscale phenomena. Explanations of a number of systems associated with midlatitude cyclones and mesoscale convective systems in the tropics and midlatitudes are presented. The examples described are: (1) conveyor belt models for midlatitude frontal systems, (2) classification of mesoscale rainbands, (3) squall lines in midlatitudes and tropics, (4) nonsquall convective systems in midlatitudes and tropics, (5) subsynoptic scale comma clouds associated with cold air vortices, and (6) polar-trough conveyor belts and instant occlusions. I.F.

A85-47805* National Aeronautics and Space Administration, Goddard Space Flight Center, Greenbelt, Md.

LANDSAT-4 AND LANDSAT-5 MSS COHERENT NOISE - CHARACTERIZATION AND REMOVAL

J. C. TILTON, B. L. MARKHAM, and W. L. ALFORD (NASA, Goddard Space Flight Center, Greenbelt, MD) *Photogrammetric Engineering and Remote Sensing* (ISSN 0099-1112), vol. 51, Sept. 1985, p. 1263-1279. refs

The Multispectral Scanner (MSS) remote sensing instrument carried by Landsat-4 and Landsat-5 is similar to MSS instruments carried by Landsat-1, Landsat-2, and Landsat-3. However, the addition of the Thematic Mapper (TM) instrument to Landsat-4 and Landsat-5 required several design changes in the MSS instruments carried on these satellites because of the lower orbit and new satellite platform. Data from the MSS onboard the Landsat-4 and Landsat-5 satellites were found to be generally

comparable to the data obtained in the case of the earlier Landsat MSSs. However, a coherent noise pattern was observed in the Landsat-4 MSS data. In the present paper, the conduction of a noise analysis is discussed along with the noise characterization results, and a technique through which the Landsat-4 MSS coherent noise can be removed. G.R.

A85-47808

THEMATIC MAPPER - OPERATIONAL ACTIVITIES AND SENSOR PERFORMANCE AT ESA/EARTHNET

L. FUSCO, U. FREI, and A. HSU (ESA, European Space Research Institute, Frascati, Italy) Photogrammetric Engineering and Remote Sensing (ISSN 0099-1112), vol. 51, Sept. 1985, p. 1299-1314. refs

The ESA-Earthnet Thematic Mapper image characterization performed in the framework of the LIDQA Program includes operational activities support, understanding of the instrument reference characterization and performance in time, and comparison of TM products generated by different processing systems. The paper overviews the different topics within the Earthnet Program investigations. Author

A85-47819* National Aeronautics and Space Administration. Ames Research Center, Moffett Field, Calif.

EVALUATION OF THEMATIC MAPPER INTERBAND REGISTRATION AND NOISE CHARACTERISTICS

R. C. WRIGLEY, C. A. HLAVKA, D. H. CARD (NASA, Ames Research Center, Moffett Field, CA), and J. S. BUIS (Technicolor Government Services, Inc., Moffett Field, CA) Photogrammetric Engineering and Remote Sensing (ISSN 0099-1112), vol. 51, Sept. 1985, p. 1417-1425. refs

It is pointed out that the Thematic Mapper (TM) instruments aboard the Landsat-4 and Landsat-5 spacecraft have provided the first digital imagery of the earth's surface with a resolution sufficient to distinguish cultural features easily. The present paper provides a description of the results of studies designed to investigate the band-to-band registration, geodetic registration to a map base, and periodic noise. In the eight TM scenes analyzed, the band-to-band registration accuracy was high even before correction, and the correction for the shift between focal planes brought all bands into registration according to tight specifications. G.R.

A85-47916

A NEW TECHNIQUE FOR INFERRING SURFACE ALBEDO FROM SATELLITE OBSERVATIONS

B. PINTY (Clermont-Ferrand II, Université, Aubière, France) and G. SZEJWACH (Ecole Polytechnique, Palaiseau, France) Journal of Climate and Applied Meteorology (ISSN 0733-3021), vol. 24, Aug. 1985, p. 741-750. refs

A technique for inferring the spatial and seasonal albedo changes over a whole climatic region from satellite data is developed. This technique uses the diurnal variation of radiances which is measured by geostationary satellites and requires the knowledge of a surface albedo value over at least one reference site. The proposed method is tested over western Africa, using Meteosat data; and surface albedo maps representative of the wet and dry seasons are derived. With regard to the considered scales and to the achievable accuracies, the technique is shown to be relevant for climatological studies. Author

A85-47917

RELATIONSHIPS BETWEEN MEASURED AND SATELLITE-ESTIMATED SOLAR IRRADIANCE IN TEXAS

W. A. DUGAS and M. L. HEUER (Texas A&M University, Temple) Journal of Climate and Applied Meteorology (ISSN 0733-3021), vol. 24, Aug. 1985, p. 751-757. refs

A85-48894#

MESSAGE COLLISION OF DATA COLLECTION SYSTEM AND ITS COMPUTER SIMULATION

C.-L. SUN (Chinese Academy of Sciences, Institute of Space Physics, Beijing, People's Republic of China) Chinese Journal of Space Science, vol. 3, July 1983, p. 254-260. In Chinese, with abstract in English

Data collection system (DCS) is a telemetry instrument using a satellite as a relay station for transmitting earth environment data. The DCS of near-earth satellites such as that of Landsat and Tiros-N, are all designed by means of the random access principle. For the design of the systems, the law of message collision which is concerned with the capacity of the systems is an important problem. In this paper, the theoretical representations which agree with the simulation results are given. Computations of the probability of the message collision for various schemes are presented. Author

A85-50022*

Centre National de la Recherche Scientifique, Verrieres-Le Buisson (France).

COMPARISON OF MESOSPHERIC OZONE MEASUREMENTS USING THE LRIR AND UVMCS SATELLITE INSTRUMENTS

F. MILLIER (CNRS, Laboratoire de Physique Stellaire et Planétaire, Verrieres-le-Buisson, France), G. P. ANDERSON (USAF, Geophysics Laboratory, Bedford, MA), A. C. AIKIN (NASA, Goddard Space Flight Center, Greenbelt, MD), and J. C. GILLE (National Center for Atmospheric Research, Boulder, CO) Annales Geophysicae (ISSN 0755-0685), vol. 3, July-Aug. 1985, p. 439-443. Research supported by the National Center for Atmospheric Research, CNES, and NASA. refs

A comparison between mesospheric ozone profiles determined by two radically different satellite-borne instruments is presented for the period of July to November, 1975. The Limb Radiance Inversion Radiometer measured 9.6-micron O3 emission, while the Ultraviolet Multiple Channel Spectrometer measured the atmospheric attenuation of solar ultraviolet radiation during passage of the OSO-8 satellite across the terminator. Only nine near coincident measurements were found. The individual instruments have estimated precision errors of + or - 10 to 15 percent. Agreement between ozone values as measured by the two techniques for specific cases varies between 10 and 20 percent. The statistical correlation is positive and significant at all altitudes where both instruments had reasonable signal-to-noise ratio. A maximum correlation of 0.76 occurred at 0.3 mb (about 59 km). Author

N85-31225# European Space Agency, Paris (France).

PRELIMINARY INVESTIGATIONS CONCERNING A 90 GHZ RADIOMETER SATELLITE EXPERIMENT

F. HEEL and H. KIETZMANN Dec 1984 68 p refs Transl. into ENGLISH of "Voruntersuchung zur Durchfuehrung eines Satellitenexpt. mit einem 90-GHz-Radiometer" Oberpfaffenhofen, West Ger. Rept DFLR-FB-84-02, 1984 Original language doc. previously announced as N84-24693 (ESA-TT-860; DFLR-FB-84-02) Avail. NTIS HC A04/MF A01, original German version available from DFLR, Cologne DM 20.50

The feasibility of satellite experiments with a 90 GHz radiometer was assessed using a computer model of the radiation temperatures of sand, vegetation, concrete, and water for different atmospheric conditions. Measurements with an uncooled airborne 90 GHz radiometer tested model results. Results are better for low reflectivity objects and for cloudy conditions. A null-balancing radiometer is proposed. In the case of null-balancing failure this system also can be operated as total power radiometer. Author (ESA)

N85-31601*# Arizona Univ., Tucson. Optical Sciences Center
SPECTRORADIOMETRIC CALIBRATION OF THE THEMATIC MAPPER AND MULTISPECTRAL SCANNER SYSTEM Quarterly Report, 1 Mar. - 31 May 1985

P. N. SLATER and J. M. PALMER, Principal Investigators 31 May 1985 26 p ERTS
 (Contract NAS5-27832)
 (E85-10104; NASA-CR-176008; NAS 1.26:176008, QR-10) Avail: NTIS HC A03/MF A01 CSCL 14B

The results of analyses of Thematic Mapper (TM) images acquired on July 8 and October 28, 1984, and of a check of the calibration of the 122-m integrating sphere at Santa Barbara Research Center (SBRC) are described. The results obtained from the in-flight calibration attempts disagree with the pre-flight calibrations for bands 2 and 4. Considerable effort was expended in an attempt to explain the disagreement. The difficult point to explain is that the difference between the radiances predicted by the radiative transfer code (the code radiances) and the radiances predicted by the preflight calibration (the pre-flight radiances) fluctuate with spectral band. Because the spectral quantities measured at White Sands show little change with spectral band, these fluctuations are not anticipated. Analyses of other targets at White Sands such as clouds, cloud shadows, and water surfaces tend to support the pre-flight and internal calibrator calibrations. The source of the disagreement has not been identified. It could be due to: (1) a computational error in the data reduction, (2) an incorrect assumption in the input to the radiative transfer code; or (3) incorrect operation of the field equipment Author

N85-31606# EG and G Energy Measurements, Inc., Las Vegas, Nev.

REMOTE SENSING TECHNOLOGY: SYMPOSIUM PROCEEDINGS

Jan 1985 445 p refs Proc. held in Las Vegas, Nev., 23 Feb. 1983

(Contract DE-AC08-83NV-10282)
 (DE85-010212, EGG-10282-1057; CONF-830286) Avail: NTIS HC A19/MF A01

Papers were presented in four subject areas: (1) applications of remote sensing; (2) data analysis, digital and analog; (3) acquisition systems; and (4) general. DOE

N85-31611# Farran Research Associates, Farnanes (Ireland)
MILLIMETRE WAVE PULSE TECHNOLOGY Final Report

Paris ESA Jul. 1983 19 p
 (Contract ESTEC-5264/82/NL-GM)
 (ESA-CR(P)-2004) Avail: NTIS HC A02/MF A01

Solid state power devices for millimeter wave generation and amplification for use in a ground mapping transmitter output stage were reviewed. The survey shows that at 35 GHz, successful ground-mapping transmitters can readily be realized, with a wide choice of individual system designs. At 64 GHz, successful transmitters can also be achieved, but with less freedom of design. Multidevice combiners are required for the output stage. Above 140 GHz, it is unlikely that sufficient transmitter power will be available in the foreseeable future for any worthwhile high altitude satellite ground-mapping studies. Other applications requiring lower transmitter power may be successful Author (ESA)

N85-31717*# National Aeronautics and Space Administration. Goddard Space Flight Center, Greenbelt, Md
TOPEX ERROR BUDGET

R. KOLENKIEWICZ In its Geodyn Branch Res. Program 6 p Aug. 1985 refs
 Avail: NTIS HC A09/MF A01 CSCL 08C

The Ocean Topography Experiment (TOPEX), a mission currently being considered as a new start is discussed. It is a dedicated satellite with an orbit that repeats to within 1 kilometer of its ground track every 10 days. The primary instrument will be a two-frequency altimeter with an anticipated precision of 2 cm. Two previous missions GEOS-3 (1975) and SEASAT (1978) had single frequency altimeters. The two frequencies help to correct for errors due to electrons in the ionosphere. The satellite will

also carry a microwave radiometer to correct for water vapor, and the TRANET doppler beacon, laser retroreflectors, and an experimental system based on the Global Positioning System (GPS) for accurate tracking of the satellite's orbit. This research aims to determine to what level of accuracy the TOPEX altimeter will be able to measure, and a means of assessing this accuracy. B.W

N85-32379*# Geological Survey, Reston, Va.
LARGE FORMAT CAMERA PHOTOGRAPHS: A NEW TOOL FOR UNDERSTANDING ARID ENVIRONMENTS

A. S. WALKER In NASA Goddard Space Flight Center Global Mega-Geomorphology p 89-90 Jul 1985
 Avail: NTIS HC A07/MF A01 CSCL 14E

Large Format Camera (LFC) was developed by NASA to produce high resolution stereo photographs from space with maximum photogrammetric fidelity. The camera has a 30.5 cm focal length lens and an f/6.0 aperture. The optics are corrected to permit operation with black and white (b/w), natural color (col) and color infrared (cir) film. Interchangeable minus-haze and minus-blue filters are located near the aperture stop, and an antivignetting filter is provided on the front element of the lens. The field-of-view of the LFC along track is 73.7 degrees (ratio 1.5 x H) and across track is 41.1 degrees (ratio 0.75 x H). The frame format of the LFC is 23x46 cm with the long dimension in the direction of flight. The camera can be operated to produce 10, 60, 70, or 80 percent forward overlap for stereoscopic coverage. With 80 percent forward overlap, the stereo model base height ratio is 0.3 for successive frames and 1.2 if every fourth frame is used. The LFC magazine has a capacity of 2400 frames. Two horizon-looking stellar cameras, one directed 45 degrees forward and the other 45 degrees aft were used to photograph the star field in synchronism with exposures of the LFC. Post flight mensuration and calculation of the stellar photographs will provide altitude information for the LFC. R.J.F

N85-32389# Army Military Personnel Center, Alexandria, Va
MICROCOMPUTER PROCESSING OF LANDSAT THEMATIC MAPPER DATA FOR THE ACQUISITION OF MILITARY TACTICAL TERRAIN DATA Final Report

S. J. MCGREGOR 12 Apr. 1985 129 p
 (AD-A154781) Avail: NTIS HC A07/MF A01 CSCL 08B

This thesis demonstrates the potential use of microcomputer digital image processing techniques for obtaining tactical terrain data from LANDSAT multispectral digital imagery. Militarily significant Level 1 and 2 land cover classes were mapped for three North Carolina study areas using a modified USGS land cover classification system, LANDSAT 4 Thematic Mapper data, and the Personal Image Processing System (APPLEPIPS). A site specific accuracy assessment technique, using a stratified, systematic, unaligned sampling design, was used to determine the classification accuracy of the three land cover maps. The classification accuracy was determined to meet the USGS minimum acceptable standard of 85 percent at the 0.05 confidence level. GRA

N85-32464*# Institute for Atmospheric Optics and Remote Sensing, Hampton, Va.

DATA ANALYSIS FOR LIDAR AND QUARTZ CRYSTAL MICROBALANCE SYSTEMS Final Report

G. S. KENT and A. DEEPAK Jun. 1985 182 p refs
 (Contract NAS1-16253)
 (NASA-CR-172601; NAS 1.26:172601) Avail: NTIS HC A09/MF A01 CSCL 04A

Results are presented of the analysis of data taken on the stratospheric aerosol, using lidar, Quartz Crystal Microbalance (QCM), and the SAGE and SAM II satellite systems. The main objective of the work reported has been to use the data, taken with the NASA-LaRC instruments to study the stratospheric effects of volcanic eruptions during the period between the launch of the SAGE and SAM II satellite systems and October 1980. Four significant volcanic eruptions, for which data are available, occurred during this period--Soufriere, Sierra Negra, Mt. St. Helens, and Ulawun. Data on these have been analyzed to determine the

08 INSTRUMENTATION AND SENSORS

changes in stratospheric mass loading produced by the eruptions, and to study the dispersion of the newly injected material

Author

N85-32558# Air Force Geophysics Lab., Hanscom AFB, Mass.
APPLICATION OF SATELLITE ACCELEROMETER DATA TO IMPROVE DENSITY MODELS Environmental Research Papers
F. A. MARCOS 9 Aug. 1984 52 p
(Contract AF PROJ. 6690)
(AD-A154904; AFGL-TR-84-0211; AFGL-ERP-887) Avail: NTIS
HC A04/MF A01 CSCL 04A

Atmospheric density measurements obtained by the satellite accelerometer experiment provide data over a wide range of solar and geophysical conditions. These results are used in a preliminary evaluation of several atmospheric models. The model accuracies are compared by their mean values and standard deviations relative to the accelerometer data. Sources of model uncertainties and problems in reducing them are described. Long-term programs involving coordinated measurements, analyses of available data and theoretical studies are required along with development of more accurate indicators of solar and geomagnetic activity before models can show significant improvement. GRA

N85-33130# Joint Publications Research Service, Arlington, Va.
COSMONAUTS PARTICIPATE IN MULTILEVEL REMOTE SENSING EXPERIMENT Abstract Only
N. BARSKIY *In its* USSR Rept.: Space (JPRS-USP-84-006) p 23 14 Nov. 1984 Transl into ENGLISH from Bakinsky Rabochiy (Maku), 30 Aug. 1984 p 3
Avail: NTIS HC A08

An international experiment was conducted for the study of natural resources by remote methods. Photography and spectrometry of the republic's territory from orbit and the spectral characteristics of natural objects in the Sheki and Zakataly rayons and at the Mingechaur Reservoir were recorded. The aerospace experiment was conducted at several levels, ranging from equipment in orbit and instruments on board airplanes and helicopters, to a ground-based automated information-and-measurement complex. The purpose of the project is to develop scientific-methodological and physical-technical bases of environmental studies from space. The information will provide farmers with recommendations, maps and charts for the rational use of agricultural lands, pastures and reservoirs based on study of mountain-meadow, forest and valley geosystems. The materials obtained from the manned complex, correlated with data from aerial photography and ground-based observations. E.A.K.

N85-33148# Joint Publications Research Service, Arlington, Va.
ENHANCING PRECISION OF REMOTE TEMPERATURE SENSING DATA FROM SATELLITES UNDER CLOUDY ATMOSPHERIC CONDITIONS Abstract Only
Y. V. PLOKHENKO and A. B. USPENSKIY *In its* USSR Rept.: Space (JPRS-USP-84-006) p 119 14 Nov. 1984 Transl. into ENGLISH from Issled. Zemli iz Kosmosa (Moscow), no. 2, Mar. - Apr. 1984 p 15-22
Avail: NTIS HC A08

Cloud cover is the major impediment to radiometric IR band measurements of thermal radiation from the Earth atmosphere system. Present algorithms for the remote determination of temperature with partial cloud cover are difficult to compare since no analysis has been made of their accuracy and the few attempts at estimating the information content and optimizing the composition of such measurements are based on considerations of a physical nature or are tied to a specific algorithm. A physical statistical model for IR measurements made in the presence of multilayer, partial cloud cover is proposed. The model is used to derive optimal estimates of the temperature distribution and the effective cloud cover density. It is assumed that the clouds can be represented by a thin absorbing layer (shield) at a specific temperature and altitude, and that the cloud layers have reflectivities close to zero. The clouds are assumed not to overlap. Cloudiness produces a sharp drop in the precision of any estimate for the atmospheric layer under the cloud cover. The information

content indicator falls off as the cloud cover altitude increases. The calculations demonstrate that the accuracy of estimates of the effective cloud cover for two adjacent layers is poor, i.e., adjacent or close layers are poorly distinguishable. The precision of estimates of the effective cloud cover improves as the spacing between the levels increases and the altitude of the top layer rises. Author

N85-33150# Joint Publications Research Service, Arlington, Va.
DETERMINATION OF ALTITUDE OF CLOUD COVER TOP FROM METEOR SATELLITE DATA Abstract Only
L. I. KOPROVA and A. Y. BAKHAMATOV *In its* USSR Rept.: Space (JPRS-USP-84-006) p 120-121 14 Nov. 1984 Transl into ENGLISH from Issled. Zemli iz Kosmosa (Moscow), no. 2, Mar. - Apr. 1984 p 25-34
Avail: NTIS HC A08

An analysis of an improved satellite measurement technique for H (upper cloud cover boundary) is presented which resolves the following problems: (1) the determination of the scope and complement of the a priori global information; (2) the generation of the requisite catalog and procedure for its timely use; (3) the automation of the identification of IR data on cloud conditions; (4) the procedure for the use of IR measurements in mapping the cloud top altitude and taking into account the effect of the atmospheric layer over the clouds on the IR measurements. The altitude determination procedure was checked by comparing synchronous radio sensing and satellite data for two regions where cloud shape and altitude differ substantially: the White Sea (1978) and the tropical latitudes of the Indian Ocean (1977). The following are summarized in extensive tables: the satellite and radio sensing data on H; the transmittance function of the atmospheric layer over the clouds as a function of latitude in both the Northern and Southern Hemispheres in July and January; the value of H based on radio sounding data and calculated from the measured radiation temperature and climatic data as well as estimates of the impact of the atmospheric layer above the clouds on the determination of H. Author

N85-33159# Joint Publications Research Service, Arlington, Va.
TERRAIN ILLUMINATION CONDITIONS WHEN TAKING SCANNING PHOTOGRAPHS FROM SPACE Abstract Only
A. M. KUZINA, I. G. MALTSEVA, and N. S. RAMM *In its* USSR Rept.: Space (JPRS-USP-84-006) p 127 14 Nov. 1984 Transl into ENGLISH from Issled. Zemli iz Kosmosa (Moscow), no. 2, Mar. - Apr. 1984 p 98-106
Avail: NTIS HC A08

Expressions for the solar altitude and azimuth are derived and analyzed for terrain points at the moment they are photographed as a function of the orbital parameters of an earth resources satellite, the photograph dates, the geographic latitude of these points and their distance from the satellite track. It is assumed that the scanner photos are taken from satellites in a circular solar synchronous orbit at an altitude of 600 to 900 km, that the photos are taken during the descending orbital trajectories, i.e., when the satellite is moving southwest in the morning or noontime hours, the Earth's surface is represented by a sphere and the orbit is strictly circular and the optical spectrum is used, employing an optical mechanical scanner with linear horizontal line scanning or using a solid state MSU-E or the HRV scanner of the SPOT system. All line elements of the photos are assumed to be recorded simultaneously. It is shown that the lighting conditions are practically independent of the satellite altitude and are completely governed by the mean local time of passage of the descending orbit. Quantitative expressions are also found for the change in illumination within any scanning photo and considerations are discussed which allow recommending an optimal value for the local mean time of descending trajectory passage. Author

N85-33160# Joint Publications Research Service, Arlington, Va.
CALCULATING SOLAR HIGHLIGHT AND SHADELESS AREAS FOR SCANNING PHOTOGRAPHS FROM SPACE AND OPTIMIZING LIGHTING CONDITIONS Abstract Only

I. G. MALTSEVA *In its* USSR Rept.: Space (JPRS-USP-84-006) p 128 14 Nov. 1984 Transl into ENGLISH from Issled. Zemli iz Kosmosa (Moscow), no. 2, Mar. - Apr. 1984 p 107-116
 Avail: NTIS HC A08

Light scattering by natural landscape objects exhibits two maxima which fall within the vertical plane having an azimuth coincident with the azimuth of the Sun. The first maximum corresponds to the direction of the solar rays (the unshaded region) and the second to the direction of the mirror reflection of these rays from the horizontal plane (the highlighting region). In these two regions, the brightness coefficients of the majority of terrain elements increase sharply and become strongly variable, while the contrasts between different objects as a rule decrease. The images of terrain objects in these regions yield the maximum information on the scattering indices of the objects. These two regions are described as applied to the case of multispectrum space scanner photography from earth resources satellites and the optimization of the ground illumination conditions. The analysis is based on the geometry of the Sun-satellite-Earth surface system and also treats the question of the duration of the space photography season and its dependence on lighting conditions. Equations are solved for the isolines and centers of the shadeless and high-light regions

Author

N85-33534*# Hughes Aircraft Co., El Segundo, Calif.
SIX MECHANISMS USED ON THE SSM/1 RADIOMETER

H. R. LUDWIG *In* NASA Ames Research Center 19th Aerospace Mech. Symp. p 347-362 Aug. 1985 refs
 Avail: NTIS HC A17/MF A01 CSCL 13M

Future USAF Block 5D Defense Meteorological Satellites will carry a scanning microwave radiometer sensor (SSM/1). SSM/1 senses the emission of microwave energy and returns to earth data used to determine weather conditions, such as rainfall rates, soil moisture, and oceanic wind speed. The overall design of the SSM/1 radiometer was largely influenced by the mechanisms. The radiometer was designed to be stowed in a cavity on the existing spacecraft. The deployment of the sensor is complex due to the constraint of this cavity and the need for precision in the deployment. The radiometer will continuously rotate, instead of oscillate, creating the need for a bearing and power transfer assembly and a momentum compensation device. The six mechanisms developed for this program are described

Author

N85-35217# Naval Postgraduate School, Monterey, Calif.
TARGET OBSERVABILITY FOR SATELLITE-BASED SENSORS M.S. Thesis

R. E. L. BOND Mar. 1985 130 p
 (AD-A156139) Avail: NTIS HC A07/MF A01 CSCL 17G

The purpose of this thesis is to discuss the observability of targets moving on or near the Earth's surface when viewed from space by an orbiting satellite. A simplified derivation of the satellite's orbital mechanics is undertaken, when taken in conjunction with a description of the target's motion allows for the derivation of a system of relative coordinates. An observability analysis is then performed on the resulting series of nonlinear equations, which in turn forms the basis for the design of a deterministic nonlinear observer and an Extended Kalman Filter to track the target.

GRA

N85-35218# National Environmental Satellite Service, Washington, D. C.

SPACE STATION POLAR PLATFORM: INTEGRATING RESEARCH AND OPERATIONAL MISSIONS

J. H. MCELROY and S. R. SCHNEIDER Jan 1985 27 p
 (PB85-195279, NOAA-TR-NESDIS-19) Avail: NTIS HC A03/MF A01 CSCL 22B

This report describes how an operational payload proposed by NOAA for the Space Station Polar Platform may be merged together with the research sensors scheduled to be carried on the Platform

as part of NASA's Earth Observing System (EOS). This is the third in a series of NOAA/NESDIS Technical Reports on the space station project. Issues addressed include studies of solar terrestrial interactions, as well as monitoring of the Earth's atmosphere, oceans and land masses using both operational and R&D sensors.

GRA

N85-35565# Bureau of Reclamation, Denver, Colo.
PROJECT SKYWATER, 1983-84 SCPP (SIERRA COOPERATIVE PILOT PROJECT) DATA INVENTORY

Oct. 1984 181 p
 (PB85-187052) Avail: NTIS HC A09/MF A01 CSCL 05B

An inventory of all data collected from October 15, 1983, through April 1984, in association with the SCPP (Sierra Cooperative Pilot Project), a weather modification research project in winter orographic cloud seeding. It is subdivided into an introduction plus 12 sections and appendixes A, B, C and D Forecasting, Radar, Satellite, Aircraft, Rawinsondes, Surface Meteorological Observations, Precipitation Gage Network, Ground based Microphysical Observations, Radiometer, Cooperative and Operational Seeding Activities, Snow Chemistry Measurements, National Weather Service, Federal Aviation Administration, and National Climatic Center Products, and Sierra PROBE Data Availability, SCPP Operations for 1983-84, University of Wyoming King Air Flight Summary Notes.

GRA

09

GENERAL

Includes economic analysis

A85-40793
PRINCIPLES OF REMOTE SENSING

P. J. CURRAN London, Longman, 1985, 293 p refs

This book is produced for undergraduate and graduate courses in remote sensing. A review of remote sensing today is presented, taking into account recent developments in remote sensing, social and legal implications of remote sensing, the status of remote sensing, and recommended reading. Other topics explored are related to electromagnetic radiation at the earth's surface, aerial photography, aerial sensor imagery, satellite sensor imagery, and image processing. Attention is given to the components of a remote sensing system, remote sensing terminology and units, sources and types of electromagnetic energy used in remote sensing, earth surface interactions with electromagnetic radiation, atmospheric interactions with electromagnetic radiation, the multispectral scanner, thermal infrared linescanner, sideways-looking airborne radar, earth resources satellites, manned earth resources satellites, meteorological satellites, military and USSR satellites, and geographic information systems.

G.R.

A85-41657
COMMERCIALIZATION OF REMOTE-SENSING TECHNOLOGY
 S. A. MORAIN (New Mexico, University, Albuquerque) International Journal of Remote Sensing (ISSN 0143-1161), vol. 6, June 1985, p. 837-846. refs

The Technology Application Center (TAC) of the University of New Mexico has accumulated a decade of experience in the transfer of remote sensing technology applications to assist commercialization efforts. The present management and cost information for 48 completed projects sheds light on small businesses' expectations regarding the frequency and duration of such projects, their requisite level of effort, and before-profit revenues. The presently ascertained gross average salary per full time employee equivalent, which has averaged only \$10,500 since 1975, suggests that market forces have not yet generated sufficient demand to support the level of skills entailed by this technology.

O.C.

09 GENERAL

A85-42220

THE EVOLVING CONTINENTS /2ND REVISED AND ENLARGED EDITION/

B. F. WINDLEY (Leicester, University, England) Chichester, England and New York, John Wiley and Sons, 1984, 416 p. refs

The earth's history is traced through the tectonic evolution of the continental crust from the very beginning of the geological record, rather than by studying the stratigraphy of a particular area. The topics addressed include: Archean granulite-gneiss belts; Archean greenstone belts; crustal evolution in the Archean; early to mid-Proterozoic basic ultrabasic intrusion, basins, and belts; mid-Proterozoic anorogenic magmatism and abortive rifting; mid-late Proterozoic basins, dykes, glaciations, and life forms; late Proterozoic mobile belts; and crustal evolution in the Proterozoic. Also considered are: paleomagnetism and continental drift; paleoclimatology and the fossil record, Caledonian-Appalachian fold belt; the Hercynian fold belt; Pangaea and its breakup; plate tectonics and sea-floor spreading; island arcs; continental margin orogenic belts; the Western Americas, the Alpine fold belt; the Himalayas; and the evolving continents. C.D.

A85-42223

THE SPACE STATION: AN IDEA WHOSE TIME HAS COME

T. R. SIMPSON, ED. New York, IEEE Press, 1985, 314 p. No individual items are abstracted in this volume

A general overview of the goals and technologies to be used in the assembly of the Space Station in the 1990s is presented. Among the topics addressed are: the historical background of American and Russian manned Space Station concepts, the views of key decision-makers in the Federal Government with respect to the Space Station; the capabilities and structure of various Space Station design concepts; and the long term potential of space systems to support manned spaceflight within the solar system in the 21st century. Excerpts from the major Presidential documents concerned with manned space flight over the past 24 years are provided in an appendix. I.H.

A85-45686* National Aeronautics and Space Administration. Goddard Inst. for Space Studies, New York.

THE EARTH'S SURFACE STUDIED FROM SPACE; PROCEEDINGS OF WORKSHOP II OF THE COSPAR 25TH PLENARY MEETING, GRAZ, AUSTRIA, JUNE 25-JULY 7, 1984

S. G. UNGAR, ED. (NASA, Goddard Institute for Space Studies, NY) Advances in Space Research (ISSN 0273-1177), vol. 5, no. 5, 1985, 120 p. For individual items see A85-45687 to A85-45697.

Consideration is given to: Landsat image data quality studies; a preliminary evaluation of Landsat-4 Thematic Mapper (TM) data for mineral exploration, and the early evaluation of TM data for mapping forest, agricultural and soil resources. Among other topics discussed are: shortwave infrared detection of vegetation, SPOT image quality and post-launch assessment, an evaluation of SPOT HRV simulation data for Corps of Engineers applications, and the application potential of SPOT imagery for topographic mapping. Consideration is also given to: verification studies of MOS-1 sensors; multiple sensor geocoded data; and the utility of proposed sensors for coastal engineering studies. I.H.

A85-48524

THE USSR AS VIEWED FROM SPACE [SSSR IZ KOSMOSA]

IU. P. KIENKO, ED., V. F. MARKOV, ED., E. A. VOSTOKOVA, ED., IU. G. KELNER, ED., and I. M. KOMISSAROVA, ED. Moscow, Glavnoe Upravlenie Geodezii i Kartografii, 1983, 65 p. In Russian. No individual items are abstracted in this volume.

A series of photographs of the entire territory of the Soviet Union obtained through satellite remote sensing is presented along with various maps compiled on the basis of these photographs. Emphasis is placed on images obtained with the KATE-140, FMS, and MKF-6 cameras, as well as Meteor-satellite TV images. Examples of the following types of items are included: physical and geographic photointerpretation; geological-structural, geomorphological, and glaciological maps; and forest surveys. B.J.

N85-31584# Committee on Commerce, Science, and Transportation (U. S. Senate).

ANTARCTICA

Washington GPO 1984 91 p. Hearing before the Subcommittee on Sci., Technol. and Space, of the Comm. on Com., Sci. and Transportation, 98th Congr., 2nd Sess., 24 Sep. 1984 (S-HRG-98-1181; GPO-40-553) Avail. Subcommittee on Science, Technology, and Space

The conduct of scientific research on Antarctica was discussed at a hearing before the House Subcommittee on Science, Technology and Space. The Antarctic treaty of 1961 and research in the areas of resource exploitation, oceanography, glaciology, polar meteorology and medicine are among the topics discussed. R.J.F.

N85-32386# Geological Survey, Washington, D.C.

WORLDWIDE DIRECTORY OF NATIONAL EARTH-SCIENCE AGENCIES AND RELATED INTERNATIONAL ORGANIZATIONS

E. J. TINSLEY, comp. and J. P. HOLLANDER, comp. 1984 107 p.

(GS-CIRC-934; LC-84-600161) Avail. NTIS HC A06/MF A01

The Directory provides addresses of government earth science agencies around the world that have functions similar to those of one or more of the operating divisions of the U.S. Geological Survey (USGS). It also lists addresses of major international organizations that are concerned with some phase of the earth sciences. The directory is arranged alphabetically by country name. The location of each country is shown on a small index map, which is keyed to one of 10 reference maps showing the major regions of the world. The principal functions of the agencies listed are keyed to those of the USGS and are indicated by code letters. Author

N85-33127# Centre National d'Etudes Spatiales, Toulouse (France).

THE FRENCH SPACE PROGRAM [PROGRAMME SPATIAL FRANCAIS]

1984 194 p. refs. In FRENCH Presented at 25th COSPAR Plenary Meeting, Graz, 25 Jun. - 7 Jul. 1984. Avail. NTIS HC A09/MF A01

The French space research program includes astronomy, solar physics, solar system, ionosphere, magnetosphere, meteorology, oceanography, earth resources, space geodesics, material science and life sciences. Author (ESA)

N85-35144*# Pennsylvania Univ., Philadelphia.

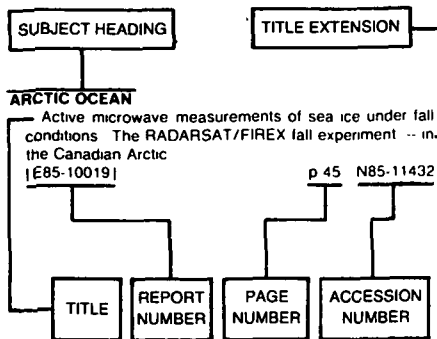
SATELLITES AND POLITICS: WEATHER, COMMUNICATIONS, AND EARTH RESOURCES

P. MACK. In NASA, Washington A Spacefaring People p 32-38 1985 refs

Avail. NTIS HC A08/MF A01; also available SOD HC \$3 50 as 033-000-009-33-0 CSCL 05D

Political problems surrounding the development of weather, communications, and Earth resources satellites are discussed. Tiros satellites, LANDSAT satellites, and Nimbus satellites are discussed. R.J.F.

Typical Subject Index Listing



The subject heading is a key to the subject content of the document. The title is used to provide a description of the subject matter. When the title is insufficiently descriptive of the document content, the title extension is added, separated from the title by three hyphens. The (NASA or AIAA) accession number and the page number are included in each entry to assist the user in locating the abstract in the abstract section. If applicable, a report number is also included as an aid in identifying the document. Under any one subject heading, the accession numbers are arranged in sequence with the AIAA accession numbers appearing first.

A

ACCELEROMETERS

Application of satellite accelerometer data to improve density models [AD-A154904] p 48 N85-32558

ACCURACY

TOPEX error budget p 47 N85-31717

ACTINOMETERS

Impact of fluctuations in optical properties of atmosphere on the ratio of spectral brightness from remote sensing of agricultural land p 5 N85-33149

ADVECTION

Mesoscale features and atmospheric refraction conditions of the Arctic marginal ice zone [AD-A155139] p 33 N85-32584

AERIAL PHOTOGRAPHY

Measurement and analysis of 2-D infrared natural background p 37 N85-42511

Remote sensing investigations on some fruit orchards in El Fayoum area, Egypt p 1 N85-42581
Vegetation profiles from color-infrared airphotos p 1 N85-42650

SPOT simulation imagery for urban monitoring - A comparison with Landsat TM and MSS imagery and with high altitude color infrared photography p 6 N85-45871

Handbook for obtaining and using aerial photography to map aquatic plant distribution [AD-A154584] p 33 N85-32388

Coastal erosion along Monterey Bay [AD-A155610] p 34 N85-32707

Cataloging the spectral brightness coefficients of the forested region of the European territory of the USSR p 5 N85-33155

AEROMAGNETISM

Long-wavelength magnetic and gravity anomaly correlations on Africa and Europe p 12 N85-31597

AEROSOLS

On observation of middle atmosphere with LAS (limb-atmospheric infrared spectrometer) on board of satellite 'Ohzora' (EXOS-C) p 42 N85-41362

Satellite measurement of sea surface temperature in the presence of volcanic aerosols p 25 N85-41993
Variation in the stratospheric aerosol associated with the North Cyclonic Polar Vortex as measured by the SAM II satellite sensor --- Stratospheric Aerosol Measurement p 45 N85-46424

Satellite measurements of atmospheric aerosols [AD-A153807] p 32 N85-30556

Data analysis for lidar and quartz crystal microbalance systems [NASA-CR-172601] p 47 N85-32464

Properties of aerosol particles detected by satellites in coastal regions p 34 N85-32622

The variability of aerosol microstructure in continental and oceanic surface layers of the atmosphere in anticyclones p 34 N85-32660

AFRICA

Directional reflectance factor distributions for cover types of Northern Africa p 1 N85-43114

Reduced to pole long-wavelength magnetic anomalies of Africa and Europe p 18 N85-31595

Euro-African MAGSAT anomaly-tectonic observations p 18 N85-31596

Long-wavelength magnetic and gravity anomaly correlations on Africa and Europe p 12 N85-31597

Microwave hydrology. A trilogy [NASA-CR-176042] p 36 N85-31603

AGRICULTURE

Evaluation of Thematic Mapper data for mapping forest, agricultural and soil resources p 2 N85-45690

Evaluation of simulated SPOT imagery for the interpretation of agricultural resources in California p 2 N85-45872

AIR FLOW

Mesoscale features and atmospheric refraction conditions of the Arctic marginal ice zone [AD-A155139] p 33 N85-32584

AIR SEA ICE INTERACTIONS

Results of the MIZEX preliminary campaign 29 June to 19 July 1983 --- Marginal Ice Zone Experiment (MIZEX), satellite observation [CNES-84/142/T/CT/DRT/TIT/R] p 32 N85-31609

AIR WATER INTERACTIONS

Satellite observations of the circulation east of the Mississippi Delta - Cold-air outbreak conditions p 27 N85-43117

Ordered mesoscale structures on the ocean surface identified from satellite radar data p 28 N85-46257

Geodynamics Branch research program [NASA-TM-86223] p 18 N85-31688

Tropical Ocean and Global Atmosphere (TOGA) heat exchange project. A summary report [NASA-CR-176038] p 33 N85-31738

Mesoscale features and atmospheric refraction conditions of the Arctic marginal ice zone [AD-A155139] p 33 N85-32584

Properties of aerosol particles detected by satellites in coastal regions p 34 N85-32622

AIRBORNE EQUIPMENT

Investigation of ice cover from platforms in the air and in space using radar equipment p 25 N85-40644

Probabilities, problems, and perspectives of microwave long-range reconnaissance p 42 N85-41570

Signature measurements using cooled microwave radiometers at frequencies from 90 GHz to 140 GHz p 43 N85-41571

Aerial and space-based remote sensing in ecological prognosis p 6 N85-46249

AIRCRAFT DESIGN

To fly on the wings of the sun - A study of solar-powered aircraft p 44 N85-43691

AIRCRAFT INSTRUMENTS

MIZEX, 1984, NASA CV-990 flight report [NASA-TM-86216] p 31 N85-30451

ALASKA

The U S Geological Survey in Alaska Accomplishments during 1982 [US-GEOL-SURV-CIRC-939] p 19 N85-31719

The United States Geological Survey in Alaska Accomplishments during 1983 [USGS-CIRC-945] p 23 N85-34468

ALBEDO

Albedo of a water surface, spectral variation, effects of atmospheric transmittance, sun angle and wind speed p 27 N85-42259

The albedo field and cloud radiative forcing produced by a general circulation model with internally generated cloud optics p 27 N85-43373

ALGORITHMS

Enhancing precision of remote temperature sensing data from satellites under cloudy atmospheric conditions p 48 N85-33148

ALTIMETERS

Global mean sea surface based upon a combination of the GEOS-3 and SEASAT altimeter data p 32 N85-31710

SEASAT altimetry for surface height of inland seas p 32 N85-31714

TOPEX error budget p 47 N85-31717

Global geoid and gravity anomaly predictions using the collocation and point mass techniques [AD-A154517] p 13 N85-32387

ALTITUDE

Terrain illumination conditions when taking scanning photographs from space p 48 N85-33159

ALUMINUM SILICATES

Conditions for formation of parageneses containing kyanite-orthoclase in region of Mount Provender and Pratt Peak (Shackleton Range, Antarctica) p 16 N85-30447

ANGULAR DISTRIBUTION

Two-dimensional leaf orientation distributions p 2 N85-49104

Remote sensing of angular characteristics of canopy reflectances p 3 N85-49105

ANNUAL VARIATIONS

The variability of aerosol microstructure in continental and oceanic surface layers of the atmosphere in anticyclones p 34 N85-32660

ANTARCTIC REGIONS

The Antarctic ice p 14 N85-42171

Radar maps of the Arctic and Antarctic compiled on the basis of Cosmos-1500 satellite data, and preliminary results of their analysis p 29 N85-46259

ANTARCTICA

[S-HRG-98-1181] p 50 N85-31584

Petroleum and mineral resources of Antarctica [US-GEOL-SURV-CIRC-909] p 18 N85-31605

Use of the synoptic view. Examples from Earth and other planets p 20 N85-32371

ANTICYCLONES

Mesoscale features and atmospheric refraction conditions of the Arctic marginal ice zone [AD-A155139] p 33 N85-32584

The variability of aerosol microstructure in continental and oceanic surface layers of the atmosphere in anticyclones p 34 N85-32660

AQUATIC PLANTS

Handbook for obtaining and using aerial photography to map aquatic plant distribution [AD-A154584] p 33 N85-32388

AQUIFERS

Hydrogeology of the lower Glen Rose Aquifer, south-central Texas p 36 N85-35466

ARCTIC REGIONS

Radar maps of the Arctic and Antarctic compiled on the basis of Cosmos-1500 satellite data, and preliminary results of their analysis p 29 N85-46259

Mesoscale features and atmospheric refraction conditions of the Arctic marginal ice zone [AD-A155139] p 33 N85-32584

Arctic and offshore research [DE85-001995] p 34 N85-33653

ARID LANDS

A new technique for inferring surface albedo from satellite observations p 46 N85-47916

Comprehensive mapping of arid and semiarid regions of Arizona using space photography p 14 N85-33164

Remote sensing of hydrologic transport processes using spot simulation data [DE85-012412] p 37 N85-35467

ARTIFICIAL SATELLITES

Global geoid and gravity anomaly predictions using the collocation and point mass techniques
[AD-A154517] p 13 N85-32387

ASHES

Eruption of Mount Ontake in 1979 - Detection of volcanic ash fall area from Landsat MSS CCT data p 15 A85-42583

ASSESSMENTS

Some recent deposit modeling efforts p 23 N85-35453

ATLANTIC OCEAN

Thermal isostasy in the South Atlantic Ocean from geoid anomalies p 27 A85-44925
Marine phosphorite deposits model for exploration, with emphasis on deposits in the US Atlantic coastal plain p 35 N85-35439

ATMOSPHERIC ATTENUATION

Profile statistics of rain in slant path as measured with a radar p 35 A85-40098
Satellite propagation in the South Pacific region p 26 A85-42050
Solid-state spectral transmissometer and radiometer p 30 A85-48670

ATMOSPHERIC BOUNDARY LAYER

Properties of aerosol particles detected by satellites in coastal regions p 34 N85-32622

ATMOSPHERIC CIRCULATION

The albedo field and cloud radiative forcing produced by a general circulation model with internally generated cloud optics p 27 A85-43373
Measuring the global distribution of intense convection over land with passive microwave radiometry p 36 A85-47923

ATMOSPHERIC COMPOSITION

The origin of temporal variance in long-lived trace constituents in the summer stratosphere p 6 A85-43375
The variability of aerosol microstructure in continental and oceanic surface layers of the atmosphere in anticyclones p 34 N85-32660

ATMOSPHERIC CORRECTION

The determination of the albedo of natural covers of the earth on the basis of remote measurement results p 10 A85-46132

ATMOSPHERIC DENSITY

Application of satellite accelerometer data to improve density models [AD-A154904] p 48 N85-32558

ATMOSPHERIC DIFFUSION

Impact of fluctuations in optical properties of atmosphere on the ratio of spectral brightness from remote sensing of agricultural land p 5 N85-33149

ATMOSPHERIC EFFECTS

The atmospheric effect on the separability of field classes measured from satellites p 44 A85-43115
The effect of the interface albedo of the underlying surface on the reflected radiation p 10 A85-46131
The determination of the albedo of natural covers of the earth on the basis of remote measurement results p 10 A85-46132
Remote sensing of angular characteristics of canopy reflectances p 3 A85-49105

ATMOSPHERIC HEAT BUDGET

Motor glider measurements during the Urban Atmosphere Energy Budget Experiment (EESA 1) p 7 N85-35553

ATMOSPHERIC MODELS

Application of satellite accelerometer data to improve density models [AD-A154904] p 48 N85-32558

ATMOSPHERIC OPTICS

The determination of the albedo of natural covers of the earth on the basis of remote measurement results p 10 A85-46132

ATMOSPHERIC PHYSICS

Proceedings of Meteorological Motor Glider (MEMO) Workshop '84 [DFVLR-MITT-85-04] p 7 N85-35542

ATMOSPHERIC RADIATION

Determination of altitude of cloud cover top from Meteor satellite data p 48 N85-33150

ATMOSPHERIC REFRACTION

Mesoscale features and atmospheric refraction conditions of the Arctic marginal ice zone [AD-A155139] p 33 N85-32584

ATMOSPHERIC SCATTERING

The effect of the interface albedo of the underlying surface on the reflected radiation p 10 A85-46131
Scattering in precipitation during microwave-beam power transmission p 45 A85-46297
Properties of aerosol particles detected by satellites in coastal regions p 34 N85-32622

ATMOSPHERIC TEMPERATURE

Remote sensing of temperature profiles from a combination of observations from the satellite-based Microwave Sounding Unit and the ground-based Profiler p 43 A85-42292

ATMOSPHERIC TURBULENCE

Environmental-physical measurements and determination of atmospheric turbulence with the ASK-16 motor glider p 7 N85-35549

AURORAL ELECTROJETS

High-latitude mesopause neutral winds and geomagnetic activity - A cross-correlation analysis p 16 A85-49227

AVALANCHE DIODES

Millimetre wave pulse technology --- satellite mapping [ESA-CR(P)-2004] p 47 N85-31611

AZIMUTH

View azimuth and zenith, and solar angle effects on wheat canopy reflectance p 2 A85-43120
Terrain illumination conditions when taking scanning photographs from space p 48 N85-33159
Calculating solar highlight and shadeless areas for scanning photographs from space and optimizing lighting conditions p 49 N85-33160

B

BACKSCATTERING

Backscattering of centimeter and millimeter radio waves by the earth surface at low grazing angles (Review) p 9 A85-46078
Microwave inversion of leaf area and inclination angle distributions from backscattered data p 3 A85-49109
Sources of scattering from vegetation canopies at 10 GHz p 4 A85-49114

BALLOON SOUNDING

Environmental-physical measurements and determination of atmospheric turbulence with the ASK-16 motor glider p 7 N85-35549

BEACHES

Coastal erosion along Monterey Bay [AD-A155610] p 34 N85-32707

BEDROCK

The Antarctic ice p 14 A85-42171
Reduced to pole long-wavelength magnetic anomalies of Africa and Europe p 18 N85-31595
Euro-African MAGSAT anomaly-tectonic observations p 18 N85-31596

BELGIUM

Satellite-determined stresses in the crust of Europe with particular consideration to the Liege earthquake of November 8, 1983 p 13 N85-31694

BERING SEA

Dispersion of sea ice in the Bering Sea p 26 A85-42257

BOUNDARY LAYER STABILITY

Mesoscale features and atmospheric refraction conditions of the Arctic marginal ice zone [AD-A155139] p 33 N85-32584

BRAGG ANGLE

The impact of higher-order Bragg terms on radar sea return p 24 A85-40237

BRIGHTNESS DISTRIBUTION

Contrasts among bidirectional reflectance of leaves, canopies, and soils p 3 A85-49106

C

CALIBRATING

Calibration of Doppler receivers p 8 A85-41195
Interferometric analysis of Doppler measurements for differential receiver calibration p 8 A85-41203
Comments on the intercalibration of multisensor, multitemporal, multichannel digital radiance data p 38 A85-42853
Spectroradiometric calibration of the Thematic Mapper and Multispectral Scanner system [E85-10104] p 47 N85-31601
TOPEX error budget p 47 N85-31717

CAMERAS

Large format camera photographs A new tool for understanding and environments p 47 N85-32379

CANOPIES (VEGETATION)

Specular, diffuse, and polarized light scattered by two wheat canopies p 1 A85-42865
View azimuth and zenith, and solar angle effects on wheat canopy reflectance p 2 A85-43120
Two-dimensional leaf orientation distributions p 2 A85-49104
Remote sensing of angular characteristics of canopy reflectances p 3 A85-49105
Contrasts among bidirectional reflectance of leaves, canopies, and soils p 3 A85-49106
A Monte Carlo reflectance model for soil surfaces with three-dimensional structure p 3 A85-49107

Evaluation of a canopy reflectance model for LAI estimation through its inversion --- leaf area index p 3 A85-49108

Modeling the radiant transfers of sparse vegetation canopies p 3 A85-49110

Geometric-optical modeling of a conifer forest canopy p 4 A85-49111

Plant canopy specular reflectance model p 4 A85-49112

Inclusion of specular reflectance in vegetative canopy models p 4 A85-49113

Sources of scattering from vegetation canopies at 10 GHz p 4 A85-49114

Microwave attenuation properties of vegetation canopies p 4 A85-49115

CELESTIAL GEODESY

Further improvements of the orbital program system Potsdam-5 and their utilization in geodetic-geodynamic investigations p 7 A85-41189
Calibration of Doppler receivers p 8 A85-41195
Space-age geodesy - The NASA Crustal Dynamics Project p 8 A85-42452
Lasers in space p 43 A85-42576
Establishment of three-dimensional geodetic control by interferometry with the global positioning system p 9 A85-44102
Comparative evaluations of the geodetic accuracy and cartographic potential of Landsat-4 and Landsat-5 Thematic Mapper image data p 10 A85-47804

CHLOROPHYLLS

Solid-state spectral transmissometer and radiometer p 30 A85-48670

CHROMITES

Some recent deposit modeling efforts p 23 N85-35453

CHROMIUM

Applications of the mineral resources data system and the international strategic minerals inventory in mineral-resource assessments by region and commodity p 23 N85-35451
The Conterminous United States Mineral Assessment Program p 24 N85-35458
The Alaska Mineral Resources Assessment Program p 24 N85-35460

CHRONOLOGY

A new global geomorphology? p 19 N85-32358

CITIES

SPOT simulation imagery for urban monitoring - A comparison with Landsat TM and MSS imagery and with high altitude color infrared photography p 6 A85-45871
Motor glider measurements during the Urban Atmosphere Energy Budget Experiment (EESA 1) p 7 N85-35553

CLASSIFICATIONS

Geomorphic classification of Icelandic and Martian volcanoes Limitations of comparative planetology research from LANDSAT and Viking orbiter images p 20 N85-32372

CLIFFS

Coastal erosion along Monterey Bay [AD-A155610] p 34 N85-32707

CLIMATOLOGY

Satellite propagation in the South Pacific region p 26 A85-42050
A global climatology of total ozone from the Nimbus 7 total ozone mapping spectrometer p 44 A85-45235

CLOUD COVER

Enhancing precision of remote temperature sensing data from satellites under cloudy atmospheric conditions p 48 N85-33148
Determination of altitude of cloud cover top from Meteor satellite data p 48 N85-33150
Repetition of dense cloud cover above Indian Ocean from generalized satellite data p 41 N85-33165

CLOUD PHOTOGRAPHY

Determination of altitude of cloud cover top from Meteor satellite data p 48 N85-33150

CLOUD SEEDING

Project Skywater, 1983-84 SCPP (Sierra Cooperative Pilot Project) data inventory [PB85-187052] p 49 N85-35565

CLOUDS (METEOROLOGY)

The albedo field and cloud radiative forcing produced by a general circulation model with internally generated cloud optics p 27 A85-43373
Satellite measurements of atmospheric aerosols [AD-A153807] p 32 N85-30556

COASTAL CURRENTS

Satellite observations of the circulation east of the Mississippi Delta - Cold-air outbreak conditions p 27 A85-43117

COASTAL WATER

Thermal satellite imagery applied to a littoral macrobenthos investigation in the Gulf of Maine p 25 A85-41662

- Methods of obtaining offshore wind direction and sea-state data from X-band aircraft SAR imagery of coastal waters p 25 A85-41753
- Evaluation of SPOT HRV simulation data for Corps of Engineers applications p 36 A85-45693
- A comparison of SPOT simulator data with Landsat MSS imagery for delineating water masses in Delaware Bay, Broadkill River, and adjacent wetlands p 27 A85-45875
- Properties of aerosol particles detected by satellites in coastal regions p 34 A85-32622
- Coastal erosion along Monterey Bay [AD-A155610] p 34 A85-32707
- Arctic and offshore research [DE85-001995] p 34 A85-33653
- COASTAL ZONE COLOR SCANNER**
- Utility of proposed sensors for coastal engineering studies p 45 A85-45697
- Solid-state spectral transmissometer and radiometer p 30 A85-48670
- Nimbus 7 Coastal Zone Color Scanner (CZCS) Level 2 data product users' guide [NASA-TM-86202] p 31 A85-30452
- Nimbus 7 Coastal Zone Color Scanner (CZCS) Level 1 data product users' guide [NASA-TM-86203] p 31 A85-30453
- COASTS**
- Properties of aerosol particles detected by satellites in coastal regions p 34 A85-32622
- Marine phosphonate deposits model for exploration, with emphasis on deposits in the US Atlantic coastal plain p 35 A85-35439
- USGS coastal research, studies and maps. A source of information for coastal decision making [USGS-CIRC-883] p 35 A85-35465
- COBALT**
- Applications of the mineral resources data system and the international strategic minerals inventory in mineral-resource assessments by region and commodity p 23 A85-35451
- The Conterminous United States Mineral Assessment Program p 24 A85-35458
- The Alaska Mineral Resources Assessment Program p 24 A85-35460
- COHERENT ACOUSTIC RADIATION**
- LANDSAT-4/5 image data quality analysis [E85-10105] p 41 A85-35463
- COLD FRONTS**
- Satellite observations of the circulation east of the Mississippi Delta - Cold-air outbreak conditions p 27 A85-43117
- COLOR INFRARED PHOTOGRAPHY**
- Vegetation profiles from color-infrared airphotos p 1 A85-42650
- SPOT simulation imagery for urban monitoring - A comparison with Landsat TM and MSS imagery and with high altitude color infrared photography p 6 A85-45871
- COLOR PHOTOGRAPHY**
- A survey of the Rehamna Hercynian Range in western Morocco using Landsat color composite imagery p 15 A85-42582
- COLORADO**
- Aeromagnetic and gravity models of the pluton below the Lake City caldera, Colorado p 23 A85-35442
- COMMITTEE ON SPACE RESEARCH**
- The French space program p 50 A85-33127
- COMMUNICATION SATELLITES**
- Satellites and politics Weather, communications, and earth resources p 50 A85-35144
- COMPARISON**
- Large-scale sea surface temperature variability from satellite and shipboard measurements [NASA-CR-176123] p 34 A85-33651
- COMPUTATION**
- Global mean sea surface based upon a combination of the GEOS-3 and SEASAT altimeter data p 32 A85-31710
- COMPUTER AIDED MAPPING**
- Interactive procedures for discriminating and restoring contour line networks p 41 A85-33158
- The scientific and technical issues in integrating remotely sensed imagery with geocoded data bases p 41 A85-34547
- Applied computer graphics in a geographic information system Problems and successes p 6 A85-34563
- COMPUTER GRAPHICS**
- Interactive procedures for discriminating and restoring contour line networks p 41 A85-33158
- Selection of segment similarity measures for hierarchical picture segmentation p 41 A85-34548
- Applied computer graphics in a geographic information system Problems and successes p 6 A85-34563
- COMPUTER PROGRAMS**
- Further improvements of the orbital program system Potsdam-5 and their utilization in geodetic-geodynamic investigations p 7 A85-41189
- Nimbus 7 Coastal Zone Color Scanner (CZCS) Level 2 data product users' guide [NASA-TM-86202] p 31 A85-30452
- Geodyn systems development p 13 A85-31708
- COMPUTER SYSTEMS DESIGN**
- Selection of segment similarity measures for hierarchical picture segmentation p 41 A85-34548
- COMPUTER TECHNIQUES**
- A fast Fourier transform method for computing terrain corrections p 37 A85-41396
- Interactive procedures for discriminating and restoring contour line networks p 41 A85-33158
- Discrimination of linear contour elements of space photographs based on visual perception model p 13 A85-33161
- COMPUTERIZED SIMULATION**
- Message collision of data collection system and its computer simulation p 46 A85-48894
- Comparative study of fracture planes computed from topography and lineaments from imagery with structures and mineralization in the magnetic belt of Washington State [DE85-010972] p 18 A85-31608
- CONFERENCES**
- The earth's surface studied from space, Proceedings of Workshop II of the COSPAR 25th Plenary Meeting, Graz, Austria, June 25-July 7, 1984 p 50 A85-45686
- Space methods for geological research p 16 A85-30429
- Remote Sensing Technology Symposium Proceedings [DE85-010212] p 47 A85-31606
- Commission for Marine Meteorology [WMO-640] p 33 A85-31735
- Proceedings of Meteorological Motor Glider (MEMO) Workshop '84 [DFVLR-MITT-85-04] p 7 A85-35542
- CONGRESSIONAL REPORTS**
- Antarctica [S-HRG-98-1181] p 50 A85-31584
- CONIFERS**
- Geometric-optical modeling of a conifer forest canopy p 4 A85-49111
- CONTINENTAL DRIFT**
- The evolving continents / 2nd revised and enlarged edition/ --- Book p 50 A85-42220
- CONTINENTAL SHELVES**
- A wind-induced mesoscale eddy over the Vancouver Island continental slope p 30 A85-49863
- CONTINENTS**
- Continental and oceanic magnetic anomalies Enhancement through GRM p 32 A85-31598
- Continental magnetic anomaly constraints on continental reconstruction p 12 A85-31599
- Regional magnetic anomaly constraints on continental rifting p 12 A85-31600
- CONTOUR SENSORS**
- LANDSAT-4/5 image data quality analysis [E85-10105] p 41 A85-35463
- CONTOURS**
- SEASAT altimetry for surface height of inland seas p 32 A85-31714
- Interactive procedures for discriminating and restoring contour line networks p 41 A85-33158
- Discrimination of linear contour elements of space photographs based on visual perception model p 13 A85-33161
- Evaluation Close-range photogrammetry for slope inventory and monitoring [PB85-192755] p 24 A85-35470
- CONVECTION CLOUDS**
- Conceptual models of precipitation systems p 45 A85-47245
- Mesoscale features and atmospheric refraction conditions of the Arctic marginal ice zone [AD-A155139] p 33 A85-32584
- CONVECTIVE FLOW**
- Measuring the global distribution of intense convection over land with passive microwave radiometry p 36 A85-47923
- CONVECTIVE HEAT TRANSFER**
- Lidar observations of vertically organized convection in the planetary boundary layer over the ocean p 30 A85-47921
- COPPER**
- Some recent deposit modeling efforts p 23 A85-35453
- The Conterminous United States Mineral Assessment Program p 24 A85-35458
- The Alaska Mineral Resources Assessment Program p 24 A85-35460
- COSMOS SATELLITES**
- Program of experiments on the Cosmos-1500 satellite p 28 A85-46251
- Determination of the ice-cover characteristics of the Sea of Okhotsk in the winter of 1983-1984 on the basis of radar-sounding data p 28 A85-46253
- The use of radar images obtained with the Cosmos-1500 satellite to study the distribution and dynamics of sea ice p 28 A85-46254
- Radar maps of the Arctic and Antarctic compiled on the basis of Cosmos-1500 satellite data, and preliminary results of their analysis p 29 A85-46259
- The data acquisition system on the Cosmos-1500 satellite p 29 A85-46260
- Investigation of the ocean with low-resolution multispectral scanners p 29 A85-46261
- The sidelooking radar on the Cosmos-1500 satellite p 29 A85-46262
- Informational potential of the sidelooking radar of the Cosmos-1500 satellite p 29 A85-46263
- Automated processing of remote-sensing data obtained with the microwave radiometer of the Cosmos-1500 satellite p 29 A85-46265
- Digital processing of radar images obtained with the Cosmos-1500 satellite p 29 A85-46266
- The experimental oceanographic satellite Cosmos-1500 p 30 A85-46267
- CROP IDENTIFICATION**
- Shortwave infrared detection of vegetation p 2 A85-45691
- Interpretation of multiband photographs made during Telefoto-80 experiment for the purpose of discriminating agricultural crops p 5 A85-33152
- CROSS CORRELATION**
- High-latitude mesopause neutral winds and geomagnetic activity - A cross-correlation analysis p 16 A85-49227
- CROSSBEDDING (GEOLOGY)**
- The U.S. Geological Survey in Alaska Accomplishments during 1982 [US-GEOL-SURV-CIRC-939] p 19 A85-31719
- CRUDE OIL**
- Visible fluorescence from ultraviolet excited crude oil p 27 A85-42512
- Petroleum and mineral resources of Antarctica [US-GEOL-SURV-CIRC-909] p 18 A85-31605
- CRUSTAL FRACTURES**
- Geodynamics Branch research program [NASA-TM-86223] p 18 A85-31688
- The global VLBL fiducial network p 12 A85-31690
- First epoch measurements by Mark III VLBL of the San Andreas Fault experiment baseline p 12 A85-31691
- Geophysical interpretation of satellite laser ranging measurements p 19 A85-31692
- Satellite-determined stresses in the crust of Europe with particular consideration to the Liege earthquake of November 8, 1983 p 13 A85-31694
- Mega-geomorphology and neotectonics p 20 A85-32366
- Use of space photographs for analysis of structural and dynamic conditions of formation of ancient phlogopite and apatite deposits p 22 A85-33153
- CRYOGENIC EQUIPMENT**
- Cryogenic magnetic gradiometers for space applications p 43 A85-42475
- CV-990 AIRCRAFT**
- MIZEX, 1984, NASA CV-990 flight report [NASA-TM-86216] p 31 A85-30451
- CYCLOGENESIS**
- Surface cyclogenesis as indicated by satellite imagery [PB85-191815] p 42 A85-35566
- CYCLOONES**
- Geopotential heights and thicknesses as predictors of Atlantic tropical cyclone motion and intensity p 26 A85-42177
- Small-scale cyclones on the periphery of a Gulf Stream warm-core ring p 30 A85-49855

D

DATA ACQUISITION

- Data acquisition and processing system based on a microprocessor set for the study of earth resources p 43 A85-43074
- Remote Sensing Technology Symposium Proceedings [DE85-010212] p 47 A85-31606
- Tropical Ocean and Global Atmosphere (TOGA) heat exchange project A summary report [NASA-CR-176038] p 33 A85-31738
- Microcomputer processing of LANDSAT Thematic Mapper data for the acquisition of military tactical terrain data [AD-A154781] p 47 A85-32389
- Federal Mineral Land Information System p 7 A85-35459

DATA BASES

- Remote Sensing Technology Symposium
Proceedings
[DE85-010212] p 47 N85-31606
Applications of the mineral resources data system and the international strategic minerals inventory in mineral-resource assessments by region and commodity p 23 N85-35451

DATA COLLECTION PLATFORMS

- Message collision of data collection system and its computer simulation p 46 A85-48894

DATA PROCESSING

- Federal Mineral Land Information System p 7 N85-35459

DATA RETRIEVAL

- Federal Mineral Land Information System p 7 N85-35459

DEFOLIATION

- Forest cover type mapping and spruce budworm defoliation detection using simulated SPOT imagery p 2 A85-45874

DEFORMATION

- Crustal Dynamics Project Catalogue of site information [NASA-TM-86218] p 14 N85-33552

DELTAS

- Mapping of dynamics of deltas by space photography p 14 N85-33163

DEMOGRAPHY

- Estimation of rural population in Kordofan, Sudan p 6 A85-42579

DENSITY MEASUREMENT

- Application of satellite accelerometer data to improve density models [AD-A154904] p 48 N85-32558

DESORPTION

- Evaluation Close-range photogrammetry for slope inventory and monitoring [PB85-192755] p 24 N85-35470

DETECTION

- A microprocessor-controlled, multichannel fluorimeter for analysis of sea water [AD-A154986] p 33 N85-32310
LANDSAT-4/5 image data quality analysis [E85-10105] p 41 N85-35463

DIELECTRICS

- Modeling of radio-wave scattering by ice cover p 30 A85-49477

DIGITAL DATA

- Contextual classification post-processing of Landsat data using a probabilistic relaxation model p 37 A85-41658

- Comments on the intercalibration of multisensor, multitemporal, multichannel digital radiance data p 38 A85-42853

- Systematic and random variations in Thematic Mapper digital radiance data p 40 A85-47820

DIGITAL SYSTEMS

- Microcomputer processing of LANDSAT Thematic Mapper data for the acquisition of military tactical terrain data [AD-A154781] p 47 N85-32389

DIGITAL TECHNIQUES

- Digital processing of radar images obtained with the Cosmos-1500 satellite p 29 A85-46266

- Spectral reflectances of natural targets for use in remote sensing studies [NASA-RP-1139] p 41 N85-30450

- Interactive procedures for discriminating and restoring contour line networks p 41 N85-33158

- The scientific and technical issues in integrating remotely sensed imagery with geocoded data bases p 41 N85-34547

- Processing of LANDSAT imagery to map surface mineral alteration on the Alaska Peninsula, Alaska p 23 N85-35455

- Remote sensing of hydrologic transport processes using spot simulation data [DE85-012412] p 37 N85-35467

DIODES

- A microprocessor-controlled, multichannel fluorimeter for analysis of sea water [AD-A154986] p 33 N85-32310

DIRECTORIES

- Worldwide directory of national Earth-science agencies and related international organizations [GS-CIRC-934] p 50 N85-32386

DISPERSING

- Dispersion of sea ice in the Bering Sea p 26 A85-42257

DISTANCE MEASURING EQUIPMENT

- Comparison of survey and photogrammetry methods to position gravity data, Yucca Mountain, Nevada [DE85-011685] p 13 N85-32316

DOPPLER RADAR

- The impact of higher-order Bragg terms on radar sea return p 24 A85-40237
Interferometric analysis of Doppler measurements for differential receiver calibration p 8 A85-41203

DRAINAGE

- Geomorphic analyses from space imagery p 20 N85-32374

E

EARTH ALBEDO

- The effect of the interface albedo of the underlying surface on the reflected radiation p 10 A85-46131
The determination of the albedo of natural covers of the earth on the basis of remote measurement results p 10 A85-46132
A new technique for inferring surface albedo from satellite observations p 46 A85-47916

EARTH ATMOSPHERE

- Impact of fluctuations in optical properties of atmosphere on the ratio of spectral brightness from remote sensing of agricultural land p 5 N85-33149
Determination of altitude of cloud cover top from Meteor satellite data p 48 N85-33150

EARTH CRUST

- The evolving continents /2nd revised and enlarged edition/ --- Book p 50 A85-42220
Space-age geodesy - The NASA Crustal Dynamics Project p 8 A85-42452
Secular variation, crustal contributions, and tectonic activity in California, 1976-1984 p 15 A85-47898
Discovery in earthquake forecasting and seismic zoning recorded p 16 N85-30426
Improving the geological interpretation of magnetic and gravity satellite anomalies [E85-10103] p 11 N85-31585
The south-central United States magnetic anomaly p 17 N85-31591
The south-central United States magnetic anomaly p 18 N85-31592
Continental and oceanic magnetic anomalies Enhancement through GRM p 32 N85-31598
Continental magnetic anomaly constraints on continental reconstruction p 12 N85-31599
Regional magnetic anomaly constraints on continental rifting p 12 N85-31600
The global VLBI fiducial network p 12 N85-31690
Spacecraft-aided research discussed at geology Congress p 22 N85-33147

EARTH MANTLE

- Landscape interpretation capabilities using space photographs of regions of a multistage platform mantle structure p 22 N85-33151

EARTH MOVEMENTS

- Satellite geodynamics p 8 A85-42451
Space-age geodesy - The NASA Crustal Dynamics Project p 8 A85-42452
The global VLBI fiducial network p 12 N85-31690
Mapping of dynamics of deltas by space photography p 14 N85-33163
Crustal Dynamics Project Catalogue of site information [NASA-TM-86218] p 14 N85-33552

EARTH OBSERVATIONS (FROM SPACE)

- Commercialization of remote-sensing technology p 49 A85-41657
Cartographic-photogrammetric analysis and analytical correction of space scanner images p 38 A85-44864
The earth's surface studied from space, Proceedings of Workshop II of the COSPAR 25th Plenary Meeting, Graz, Austria, June 25-July 7, 1984 p 50 A85-45686
Evaluation of SPOT simulator data for the detection of alteration in Goldfield/Cupente, Nevada p 15 A85-45873

EARTH MOVEMENTS

- Aerial and space-based remote sensing in ecological prognosis p 6 A85-46249
The USSR as viewed from space p 50 A85-48524
Message collision of data collection system and its computer simulation p 46 A85-48894
Large format camera photographs A new tool for understanding and environments p 47 N85-32379
Quantitative geomorphologic studies from spaceborne platforms p 21 N85-32381
Process thresholds Report of Working Group Number 3 p 21 N85-32384
Planetary perspective Report of Working Group Number 4 p 22 N85-32385
Properties of aerosol particles detected by satellites in coastal regions p 34 N85-32622
Cosmonauts participate in multilevel remote sensing experiment p 48 N85-33130
Physico-geographical regionalization of Caspian lowland based on space survey materials p 14 N85-33162

- Aerial and space-based remote sensing in ecological prognosis p 6 A85-46249
The USSR as viewed from space p 50 A85-48524
Message collision of data collection system and its computer simulation p 46 A85-48894
Large format camera photographs A new tool for understanding and environments p 47 N85-32379
Quantitative geomorphologic studies from spaceborne platforms p 21 N85-32381
Process thresholds Report of Working Group Number 3 p 21 N85-32384
Planetary perspective Report of Working Group Number 4 p 22 N85-32385
Properties of aerosol particles detected by satellites in coastal regions p 34 N85-32622
Cosmonauts participate in multilevel remote sensing experiment p 48 N85-33130
Physico-geographical regionalization of Caspian lowland based on space survey materials p 14 N85-33162

- Aerial and space-based remote sensing in ecological prognosis p 6 A85-46249
The USSR as viewed from space p 50 A85-48524
Message collision of data collection system and its computer simulation p 46 A85-48894
Large format camera photographs A new tool for understanding and environments p 47 N85-32379
Quantitative geomorphologic studies from spaceborne platforms p 21 N85-32381
Process thresholds Report of Working Group Number 3 p 21 N85-32384
Planetary perspective Report of Working Group Number 4 p 22 N85-32385
Properties of aerosol particles detected by satellites in coastal regions p 34 N85-32622
Cosmonauts participate in multilevel remote sensing experiment p 48 N85-33130
Physico-geographical regionalization of Caspian lowland based on space survey materials p 14 N85-33162

- Aerial and space-based remote sensing in ecological prognosis p 6 A85-46249
The USSR as viewed from space p 50 A85-48524
Message collision of data collection system and its computer simulation p 46 A85-48894
Large format camera photographs A new tool for understanding and environments p 47 N85-32379
Quantitative geomorphologic studies from spaceborne platforms p 21 N85-32381
Process thresholds Report of Working Group Number 3 p 21 N85-32384
Planetary perspective Report of Working Group Number 4 p 22 N85-32385
Properties of aerosol particles detected by satellites in coastal regions p 34 N85-32622
Cosmonauts participate in multilevel remote sensing experiment p 48 N85-33130
Physico-geographical regionalization of Caspian lowland based on space survey materials p 14 N85-33162

- Aerial and space-based remote sensing in ecological prognosis p 6 A85-46249
The USSR as viewed from space p 50 A85-48524
Message collision of data collection system and its computer simulation p 46 A85-48894
Large format camera photographs A new tool for understanding and environments p 47 N85-32379
Quantitative geomorphologic studies from spaceborne platforms p 21 N85-32381
Process thresholds Report of Working Group Number 3 p 21 N85-32384
Planetary perspective Report of Working Group Number 4 p 22 N85-32385
Properties of aerosol particles detected by satellites in coastal regions p 34 N85-32622
Cosmonauts participate in multilevel remote sensing experiment p 48 N85-33130
Physico-geographical regionalization of Caspian lowland based on space survey materials p 14 N85-33162

- Aerial and space-based remote sensing in ecological prognosis p 6 A85-46249
The USSR as viewed from space p 50 A85-48524
Message collision of data collection system and its computer simulation p 46 A85-48894
Large format camera photographs A new tool for understanding and environments p 47 N85-32379
Quantitative geomorphologic studies from spaceborne platforms p 21 N85-32381
Process thresholds Report of Working Group Number 3 p 21 N85-32384
Planetary perspective Report of Working Group Number 4 p 22 N85-32385
Properties of aerosol particles detected by satellites in coastal regions p 34 N85-32622
Cosmonauts participate in multilevel remote sensing experiment p 48 N85-33130
Physico-geographical regionalization of Caspian lowland based on space survey materials p 14 N85-33162

- Aerial and space-based remote sensing in ecological prognosis p 6 A85-46249
The USSR as viewed from space p 50 A85-48524
Message collision of data collection system and its computer simulation p 46 A85-48894
Large format camera photographs A new tool for understanding and environments p 47 N85-32379
Quantitative geomorphologic studies from spaceborne platforms p 21 N85-32381
Process thresholds Report of Working Group Number 3 p 21 N85-32384
Planetary perspective Report of Working Group Number 4 p 22 N85-32385
Properties of aerosol particles detected by satellites in coastal regions p 34 N85-32622
Cosmonauts participate in multilevel remote sensing experiment p 48 N85-33130
Physico-geographical regionalization of Caspian lowland based on space survey materials p 14 N85-33162

- Aerial and space-based remote sensing in ecological prognosis p 6 A85-46249
The USSR as viewed from space p 50 A85-48524
Message collision of data collection system and its computer simulation p 46 A85-48894
Large format camera photographs A new tool for understanding and environments p 47 N85-32379
Quantitative geomorphologic studies from spaceborne platforms p 21 N85-32381
Process thresholds Report of Working Group Number 3 p 21 N85-32384
Planetary perspective Report of Working Group Number 4 p 22 N85-32385
Properties of aerosol particles detected by satellites in coastal regions p 34 N85-32622
Cosmonauts participate in multilevel remote sensing experiment p 48 N85-33130
Physico-geographical regionalization of Caspian lowland based on space survey materials p 14 N85-33162

- Aerial and space-based remote sensing in ecological prognosis p 6 A85-46249
The USSR as viewed from space p 50 A85-48524
Message collision of data collection system and its computer simulation p 46 A85-48894
Large format camera photographs A new tool for understanding and environments p 47 N85-32379
Quantitative geomorphologic studies from spaceborne platforms p 21 N85-32381
Process thresholds Report of Working Group Number 3 p 21 N85-32384
Planetary perspective Report of Working Group Number 4 p 22 N85-32385
Properties of aerosol particles detected by satellites in coastal regions p 34 N85-32622
Cosmonauts participate in multilevel remote sensing experiment p 48 N85-33130
Physico-geographical regionalization of Caspian lowland based on space survey materials p 14 N85-33162

- Aerial and space-based remote sensing in ecological prognosis p 6 A85-46249
The USSR as viewed from space p 50 A85-48524
Message collision of data collection system and its computer simulation p 46 A85-48894
Large format camera photographs A new tool for understanding and environments p 47 N85-32379
Quantitative geomorphologic studies from spaceborne platforms p 21 N85-32381
Process thresholds Report of Working Group Number 3 p 21 N85-32384
Planetary perspective Report of Working Group Number 4 p 22 N85-32385
Properties of aerosol particles detected by satellites in coastal regions p 34 N85-32622
Cosmonauts participate in multilevel remote sensing experiment p 48 N85-33130
Physico-geographical regionalization of Caspian lowland based on space survey materials p 14 N85-33162

- Aerial and space-based remote sensing in ecological prognosis p 6 A85-46249
The USSR as viewed from space p 50 A85-48524
Message collision of data collection system and its computer simulation p 46 A85-48894
Large format camera photographs A new tool for understanding and environments p 47 N85-32379
Quantitative geomorphologic studies from spaceborne platforms p 21 N85-32381
Process thresholds Report of Working Group Number 3 p 21 N85-32384
Planetary perspective Report of Working Group Number 4 p 22 N85-32385
Properties of aerosol particles detected by satellites in coastal regions p 34 N85-32622
Cosmonauts participate in multilevel remote sensing experiment p 48 N85-33130
Physico-geographical regionalization of Caspian lowland based on space survey materials p 14 N85-33162

- Aerial and space-based remote sensing in ecological prognosis p 6 A85-46249
The USSR as viewed from space p 50 A85-48524
Message collision of data collection system and its computer simulation p 46 A85-48894
Large format camera photographs A new tool for understanding and environments p 47 N85-32379
Quantitative geomorphologic studies from spaceborne platforms p 21 N85-32381
Process thresholds Report of Working Group Number 3 p 21 N85-32384
Planetary perspective Report of Working Group Number 4 p 22 N85-32385
Properties of aerosol particles detected by satellites in coastal regions p 34 N85-32622
Cosmonauts participate in multilevel remote sensing experiment p 48 N85-33130
Physico-geographical regionalization of Caspian lowland based on space survey materials p 14 N85-33162

- Aerial and space-based remote sensing in ecological prognosis p 6 A85-46249
The USSR as viewed from space p 50 A85-48524
Message collision of data collection system and its computer simulation p 46 A85-48894
Large format camera photographs A new tool for understanding and environments p 47 N85-32379
Quantitative geomorphologic studies from spaceborne platforms p 21 N85-32381
Process thresholds Report of Working Group Number 3 p 21 N85-32384
Planetary perspective Report of Working Group Number 4 p 22 N85-32385
Properties of aerosol particles detected by satellites in coastal regions p 34 N85-32622
Cosmonauts participate in multilevel remote sensing experiment p 48 N85-33130
Physico-geographical regionalization of Caspian lowland based on space survey materials p 14 N85-33162

EARTH PLANETARY STRUCTURE

- Highly important features of regional tectonics of Earth's Arctic sector p 17 N85-30449
Landscape interpretation capabilities using space photographs of regions of a multistage platform mantle structure p 22 N85-33151

EARTH RADIATION BUDGET EXPERIMENT

- Space Station Polar Platform Integrating research and operational missions [PB85-195279] p 49 N85-35218

EARTH RESOURCES

- The selection of optimum spectral channels for multispectral remote sensing p 43 A85-42484
Data acquisition and processing system based on a microprocessor set for the study of earth resources p 43 A85-43074
Evaluation of simulated SPOT imagery for the interpretation of agricultural resources in California p 2 A85-45872

- Remote Sensing Technology Symposium Proceedings [DE85-010212] p 47 N85-31606
The U S Geological Survey in Alaska Accomplishments during 1982 p 19 N85-31719
[US-GEOL-SURV-CIRC-939] Handbook for obtaining and using aerial photography to map aquatic plant distribution [AD-A154584] p 33 N85-32388

- Cosmonauts participate in multilevel remote sensing experiment p 48 N85-33130
The scientific and technical issues in integrating remotely sensed imagery with geocoded data bases p 41 N85-34547

- Selection of segment similarity measures for hierarchical picture segmentation p 41 N85-34548
Satellites and politics Weather, communications, and earth resources p 50 N85-35144

- Microwave properties of a quiet sea [NASA-CR-176199] p 35 N85-35322
USGS coastal research, studies and maps A source of information for coastal decision making [USGS-CIRC-883] p 35 N85-35465

- Remote sensing of hydrologic transport processes using spot simulation data [DE85-012412] p 37 N85-35467

- Remote sensing of hydrologic transport processes using spot simulation data [DE85-012412] p 37 N85-35467

- Remote sensing of hydrologic transport processes using spot simulation data [DE85-012412] p 37 N85-35467

- Remote sensing of hydrologic transport processes using spot simulation data [DE85-012412] p 37 N85-35467

- Remote sensing of hydrologic transport processes using spot simulation data [DE85-012412] p 37 N85-35467

- Remote sensing of hydrologic transport processes using spot simulation data [DE85-012412] p 37 N85-35467

- Remote sensing of hydrologic transport processes using spot simulation data [DE85-012412] p 37 N85-35467

- Remote sensing of hydrologic transport processes using spot simulation data [DE85-012412] p 37 N85-35467

- Remote sensing of hydrologic transport processes using spot simulation data [DE85-012412] p 37 N85-35467

- Remote sensing of hydrologic transport processes using spot simulation data [DE85-012412] p 37 N85-35467

- Remote sensing of hydrologic transport processes using spot simulation data [DE85-012412] p 37 N85-35467

- Remote sensing of hydrologic transport processes using spot simulation data [DE85-012412] p 37 N85-35467

- Remote sensing of hydrologic transport processes using spot simulation data [DE85-012412] p 37 N85-35467

- Remote sensing of hydrologic transport processes using spot simulation data [DE85-012412] p 37 N85-35467

- Remote sensing of hydrologic transport processes using spot simulation data [DE85-012412] p 37 N85-35467

- Remote sensing of hydrologic transport processes using spot simulation data [DE85-012412] p 37 N85-35467

- Remote sensing of hydrologic transport processes using spot simulation data [DE85-012412] p 37 N85-35467

- Remote sensing of hydrologic transport processes using spot simulation data [DE85-012412] p 37 N85-35467

- Remote sensing of hydrologic transport processes using spot simulation data [DE85-012412] p 37 N85-35467

- Remote sensing of hydrologic transport processes using spot simulation data [DE85-012412] p 37 N85-35467

- Remote sensing of hydrologic transport processes using spot simulation data [DE85-012412] p 37 N85-35467

- Remote sensing of hydrologic transport processes using spot simulation data [DE85-012412] p 37 N85-35467

- Remote sensing of hydrologic transport processes using spot simulation data [DE85-012412] p 37 N85-35467

- Remote sensing of hydrologic transport processes using spot simulation data [DE85-012412] p 37 N85-35467

EDUCATION

- One application of mega-geomorphology in education
p 6 N85-32370

ELECTROMAGNETIC SCATTERING

- A comparison between active and passive sensing of soil moisture from vegetated terrains p 4 A85-49118
Active and passive remote sensing of ice
[AD-A154406] p 31 N85-30459

ELECTRON PRECIPITATION

- Wave-induced precipitation as a loss process for radiation belt particles p 25 A85-41961

ELECTRONIC CONTROL

- A microprocessor-controlled, multichannel fluorimeter for analysis of sea water
[AD-A154986] p 33 N85-32310

ELEVATION

- Comparison of survey and photogrammetry methods to position gravity data, Yucca Mountain, Nevada
[DE85-011685] p 13 N85-32316

ENERGETIC PARTICLES

- Wave-induced precipitation as a loss process for radiation belt particles p 25 A85-41961

ENERGY TECHNOLOGY

- Arctic and offshore research
[DE85-001995] p 34 N85-33653

ENVIRONMENTAL MONITORING

- Aerial and space-based remote sensing in ecological prognosis p 6 A85-46249

ENVIRONMENTAL SURVEYS

- Environmental-physical measurements and determination of atmospheric turbulence with the ASK-16 motor glider p 7 N85-35549

ENVIRONMENTS

- Satellite measurements of atmospheric aerosols
[AD-A153807] p 32 N85-30556

EROSION

- Coastal erosion along Monterey Bay
[AD-A155610] p 34 N85-32707

ERROR ANALYSIS

- Satellite measurements of atmospheric aerosols
[AD-A153807] p 32 N85-30556

- Spaceborne gradiometer error analysis
p 13 N85-31707

- TOPEX error budget
p 47 N85-31717

ERROR CORRECTING DEVICES

- A fast Fourier transform method for computing terrain corrections p 37 A85-41396

ERROR SIGNALS

- LANDSAT-4/5 image data quality analysis
[E85-10105] p 41 N85-35463

ERRORS

- Comparison of survey and photogrammetry methods to position gravity data, Yucca Mountain, Nevada
[DE85-011685] p 13 N85-32316

ERS-1 (ESA SATELLITE)

- The ERS-1 synthetic aperture radar and scatterometer
p 45 A85-46849

ESTIMATING

- LANDSAT-4/5 image data quality analysis
[E85-10105] p 41 N85-35463

EUROPE

- Reduced to pole long-wavelength magnetic anomalies of Africa and Europe p 18 N85-31595
Euro-African MAGSAT anomaly-tectonic observations
p 18 N85-31596

- Long-wavelength magnetic and gravity anomaly correlations on Africa and Europe p 12 N85-31597

EVAPORATION

- Influence of spatial variability of hydraulic characteristics of soils on surface parameters obtained from remote sensing data in infrared and microwaves
[NASA-TM-77902] p 5 N85-31604

EXPLORATION

- Some recent deposit modeling efforts
p 23 N85-35453

EXTRAPOLATION

- Application of pattern-recognition and extrapolation techniques to forecasting p 45 A85-47244

EXTREMELY HIGH FREQUENCIES

- Preliminary investigations concerning a 90 GHz radiometer satellite experiment
[ESA-TT-860] p 46 N85-31225

F**FAST FOURIER TRANSFORMATIONS**

- A fast Fourier transform method for computing terrain corrections p 37 A85-41396

FEASIBILITY ANALYSIS

- Methods for destriping Landsat Thematic Mapper images - A feasibility study for an online destriping process in the Thematic Mapper Image Processing System (TIPS) p 39 A85-47813

- Preliminary investigations concerning a 90 GHz radiometer satellite experiment
[ESA-TT-860] p 46 N85-31225
Rain volume estimation over areas using satellite and radar data
[NASA-CR-176050] p 36 N85-32570

FELDSPARS

- Conditions for formation of parageneses containing kyanite-orthoclase in region of Mount Provender and Pratt Peak (Shackleton Range, Antarctica) p 16 N85-30447

FINE STRUCTURE

- Fine structure of the preliminary impulse of a sudden storm commencement p 14 A85-40612

FLOW STABILITY

- Some features of the Algerian Current
p 26 A85-42255

FLUORESCENCE

- Visible fluorescence from ultraviolet excited crude oil
p 27 A85-42512

- A microprocessor-controlled, multichannel fluorimeter for analysis of sea water
[AD-A154986] p 33 N85-32310

FOLDS (GEOLOGY)

- Using remote photographs in prospecting for hydrocarbons on the Kerch Peninsula p 22 N85-33154

FORECASTING

- Discovery in earthquake forecasting and seismic zoning recorded p 16 N85-30426

FOREST FIRE DETECTION

- Aerospace technology determines forest-fire danger
[AD-A154986] p 5 N85-30427

FORESTS

- Evaluation of Thematic Mapper data for mapping forest, agricultural and soil resources p 2 A85-45690

- Forest cover type mapping and spruce budworm defoliation detection using simulated SPOT imagery
p 2 A85-45874

- Interpretation of Landsat-4 Thematic Mapper and Multispectral Scanner data for forest surveys
p 2 A85-47806

- Geometric-optical modeling of a conifer forest canopy
p 4 A85-49111

FRENCH SPACE PROGRAMS

- The French space program p 50 N85-33127

FRUITS

- Remote sensing investigations on some fruit orchards in El Fayoum area, Egypt p 1 A85-42581

G**GALLIUM ARSENIDES**

- Millimetre wave pulse technology --- satellite mapping
[ESA-CR(P)-2004] p 47 N85-31611

GAS COMPOSITION

- The origin of temporal variance in long-lived trace constituents in the summer stratosphere
p 6 A85-43375

GEOCHEMISTRY

- The U.S. Geological Survey in Alaska Accomplishments during 1982
[US-GEOL-SURV-CIRC-939] p 19 N85-31719

- Global Mega-Geomorphology
[NASA-CP-2312] p 19 N85-32357

- The development of assessment techniques program
p 24 N85-35457

- The Alaska Mineral Resources Assessment Program
p 24 N85-35460

GEOCHRONOLOGY

- The evolving continents /2nd revised and enlarged edition/ --- Book p 50 A85-42220

- Global Mega-Geomorphology
[NASA-CP-2312] p 19 N85-32357

- Landscape inheritance Report of Working Group Number 2 p 21 N85-32383

- Hydrogeology of the lower Glen Rose Aquifer, south-central Texas p 36 N85-35466

GEODESY

- Preliminary results of Finnish-Hungarian Doppler Observation Campaign /FHDOC/ p 8 A85-41199

- Interferometric analysis of Doppler measurements for differential receiver calibration p 8 A85-41203

- The research work at the Central Institute for Physics of the Earth, Potsdam, GDR, in the field of Doppler satellite geodesy p 8 A85-41204

- A water-vapor radiometer error model --- for ionosphere in geodetic microwave techniques p 8 A85-42464

- Intrinsic geodesy --- Book p 9 A85-43958

- Geodyn systems development p 13 N85-31708

- Crustal Dynamics Project Catalogue of site information
[NASA-TM-86218] p 14 N85-33552

GEODETTIC ACCURACY

- Comparative evaluations of the geodetic accuracy and cartographic potential of Landsat-4 and Landsat-5 Thematic Mapper image data p 10 A85-47804
Evaluation of Thematic Mapper interband registration and noise characteristics p 46 A85-47819

GEODETTIC COORDINATES

- Preliminary results of Finnish-Hungarian Doppler Observation Campaign /FHDOC/ p 8 A85-41199

GEODETTIC SURVEYS

- Geodetic and geophysical results from Lageos p 7 A85-40003

- Further improvements of the orbital program system Potsdam-5 and their utilization in geodetic-geodynamic investigations p 7 A85-41189

- Calibration of Doppler receivers p 8 A85-41195

- Space-age geodesy - The NASA Crustal Dynamics Project p 8 A85-42452

- Application of GPS in a high precision engineering survey network
[DE85-010556] p 10 N85-30539

GEODYNAMICS

- Further improvements of the orbital program system Potsdam-5 and their utilization in geodetic-geodynamic investigations p 7 A85-41189

- Satellite geodynamics p 8 A85-42451

- Space-age geodesy - The NASA Crustal Dynamics Project p 8 A85-42452

- Geodynamics Branch research program
[NASA-TM-86223] p 18 N85-31688

- Mapping of dynamics of deltas by space photography
p 14 N85-33163

GEOGRAPHIC INFORMATION SYSTEMS

- Data acquisition and processing system based on a microprocessor set for the study of earth resources

- Multiple sensor geocoded data p 38 A85-45695

GEOGRAPHY

- Applied computer graphics in a geographic information system Problems and successes p 6 N85-34563

GEOIDS

- Thermal isostasy in the South Atlantic Ocean from geoid anomalies p 27 A85-44925

- Application of GPS in a high precision engineering survey network
[DE85-010556] p 10 N85-30539

- Spaceborne gradiometer error analysis
p 13 N85-31707

- Global mean sea surface based upon a combination of the GEOS-3 and SEASAT altimeter data
p 32 N85-31710

GEOLOGICAL FAULTS

- Discovery in earthquake forecasting and seismic zoning recorded p 16 N85-30426

- Comparative study of fracture planes computed from topography and lineaments from imagery with structures and mineralization in the magnetic belt of Washington State
[DE85-010972] p 18 N85-31608

- Spacecraft-aided research discussed at geology Congress p 22 N85-33147

- Landscape interpretation capabilities using space photographs of regions of a multistage platform mantle structure p 22 N85-33151

GEOLOGICAL SURVEYS

- The Antarctic ice p 14 A85-42171

- Geology and structures study of the Nuba Mountains, Sudan, using Landsat images p 15 A85-42580

- Space methods for geological research
p 16 N85-30429

- Highly important features of regional tectonics of Earth's Arctic sector p 17 N85-30449

- Engineering geology of selected areas, US army engineer division, lower Mississippi valley The American bottom area, MO-IL Volume 1 p 17 N85-30455

- Petroleum and mineral resources of Antarctica
[US-GEOL-SURV-CIRC-909] p 18 N85-31605

- The U.S. Geological Survey in Alaska Accomplishments during 1982
[US-GEOL-SURV-CIRC-939] p 19 N85-31719

- Worldwide directory of national Earth-science agencies and related international organizations
[GS-CIRC-934] p 50 N85-32386

- The United States Geological Survey in Alaska Accomplishments during 1983
[USGS-CIRC-945] p 23 N85-34468

- The development of assessment techniques program
p 24 N85-35457

- The Conterminous United States Mineral Assessment Program p 24 N85-35458

- Federal Mineral Land Information System
p 7 N85-35459

- The Alaska Mineral Resources Assessment Program
p 24 N85-35460

- USGS coastal research, studies and maps A source of information for coastal decision making [USGS-CIRC-883] p 35 N85-35465
- Evaluation Close-range photogrammetry for slope inventory and monitoring [PB85-192755] p 24 N85-35470
- GEOLOGY**
- Improving the geological interpretation of magnetic and gravity satellite anomalies [E85-10103] p 11 N85-31585
- Geologic analysis of averaged magnetic satellite anomalies p 17 N85-31588
- Statistical magnetic anomalies from satellite measurements for geologic analysis p 17 N85-31589
- Binning of satellite magnetic anomalies p 11 N85-31590
- The south-central United States magnetic anomaly p 17 N85-31591
- The south-central United States magnetic anomaly p 18 N85-31592
- Global Mega-Geomorphology [NASA-CP-2312] p 19 N85-32357
- Space imagery and some geomorphological problems of the Guiana Shield, South America p 20 N85-32368
- One application of mega-geomorphology in education p 6 N85-32370
- Worldwide directory of national Earth-science agencies and related international organizations [GS-CIRC-934] p 50 N85-32386
- Spacecraft-aided research discussed at geology Congress p 22 N85-33147
- GEOMAGNETIC PULSATIONS**
- Fine structure of the preliminary impulse of a sudden storm commencement p 14 A85-40612
- GEOMAGNETISM**
- Geopotential Research Mission - Status report p 8 A85-42469
- The magnetic field of the earth - Performance considerations for space-based observing systems p 9 A85-42474
- Cryogenic magnetic gradiometers for space applications p 43 A85-42475
- Secular variation, crustal contributions, and tectonic activity in California, 1976-1984 p 15 A85-47898
- High-latitude mesopause neutral winds and geomagnetic activity - A cross-correlation analysis p 16 A85-49227
- MAGSAT scalar anomaly map of South America p 11 N85-31586
- MAGSAT satellite magnetic anomaly map over South America p 11 N85-31587
- Geologic analysis of averaged magnetic satellite anomalies p 17 N85-31588
- Statistical magnetic anomalies from satellite measurements for geologic analysis p 17 N85-31589
- Binning of satellite magnetic anomalies p 11 N85-31590
- The south-central United States magnetic anomaly p 17 N85-31591
- The south-central United States magnetic anomaly p 18 N85-31592
- Reduced to pole long-wavelength magnetic anomalies of Africa and Europe p 18 N85-31595
- Euro-African MAGSAT anomaly-tectonic observations p 18 N85-31596
- Continental and oceanic magnetic anomalies Enhancement through GRM p 32 N85-31598
- Continental magnetic anomaly constraints on continental reconstruction p 12 N85-31599
- Regional magnetic anomaly constraints on continental rifting p 12 N85-31600
- GEOMETRIC ACCURACY**
- Landsat-4 and Landsat-5 Thematic Mapper data quality analysis p 39 A85-47818
- GEOMETRIC RECTIFICATION (IMAGERY)**
- LANDSAT-4/5 image data quality analysis [E85-10105] p 41 N85-35463
- GEOMETRICAL OPTICS**
- Geometric-optical modeling of a conifer forest canopy p 4 A85-49111
- GEOMORPHOLOGY**
- Polar motion measurements - Subdecimeter accuracy verified by intercomparison p 16 A85-48873
- Space methods for geological research p 16 N85-30429
- Engineering geology of selected areas, US army engineer division, lower Mississippi valley The American bottom area, MO-IL Volume 1 [AD-A154258] p 17 N85-30455
- Global Mega-Geomorphology [NASA-CP-2312] p 19 N85-32357
- A new global geomorphology? p 19 N85-32358
- Geomorphological similarity and uniqueness p 19 N85-32361
- Regional landform thresholds p 19 N85-32362
- Geomorphology, tectonics, and exploration p 19 N85-32365
- Mega-geomorphology and neotectonics p 20 N85-32366
- Andean examples of mega-geomorphology themes p 20 N85-32367
- Space imagery and some geomorphological problems of the Guiana Shield, South America p 20 N85-32368
- Deep sea mega-geomorphology Progress and problems p 33 N85-32369
- One application of mega-geomorphology in education p 6 N85-32370
- Use of the synoptic view Examples from Earth and other planets p 20 N85-32371
- Geomorphic classification of Icelandic and Martian volcanoes Limitations of comparative planetology research from LANDSAT and Viking orbiter images p 20 N85-32372
- Geomorphic analyses from space imagery p 20 N85-32374
- Use of spaceborne imaging radar in regional geomorphic studies p 20 N85-32377
- Techniques, problems and uses of mega-geomorphological mapping p 21 N85-32378
- Quantitative analysis of geomorphic processes using satellite image data at different scales p 21 N85-32380
- Quantitative geomorphologic studies from spaceborne platforms p 21 N85-32381
- Global geomorphology Report of Working Group Number 1 p 21 N85-32382
- Process thresholds Report of Working Group Number 3 p 21 N85-32384
- Planetary perspective Report of Working Group Number 4 p 22 N85-32385
- The United States Geological Survey in Alaska Accomplishments during 1983 [USGS-CIRC-945] p 23 N85-34468
- GEOGRAPHICAL SATELLITES**
- Application of satellite accelerometer data to improve density models [AD-A154904] p 48 N85-32558
- GEOPHYSICS**
- Geophysics 2001 p 10 A85-49660
- Contemporary plate motions from LAGEOS p 19 N85-31689
- Geodyn systems development p 13 N85-31708
- Global Mega-Geomorphology [NASA-CP-2312] p 19 N85-32357
- Deep sea mega-geomorphology Progress and problems p 33 N85-32369
- Landscape interpretation capabilities using space photographs of regions of a multistage platform mantle structure p 22 N85-33151
- The development of assessment techniques program p 24 N85-35457
- The Alaska Mineral Resources Assessment Program p 24 N85-35460
- GEOPOTENTIAL**
- Geopotential Research Mission - Status report p 8 A85-42469
- Improving the geological interpretation of magnetic and gravity satellite anomalies [E85-10103] p 11 N85-31585
- A comparative study of spherical and flat-Earth geopotential modeling at satellite elevations p 11 N85-31593
- A comparative study of spherical and flat-Earth geopotential modeling at satellite elevations p 12 N85-31594
- Long-wavelength magnetic and gravity anomaly correlations on Africa and Europe p 12 N85-31597
- Comparison of survey and photogrammetry methods to position gravity data, Yucca Mountain, Nevada [DE85-011685] p 13 N85-32316
- Global geoid and gravity anomaly predictions using the collocation and point mass techniques [AD-A154517] p 13 N85-32387
- GRAZING INCIDENCE**
- Backscattering of centimeter and millimeter radio waves by the earth surface at low grazing angles (Review) p 9 A85-46078
- Distribution of the effective scattering area of the earth surface at low grazing angles p 10 A85-46079
- GROUND BASED CONTROL**
- The development of assessment techniques program p 24 N85-35457
- GROUND STATIONS**
- Remote sensing of temperature profiles from a combination of observations from the satellite-based Microwave Sounding Unit and the ground-based Profiler p 43 A85-42292
- GROUND TRUTH**
- Relationships between measured and satellite-estimated solar irradiance in Texas p 46 A85-47917
- Handbook for obtaining and using aerial photography to map aquatic plant distribution [AD-A154584] p 33 N85-32388
- Interpretation of multiband photographs made during Telefoto-80 experiment for the purpose of discriminating agricultural crops p 5 N85-33152
- LANDSAT-4/5 image data quality analysis [E85-10105] p 41 N85-35463
- GROUND WATER**
- Microwave hydrology: A trilogy [NASA-CR-176042] p 36 N85-31603
- GULF OF MEXICO**
- Satellite observations of the circulation east of the Mississippi Delta - Cold-air outbreak conditions p 27 A85-43117
- Motor glider measurements during the Urban Atmosphere Energy Budget Experiment (EESA 1) p 7 N85-35553

GULF STREAM

Small-scale cyclones on the periphery of a Gulf Stream warm-core ring p 30 A85-49855

GUNN DIODES

Millimetre wave pulse technology --- satellite mapping [ESA-CRP(P)-2004] p 47 N85-31611

H**HEAT BUDGET**

Tropical Ocean and Global Atmosphere (TOGA) heat exchange project A summary report [NASA-CR-176038] p 33 N85-31738

HEAT CAPACITY MAPPING MISSION

On the analysis of thermal infrared imagery - The limited utility of apparent thermal inertia --- for Heat Capacity Mapping Mission data of surface temperature p 38 A85-43118

HEAT TRANSFER

Influence of spatial variability of hydraulic characteristics of soils on surface parameters obtained from remote sensing data in infrared and microwaves [NASA-TM-77902] p 5 N85-31604

HIERARCHIES

Selection of segment similarity measures for hierarchical picture segmentation p 41 N85-34548

HIGH RESOLUTION

Sources of scattering from vegetation canopies at 10 GHz p 4 A85-49114

HISTOGRAMS

Study of spectral/radiometric characteristics of the Thematic Mapper for land use applications [E85-10106] p 42 N85-35464

HISTORIES

One application of mega-geomorphology in education p 6 N85-32370

HUMIDITY MEASUREMENT

Tropical Ocean and Global Atmosphere (TOGA) heat exchange project A summary report [NASA-CR-176038] p 33 N85-31738

HYDROCARBONS

Using remote photographs in prospecting for hydrocarbons on the Kerch Peninsula p 22 N85-33154

The Conterminous United States Mineral Assessment Program p 24 N85-35458

HYDRODYNAMIC COEFFICIENTS

Influence of spatial variability of hydraulic characteristics of soils on surface parameters obtained from remote sensing data in infrared and microwaves [NASA-TM-77902] p 5 N85-31604

HYDROGEOLOGY

Deep sea mega-geomorphology Progress and problems p 33 N85-32369
Hydrogeology of the lower Glen Rose Aquifer, south-central Texas p 36 N85-35466

HYDROGRAPHY

Federal Mineral Land Information System p 7 N85-35459

HYDROLOGY

Hydrologic and land sciences applications of NOAA polar-orbiting satellite data --- Book p 35 A85-41320
Microwave hydrology A trilogy [NASA-CR-176042] p 36 N85-31603
SEASAT altimetry for surface height of inland seas p 32 N85-31714
Mega-geomorphology and neotectonics p 20 N85-32366

Space imagery and some geomorphological problems of the Guiana Shield, South America p 20 N85-32368
USGS coastal research, studies and maps A source of information for coastal decision making [USGS-CIRC-883] p 35 N85-35465

HYDROLOGY MODELS

The development of assessment techniques program p 24 N85-35457

HYDROTHERMAL SYSTEMS

A comparison of LANDSAT thematic mapper, multispectral scanner and airborne sensors for mapping the distribution of alteration minerals Examples from the southwestern United States p 23 N85-35452

I**ICE**

The Antarctic ice p 14 A85-42171
Active and passive remote sensing of ice [AD-A154406] p 31 N85-30459
Mesoscale features and atmospheric refraction conditions of the Arctic marginal ice zone [AD-A155139] p 33 N85-32584

ICE FLOES

Dispersion of sea ice in the Bering Sea p 26 A85-42257

The use of radar images obtained with the Cosmos-1500 satellite to study the distribution and dynamics of sea ice p 28 A85-46254

ICE MAPPING

Determination of the ice-cover characteristics of the Sea of Okhotsk in the winter of 1983-1984 on the basis of radar-sounding data p 28 A85-46253

The use of radar images obtained with the Cosmos-1500 satellite to study the distribution and dynamics of sea ice p 28 A85-46254

Quantitative interpretation of satellite radar images of sea ice using a priori data p 28 A85-46255

Radar maps of the Arctic and Antarctic compiled on the basis of Cosmos-1500 satellite data, and preliminary results of their analysis p 29 A85-46259

ICE REPORTING

Investigation of ice cover from platforms in the air and in space using radar equipment p 25 A85-40644
Program of experiments on the Cosmos-1500 satellite p 28 A85-46251

Interpretation of sea ice on satellite radar images p 28 A85-46252

Informational potential of the sidelooking radar of the Cosmos-1500 satellite p 29 A85-46263

Modeling of radio-wave scattering by ice cover p 30 A85-49477

Results of the MIZEX preliminary campaign 29 June to 19 July 1983 --- Marginal Ice Zone Experiment (MIZEX), satellite observation [CNES-84/142/T/CT/DRT/TIT/R] p 32 N85-31609

ICELAND

Geomorphic classification of Icelandic and Martian volcanoes Limitations of comparative planetology research from LANDSAT and Viking orbiter images p 20 N85-32372

IGNEOUS ROCKS

Aeromagnetic and gravity models of the pluton below the Lake City caldera, Colorado p 23 N85-35442

ILLUMINATING

Terrain illumination conditions when taking scanning photographs from space p 48 N85-33159

IMAGE ANALYSIS

Preliminary spectral and geologic analysis of Landsat-4 Thematic Mapper data, Wind River Basin area, Wyoming p 15 A85-42476

Modeling manual extraction of textural elements by mathematical morphology p 38 A85-42584

On the analysis of thermal infrared imagery - The limited utility of apparent thermal inertia --- for Heat Capacity Mapping Mission data of surface temperature p 38 A85-43118

Landsat image data quality studies p 38 A85-45687

Evaluation of Thematic Mapper data for mapping forest, agricultural and soil resources p 2 A85-45690

SPOT image quality and post-launch assessment p 38 A85-45692

Interpretation of sea ice on satellite radar images p 28 A85-46252

Identification of eddy formations in a radar image of the ocean surface p 28 A85-46256

Combined analysis of radar and optical images of the northwest Pacific on December 6, 1983 p 29 A85-46258

Thematic Mapper - Operational activities and sensor performance at ESA/Earthnet p 46 A85-47808

Systematic and random variations in Thematic Mapper digital radiance data p 40 A85-47820

IMAGE ENHANCEMENT

Restoration of multichannel microwave radiometric images p 42 A85-41089

Standardized principal components p 37 A85-41660

Cartographic-photogrammetric analysis and analytical correction of space scanner images p 38 A85-44864

IMAGE PROCESSING

Contextual classification post-processing of Landsat data using a probabilistic relaxation model p 37 A85-41658

The generation and interpretation of false-colour composite principal component images p 37 A85-41659

Multiple sensor geocoded data p 38 A85-45695

Cartographic potential of SPOT image data p 9 A85-45870

Quantitative interpretation of satellite radar images of sea ice using a priori data p 28 A85-46255

Digital processing of radar images obtained with the Cosmos-1500 satellite p 29 A85-46266

Investigation of Landsat-4 Thematic Mapper line-to-line and band-to-band registration and relative detector calibration p 39 A85-47807

Intraband radiometric performance of the Landsat Thematic Mappers p 39 A85-47810

Methods for destriping Landsat Thematic Mapper images - A feasibility study for an online destriping process in the Thematic Mapper Image Processing System (TIPS) p 39 A85-47813

Landsat-4 Thematic Mapper scene characteristics of a suburban and rural area p 40 A85-47824

Microcomputer processing of LANDSAT Thematic Mapper data for the acquisition of military tactical terrain data [AD-A154781] p 47 N85-32389

IMAGERY

Geomorphic classification of Icelandic and Martian volcanoes Limitations of comparative planetology research from LANDSAT and Viking orbiter images p 20 N85-32372

Geomorphic analyses from space imagery p 20 N85-32374

Process thresholds Report of Working Group Number 3 p 21 N85-32384

IMAGES

Remote sensing of hydrologic transport processes using spot simulation data [DE85-012412] p 37 N85-35467

IMAGING TECHNIQUES

One application of mega-geomorphology in education p 6 N85-32370

Physico-geographical regionalization of Caspian lowland based on space survey materials p 14 N85-33162

Method and apparatus for Delta Kappa synthetic aperture radar measurement of ocean current [NASA-CASE-NPO-15704-1] p 35 N85-34327

The scientific and technical issues in integrating remotely sensed imagery with geocoded data bases p 41 N85-34547

Selection of segment similarity measures for hierarchical picture segmentation p 41 N85-34548

Processing of LANDSAT imagery to map surface mineral alteration on the Alaska Peninsula, Alaska p 23 N85-35455

INCLINATION

Microwave inversion of leaf area and inclination angle distributions from backscattered data p 3 A85-49109

INCOHERENT SCATTER RADAR

Active and passive remote sensing of ice [AD-A154406] p 31 N85-30459

INCOHERENT SCATTERING

A Monte Carlo reflectance model for soil surfaces with three-dimensional structure p 3 A85-49107

INFESTATION

Forest cover type mapping and spruce budworm defoliation detection using simulated SPOT imagery p 2 A85-45874

INFORMATION DISSEMINATION

USGS coastal research, studies and maps A source of information for coastal decision making [USGS-CIRC-883] p 35 N85-35465

INFORMATION SYSTEMS

Applied computer graphics in a geographic information system Problems and successes p 6 N85-34563

INFORMATION THEORY

The selection of optimum spectral channels for multispectral remote sensing p 43 A85-42484

INFRARED DETECTORS

Shortwave infrared detection of vegetation p 2 A85-45691

Enhancing precision of remote temperature sensing data from satellites under cloudy atmospheric conditions p 48 N85-33148

Determination of altitude of cloud cover top from Meteor satellite data p 48 N85-33150

INFRARED IMAGERY

Some features of the Algerian Current p 26 A85-42255

Measurement and analysis of 2-D infrared natural background p 37 A85-42511

On the analysis of thermal infrared imagery - The limited utility of apparent thermal inertia --- for Heat Capacity Mapping Mission data of surface temperature p 38 A85-43118

Influence of spatial variability of hydraulic characteristics of soils on surface parameters obtained from remote sensing data in infrared and microwaves [NASA-TM-77902] p 5 N85-31604

Surface cyclogenesis as indicated by satellite imagery [PB85-191815] p 42 N85-35566

INFRARED PHOTOGRAPHY

Interpretation of multiband photographs made during Telefoto-80 experiment for the purpose of discriminating agricultural crops p 5 N85-33152

INFRARED SPECTROMETERS

On observation of middle atmosphere with LAS (limb-atmospheric infrared spectrometer) on board of satellite 'Ohzora' (EXOS-C) p 42 A85-41362

INFRARED WINDOWS

Satellite measurement of sea surface temperature in the presence of volcanic aerosols p 25 A85-41993

INTEGRAL EQUATIONS

A fast Fourier transform method for computing terrain corrections p 37 A85-41396

INTERFEROMETRY

Preliminary results of Finnish-Hungarian Doppler Observation Campaign /FHDOC/ p 8 A85-41199
Interferometric analysis of Doppler measurements for differential receiver calibration p 8 A85-41203
Establishment of three-dimensional geodetic control by interferometry with the global positioning system p 9 A85-44102

INTERNATIONAL COOPERATION

Antarctica [S-HRG-98-1181] p 50 N85-31584

INVERSE SCATTERING

Inverse methods for ocean wave imaging by SAR p 30 A85-48970

IONOSPHERIC PROPAGATION

Satellite propagation in the South Pacific region p 26 A85-42050

IRAN

Microwave hydrology A trilogy [NASA-CR-176042] p 36 N85-31603

IRRADIANCE

Relationships between measured and satellite-estimated solar irradiance in Texas p 46 A85-47917

ITERATIVE SOLUTION

Restoration of multichannel microwave radiometric images p 42 A85-41089

J

JAPANESE SPACECRAFT

On observation of middle atmosphere with LAS (limb-atmospheric infrared spectrometer) on board of satellite 'Ohzora' (EXOS-C) p 42 A85-41362
Verification studies of MOS-1 sensors p 44 A85-45696

K

KINEMATICS

Dispersion of sea ice in the Bering Sea p 26 A85-42257

L

LAGEOS (SATELLITE)

Geodetic and geophysical results from Lageos p 7 A85-40003
Ocean tidal parameters from LAGEOS p 32 N85-31716

LAKES

Evaluation of SPOT HRV simulation data for Corps of Engineers applications p 36 A85-45693
Microwave hydrology A trilogy [NASA-CR-176042] p 36 N85-31603

LAND

Improving Thematic Mapper land cover classification using filtered data p 37 A85-41664

LAND USE

Hydrologic and land sciences applications of NOAA polar-orbiting satellite data --- Book p 35 A85-41320
Microcomputer processing of LANDSAT Thematic Mapper data for the acquisition of military tactical terrain data [AD-A154781] p 47 N85-32389
Cosmonauts participate in multilevel remote sensing experiment p 48 N85-33130

LANDFORMS

Global Mega-Geomorphology [NASA-CP-2312] p 19 N85-32357
Global geomorphology Report of Working Group Number 1 p 21 N85-32382
Planetary perspective Report of Working Group Number 4 p 22 N85-32385

LANDSAT SATELLITES

Contextual classification post-processing of Landsat data using a probabilistic relaxation model p 37 A85-41658
Geology and structures study of the Nuba Mountains, Sudan, using Landsat images p 15 A85-42580
A survey of the Rehanna Hercynian Range in western Morocco using Landsat color composite imagery p 15 A85-42582
Sensor-induced temporal variability of Landsat MSS data p 44 A85-43116
Landsat image data quality studies p 38 A85-45687
Utility of proposed sensors for coastal engineering studies p 45 A85-45697
Performance comparisons between information extraction techniques using variable spatial resolution data p 40 A85-47823

Geomorphic classification of Icelandic and Martian volcanoes Limitations of comparative planetology research from LANDSAT and Viking orbiter images p 20 N85-32372

Use of spaceborne imaging radar in regional geomorphic studies p 20 N85-32377

Quantitative geomorphologic studies from spaceborne platforms p 21 N85-32381

Microcomputer processing of LANDSAT Thematic Mapper data for the acquisition of military tactical terrain data [AD-A154781] p 47 N85-32389

Satellites and politics Weather, communications, and earth resources p 50 N85-35144

A comparison of LANDSAT thematic mapper, multispectral scanner and airborne sensors for mapping the distribution of alteration minerals Examples from the southwestern United States p 23 N85-35452

Processing of LANDSAT imagery to map surface mineral alteration on the Alaska Peninsula, Alaska p 23 N85-35455

LANDSAT 3

A comparison of SPOT simulator data with Landsat MSS imagery for delineating water masses in Delaware Bay, Broadkill River, and adjacent wetlands p 27 A85-45875

LANDSAT 4

Preliminary spectral and geologic analysis of Landsat-4 Thematic Mapper data, Wind River Basin area, Wyoming p 15 A85-42476
Preliminary evaluation of the Landsat-4 Thematic Mapper data for mineral exploration p 15 A85-45688
Comparative evaluations of the geodetic accuracy and cartographic potential of Landsat-4 and Landsat-5 Thematic Mapper image data p 10 A85-47804
Landsat-4 and Landsat-5 MSS coherent noise - Characterization and removal p 45 A85-47805
Interpretation of Landsat-4 Thematic Mapper and Multispectral Scanner data for forest surveys p 2 A85-47806

Investigation of Landsat-4 Thematic Mapper line-to-line and band-to-band registration and relative detector calibration p 39 A85-47807

Thematic Mapper - Operational activities and sensor performance at ESA/Earthnet p 46 A85-47808

Characterization and comparison of Landsat-4 and Landsat-5 Thematic Mapper data p 39 A85-47809

Intraband radiometric performance of the Landsat Thematic Mappers p 39 A85-47810

Assessment of radiometric accuracy of Landsat-4 and Landsat-5 Thematic Mapper data products from Canadian production systems p 39 A85-47812

Methods for destriping Landsat Thematic Mapper images - A feasibility study for an online destriping process in the Thematic Mapper Image Processing System (TIPS) p 39 A85-47813

Landsat Thematic Mapper image-derived MTF p 39 A85-47817

Landsat-4 and Landsat-5 Thematic Mapper data quality analysis p 39 A85-47818

Evaluation of Thematic Mapper interband registration and noise characteristics p 46 A85-47819

Systematic and random variations in Thematic Mapper digital radiance data p 40 A85-47820

An analysis of Landsat Thematic Mapper P-Product internal geometry and conformity to earth surface geometry p 40 A85-47821

Comparison of the information contents of Landsat TM and MSS data p 40 A85-47822

Landsat-4 Thematic Mapper scene characteristics of a suburban and rural area p 40 A85-47824

LANDSAT-4/5 image data quality analysis [E85-10105] p 41 N85-35463

Study of spectral/radiometric characteristics of the Thematic Mapper for land use applications [E85-10106] p 42 N85-35464

LANDSAT 5

Comparative evaluations of the geodetic accuracy and cartographic potential of Landsat-4 and Landsat-5 Thematic Mapper image data p 10 A85-47804

Landsat-4 and Landsat-5 MSS coherent noise - Characterization and removal p 45 A85-47805

Thematic Mapper - Operational activities and sensor performance at ESA/Earthnet p 46 A85-47808

Characterization and comparison of Landsat-4 and Landsat-5 Thematic Mapper data p 39 A85-47809

Intraband radiometric performance of the Landsat Thematic Mappers p 39 A85-47810

Assessment of radiometric accuracy of Landsat-4 and Landsat-5 Thematic Mapper data products from Canadian production systems p 39 A85-47812

Landsat Thematic Mapper image-derived MTF p 39 A85-47817

Landsat-4 and Landsat-5 Thematic Mapper data quality analysis p 39 A85-47818

Evaluation of Thematic Mapper interband registration and noise characteristics p 46 A85-47819

Systematic and random variations in Thematic Mapper digital radiance data p 40 A85-47820

An analysis of Landsat Thematic Mapper P-Product internal geometry and conformity to earth surface geometry p 40 A85-47821

Spectroradiometric calibration of the Thematic Mapper and Multispectral Scanner system [E85-10104] p 47 N85-31601

LANDSAT-4/5 image data quality analysis [E85-10105] p 41 N85-35463

Study of spectral/radiometric characteristics of the Thematic Mapper for land use applications [E85-10106] p 42 N85-35464

LASER APPLICATIONS

Further improvements of the orbital program system Potsdam-5 and their utilization in geodetic-geodynamic investigations p 7 A85-41189

Lasers in space p 43 A85-42576

Ocean tidal parameters from LAGEOS p 32 N85-31716

LASER RANGE FINDERS

Polar motion measurements - Subdecimeter accuracy verified by intercomparison p 16 A85-48873

Contemporary plate motions from LAGEOS p 19 N85-31689

LASER RANGER/TRACKER

Geodetic and geophysical results from Lageos p 7 A85-40003

LEAD (METAL)

The Conterminous United States Mineral Assessment Program p 24 N85-35458

LEAVES

Two-dimensional leaf orientation distributions p 2 A85-49104

Contrasts among bidirectional reflectance of leaves, canopies, and soils p 3 A85-49106

Evaluation of a canopy reflectance model for LAI estimation through its inversion --- leaf area index p 3 A85-49108

Microwave inversion of leaf area and inclination angle distributions from backscattered data p 3 A85-49109

Inclusion of specular reflectance in vegetative canopy models p 4 A85-49113

LIGHT SCATTERING

Specular, diffuse, and polarized light scattered by two wheat canopies p 1 A85-42865

Calculating solar highlight and shadeless areas for scanning photographs from space and optimizing lighting conditions p 49 N85-33160

LIGHT TRANSMISSION

Model computations of light reflection from sea surface p 31 N85-30411

LIMNOLOGY

Microwave hydrology A trilogy [NASA-CR-176042] p 36 N85-31603

LIMONITE

A comparison of LANDSAT thematic mapper, multispectral scanner and airborne sensors for mapping the distribution of alteration minerals Examples from the southwestern United States p 23 N85-35452

LINE OF SIGHT COMMUNICATION

Strong fluctuation theory for scattering, attenuation, and transmission of microwaves through snowfall p 36 A85-49116

LINEAR ACCELERATORS

Application of GPS in a high precision engineering survey network [DE85-010556] p 10 N85-30539

LINES (GEOMETRY)

Selection of segment similarity measures for hierarchical picture segmentation p 41 N85-34548

LITHIUM

The Conterminous United States Mineral Assessment Program p 24 N85-35458

LITHOLOGY

Reduced to pole long-wavelength magnetic anomalies of Africa and Europe p 18 N85-31595

Some recent deposit modeling efforts p 23 N85-35453

Hydrogeology of the lower Glen Rose Aquifer, south-central Texas p 36 N85-35466

LITHOSPHERE

Euro-African MAGSAT anomaly-tectonic observations p 18 N85-31596

Satellite-determined stresses in the crust of Europe with particular consideration to the Liege earthquake of November 8, 1983 p 13 N85-31694

LITTORAL DRIFT

Utility of proposed sensors for coastal engineering studies p 45 A85-45697

LOW PASS FILTERS

Landsat-4 and Landsat-5 MSS coherent noise - Characterization and removal p 45 A85-47805

MIDLATITUDE ATMOSPHERE

MIDLATITUDE ATMOSPHERE

The origin of temporal variance in long-lived trace constituents in the summer stratosphere

p 6 A85-43375

MILLIMETER WAVES

Propagation and diffraction of radio waves in the millimeter and submillimeter ranges p 9 A85-46076
Specific effective scattering surfaces of certain terrains in the millimeter wave band p 10 A85-46081
Millimetre wave pulse technology --- satellite mapping [ESA-CR(P)-2004] p 47 N85-31611

MINERAL DEPOSITS

Petroleum and mineral resources of Antarctica [US-GEOL-SURV-CIRC-909] p 18 N85-31605
Comparative study of fracture planes computed from topography and lineaments from imagery with structures and mineralization in the magnetic belt of Washington State

[DE85-010972] p 18 N85-31608
The U S Geological Survey in Alaska Accomplishments during 1982

[US-GEOL-SURV-CIRC-939] p 19 N85-31719
Geomorphology, tectonics, and exploration p 19 N85-32365

The United States Geological Survey in Alaska Accomplishments during 1983

[USGS-CIRC-945] p 23 N85-34468
Aeromagnetic and radiometric signatures of a possible porphyry system in the western Tushar Mountains, Utah p 23 N85-35437

Manne phosphonite deposits model for exploration, with emphasis on deposits in the US Atlantic coastal plain

p 35 N85-35439
Aeromagnetic and gravity models of the pluton below the Lake City caldera, Colorado p 23 N85-35442

New silver resource map of the United States Potential for increased domestic silver production

p 23 N85-35445

Applications of the mineral resources data system and the international strategic minerals inventory in mineral-resource assessments by region and commodity p 23 N85-35451

A comparison of LANDSAT thematic mapper, multispectral scanner and airborne sensors for mapping the distribution of alteration minerals Examples from the southwestern United States p 23 N85-35452

Some recent deposit modeling efforts

p 23 N85-35453

Processing of LANDSAT imagery to map surface mineral alteration on the Alaska Peninsula, Alaska

p 23 N85-35455

Mineral resources programs

p 24 N85-35456

The development of assessment techniques program

p 24 N85-35457

The Conterminous United States Mineral Assessment Program

p 24 N85-35458

Federal Mineral Land Information System

p 7 N85-35459

The Alaska Mineral Resources Assessment Program

p 24 N85-35460

Hydrogeology of the lower Glen Rose Aquifer, south-central Texas

p 36 N85-35466

MINERAL EXPLORATION

The significance of lineaments mapped from remotely sensed images of the 1 250,000 Lau Sheet in Benue trough of Nigeria p 14 A85-41661

Preliminary evaluation of the Landsat-4 Thematic Mapper data for mineral exploration p 15 A85-45688

Comparative study of fracture planes computed from topography and lineaments from imagery with structures and mineralization in the magnetic belt of Washington State

[DE85-010972] p 18 N85-31608

Geomorphology, tectonics, and exploration

p 19 N85-32365

Use of space photographs for analysis of structural and dynamic conditions of formation of ancient phlogopite and apatite deposits p 22 N85-33153

Aeromagnetic and radiometric signatures of a possible porphyry system in the western Tushar Mountains, Utah p 23 N85-35437

Manne phosphonite deposits model for exploration, with emphasis on deposits in the US Atlantic coastal plain

p 35 N85-35439

Aeromagnetic and gravity models of the pluton below the Lake City caldera, Colorado p 23 N85-35442

Mineral resources programs

p 24 N85-35456

The Conterminous United States Mineral Assessment Program

p 24 N85-35458

Federal Mineral Land Information System

p 7 N85-35459

The Alaska Mineral Resources Assessment Program

p 24 N85-35460

MINERALOGY

Evaluation of SPOT simulator data for the detection of alteration in Goldfield/Cuprite, Nevada

p 15 A85-45873

MINES (EXCAVATIONS)

New silver resource map of the United States Potential for increased domestic silver production

p 23 N85-35445

Federal Mineral Land Information System

p 7 N85-35459

MISSISSIPPI RIVER (US)

Satellite observations of the circulation east of the Mississippi Delta - Cold-air outbreak conditions

p 27 A85-43117

MODELS

The development of assessment techniques program

p 24 N85-35457

MODULATION TRANSFER FUNCTION

Landsat Thematic Mapper image-derived MTF

p 39 A85-47817

MOISTURE CONTENT

Aerospace technology determines forest-fire danger

p 5 N85-30427

MOLYBDENUM

Some recent deposit modeling efforts

p 23 N85-35453

The Conterminous United States Mineral Assessment Program

p 24 N85-35458

MONITORS

Evaluation Close-range photogrammetry for slope inventory and monitoring [PB85-192755] p 24 N85-35470

MONTE CARLO METHOD

A Monte Carlo reflectance model for soil surfaces with three-dimensional structure p 3 A85-49107

MONTEREY BAY (CA)

Coastal erosion along Monterey Bay

[AD-A155610] p 34 N85-32707

MOUNTAINS

Aeromagnetic and radiometric signatures of a possible porphyry system in the western Tushar Mountains, Utah

p 23 N85-35437

MULTISENSOR APPLICATIONS

Comments on the intercalibration of multisensor, multitemporal, multichannel digital radiance data

p 38 A85-42853

Multiple sensor geocoded data

p 38 A85-45695

MULTISPECTRAL BAND SCANNERS

Restoration of multichannel microwave radiometric images p 42 A85-41089

The selection of optimum spectral channels for multispectral remote sensing p 43 A85-42484

Sensor-induced temporal variability of Landsat MSS data p 44 A85-43116

Cartographic-photogrammetric analysis and analytical correction of space scanner images p 38 A85-44864

Investigation of the ocean with low-resolution multispectral scanners p 29 A85-46261

Landsat-4 and Landsat-5 MSS coherent noise - Characterization and removal p 45 A85-47805

Interpretation of Landsat-4 Thematic Mapper and Multispectral Scanner data for forest surveys

p 2 A85-47806

Comparison of the information contents of Landsat TM and MSS data p 40 A85-47822

Nimbus 7 Coastal Zone Color Scanner (CZCS) Level 2 data product users' guide

[NASA-TM-86202] p 31 N85-30452

Nimbus 7 Coastal Zone Color Scanner (CZCS) Level 1 data product users' guide

[NASA-TM-86203] p 31 N85-30453

Spectroradiometric calibration of the Thematic Mapper and Multispectral Scanner system

[E85-10104] p 47 N85-31601

Use of spaceborne imaging radar in regional geomorphic studies p 20 N85-32377

Quantitative geomorphologic studies from spaceborne platforms p 21 N85-32381

Calculating solar highlight and shadeless areas for scanning photographs from space and optimizing lighting conditions p 49 N85-33160

Comprehensive mapping of and territories of Arizona using space photography p 14 N85-33164

MULTISPECTRAL LINEAR ARRAYS

Nimbus 7 Coastal Zone Color Scanner (CZCS) Level 1 data product users' guide

[NASA-TM-86203] p 31 N85-30453

MULTISPECTRAL PHOTOGRAPHY

The generation and interpretation of false-colour composite principal component images

p 37 A85-41659

Remote sensing investigations on some fruit orchards in El Fayoum area, Egypt p 1 A85-42581

Eruption of Mount Ontake in 1979 - Detection of volcanic ash fall area from Landsat MSS CCT data

p 15 A85-42583

Interpretation of multiband photographs made during Telefoto-80 experiment for the purpose of discriminating agricultural crops p 5 N85-33152

Cataloging the spectral brightness coefficients of the forested region of the European territory of the USSR

p 5 N85-33155

Regression analysis of aircraft and ground measurement data on vegetation cover p 5 N85-33156

MULTISPECTRAL RESOURCE SAMPLER

A comparison of LANDSAT thematic mapper, multispectral scanner and airborne sensors for mapping the distribution of alteration minerals Examples from the southwestern United States p 23 N85-35452

N

NASA PROGRAMS

Space-age geodesy - The NASA Crustal Dynamics Project p 8 A85-42452

Geopotential Research Mission - Status report p 8 A85-42469

NATURAL GAS

Reflections of possible oil- and gas-bearing structures of the pre-Jurassic complex in the present-day terrain of Western Sibena p 16 A85-48387

NATURAL GAS EXPLORATION

Using remote photographs in prospecting for hydrocarbons on the Kerch Peninsula

p 22 N85-33154

NETWORK CONTROL

Establishment of three-dimensional geodetic control by interferometry with the global positioning system

p 9 A85-44102

NEVADA

Comparison of survey and photogrammetry methods to position gravity data, Yucca Mountain, Nevada [DE85-011685] p 13 N85-32316

NEW MEXICO

Remote sensing of hydrologic transport processes using spot simulation data [DE85-012412] p 37 N85-35467

NICKEL

Applications of the mineral resources data system and the international strategic minerals inventory in mineral-resource assessments by region and commodity p 23 N85-35451

The Conterminous United States Mineral Assessment Program p 24 N85-35458

NIMBUS SATELLITES

Satellites and politics Weather, communications, and earth resources p 50 N85-35144

NIMBUS 7 SATELLITE

A global climatology of total ozone from the Nimbus 7 total ozone mapping spectrometer p 44 A85-45235

MIZEX, 1984, NASA CV-990 flight report [NASA-TM-86216] p 31 N85-30451

NOAA SATELLITES

Hydrologic and land sciences applications of NOAA polar-orbiting satellite data --- Book p 35 A85-41320

Remote sensing of temperature profiles from a combination of observations from the satellite-based Microwave Sounding Unit and the ground-based Profiler p 43 A85-42292

NOISE REDUCTION

Landsat-4 and Landsat-5 MSS coherent noise - Characterization and removal p 45 A85-47805

Effect of spatial filtering on scene noise and boundary detail in Thematic Mapper imagery p 40 A85-47825

NOWCASTING

Application of pattern-recognition and extrapolation techniques to forecasting p 45 A85-47244

Conceptual models of precipitation systems p 45 A85-47245

O

OCEAN BOTTOM

Deep sea mega-geomorphology Progress and problems p 33 N85-32369

Arctic and offshore research

[DE85-001995] p 34 N85-33653

Manne phosphonite deposits model for exploration, with emphasis on deposits in the US Atlantic coastal plain

p 35 N85-35439

OCEAN CURRENTS

Wave refraction by warm core rings --- ocean swells p 26 A85-42254

Some features of the Algenan Current p 26 A85-42255

A wind-induced mesoscale eddy over the Vancouver Island continental slope p 30 A85-49863

Ocean circulation studies p 32 N85-31712

- Method and apparatus for Delta Kappa synthetic aperture radar measurement of ocean current [NASA-CASE-NPO-15704-1] p 35 N85-34327
- OCEAN DATA ACQUISITIONS SYSTEMS**
- Optical-physical methods for the study of the ocean --- Russian book p 26 A85-42134
- The data acquisition system on the Cosmos-1500 satellite p 29 A85-46260
- Investigation of the ocean with low-resolution multispectral scanners p 29 A85-46261
- Informational potential of the sidelooking radar of the Cosmos-1500 satellite p 29 A85-46263
- Automated processing of remote-sensing data obtained with the microwave radiometer of the Cosmos-1500 satellite p 29 A85-46265
- The experimental oceanographic satellite Cosmos-1500 p 30 A85-46267
- Comment on 'Measurement of high-frequency waves using a wave follower' by S. Tang and O. H. Shemdin p 31 A85-49872
- Tropical Ocean and Global Atmosphere (TOGA) heat exchange project. A summary report [NASA-CR-176038] p 33 N85-31738
- Large-scale sea surface temperature variability from satellite and shipboard measurements [NASA-CR-176123] p 34 N85-33651
- OCEAN DYNAMICS**
- Some features of the Algenan Current p 26 A85-42255
- Identification of eddy formations in a radar image of the ocean surface p 28 A85-46256
- Ordered mesoscale structures on the ocean surface identified from satellite radar data p 28 A85-46257
- Large-scale sea surface temperature variability from satellite and shipboard measurements [NASA-CR-176123] p 34 N85-33651
- OCEAN MODELS**
- Wave refraction by warm core rings --- ocean swells p 26 A85-42254
- OCEAN SURFACE**
- The impact of higher-order Bragg terms on radar sea return p 24 A85-40237
- Albedo of a water surface, spectral variation, effects of atmospheric transmittance, sun angle and wind speed p 27 A85-42259
- Identification of eddy formations in a radar image of the ocean surface p 28 A85-46256
- Ordered mesoscale structures on the ocean surface identified from satellite radar data p 28 A85-46257
- Combined analysis of radar and optical images of the northwest Pacific on December 6, 1983 p 29 A85-46258
- The sidelooking radar on the Cosmos-1500 satellite p 29 A85-46262
- Inverse methods for ocean wave imaging by SAR p 30 A85-48970
- Model computations of light reflection from sea surface p 31 N85-30411
- Geodynamics Branch research program [NASA-TM-86223] p 18 N85-31688
- Global mean sea surface based upon a combination of the GEOS-3 and SEASAT altimeter data p 32 N85-31710
- Using ship wake patterns to evaluate SAR (Synthetic Aperture Radar) ocean wave imaging mechanisms. Joint US-Canadian Ocean Wave Investigation Project [AD-A154633] p 33 N85-32223
- Basic properties and interpretation of synthesized radar images of sea waves with long synthesize time p 34 N85-33384
- Large-scale sea surface temperature variability from satellite and shipboard measurements [NASA-CR-176123] p 34 N85-33651
- Microwave properties of a quiet sea [NASA-CR-176199] p 35 N85-35322
- OCEAN TEMPERATURE**
- Large-scale sea surface temperature variability from satellite and shipboard measurements [NASA-CR-176123] p 34 N85-33651
- OCEANOGRAPHIC PARAMETERS**
- Radar sensing of the ocean p 25 A85-41752
- Digital processing of radar images obtained with the Cosmos-1500 satellite p 29 A85-46266
- Tropical Ocean and Global Atmosphere (TOGA) heat exchange project. A summary report [NASA-CR-176038] p 33 N85-31738
- Basic properties and interpretation of synthesized radar images of sea waves with long synthesize time p 34 N85-33384
- OCEANOGRAPHY**
- Optical-physical methods for the study of the ocean --- Russian book p 26 A85-42134
- Satellite oceanography --- Book p 26 A85-42222
- Program of experiments on the Cosmos-1500 satellite p 28 A85-46251
- The data acquisition system on the Cosmos-1500 satellite p 29 A85-46260
- Investigation of the ocean with low-resolution multispectral scanners p 29 A85-46261
- Ocean circulation studies p 32 N85-31712
- Ocean tidal parameters from LAGEOS p 32 N85-31716
- Microwave properties of a quiet sea [NASA-CR-176199] p 35 N85-35322
- OCEANS**
- MIZEX, 1984, NASA CV-990 flight report [NASA-TM-86216] p 31 N85-30451
- Satellite measurements of atmospheric aerosols [AD-A153807] p 32 N85-30556
- Continental and oceanic magnetic anomalies Enhancement through GRM p 32 N85-31598
- Global Mega-Geomorphology [NASA-CP-2312] p 19 N85-32357
- The variability of aerosol microstructure in continental and oceanic surface layers of the atmosphere in anticyclones p 34 N85-32660
- OIL EXPLORATION**
- Using remote photographs in prospecting for hydrocarbons on the Kerch Peninsula p 22 N85-33154
- OIL FIELDS**
- Reflections of possible oil- and gas-bearing structures of the pre-Jurassic complex in the present-day terrain of Western Siberia p 16 A85-48387
- OIL POLLUTION**
- Optical-physical methods for the study of the ocean --- Russian book p 26 A85-42134
- Visible fluorescence from ultraviolet excited crude oil p 27 A85-42512
- OIL SLICKS**
- The impact of higher-order Bragg terms on radar sea return p 24 A85-40237
- ONBOARD DATA PROCESSING**
- The data acquisition system on the Cosmos-1500 satellite p 29 A85-46260
- Automated processing of remote-sensing data obtained with the microwave radiometer of the Cosmos-1500 satellite p 29 A85-46265
- OPTICAL COMMUNICATION**
- Lasers in space p 43 A85-42576
- OPTICAL MEASUREMENT**
- Remote Sensing Technology Symposium Proceedings [DE85-010212] p 47 N85-31606
- OPTICAL PROPERTIES**
- The albedo field and cloud radiative forcing produced by a general circulation model with internally generated cloud optics p 27 A85-43373
- Variation in the stratospheric aerosol associated with the North Cyclonic Polar Vortex as measured by the SAM II satellite sensor --- Stratospheric Aerosol Measurement p 45 A85-46424
- Properties of aerosol particles detected by satellites in coastal regions p 34 N85-32622
- Impact of fluctuations in optical properties of atmosphere on the ratio of spectral brightness from remote sensing of agricultural land p 5 N85-33149
- OPTICAL RADAR**
- Lasers in space p 43 A85-42576
- Lidar observations of vertically organized convection in the planetary boundary layer over the ocean p 30 A85-47921
- Data analysis for lidar and quartz crystal microbalance systems [NASA-CR-172601] p 47 N85-32464
- OPTICAL REFLECTION**
- Model computations of light reflection from sea surface p 31 N85-30411
- OPTICAL SCANNERS**
- Applied computer graphics in a geographic information system. Problems and successes p 6 N85-34563
- OPTICAL THICKNESS**
- Impact of fluctuations in optical properties of atmosphere on the ratio of spectral brightness from remote sensing of agricultural land p 5 N85-33149
- ORBIT CALCULATION**
- Geodyn systems development p 13 N85-31708
- ORBITAL ELEMENTS**
- Geodyn systems development p 13 N85-31708
- ORBITAL MECHANICS**
- Further improvements of the orbital program system Potsdam-5 and their utilization in geodetic-geodynamic investigations p 7 A85-41189
- Target observability for satellite-based sensors [AD-A156139] p 49 N85-35217
- ORGANIZATIONS**
- Worldwide directory of national Earth-science agencies and related international organizations [GS-CIRC-934] p 50 N85-32386
- OROGRAPHY**
- Project Skywater, 1983-84 SCPP (Sierra Cooperative Pilot Project) data inventory [PB85-187052] p 49 N85-35565
- OZONE**
- A global climatology of total ozone from the Nimbus 7 total ozone mapping spectrometer p 44 A85-45235
- Space Station Polar Platform. Integrating research and operational missions [PB85-195279] p 49 N85-35218
- OZONOMETRY**
- A global climatology of total ozone from the Nimbus 7 total ozone mapping spectrometer p 44 A85-45235
- Comparison of mesospheric ozone measurements using the LRIR and UVMCS satellite instruments --- Limb Radiance Inversion Radiometer and Ultraviolet Multiple Channel Spectrometer p 46 A85-50022
- P**
- PACIFIC OCEAN**
- Combined analysis of radar and optical images of the northwest Pacific on December 6, 1983 p 29 A85-46258
- PALEONTOLOGY**
- Global Mega-Geomorphology [NASA-CP-2312] p 19 N85-32357
- PARAMETER IDENTIFICATION**
- Geodyn systems development p 13 N85-31708
- PATTERN RECOGNITION**
- Application of pattern-recognition and extrapolation techniques to forecasting p 45 A85-47244
- PATTERN REGISTRATION**
- Repetition of dense cloud cover above Indian Ocean from generalized satellite data p 41 N85-33165
- PENNSYLVANIA**
- Remote sensing of hydrologic transport processes using spot simulation data [DE85-012412] p 37 N85-35467
- PHOSPHATES**
- Applications of the mineral resources data system and the international strategic minerals inventory in mineral-resource assessments by region and commodity p 23 N85-35451
- PHOSPHORUS**
- Manne phosphorite deposits model for exploration, with emphasis on deposits in the US Atlantic coastal plain p 35 N85-35439
- PHOTO GEOLOGY**
- Preliminary spectral and geologic analysis of Landsat-4 Thematic Mapper data, Wind River Basin area, Wyoming p 15 A85-42476
- Geology and structures study of the Nuba Mountains, Sudan, using Landsat images p 15 A85-42580
- A survey of the Rehanna Hercynian Range in western Morocco using Landsat color composite imagery p 15 A85-42582
- Preliminary evaluation of the Landsat-4 Thematic Mapper data for mineral exploration p 15 A85-45688
- Evaluation of SPOT simulator data for the detection of alteration in Goldfield/Cuprite, Nevada p 15 A85-45873
- Space methods for geological research p 16 N85-30429
- Quantitative geomorphologic studies from spaceborne platforms p 21 N85-32381
- Use of space photographs for analysis of structural and dynamic conditions of formation of ancient phlogopite and apatite deposits p 22 N85-33153
- Using remote photographs in prospecting for hydrocarbons on the Kerch Peninsula p 22 N85-33154
- PHOTOGRAMMETRY**
- Cartographic-photogrammetric analysis and analytical correction of space scanner images p 38 A85-44864
- Comparison of survey and photogrammetry methods to position gravity data, Yucca Mountain, Nevada [DE85-011685] p 13 N85-32316
- Coastal erosion along Monterey Bay [AD-A155610] p 34 N85-32707
- Evaluation. Close-range photogrammetry for slope inventory and monitoring [PB85-192755] p 24 N85-35470
- PHOTOINTERPRETATION**
- Modeling manual extraction of textural elements by mathematical morphology p 38 A85-42584
- Evaluation of simulated SPOT imagery for the interpretation of agricultural resources in California p 2 A85-45872
- Handbook for obtaining and using aerial photography to map aquatic plant distribution [AD-A154584] p 33 N85-32388

PHOTOMAPPING

- The significance of lineaments mapped from remotely sensed images of the 1:250,000 Lau Sheet in Benue trough of Nigeria p 14 A85-41661
- Application potential of SPOT imagery for topographic mapping p 9 A85-45694
- Cartographic potential of SPOT image data p 9 A85-45870
- SPOT simulation imagery for urban monitoring - A comparison with Landsat TM and MSS imagery and with high altitude color infrared photography p 6 A85-45871
- A comparison of SPOT simulator data with Landsat MSS imagery for delineating water masses in Delaware Bay, Broadkill River, and adjacent wetlands p 27 A85-45875
- The USSR as viewed from space p 50 A85-48524
- Mapping of dynamics of deltas by space photography p 14 A85-33163
- Comprehensive mapping of and terrones of Arizona using space photography p 14 A85-33164
- PLANETARY BOUNDARY LAYER**
- Lidar observations of vertically organized convection in the planetary boundary layer over the ocean p 30 A85-47921
- PLANETARY EVOLUTION**
- The evolving continents /2nd revised and enlarged edition/ --- Book p 50 A85-42220
- Global geomorphology Report of Working Group Number 1 p 21 A85-32382
- Landscape inheritance Report of Working Group Number 2 p 21 A85-32383
- PLANETARY GEOLOGY**
- Landscape inheritance Report of Working Group Number 2 p 21 A85-32383
- PLANETARY GRAVITATION**
- Geodetic and geophysical results from Lageos p 7 A85-40003
- PLANETARY TEMPERATURE**
- Thermal isostasy in the South Atlantic Ocean from geoid anomalies p 27 A85-44925
- PLANETOLOGY**
- Geophysics 2001 p 10 A85-49660
- Geomorphologic classification of Icelandic and Martian volcanoes Limitations of comparative planetology research from LANDSAT and Viking orbiter images p 20 A85-32372
- Spacecraft-aided research discussed at geology Congress p 22 A85-33147
- PLATES (TECTONICS)**
- Geodynamics Branch research program [NASA-TM-86223] p 18 A85-31688
- Contemporary plate motions from LAGEOS p 19 A85-31689
- Techniques, problems and uses of mega-geomorphological mapping p 21 A85-32378
- Planetary perspective Report of Working Group Number 4 p 22 A85-32385
- PLATINUM**
- Applications of the mineral resources data system and the international strategic minerals inventory in mineral-resource assessments by region and commodity p 23 A85-35451
- PLOTTERS**
- Applied computer graphics in a geographic information system Problems and successes p 6 A85-34563
- POLAR ORBITS**
- Hydrologic and land sciences applications of NOAA polar-orbiting satellite data --- Book p 35 A85-41320
- Space Station Polar Platform Integrating research and operational missions [PB85-195279] p 49 A85-35218
- POLAR REGIONS**
- Variation in the stratospheric aerosol associated with the North Cyclonic Polar Vortex as measured by the SAM II satellite sensor --- Stratospheric Aerosol Measurement p 45 A85-46424
- POLAR WANDERING (GEOLOGY)**
- Polar motion measurements - Subdecimeter accuracy verified by intercomparison p 16 A85-48873
- POLARIZED ELECTROMAGNETIC RADIATION**
- Microwave attenuation properties of vegetation canopies p 4 A85-49115
- POLARIZED LIGHT**
- Specular, diffuse, and polarized light scattered by two wheat canopies p 1 A85-42865
- Plant canopy specular reflectance model p 4 A85-49112
- POLITICS**
- Satellites and politics Weather, communications, and earth resources p 50 A85-35144
- POLLUTION MONITORING**
- Visible fluorescence from ultraviolet excited crude oil p 27 A85-42512

POLYSTATION DOPPLER TRACKING SYSTEM

- Preliminary results of Finnish-Hungarian Doppler Observation Campaign /FHDOC/ p 8 A85-41199
- POSTLAUNCH REPORTS**
- SPOT image quality and post-launch assessment p 38 A85-45692
- POWER SPECTRA**
- Inverse methods for ocean wave imaging by SAR p 30 A85-48970
- PRECAMBRIAN PERIOD**
- Use of space photographs for analysis of structural and dynamic conditions of formation of ancient phlogopite and apatite deposits p 22 A85-33153
- PRECIPITATION (METEOROLOGY)**
- Conceptual models of precipitation systems p 45 A85-47245
- PREDICTION ANALYSIS TECHNIQUES**
- Methods for the prediction of the attenuation statistics of radio waves in the 10-100 GHz range in rain - Inclined paths p 44 A85-44015
- PRINCIPAL COMPONENTS ANALYSIS**
- The generation and interpretation of false-colour composite principal component images p 37 A85-41659
- Standardized principal components p 37 A85-41660
- Preliminary spectral and geologic analysis of Landsat-4 Thematic Mapper data, Wind River Basin area, Wyoming p 15 A85-42476
- PROFILE METHOD (FORECASTING)**
- Profile statistics of rain in slant path as measured with a radar p 35 A85-40098
- PROJECT MANAGEMENT**
- Commission for Marine Meteorology [WMO-840] p 33 A85-31735
- PULSE RADAR**
- Millimetre wave pulse technology --- satellite mapping [ESA-CR(P)-2004] p 47 A85-31611
- Q**
- QUANTITATIVE ANALYSIS**
- Quantitative analysis of geomorphic processes using satellite image data at different scales p 21 A85-32380
- Quantitative geomorphologic studies from spaceborne platforms p 21 A85-32381
- QUARTZ CRYSTALS**
- Data analysis for lidar and quartz crystal microbalance systems [NASA-CR-172601] p 47 A85-32464
- R**
- RADAR ECHOES**
- Techniques of radar reflectivity measurement --- Book p 44 A85-43944
- RADAR IMAGERY**
- Investigation of ice cover from platforms in the air and in space using radar equipment p 25 A85-40644
- Radar sensing of the ocean p 25 A85-41752
- Methods of obtaining offshore wind direction and sea-state data from X-band aircraft SAR imagery of coastal waters p 25 A85-41753
- Interpretation of sea ice on satellite radar images p 28 A85-46252
- Determination of the ice-cover characteristics of the Sea of Okhotsk in the winter of 1983-1984 on the basis of radar-sounding data p 28 A85-46253
- The use of radar images obtained with the Cosmos-1500 satellite to study the distribution and dynamics of sea ice p 28 A85-46254
- Quantitative interpretation of satellite radar images of sea ice using a priori data p 28 A85-46255
- Identification of eddy formations in a radar image of the ocean surface p 28 A85-46256
- Ordered mesoscale structures on the ocean surface identified from satellite radar data p 28 A85-46257
- Combined analysis of radar and optical images of the northwest Pacific on December 6, 1983 p 29 A85-46258
- The sidelooking radar on the Cosmos-1500 satellite p 29 A85-46262
- Informational potential of the sidelooking radar of the Cosmos-1500 satellite p 29 A85-46263
- Digital processing of radar images obtained with the Cosmos-1500 satellite p 29 A85-46266
- The ERS-1 synthetic aperture radar and scatterometer p 45 A85-46849
- Conceptual models of precipitation systems p 45 A85-47245
- Inverse methods for ocean wave imaging by SAR p 30 A85-48970
- Using ship wake patterns to evaluate SAR (Synthetic Aperture Radar) ocean wave imaging mechanisms Joint US-Canadian Ocean Wave Investigation Project [AD-A154633] p 33 A85-32223
- Use of spaceborne imaging radar in regional geomorphic studies p 20 A85-32377
- Basic properties and interpretation of synthesized radar images of sea waves with long synthesize time p 34 A85-33384
- Surface cyclogenesis as indicated by satellite imagery [PB85-191815] p 42 A85-35566
- RADAR MAPS**
- The Antarctic ice p 14 A85-42171
- Radar maps of the Arctic and Antarctic compiled on the basis of Cosmos-1500 satellite data, and preliminary results of their analysis p 29 A85-46259
- Millimetre wave pulse technology --- satellite mapping [ESA-CR(P)-2004] p 47 A85-31611
- RADAR MEASUREMENT**
- Techniques of radar reflectivity measurement --- Book p 44 A85-43944
- RADAR RECEIVERS**
- Interferometric analysis of Doppler measurements for differential receiver calibration p 8 A85-41203
- RADAR SCATTERING**
- The impact of higher-order Bragg terms on radar sea return p 24 A85-40237
- Radar sensing of the ocean p 25 A85-41752
- Sources of scattering from vegetation canopies at 10 GHz p 4 A85-49114
- A comparison between active and passive sensing of soil moisture from vegetated terrains p 4 A85-49118
- RADIANCE**
- Comments on the intercalibration of multisensor, multitemporal, multichannel digital radiance data p 38 A85-42853
- The atmospheric effect on the separability of field classes measured from satellites p 44 A85-43115
- Systematic and random variations in Thematic Mapper digital radiance data p 40 A85-47820
- RADIATION BELTS**
- Wave-induced precipitation as a loss process for radiation belt particles p 25 A85-41961
- RADIATIVE TRANSFER**
- The albedo field and cloud radiative forcing produced by a general circulation model with internally generated cloud optics p 27 A85-43373
- Remote sensing of angular characteristics of canopy reflectances p 3 A85-49105
- Modeling the radiant transfers of sparse vegetation canopies p 3 A85-49110
- Inclusion of specular reflectance in vegetative canopy models p 4 A85-49113
- Modeling of radio-wave scattering by ice cover p 30 A85-49477
- RADIO ALTIMETERS**
- Radar sensing of the ocean p 25 A85-41752
- RADIO ATTENUATION**
- Methods for the prediction of the attenuation statistics of radio waves in the 10-100 GHz range in rain - Inclined paths p 44 A85-44015
- RADIO INTERFEROMETERS**
- The research work at the Central Institute for Physics of the Earth, Potsdam, GDR, in the field of Doppler satellite geodesy p 8 A85-41204
- RADIO RECEIVERS**
- The research work at the Central Institute for Physics of the Earth, Potsdam, GDR, in the field of Doppler satellite geodesy p 8 A85-41204
- RADIO SCATTERING**
- Backscattering of centimeter and millimeter radio waves by the earth surface at low grazing angles (Review) p 9 A85-46078
- Distribution of the effective scattering area of the earth surface at low grazing angles p 10 A85-46079
- Modeling of radio-wave scattering by ice cover p 30 A85-49477
- RADIO TRANSMISSION**
- Propagation and diffraction of radio waves in the millimeter and submillimeter ranges p 9 A85-46076
- RADIOMETERS**
- Comparison of mesospheric ozone measurements using the LRIR and UVMCS satellite instruments --- Limb Radiance Inversion Radiometer and Ultraviolet Multiple Channel Spectrometer p 46 A85-50022
- Ocean circulation studies p 32 A85-31712
- Enhancing precision of remote temperature sensing data from satellites under cloudy atmospheric conditions p 48 A85-33148
- Determination of altitude of cloud cover top from Meteor satellite data p 48 A85-33150
- Aeromagnetic and radiometric signatures of a possible porphyry system in the western Tushar Mountains, Utah p 23 A85-35437

RADIOMETRIC CORRECTION

- A water-vapor radiometer error model --- for ionosphere in geodetic microwave techniques p 8 A85-42464
- Intraband radiometric performance of the Landsat Thematic Mappers p 39 A85-47810
- Assessment of radiometric accuracy of Landsat-4 and Landsat-5 Thematic Mapper data products from Canadian production systems p 39 A85-47812
- Landsat-4 and Landsat-5 Thematic Mapper data quality analysis p 39 A85-47818
- LANDSAT-4/5 image data quality analysis [E85-10105] p 41 N85-35463

RADIOMETRIC RESOLUTION

- Probabilities, problems, and perspectives of microwave long-range reconnaissance p 42 A85-41570
- Study of spectral/land use characteristics of the Thematic Mapper for radiometric applications [E85-10106] p 42 N85-35464

RAIN

- Profile statistics of rain in slant path as measured with a radar p 35 A85-40098
- Satellite propagation in the South Pacific region p 26 A85-42050
- Methods for the prediction of the attenuation statistics of radio waves in the 10-100 GHz range in rain - Inclined paths p 44 A85-44015
- Scattering in precipitation during microwave-beam power transmission p 45 A85-46297
- Rain volume estimation over areas using satellite and radar data [NASA-CR-176050] p 36 N85-32570

RAINSTORMS

- Measuring the global distribution of intense convection over land with passive microwave radiometry p 36 A85-47923

RANGE (EXTREMES)

- Evaluation Close-range photogrammetry for slope inventory and monitoring [PB85-192755] p 24 N85-35470

RECONNAISSANCE SPACECRAFT

- Target observability for satellite-based sensors [AD-A156139] p 49 N85-35217

REFLECTANCE

- Techniques of radar reflectivity measurement --- Book p 44 A85-43944
- Two-dimensional leaf orientation distributions p 2 A85-49104
- Remote sensing of angular characteristics of canopy reflectances p 3 A85-49105
- Contrasts among bidirectional reflectance of leaves, canopies, and soils p 3 A85-49106
- Evaluation of a canopy reflectance model for LAI estimation through its inversion --- leaf area index p 3 A85-49108
- Modeling the radiant transfers of sparse vegetation canopies p 3 A85-49110
- Spectral reflectances of natural targets for use in remote sensing studies [NASA-RP-1139] p 41 N85-30450
- Preliminary investigations concerning a 90 GHz radiometer satellite experiment [ESA-TT-860] p 46 N85-31225
- Enhancing precision of remote temperature sensing data from satellites under cloudy atmospheric conditions p 48 N85-33148

REFLECTION

- Calculating solar highlight and shadeless areas for scanning photographs from space and optimizing lighting conditions p 49 N85-33160

REFRACTION

- Wave refraction by warm core rings --- ocean swells p 26 A85-42254

REGIONS

- Discovery in earthquake forecasting and seismic zoning recorded p 16 N85-30426

REGRESSION ANALYSIS

- Regression analysis of aircraft and ground measurement data on vegetation cover p 5 N85-33156

RELAXATION METHOD (MATHEMATICS)

- Contextual classification post-processing of Landsat data using a probabilistic relaxation model p 37 A85-41658

REMOTE SENSING

- Theory of microwave remote sensing --- Book p 42 A85-40792
- Principles of remote sensing --- Book p 49 A85-40793
- The contribution of SPOT images to soil mapping - A SPOT simulation study on Lauragais (1981) p 1 A85-41350
- Probabilities, problems, and perspectives of microwave long-range reconnaissance p 42 A85-41570
- Signature measurements using cooled microwave radiometers at frequencies from 90 GHz to 140 GHz p 43 A85-41571

- Commercialization of remote-sensing technology p 49 A85-41657
- Contextual classification post-processing of Landsat data using a probabilistic relaxation model p 37 A85-41658
- Standardized principal components p 37 A85-41660
- The significance of lineaments mapped from remotely sensed images of the 1 250,000 Lau Sheet in Benue trough of Nigeria p 14 A85-41661
- Thermal satellite imagery applied to a littoral macrobenthos investigation in the Gulf of Maine p 25 A85-41662
- Improving Thematic Mapper land cover classification using filtered data p 37 A85-41664
- Radar sensing of the ocean p 25 A85-41752
- Transmission model and ground-truth investigation of satellite-derived sea surface temperatures p 25 A85-41994
- Satellite oceanography --- Book p 26 A85-42222
- Remote sensing of temperature profiles from a combination of observations from the satellite-based Microwave Sounding Unit and the ground-based Profiler p 43 A85-42292
- The selection of optimum spectral channels for multispectral remote sensing p 43 A85-42484
- Lasers in space p 43 A85-42576
- Estimation of rural population in Kordofan, Sudan p 6 A85-42579
- Remote sensing investigations on some fruit orchards in El Fayoum area, Egypt p 1 A85-42581
- Comments on the intercalibration of multisensor, multitemporal, multichannel digital radiance data p 38 A85-42853
- Specular, diffuse, and polarized light scattered by two wheat canopies p 1 A85-42865
- Data acquisition and processing system based on a microprocessor set for the study of earth resources p 43 A85-43074
- Directional reflectance factor distributions for cover types of Northern Africa p 1 A85-43114
- The atmospheric effect on the separability of field classes measured from satellites p 44 A85-43115
- View azimuth and zenith, and solar angle effects on wheat canopy reflectance p 2 A85-43120
- Cartographic-photogrammetric analysis and analytical correction of space scanner images p 38 A85-44864
- The earth's surface studied from space, Proceedings of Workshop II of the COSPAR 25th Plenary Meeting, Graz, Austria, June 25-July 7, 1984 p 50 A85-45686
- Shortwave infrared detection of vegetation p 2 A85-45691
- Multiple sensor geocoded data p 38 A85-45695
- The determination of the albedo of natural covers of the earth on the basis of remote measurement results p 10 A85-46132
- Aerial and space-based remote sensing in ecological prognosis p 6 A85-46249
- Program of experiments on the Cosmos-1500 satellite p 28 A85-46251
- The experimental oceanographic satellite Cosmos-1500 p 30 A85-46267
- Application of pattern-recognition and extrapolation techniques to forecasting p 45 A85-47244
- Solid-state spectral transmissometer and radiometer p 30 A85-48670
- Two-dimensional leaf orientation distributions p 2 A85-49104
- Remote sensing of angular characteristics of canopy reflectances p 3 A85-49105
- A Monte Carlo reflectance model for soil surfaces with three-dimensional structure p 3 A85-49107
- Evaluation of a canopy reflectance model for LAI estimation through its inversion --- leaf area index p 3 A85-49108
- Modeling the radiant transfers of sparse vegetation canopies p 3 A85-49110
- Geometric-optical modeling of a conifer forest canopy p 4 A85-49111
- Plant canopy specular reflectance model p 4 A85-49112
- Sources of scattering from vegetation canopies at 10 GHz p 4 A85-49114
- Microwave attenuation properties of vegetation canopies p 4 A85-49115
- A comparison between active and passive sensing of soil moisture from vegetated terrains p 4 A85-49118
- Space methods for geological research p 16 N85-30429
- Spectral reflectances of natural targets for use in remote sensing studies [NASA-RP-1139] p 41 N85-30450
- Nimbus 7 Coastal Zone Color Scanner (CZCS) Level 2 data product users' guide p 31 N85-30452

- Nimbus 7 Coastal Zone Color Scanner (CZCS) Level 1 data product users' guide [NASA-TM-86203] p 31 N85-30453
- Active and passive remote sensing of ice [AD-A154406] p 31 N85-30459
- Microwave hydrology A trilogy [NASA-CR-176042] p 36 N85-31603
- Influence of spatial variability of hydraulic characteristics of soils on surface parameters obtained from remote sensing data in infrared and microwaves [NASA-TM-77902] p 5 N85-31604
- Remote Sensing Technology Symposium Proceedings [DE85-010212] p 47 N85-31606
- Millimetre wave pulse technology --- satellite mapping [ESA-CR(P)-2004] p 47 N85-31611
- Tropical Ocean and Global Atmosphere (TOGA) heat exchange project A summary report [NASA-CR-176038] p 33 N85-31738
- A new global geomorphology? p 19 N85-32358
- Geomorphological similarity and uniqueness p 19 N85-32361
- Regional landform thresholds p 19 N85-32362
- Mega-geomorphology and neotectonics p 20 N85-32366
- Andean examples of mega-geomorphology themes p 20 N85-32367
- Space imagery and some geomorphological problems of the Guiana Shield, South America p 20 N85-32368
- Deep sea mega-geomorphology: Progress and problems p 33 N85-32369
- Use of the synoptic view Examples from Earth and other planets p 20 N85-32371
- Geomorphic analyses from space imagery p 20 N85-32374
- Use of spaceborne imaging radar in regional geomorphic studies p 20 N85-32377
- Techniques, problems and uses of mega-geomorphological mapping p 21 N85-32378
- Global geomorphology Report of Working Group Number 1 p 21 N85-32382
- Process thresholds Report of Working Group Number 3 p 21 N85-32384
- Cosmonauts participate in multilevel remote sensing experiment p 48 N85-33130
- Spacecraft-aided research discussed at geology Congress p 22 N85-33147
- Enhancing precision of remote temperature sensing data from satellites under cloudy atmospheric conditions p 48 N85-33148
- Impact of fluctuations in optical properties of atmosphere on the ratio of spectral brightness from remote sensing of agricultural land p 5 N85-33149
- Determination of altitude of cloud cover top from Meteor satellite data p 48 N85-33150
- Landscape interpretation capabilities using space photographs of regions of a multistage platform mantle structure p 22 N85-33151
- Interpretation of multiband photographs made during Telefoto-80 experiment for the purpose of discriminating agricultural crops p 5 N85-33152
- Using remote photographs in prospecting for hydrocarbons on the Kerch Peninsula p 22 N85-33154
- Cataloging the spectral brightness coefficients of the forested region of the European territory of the USSR p 5 N85-33155
- Regression analysis of aircraft and ground measurement data on vegetation cover p 5 N85-33156
- The scientific and technical issues in integrating remotely sensed imagery with geocoded data bases p 41 N85-34547
- Selection of segment similarity measures for hierarchical picture segmentation p 41 N85-34548
- Microwave properties of a quiet sea [NASA-CR-176199] p 35 N85-35322
- Processing of LANDSAT imagery to map surface mineral alteration on the Alaska Peninsula, Alaska p 23 N85-35455
- The development of assessment techniques program p 24 N85-35457
- Remote sensing of hydrologic transport processes using spot simulation data [DE85-012412] p 37 N85-35467
- REMOTE SENSORS**
- Landsat image data quality studies p 38 A85-45687
- Verification studies of MOS-1 sensors p 44 A85-45696
- The ERS-1 synthetic aperture radar and scatterometer p 45 A85-46849
- Investigation of Landsat-4 Thematic Mapper line-to-line and band-to-band registration and relative detector calibration p 39 A85-47807
- Evaluation of Thematic Mapper interband registration and noise characteristics p 46 A85-47819

- Spectroradiometric calibration of the Thematic Mapper and Multispectral Scanner system p 47 N85-31601 [E85-10104]
- Target observability for satellite-based sensors [AD-A156139] p 49 N85-35217

RESEARCH AND DEVELOPMENT

- The Space Station An idea whose time has come --- Book p 50 A85-42223

RESEARCH MANAGEMENT

- Commission for Marine Meteorology [WMO-640] p 33 N85-31735

RESOLUTION

- LANDSAT-4/5 image data quality analysis [E85-10105] p 41 N85-35463

RESOURCES

- Arctic and offshore research [DE85-001995] p 34 N85-33653
- Applications of the mineral resources data system and the international strategic minerals inventory in mineral-resource assessments by region and commodity p 23 N85-35451

RESOURCES MANAGEMENT

- Some recent deposit modeling efforts p 23 N85-35453
- Mineral resources programs p 24 N85-35456
- Federal Mineral Land Information System p 7 N85-35459
- USGS coastal research, studies and maps A source of information for coastal decision making [USGS-CIRC-883] p 35 N85-35465

RETURN BEAM VIDEOS

- Estimation of rural population in Kordofan, Sudan p 6 A85-42579

RIVERS

- Microwave hydrology A trilogy [NASA-CR-176042] p 36 N85-31603

ROOT-MEAN-SQUARE ERRORS

- Polar motion measurements - Subdecimeter accuracy verified by intercomparison p 16 A85-48873
- Satellite measurements of atmospheric aerosols [AD-A153807] p 32 N85-30556

RURAL AREAS

- Estimation of rural population in Kordofan, Sudan p 6 A85-42579
- Motor glider measurements during the Urban Atmosphere Energy Budget Experiment (EESA 1) p 7 N85-35553

S**SAN ANDREAS FAULT**

- Geodynamics Branch research program [NASA-TM-86223] p 18 N85-31688
- First epoch measurements by Mark III VLBI of the San Andreas Fault experiment baseline p 12 N85-31691
- Geophysical interpretation of satellite laser ranging measurements p 19 N85-31692

SAN ANDREAS FAULT EXPERIMENT

- Geodynamics Branch research program [NASA-TM-86223] p 18 N85-31688
- First epoch measurements by Mark III VLBI of the San Andreas Fault experiment baseline p 12 N85-31691
- Geophysical interpretation of satellite laser ranging measurements p 19 N85-31692

SATELLITE DESIGN

- The experimental oceanographic satellite Cosmos-1500 p 30 A85-46267

SATELLITE DOPPLER POSITIONING

- Calibration of Doppler receivers p 8 A85-41195
- Preliminary results of Finnish-Hungarian Doppler Observation Campaign /FHDOP/ p 8 A85-41199
- The research work at the Central Institute for Physics of the Earth, Potsdam, GDR, in the field of Doppler satellite geodesy p 8 A85-41204

SATELLITE GROUND SUPPORT

- Automated processing of remote-sensing data obtained with the microwave radiometer of the Cosmos-1500 satellite p 29 A85-46265

SATELLITE IMAGERY

- Hydrologic and land sciences applications of NOAA polar-orbiting satellite data --- Book p 35 A85-41320
- The contribution of SPOT images to soil mapping - A SPOT simulation study on Lauragais (1981) p 1 A85-41350
- The generation and interpretation of false-colour composite principal component images p 37 A85-41659
- Standardized principal components p 37 A85-41660

- The significance of lineaments mapped from remotely sensed images of the 1:250,000 Lau Sheet in Benue trough of Nigeria p 14 A85-41661
- Thermal satellite imagery applied to a littoral macrobenthos investigation in the Gulf of Maine p 25 A85-41662

- Improving Thematic Mapper land cover classification using filtered data p 37 A85-41664

- Preliminary spectral and geologic analysis of Landsat-4 Thematic Mapper data, Wind River Basin area, Wyoming p 15 A85-42476

- Estimation of rural population in Kordofan, Sudan p 6 A85-42579

- Geology and structures study of the Nuba Mountains, Sudan, using Landsat images p 15 A85-42580
- A survey of the Rehanna Hercynian Range in western Morocco using Landsat color composite imagery p 15 A85-42582

- Eruption of Mount Ontake in 1979 - Detection of volcanic ash fall area from Landsat MSS CCT data p 15 A85-42583

- Modeling manual extraction of textural elements by mathematical morphology p 38 A85-42584
- Sensor-induced temporal variability of Landsat MSS data p 44 A85-43116
- Satellite observations of the circulation east of the Mississippi Delta - Cold-air outbreak conditions p 27 A85-43117

- On the analysis of thermal infrared imagery - The limited utility of apparent thermal inertia --- for Heat Capacity Mapping Mission data of surface temperature p 38 A85-43118

- The earth's surface studied from space, Proceedings of Workshop II of the COSPAR 25th Plenary Meeting, Graz, Austria, June 25-July 7, 1984 p 50 A85-45686
- Landsat image data quality studies p 38 A85-45687
- Preliminary evaluation of the Landsat-4 Thematic Mapper data for mineral exploration p 15 A85-45688
- Evaluation of Thematic Mapper data for mapping forest, agricultural and soil resources p 2 A85-45690
- SPOT image quality and post-launch assessment p 38 A85-45692

- Evaluation of SPOT HRV simulation data for Corps of Engineers applications p 36 A85-45693
- Application potential of SPOT imagery for topographic mapping p 9 A85-45694
- Multiple sensor geocoded data p 38 A85-45695
- Utility of proposed sensors for coastal engineering studies p 45 A85-45697
- Cartographic potential of SPOT image data p 9 A85-45870

- SPOT simulation imagery for urban monitoring - A comparison with Landsat TM and MSS imagery and with high altitude color infrared photography p 6 A85-45871

- Evaluation of simulated SPOT imagery for the interpretation of agricultural resources in California p 2 A85-45872

- Evaluation of SPOT simulator data for the detection of alteration in Goldfield/Cuprite, Nevada p 15 A85-45873

- Forest cover type mapping and spruce budworm defoliation detection using simulated SPOT imagery p 2 A85-45874

- A comparison of SPOT simulator data with Landsat MSS imagery for delineating water masses in Delaware Bay, Broadkill River, and adjacent wetlands p 27 A85-45875

- The effect of the interface albedo of the underlying surface on the reflected radiation p 10 A85-46131
- Program of experiments on the Cosmos-1500 satellite p 28 A85-46251

- Interpretation of sea ice on satellite radar images p 28 A85-46252

- The use of radar images obtained with the Cosmos-1500 satellite to study the distribution and dynamics of sea ice p 28 A85-46254

- Quantitative interpretation of satellite radar images of sea ice using a priori data p 28 A85-46255

- Combined analysis of radar and optical images of the northwest Pacific on December 6, 1983 p 29 A85-46258

- Investigation of the ocean with low-resolution multispectral scanners p 29 A85-46261
- Conceptual models of precipitation systems p 45 A85-47245

- Comparative evaluations of the geodetic accuracy and cartographic potential of Landsat-4 and Landsat-5 Thematic Mapper image data p 10 A85-47804
- Landsat-4 and Landsat-5 MSS coherent noise - Characterization and removal p 45 A85-47805
- Interpretation of Landsat-4 Thematic Mapper and Multispectral Scanner data for forest surveys p 2 A85-47806

- Thematic Mapper - Operational activities and sensor performance at ESA/Earthnet p 46 A85-47808
- Characterization and comparison of Landsat-4 and Landsat-5 Thematic Mapper data p 39 A85-47809
- Methods for destriping Landsat Thematic Mapper images - A feasibility study for an online destriping process in the Thematic Mapper Image Processing System (TIPS) p 39 A85-47813

- Landsat Thematic Mapper image-derived MTF p 39 A85-47817

- Effect of spatial filtering on scene noise and boundary detail in Thematic Mapper imagery p 40 A85-47825
- The USSR as viewed from space p 50 A85-48524

- A wind-induced mesoscale eddy over the Vancouver Island continental slope p 30 A85-49863

- Satellite measurements of atmospheric aerosols [AD-A153807] p 32 N85-30556

- Microwave hydrology A trilogy [NASA-CR-176042] p 36 N85-31603
- Regional landform thresholds p 19 N85-32362
- Geomorphology, tectonics, and exploration p 19 N85-32365

- Quantitative analysis of geomorphic processes using satellite image data at different scales p 21 N85-32380

- Use of space photographs for analysis of structural and dynamic conditions of formation of ancient phlogopite and apatite deposits p 22 N85-33153
- Physico-geographical regionalization of Caspian lowland based on space survey materials p 14 N85-33162
- Repetition of dense cloud cover above Indian Ocean from generalized satellite data p 41 N85-33165

SATELLITE INSTRUMENTS

- Six mechanisms used on the SSM/1 radiometer p 49 N85-33534

SATELLITE NETWORKS

- Methods for the prediction of the attenuation statistics of radio waves in the 10-100 GHz range in rain - Inclined paths p 44 A85-44015

SATELLITE OBSERVATION

- On observation of middle atmosphere with LAS (limb-atmospheric infrared spectrometer) on board of satellite 'Ohzora' (EXOS-C) p 42 A85-41362
- Wave-induced precipitation as a loss process for radiation belt particles p 25 A85-41961
- Satellite measurement of sea surface temperature in the presence of volcanic aerosols p 25 A85-41993
- Transmission model and ground-truth investigation of satellite-derived sea surface temperatures p 25 A85-41994

- Satellite oceanography --- Book p 26 A85-42222
- The magnetic field of the earth - Performance considerations for space-based observing systems p 9 A85-42474

- The atmospheric effect on the separability of field classes measured from satellites p 44 A85-43115
- A global climatology of total ozone from the Nimbus 7 total ozone mapping spectrometer p 44 A85-45235

- Improving the geological interpretation of magnetic and gravity satellite anomalies [E85-10103] p 11 N85-31585

- Geologic analysis of averaged magnetic satellite anomalies p 17 N85-31588
- Statistical magnetic anomalies from satellite measurements for geologic analysis p 17 N85-31589

- Binning of satellite magnetic anomalies p 11 N85-31590
- Continental and oceanic magnetic anomalies Enhancement through GRM p 32 N85-31598

- Results of the MIZEX preliminary campaign 29 June to 19 July 1983 --- Marginal Ice Zone Experiment (MIZEX), satellite observation [CNES-84/142/T/CT/DRT/TIT/R] p 32 N85-31609

- Geophysical interpretation of satellite laser ranging measurements p 19 N85-31692
- Ocean circulation studies p 32 N85-31712
- Ocean tidal parameters from LAGEOS p 32 N85-31716

- Tropical Ocean and Global Atmosphere (TOGA) heat exchange project A summary report [NASA-CR-176038] p 33 N85-31738

- Use of the synoptic view Examples from Earth and other planets p 20 N85-32371
- Rain volume estimation over areas using satellite and radar data [NASA-CR-176050] p 36 N85-32570

- Large-scale sea surface temperature variability from satellite and shipboard measurements [NASA-CR-176123] p 34 N85-33651

- Method and apparatus for Delta Kappa synthetic aperture radar measurement of ocean current [NASA-CASE-NPO-15704-1] p 35 N85-34327

- Target observability for satellite-based sensors [AD-A156139] p 49 N85-35217
- Remote sensing of hydrologic transport processes using spot simulation data [DE85-012412] p 37 N85-35467

SATELLITE ORBITS

- Satellite geodynamics p 8 A85-42451
- Spacecraft-aided research discussed at geology Congress p 22 N85-33147

SATELLITE PERTURBATION

- Spaceborne gradiometer error analysis p 13 N85-31707

SATELLITE POWER TRANSMISSION (TO EARTH)

- Scattering in precipitation during microwave-beam power transmission p 45 A85-46297

SATELLITE SOLAR POWER STATIONS

- Scattering in precipitation during microwave-beam power transmission p 45 A85-46297

SATELLITE SOUNDING

- The determination of the albedo of natural covers of the earth on the basis of remote measurement results p 10 A85-46132

- A new technique for inferring surface albedo from satellite observations p 46 A85-47916
Relationships between measured and satellite-estimated solar irradiance in Texas p 46 A85-47917

- Measuring the global distribution of intense convection over land with passive microwave radiometry p 36 A85-47923

- Comparison of mesospheric ozone measurements using the LRIR and UVMCS satellite instruments --- Lmb Radiance Inversion Radiometer and Ultraviolet Multiple Channel Spectrometer p 46 A85-50022

SATELLITE TRANSMISSION

- Satellite propagation in the South Pacific region p 26 A85-42050

SATELLITE-BORNE INSTRUMENTS

- The research work at the Central Institute for Physics of the Earth, Potsdam, GDR, in the field of Doppler satellite geodesy p 8 A85-41204

- Probabilities, problems, and perspectives of microwave long-range reconnaissance p 42 A85-41570
Signature measurements using cooled microwave radiometers at frequencies from 90 GHz to 140 GHz p 43 A85-41571

- Cryogenic magnetic gradiometers for space applications p 43 A85-42475
Visible fluorescence from ultraviolet excited crude oil p 27 A85-42512

- The data acquisition system on the Cosmos-1500 satellite p 29 A85-46260

- Investigation of the ocean with low-resolution multispectral scanners p 29 A85-46261
Automated processing of remote-sensing data obtained with the microwave radiometer of the Cosmos-1500 satellite p 29 A85-46265

- Variation in the stratospheric aerosol associated with the North Cyclonic Polar Vortex as measured by the SAM II satellite sensor --- Stratospheric Aerosol Measurement p 45 A85-46424

- Preliminary investigations concerning a 90 GHz radiometer satellite experiment [ESA-TT-860] p 46 A85-31225

- Spacecraft-aided research discussed at geology Congress p 22 A85-33147

SATELLITE-BORNE PHOTOGRAPHY

- Spacecraft-aided research discussed at geology Congress p 22 A85-33147

- Landscape interpretation capabilities using space photographs of regions of a multistage platform mantle structure p 22 A85-33151
Surface cyclogenesis as indicated by satellite imagery [PB85-191815] p 42 A85-35566

SATELLITE-BORNE RADAR

- Interpretation of sea ice on satellite radar images p 28 A85-46252

- Determination of the ice-cover characteristics of the Sea of Okhotsk in the winter of 1983-1984 on the basis of radar-sounding data p 28 A85-46253

- The use of radar images obtained with the Cosmos-1500 satellite to study the distribution and dynamics of sea ice p 28 A85-46254

- Quantitative interpretation of satellite radar images of sea ice using a priori data p 28 A85-46255

- Identification of eddy formations in a radar image of the ocean surface p 28 A85-46256

- Ordered mesoscale structures on the ocean surface identified from satellite radar data p 28 A85-46257

- Radar maps of the Arctic and Antarctic compiled on the basis of Cosmos-1500 satellite data, and preliminary results of their analysis p 29 A85-46259

- The data acquisition system on the Cosmos-1500 satellite p 29 A85-46260

- The sidelooking radar on the Cosmos-1500 satellite p 29 A85-46262

- Informational potential of the sidelooking radar of the Cosmos-1500 satellite p 29 A85-46263

- Digital processing of radar images obtained with the Cosmos-1500 satellite p 29 A85-46266

SCALE (RATIO)

- Quantitative analysis of geomorphic processes using satellite image data at different scales p 21 A85-32380

SCANNERS

- Six mechanisms used on the SSM/1 radiometer p 49 A85-33534

SCANNING

- LANDSAT-4/5 image data quality analysis [E85-10105] p 41 A85-35463

SCATTERING COEFFICIENTS

- Strong fluctuation theory for scattering, attenuation, and transmission of microwaves through snowfall p 36 A85-49116

- Active and passive remote sensing of ice [AD-A154406] p 31 A85-30459

SCATTEROMETERS

- The impact of higher-order Bragg terms on radar sea return p 24 A85-40237

- The ERS-1 synthetic aperture radar and scatterometer p 45 A85-46849

- Results of the MIZEX preliminary campaign 29 June to 19 July 1983 --- Marginal Ice Zone Experiment (MIZEX), satellite observation [CNES-84/142/T/CT/DRT/TIT/R] p 32 A85-31609

SCENE ANALYSIS

- Measurement and analysis of 2-D infrared natural background p 37 A85-42511

- An analysis of Landsat Thematic Mapper P-Product internal geometry and conformity to earth surface geometry p 40 A85-47821

- Landsat-4 Thematic Mapper scene characteristics of a suburban and rural area p 40 A85-47824

SEA ICE

- Investigation of ice cover from platforms in the air and in space using radar equipment p 25 A85-40644

- Dispersion of sea ice in the Bering Sea p 26 A85-42257

- Interpretation of sea ice on satellite radar images p 28 A85-46252

- Determination of the ice-cover characteristics of the Sea of Okhotsk in the winter of 1983-1984 on the basis of radar-sounding data p 28 A85-46253

- Quantitative interpretation of satellite radar images of sea ice using a priori data p 28 A85-46255

- A comparison between active and passive sensing of soil moisture from vegetated terrains p 4 A85-49118

- MIZEX, 1984, NASA CV-990 flight report [NASA-TM-86216] p 31 A85-30451

- Arctic and offshore research [DE85-001995] p 34 A85-33653

SEA OF OKHOTSK

- Determination of the ice-cover characteristics of the Sea of Okhotsk in the winter of 1983-1984 on the basis of radar-sounding data p 28 A85-46253

SEA ROUGHNESS

- Combined analysis of radar and optical images of the northwest Pacific on December 6, 1983 p 29 A85-46258

SEA STATES

- Methods of obtaining offshore wind direction and sea-state data from X-band aircraft SAR imagery of coastal waters p 25 A85-41753

- Comment on 'Measurement of high-frequency waves using a wave follower' by S. Tang and O. H. Shermidin p 31 A85-49872

SEA SURFACE TEMPERATURE

- Thermal satellite imagery applied to a littoral macrobenthos investigation in the Gulf of Maine p 25 A85-41662

- Satellite measurement of sea surface temperature in the presence of volcanic aerosols p 25 A85-41993

- Transmission model and ground-truth investigation of satellite-derived sea surface temperatures p 25 A85-41994

- Tropical Ocean and Global Atmosphere (TOGA) heat exchange project. A summary report [NASA-CR-176038] p 33 A85-31738

SEA TRUTH

- Transmission model and ground-truth investigation of satellite-derived sea surface temperatures p 25 A85-41994

SEA WATER

- Solid-state spectral transmissometer and radiometer p 30 A85-48670

- A microprocessor-controlled, multichannel fluorimeter for analysis of sea water [AD-A154986] p 33 A85-32310

- Microwave properties of a quiet sea [NASA-CR-176199] p 35 A85-35322

SEAS

- SEASAT altimetry for surface height of inland seas p 32 A85-31714

SEASAT SATELLITES

- Inverse methods for ocean wave imaging by SAR p 30 A85-48970

- Global mean sea surface based upon a combination of the GEOS-3 and SEASAT altimeter data p 32 A85-31710

- SEASAT altimetry for surface height of inland seas p 32 A85-31714

SECULAR VARIATIONS

- Secular variation, crustal contributions, and tectonic activity in California, 1976-1984 p 15 A85-47898

SEDIMENTARY ROCKS

- Marine phosphorite deposits model for exploration, with emphasis on deposits in the US Atlantic coastal plain p 35 A85-35439

SEGMENTS

- Selection of segment similarity measures for hierarchical picture segmentation p 41 A85-34548

SEISMIC WAVES

- Discovery in earthquake forecasting and seismic zoning recorded p 16 A85-30426

SELECTIVE DISSEMINATION OF INFORMATION

- The U.S. Geological Survey in Alaska Accomplishments during 1982 [US-GEOL-SURV-CIRC-939] p 19 A85-31719

SHORT WAVE RADIATION

- Shortwave infrared detection of vegetation p 2 A85-45691

- Global geoid and gravity anomaly predictions using the collocation and point mass techniques [AD-A154517] p 13 A85-32387

SIBERIA

- Reflections of possible oil- and gas-bearing structures of the pre-Jurassic complex in the present-day terrain of Western Siberia p 16 A85-48387

SIDE-LOOKING RADAR

- The sidelooking radar on the Cosmos-1500 satellite p 29 A85-46262

- Informational potential of the sidelooking radar of the Cosmos-1500 satellite p 29 A85-46263

SIGNAL ANALYSIS

- The selection of optimum spectral channels for multispectral remote sensing p 43 A85-42484

SIGNAL TO NOISE RATIOS

- Standardized principal components p 37 A85-41660

SIGNATURE ANALYSIS

- Signature measurements using cooled microwave radiometers at frequencies from 90 GHz to 140 GHz p 43 A85-41571

SILVER

- New silver resource map of the United States Potential for increased domestic silver production p 23 A85-35445

SIMILARITY NUMBERS

- Selection of segment similarity measures for hierarchical picture segmentation p 41 A85-34548

SIRIO SATELLITE

- Profile statistics of rain in slant path as measured with a radar p 35 A85-40098

SLOPES

- Evaluation Close-range photogrammetry for slope inventory and monitoring [PB85-192755] p 24 A85-35470

SNOW

- Strong fluctuation theory for scattering, attenuation, and transmission of microwaves through snowfall p 36 A85-49116

SNOW COVER

- A comparison between active and passive sensing of soil moisture from vegetated terrains p 4 A85-49118

SOIL MAPPING

- The contribution of SPOT images to soil mapping - A SPOT simulation study on Lauragais (1981) p 1 A85-41350

- Vegetation profiles from color-infrared airphotos p 1 A85-42650

- Cartographic-photogrammetric analysis and analytical correction of space scanner images p 38 A85-44864

- Evaluation of Thematic Mapper data for mapping forest, agricultural and soil resources p 2 A85-45690

- Space imagery and some geomorphological problems of the Guana Shield, South America p 20 A85-32368

SOIL MECHANICS

- Engineering geology of selected areas, US army engineer division, lower Mississippi valley The American bottom area, MO-IL Volume 1 [AD-A154258] p 17 A85-30455

- Influence of spatial variability of hydraulic characteristics of soils on surface parameters obtained from remote sensing data in infrared and microwaves [NASA-TM-77902] p 5 A85-31604

SOIL MOISTURE

- A comparison between active and passive sensing of soil moisture from vegetated terrains p 4 A85-49118

- Aerospace technology determines forest-fire danger p 5 A85-30427

- Influence of spatial variability of hydraulic characteristics of soils on surface parameters obtained from remote sensing data in infrared and microwaves [NASA-TM-77902] p 5 A85-31604

SOILS

- Contrasts among bidirectional reflectance of leaves, canopies, and soils p 3 A85-49106

- A Monte Carlo reflectance model for soil surfaces with three-dimensional structure p 3 A85-49107
Modeling the radiant transfers of sparse vegetation canopies p 3 A85-49110
Arctic and offshore research p 34 N85-33653
[DE85-001995]
- SOLAR HEATING**
Geodynamics Branch research program [NASA-TM-86223] p 18 N85-31688
- SOLAR POSITION**
Albedo of a water surface, spectral variation, effects of atmospheric transmittance, sun angle and wind speed p 27 A85-42259
View azimuth and zenith, and solar angle effects on wheat canopy reflectance p 2 A85-43120
Terrain illumination conditions when taking scanning photographs from space p 48 N85-33159
- SOLAR POWERED AIRCRAFT**
To fly on the wings of the sun - A study of solar-powered aircraft p 44 A85-43691
- SOLAR RADIATION**
The albedo field and cloud radiative forcing produced by a general circulation model with internally generated cloud optics p 27 A85-43373
The effect of the interface albedo of the underlying surface on the reflected radiation p 10 A85-46131
Relationships between measured and satellite-estimated solar irradiance in Texas p 46 A85-47917
Calculating solar highlight and shadeless areas for scanning photographs from space and optimizing lighting conditions p 49 N85-33160
Space Station Polar Platform Integrating research and operational missions [PB85-195279] p 49 N85-35218
- SOLAR TERRESTRIAL INTERACTIONS**
Space Station Polar Platform Integrating research and operational missions [PB85-195279] p 49 N85-35218
- SOUTH AMERICA**
MAGSAT scalar anomaly map of South America p 11 N85-31586
MAGSAT satellite magnetic anomaly map over South America p 11 N85-31587
- SPACE BASED RADAR**
The ERS-1 synthetic aperture radar and scatterometer p 45 A85-46849
- SPACE COMMERCIALIZATION**
Commercialization of remote-sensing technology p 49 A85-41657
- SPACE STATIONS**
The Space Station An idea whose time has come --- Book p 50 A85-42223
Space Station Polar Platform Integrating research and operational missions [PB85-195279] p 49 N85-35218
- SPACEBORNE EXPERIMENTS**
Program of experiments on the Cosmos-1500 satellite p 28 A85-46251
- SPACEBORNE LASERS**
Lasers in space p 43 A85-42576
- SPACEBORNE PHOTOGRAPHY**
Large format camera photographs A new tool for understanding and environments p 47 N85-32379
Terrain illumination conditions when taking scanning photographs from space p 48 N85-33159
Calculating solar highlight and shadeless areas for scanning photographs from space and optimizing lighting conditions p 49 N85-33160
Discrimination of linear contour elements of space photographs based on visual perception model p 13 N85-33161
Mapping of dynamics of deltas by space photography p 14 N85-33163
Comprehensive mapping of and territories of Arizona using space photography p 14 N85-33164
- SPACECRAFT DESIGN**
Geopotential Research Mission - Status report p 8 A85-42469
- SPACECRAFT EQUIPMENT**
Investigation of ice cover from platforms in the air and in space using radar equipment p 25 A85-40644
- SPATIAL FILTERING**
Improving Thematic Mapper land cover classification using filtered data p 37 A85-41664
Effect of spatial filtering on scene noise and boundary detail in Thematic Mapper imagery p 40 A85-47825
- SPATIAL RESOLUTION**
Restoration of multichannel microwave radiometric images p 42 A85-41089
Performance comparisons between information extraction techniques using variable spatial resolution data p 40 A85-47823
- SPECTRAL BANDS**
Evaluation of Thematic Mapper interband registration and noise characteristics p 46 A85-47819

SPECTRAL EMISSION

- A comparison between active and passive sensing of soil moisture from vegetated terrains p 4 A85-49118
Impact of fluctuations in optical properties of atmosphere on the ratio of spectral brightness from remote sensing of agricultural land p 5 N85-33149
Cataloging the spectral brightness coefficients of the forested region of the European territory of the USSR p 5 N85-33155

- A comparison of LANDSAT thematic mapper, multispectral scanner and airborne sensors for mapping the distribution of alteration minerals Examples from the southwestern United States p 23 N85-35452

SPECTRAL METHODS

- Study of spectral/radiometric characteristics of the Thematic Mapper for land use applications [E85-10106] p 42 N85-35464

SPECTRAL REFLECTANCE

- Albedo of a water surface, spectral variation, effects of atmospheric transmittance, sun angle and wind speed p 27 A85-42259

- Directional reflectance factor distributions for cover types of Northern Africa p 1 A85-43114
Sensor-induced temporal variability of Landsat MSS data p 44 A85-43116
View azimuth and zenith, and solar angle effects on wheat canopy reflectance p 2 A85-43120

- A Monte Carlo reflectance model for soil surfaces with three-dimensional structure p 3 A85-49107
Geometric-optical modeling of a conifer forest canopy p 4 A85-49111

- A comparison between active and passive sensing of soil moisture from vegetated terrains p 4 A85-49118
Spectral reflectances of natural targets for use in remote sensing studies [NASA-RP-1139] p 41 N85-30450

- Regression analysis of aircraft and ground measurement data on vegetation cover p 5 N85-33156
Processing of LANDSAT imagery to map surface mineral alteration on the Alaska Peninsula, Alaska p 23 N85-35455

- SPECTRAL SIGNATURES**
Physico-geographical regionalization of Caspian lowland based on space survey materials p 14 N85-33162

- SPECTROGRAMS**
Spacecraft-aided research discussed at geology Congress p 22 N85-33147

- SPECTROMETERS**
A microprocessor-controlled, multichannel fluorometer for analysis of sea water [AD-A154986] p 33 N85-32310

- SPECTRORADIOMETERS**
Preliminary evaluation of the Landsat-4 Thematic Mapper data for mineral exploration p 15 A85-45688
Solid-state spectral transmissometer and radiometer p 30 A85-48670

- A comparison of LANDSAT thematic mapper, multispectral scanner and airborne sensors for mapping the distribution of alteration minerals Examples from the southwestern United States p 23 N85-35452

- SPECTROSCOPY**
Cataloging the spectral brightness coefficients of the forested region of the European territory of the USSR p 5 N85-33155

- SPECULAR REFLECTION**
The effect of the interface albedo of the underlying surface on the reflected radiation p 10 A85-46131
Plant canopy specular reflectance model p 4 A85-49112

- Inclusion of specular reflectance in vegetative canopy models p 4 A85-49113

- SPOT (FRENCH SATELLITE)**
The contribution of SPOT images to soil mapping - A SPOT simulation study on Lauragais (1981) p 1 A85-41350

- SPOT image quality and post-launch assessment p 38 A85-45692
Evaluation of SPOT HRV simulation data for Corps of Engineers applications p 36 A85-45693
Application potential of SPOT imagery for topographic mapping p 9 A85-45694
Cartographic potential of SPOT image data p 9 A85-45870

- SPOT simulation imagery for urban monitoring - A comparison with Landsat TM and MSS imagery and with high altitude color infrared photography p 6 A85-45871

- Evaluation of simulated SPOT imagery for the interpretation of agricultural resources in California p 2 A85-45872

- Forest cover type mapping and spruce budworm defoliation detection using simulated SPOT imagery p 2 A85-45874

- A comparison of SPOT simulator data with Landsat MSS imagery for delineating water masses in Delaware Bay, Broadkill River, and adjacent wetlands p 27 A85-45875

- SQUID (DETECTORS)**
Cryogenic magnetic gradiometers for space applications p 43 A85-42475

- STAINING**
Processing of LANDSAT imagery to map surface mineral alteration on the Alaska Peninsula, Alaska p 23 N85-35455

- STATISTICAL ANALYSIS**
Measurement and analysis of 2-D infrared natural background p 37 A85-42511
Enhancing precision of remote temperature sensing data from satellites under cloudy atmospheric conditions p 48 N85-33148

- STATISTICAL DISTRIBUTIONS**
Profile statistics of rain in slant path as measured with a radar p 35 A85-40098

- STATISTICAL WEATHER FORECASTING**
Geopotential heights and thicknesses as predictors of Atlantic tropical cyclone motion and intensity p 26 A85-42177
Methods for the prediction of the attenuation statistics of radio waves in the 10-100 GHz range in rain - Inclined paths p 44 A85-44015

- STEREOPHOTOGRAPHY**
Cartographic potential of SPOT image data p 9 A85-45870
Large format camera photographs A new tool for understanding and environments p 47 N85-32379

- STRATEGIC MATERIALS**
Applications of the mineral resources data system and the international strategic minerals inventory in mineral-resource assessments by region and commodity p 23 N85-35451
Mineral resources programs p 24 N85-35456
The Continental United States Mineral Assessment Program p 24 N85-35458

- STRATOSPHERE**
The origin of temporal variance in long-lived trace constituents in the summer stratosphere p 6 A85-43375
Variation in the stratospheric aerosol associated with the North Cyclonic Polar Vortex as measured by the SAM II satellite sensor --- Stratospheric Aerosol Measurement p 45 A85-46424

- The effect of El Chichon on wind variability in the troposphere, stratosphere, and mesosphere over Alaska p 31 A85-49933

- STREMS**
Geomorphic analyses from space imagery p 20 N85-32374

- STRUCTURAL PROPERTIES (GEOLOGY)**
The significance of lineaments mapped from remotely sensed images of the 1:250,000 Lau Sheet in Benue trough of Nigeria p 14 A85-41661
Geology and structures study of the Nuba Mountains, Sudan, using Landsat images p 15 A85-42580

- Reflections of possible oil- and gas-bearing structures of the pre-Jurassic complex in the present-day terrain of Western Siberia p 16 A85-48387

- Comparative study of fracture planes computed from topography and lineaments from imagery with structures and mineralization in the magnetic belt of Washington State [DE85-010972] p 18 N85-31608

- Global Mega-Geomorphology [NASA-CP-2312] p 19 N85-32357
Andean examples of mega-geomorphology themes p 20 N85-32367

- SUBMILLIMETER WAVES**
Propagation and diffraction of radio waves in the millimeter and submillimeter ranges p 9 A85-46076

- SUDDEN STORM COMMENCEMENTS**
Fine structure of the preliminary impulse of a sudden storm commencement p 14 A85-40612

- SUMMER**
The origin of temporal variance in long-lived trace constituents in the summer stratosphere p 6 A85-43375

- SUN**
Terrain illumination conditions when taking scanning photographs from space p 48 N85-33159

- SUNLIGHT**
Plant canopy specular reflectance model p 4 A85-49112

- SUPERHIGH FREQUENCIES**
Satellite propagation in the South Pacific region p 26 A85-42050

- SURFACE GEOMETRY**
An analysis of Landsat Thematic Mapper P-Product internal geometry and conformity to earth surface geometry p 40 A85-47821

SURFACE PROPERTIES

A new technique for inferring surface albedo from satellite observations p 46 A85-47916

Reflections of possible oil- and gas-bearing structures of the pre-Jurassic complex in the present-day terrain of Western Siberia p 16 A85-48387

Using ship wake patterns to evaluate SAR (Synthetic Aperture Radar) ocean wave imaging mechanisms Joint US-Canadian Ocean Wave Investigation Project [AD-A154633] p 33 N85-32223

SURFACE ROUGHNESS

Specific effective scattering surfaces of certain terrains in the millimeter wave band p 10 A85-46081

Using ship wake patterns to evaluate SAR (Synthetic Aperture Radar) ocean wave imaging mechanisms Joint US-Canadian Ocean Wave Investigation Project [AD-A154633] p 33 N85-32223

SURFACE TEMPERATURE

On the analysis of thermal infrared imagery - The limited utility of apparent thermal inertia --- for Heat Capacity Mapping Mission data of surface temperature p 38 A85-43118

SURFACE WATER

Microwave hydrology A trilogy [NASA-CR-176042] p 36 N85-31603

SYNTHETIC APERTURE RADAR

Radar sensing of the ocean p 25 A85-41752
Methods of obtaining offshore wind direction and sea-state data from X-band aircraft SAR imagery of coastal waters p 25 A85-41753

Wave refraction by warm core rings --- ocean swells p 26 A85-42254

The ERS-1 synthetic aperture radar and scatterometer p 45 A85-46849

Inverse methods for ocean wave imaging by SAR p 30 A85-48970

Using ship wake patterns to evaluate SAR (Synthetic Aperture Radar) ocean wave imaging mechanisms Joint US-Canadian Ocean Wave Investigation Project [AD-A154633] p 33 N85-32223

Basic properties and interpretation of synthesized radar images of sea waves with long synthezization time p 34 N85-33384

Method and apparatus for Delta Kappa synthetic aperture radar measurement of ocean current [NASA-CASE-NPO-15704-1] p 35 N85-34327

SYSTEMS ANALYSIS

Comparison of the information contents of Landsat TM and MSS data p 40 A85-47822

SYSTEMS SIMULATION

The contribution of SPOT images to soil mapping - A SPOT simulation study on Lauragais (1981) p 1 A85-41350

T

TARGETS

Spectral reflectances of natural targets for use in remote sensing studies [NASA-RP-1139] p 41 N85-30450

Target observability for satellite-based sensors [AD-A156139] p 49 N85-35217

TECHNOLOGY ASSESSMENT

The Space Station An idea whose time has come --- Book p 50 A85-42223

Millimetre wave pulse technology --- satellite mapping [ESA-CR(P)-2004] p 47 N85-31611

TECHNOLOGY TRANSFER

Commercialization of remote-sensing technology p 49 A85-41657

TECHNOLOGY UTILIZATION

Deep sea mega-geomorphology Progress and problems p 33 N85-32369

Use of the synoptic view Examples from Earth and other planets p 20 N85-32371

TECTONICS

Geodetic and geophysical results from Lageos p 7 A85-40003

Secular variation, crustal contributions, and tectonic activity in California, 1976-1984 p 15 A85-47898

Reflections of possible oil- and gas-bearing structures of the pre-Jurassic complex in the present-day terrain of Western Siberia p 16 A85-48387

Highly important features of regional tectonics of Earth's Arctic sector p 17 N85-30449

Euro-African MAGSAT anomaly-tectonic observations p 18 N85-31596

Long-wavelength magnetic and gravity anomaly correlations on Africa and Europe p 12 N85-31597

Continental magnetic anomaly constraints on continental reconstruction p 12 N85-31599

Regional magnetic anomaly constraints on continental rifting p 12 N85-31600

Geodynamics Branch research program [NASA-TM-86223] p 18 N85-31688

Contemporary plate motions from LAGEOS

The global VLBI fiducial network p 19 N85-31689

First epoch measurements by Mark III VLBI of the San Andreas Fault experiment baseline p 12 N85-31691

Geophysical interpretation of satellite laser ranging measurements p 19 N85-31692

Global Mega-Geomorphology [NASA-CP-2312] p 19 N85-32357

Techniques, problems and uses of mega-geomorphological mapping p 21 N85-32378

Planetary perspective Report of Working Group Number 4 p 22 N85-32385

Use of space photographs for analysis of structural and dynamic conditions of formation of ancient phlogopite and apatite deposits p 22 N85-33153

Crustal Dynamics Project Catalogue of site information [NASA-TM-86218] p 14 N85-33552

Some recent deposit modeling efforts p 23 N85-35453

TELEMETRY

Message collision of data collection system and its computer simulation p 46 A85-48894

TEMPERATURE DISTRIBUTION

Enhancing precision of remote temperature sensing data from satellites under cloudy atmospheric conditions p 48 N85-33148

TERRAIN

Geomorphological similarity and uniqueness p 19 N85-32361

Landscape inheritance Report of Working Group Number 2 p 21 N85-32383

Process thresholds Report of Working Group Number 3 p 21 N85-32384

Microcomputer processing of LANDSAT Thematic Mapper data for the acquisition of military tactical terrain data [AD-A154781] p 47 N85-32389

Terrain illumination conditions when taking scanning photographs from space p 48 N85-33159

TERRAIN ANALYSIS

Theory of microwave remote sensing --- Book p 42 A85-40792

A fast Fourier transform method for computing terrain corrections p 37 A85-41396

Contextual classification post-processing of Landsat data using a probabilistic relaxation model p 37 A85-41658

Measurement and analysis of 2-D infrared natural background p 37 A85-42511

Specific effective scattering surfaces of certain terrains in the millimeter wave band p 10 A85-46081

Reflections of possible oil- and gas-bearing structures of the pre-Jurassic complex in the present-day terrain of Western Siberia p 16 A85-48387

TEXTBOOKS

Principles of remote sensing --- Book p 49 A85-40793

TEXTURES

Modeling manual extraction of textural elements by mathematical morphology p 38 A85-42584

THEMATIC MAPPING

Improving Thematic Mapper land cover classification using filtered data p 37 A85-41664

Preliminary spectral and geologic analysis of Landsat-4 Thematic Mapper data, Wind River Basin area, Wyoming p 15 A85-42476

Preliminary evaluation of the Landsat-4 Thematic Mapper data for mineral exploration p 15 A85-45688

Evaluation of Thematic Mapper data for mapping forest, agricultural and soil resources p 2 A85-45690

Shortwave infrared detection of vegetation p 2 A85-45691

Application potential of SPOT imagery for topographic mapping p 9 A85-45694

Evaluation of SPOT simulator data for the detection of alteration in Goldfield/Cuprite, Nevada p 15 A85-45873

Comparative evaluations of the geodetic accuracy and cartographic potential of Landsat-4 and Landsat-5 Thematic Mapper image data p 10 A85-47804

Interpretation of Landsat-4 Thematic Mapper and Multispectral Scanner data for forest surveys p 2 A85-47806

Investigation of Landsat-4 Thematic Mapper line-to-line and band-to-band registration and relative detector calibration p 39 A85-47807

Thematic Mapper - Operational activities and sensor performance at ESA/Earthnet p 46 A85-47808

Characterization and comparison of Landsat-4 and Landsat-5 Thematic Mapper data p 39 A85-47809

Intraband radiometric performance of the Landsat Thematic Mappers p 39 A85-47810

Assessment of radiometric accuracy of Landsat-4 and Landsat-5 Thematic Mapper data products from Canadian production systems p 39 A85-47812

Methods for destriping Landsat Thematic Mapper images - A feasibility study for an online destriping process in the Thematic Mapper Image Processing System (TIPS) p 39 A85-47813

Landsat Thematic Mapper image-derived MTF p 39 A85-47817

Landsat-4 and Landsat-5 Thematic Mapper data quality analysis p 39 A85-47818

Evaluation of Thematic Mapper interband registration and noise characteristics p 46 A85-47819

Systematic and random variations in Thematic Mapper digital radiance data p 40 A85-47820

An analysis of Landsat Thematic Mapper P-Product internal geometry and conformity to earth surface geometry p 40 A85-47821

Comparison of the information contents of Landsat TM and MSS data p 40 A85-47822

Performance comparisons between information extraction techniques using variable spatial resolution data p 40 A85-47823

Landsat-4 Thematic Mapper scene characteristics of a suburban and rural area p 40 A85-47824

Effect of spatial filtering on scene noise and boundary detail in Thematic Mapper imagery p 40 A85-47825

Microcomputer processing of LANDSAT Thematic Mapper data for the acquisition of military tactical terrain data [AD-A154781] p 47 N85-32389

Comprehensive mapping of and territories of Arizona using space photography p 14 N85-33164

LANDSAT-4/5 image data quality analysis [E85-10105] p 41 N85-35463

Study of spectral/radiometric characteristics of the Thematic Mapper for land use applications [E85-10106] p 42 N85-35464

MEASUREMENT AND ANALYSIS OF 2-D INFRARED NATURAL BACKGROUND p 37 A85-42511

ENHANCING PRECISION OF REMOTE TEMPERATURE SENSING DATA FROM SATELLITES UNDER CLOUDY ATMOSPHERIC CONDITIONS p 48 N85-33148

THE UNITED STATES GEOLOGICAL SURVEY IN ALASKA ACCOMPLISHMENTS DURING 1983 [USGS-CIRC-945] p 23 N85-34468

OCEAN TIDAL PARAMETERS FROM LAGEOS p 32 N85-31716

COASTAL EROSION ALONG MONTEREY BAY [AD-A155610] p 34 N85-32707

FOREST COVER TYPE MAPPING AND SPRUCE BUDWORM DEFOLIATION DETECTION USING SIMULATED SPOT IMAGERY p 2 A85-45874

THE CONTERMINOUS UNITED STATES MINERAL ASSESSMENT PROGRAM p 24 N85-35458

THE ALASKA MINERAL RESOURCES ASSESSMENT PROGRAM p 24 N85-35460

SATELLITES AND POLITICS Weather, communications, and earth resources p 50 N85-35144

APPLICATIONS OF THE MINERAL RESOURCES DATA SYSTEM AND THE INTERNATIONAL STRATEGIC MINERALS INVENTORY IN MINERAL-RESOURCE ASSESSMENTS BY REGION AND COMMODITY p 23 N85-35451

TOPEX TOPEX error budget p 47 N85-31717

THE ANTARCTIC ICE p 14 A85-42171

VEGETATION PROFILES FROM COLOR-INFRARED AIRPHOTOS p 1 A85-42650

APPLICATION POTENTIAL OF SPOT IMAGERY FOR TOPOGRAPHIC MAPPING p 9 A85-45694

ENGINEERING GEOLOGY OF SELECTED AREAS, US ARMY ENGINEER DIVISION, LOWER MISSISSIPPI VALLEY THE AMERICAN BOTTOM AREA, MO-IL Volume 1 p 17 N85-30455

COMPARATIVE STUDY OF FRACTURE PLANES COMPUTED FROM TOPOGRAPHY AND LINEAMENTS FROM IMAGERY WITH STRUCTURES AND MINERALIZATION IN THE MAGNETIC BELT OF WASHINGTON STATE [DE85-010972] p 18 N85-31608

GEOMORPHOLOGICAL SIMILARITY AND UNIQUENESS p 19 N85-32361

REGIONAL LANDFORM THRESHOLDS p 19 N85-32362

LANDSCAPE INHERITANCE Report of Working Group Number 2 p 21 N85-32383

PROCESS THRESHOLDS Report of Working Group Number 3 p 21 N85-32384

- Evaluation Close-range photogrammetry for slope inventory and monitoring [PB85-192755] p 24 N85-35470
- TOPOLOGY**
Global Mega-Geomorphology [NASA-CP-2312] p 19 N85-32357
- TRACE CONTAMINANTS**
The origin of temporal variance in long-lived trace constituents in the summer stratosphere p 6 A85-43375
- TRANSISTORS**
Millimetre wave pulse technology --- satellite mapping [ESA-CR(P)-2004] p 47 N85-31611
- TRANSMISSION EFFICIENCY**
Methods for the prediction of the attenuation statistics of radio waves in the 10-100 GHz range in rain - Inclined paths p 44 A85-44015
- TRANSMITTANCE**
Transmission model and ground-truth investigation of satellite-derived sea surface temperatures p 25 A85-41994
Albedo of a water surface, spectral variation, effects of atmospheric transmittance, sun angle and wind speed p 27 A85-42259
- TROPICAL METEOROLOGY**
Geopotential heights and thicknesses as predictors of Atlantic tropical cyclone motion and intensity p 26 A85-42177
Tropical Ocean and Global Atmosphere (TOGA) heat exchange project A summary report [NASA-CR-176038] p 33 N85-31738
- TROPOSPHERE**
The effect of El Chichon on wind variability in the troposphere, stratosphere, and mesosphere over Alaska p 31 A85-49933
- TUNGSTEN**
Applications of the mineral resources data system and the international strategic minerals inventory in mineral-resource assessments by region and commodity p 23 N85-35451
The Conterminous United States Mineral Assessment Program p 24 N85-35458
- TURBULENT DIFFUSION**
Dispersion of sea ice in the Bering Sea p 26 A85-42257
- TURBULENT FLOW**
Some features of the Algerian Current p 26 A85-42255

U

- U.S.S.R.**
The USSR as viewed from space p 50 A85-48524
Microwave hydrology A trilogy [NASA-CR-176042] p 36 N85-31603
- ULTRAVIOLET RADIATION**
Visible fluorescence from ultraviolet excited crude oil p 27 A85-42512
- ULTRAVIOLET SPECTROMETERS**
Comparison of mesospheric ozone measurements using the LRIR and UVMCS satellite instruments --- Limb Radiance Inversion Radiometer and Ultraviolet Multiple Channel Spectrometer p 46 A85-50022
- UNDERWATER OPTICS**
Optical-physical methods for the study of the ocean --- Russian book p 26 A85-42134
- UNITED STATES**
The south-central United States magnetic anomaly p 17 N85-31591
The south-central United States magnetic anomaly p 18 N85-31592
New silver resource map of the United States Potential for increased domestic silver production p 23 N85-35445
- UPPER ATMOSPHERE**
Space Station Polar Platform Integrating research and operational missions [PB85-195279] p 49 N85-35218
- USER MANUALS (COMPUTER PROGRAMS)**
Nimbus 7 Coastal Zone Color Scanner (CZCS) Level 2 data product users' guide [NASA-TM-86202] p 31 N85-30452
- UTAH**
Aeromagnetic and radiometric signatures of a possible porphyry system in the western Tushar Mountains, Utah p 23 N85-35437

V

- VANADIUM**
Applications of the mineral resources data system and the international strategic minerals inventory in mineral-resource assessments by region and commodity p 23 N85-35451

- VARIABILITY**
Influence of spatial variability of hydraulic characteristics of soils on surface parameters obtained from remote sensing data in infrared and microwaves [NASA-TM-77902] p 5 N85-31604
- VARIATIONS**
Impact of fluctuations in optical properties of atmosphere on the ratio of spectral brightness from remote sensing of agricultural land p 5 N85-33149
- VEGETATION**
Vegetation profiles from color-infrared airphotos p 1 A85-42650
Directional reflectance factor distributions for cover types of Northern Africa p 1 A85-43114
A comparison between active and passive sensing of soil moisture from vegetated terrain p 4 A85-49118
Space imagery and some geomorphological problems of the Guiana Shield, South America p 20 N85-32368
- VEGETATION GROWTH**
Shortwave infrared detection of vegetation p 2 A85-45691
Regression analysis of aircraft and ground measurement data on vegetation cover p 5 N85-33156
- VEGETATIVE INDEX**
Evaluation of a canopy reflectance model for LAI estimation through its inversion --- leaf area index p 3 A85-49108
- VERY LONG BASE INTERFEROMETRY**
A water-vapor radiometer error model --- for ionosphere in geodetic microwave techniques p 8 A85-42464
Polar motion measurements - Subdecimeter accuracy verified by intercomparison p 16 A85-48873
Crustal Dynamics Project Catalogue of site information [NASA-TM-86218] p 14 N85-33552
- VERY LOW FREQUENCIES**
Wave-induced precipitation as a loss process for radiation belt particles p 25 A85-41961
- VIKING ORBITER SPACECRAFT**
Geomorphic classification of Icelandic and Martian volcanoes Limitations of comparative planetology research from LANDSAT and Viking orbiter images p 20 N85-32372
- VISUAL DISCRIMINATION**
Discrimination of linear contour elements of space photographs based on visual perception model p 13 N85-33161
- VISUAL PERCEPTION**
Discrimination of linear contour elements of space photographs based on visual perception model p 13 N85-33161
- VOLCANOES**
Satellite measurement of sea surface temperature in the presence of volcanic aerosols p 25 A85-41993
Eruption of Mount Ontake in 1979 - Detection of volcanic ash fall area from Landsat MSS CCT data p 15 A85-42583
The effect of El Chichon on wind variability in the troposphere, stratosphere, and mesosphere over Alaska p 31 A85-49933
Data analysis for lidar and quartz crystal microbalance systems [NASA-CR-172601] p 47 N85-32464
- VOLCANOLOGY**
Eruption of Mount Ontake in 1979 - Detection of volcanic ash fall area from Landsat MSS CCT data p 15 A85-42583
Andean examples of mega-geomorphology themes p 20 N85-32367
- VORTICES**
Some features of the Algerian Current p 26 A85-42255
Small-scale cyclones on the periphery of a Gulf Stream warm-core ring p 30 A85-49855
A wind-induced mesoscale eddy over the Vancouver Island continental slope p 30 A85-49863

W

- WAKES**
Using ship wake patterns to evaluate SAR (Synthetic Aperture Radar) ocean wave imaging mechanisms Joint US-Canadian Ocean Wave Investigation Project [AD-A154633] p 33 N85-32223
- WATER CIRCULATION**
Small-scale cyclones on the periphery of a Gulf Stream warm-core ring p 30 A85-49855
- WATER QUALITY**
Evaluation of SPOT HRV simulation data for Corps of Engineers applications p 36 A85-45693
- WATER RESOURCES**
Microwave hydrology A trilogy [NASA-CR-176042] p 36 N85-31603

- WATER VAPOR**
A water-vapor radiometer error model --- for ionosphere in geodetic microwave techniques p 8 A85-42464
- WATER WAVES**
Wave refraction by warm core rings --- ocean swells p 26 A85-42254
Comment on 'Measurement of high-frequency waves using a wave follower' by S Tang and O H Shemdin p 31 A85-49872
Coastal erosion along Monterey Bay [AD-A155610] p 34 N85-32707
Basic properties and interpretation of synthesized radar images of sea waves with long synthesize time p 34 N85-33384
- WAVE DIFFRACTION**
Propagation and diffraction of radio waves in the millimeter and submillimeter ranges p 9 A85-46076
- WAVE DISPERSION**
Wave refraction by warm core rings --- ocean swells p 26 A85-42254
- WAVE PROPAGATION**
Propagation and diffraction of radio waves in the millimeter and submillimeter ranges p 9 A85-46076
- WAVE SCATTERING**
Method and apparatus for Delta Kappa synthetic aperture radar measurement of ocean current [NASA-CASE-NPO-15704-1] p 35 N85-34327
- WAVELENGTHS**
Reduced to pole long-wavelength magnetic anomalies of Africa and Europe p 18 N85-31595
Long-wavelength magnetic and gravity anomaly correlations on Africa and Europe p 12 N85-31597
- WEATHER**
Satellites and politics Weather, communications, and earth resources p 50 N85-35144
- WEATHER FORECASTING**
Application of pattern-recognition and extrapolation techniques to forecasting p 45 A85-47244
Project Skywater, 1983-84 SCPP (Sierra Cooperative Pilot Project) data inventory [PB85-187052] p 49 N85-35565
Surface cyclogenesis as indicated by satellite imagery [PB85-191815] p 42 N85-35566
- WEATHER MODIFICATION**
Project Skywater, 1983-84 SCPP (Sierra Cooperative Pilot Project) data inventory [PB85-187052] p 49 N85-35565
- WETLANDS**
A comparison of SPOT simulator data with Landsat MSS imagery for delineating water masses in Delaware Bay, Broadkill River, and adjacent wetlands p 27 A85-45875
- WHEAT**
Spectral, diffuse, and polarized light scattered by two wheat canopies p 1 A85-42865
View azimuth and zenith, and solar angle effects on wheat canopy reflectance p 2 A85-43120
Regression analysis of aircraft and ground measurement data on vegetation cover p 5 N85-33156
- WIND (METEOROLOGY)**
Remote sensing of temperature profiles from a combination of observations from the satellite-based Microwave Sounding Unit and the ground-based Profiler p 43 A85-42292
- WIND DIRECTION**
Methods of obtaining offshore wind direction and sea-state data from X-band aircraft SAR imagery of coastal waters p 25 A85-41753
- WIND MEASUREMENT**
Tropical Ocean and Global Atmosphere (TOGA) heat exchange project A summary report [NASA-CR-176038] p 33 N85-31738
- WIND VARIATIONS**
The effect of El Chichon on wind variability in the troposphere, stratosphere, and mesosphere over Alaska p 31 A85-49933
- WIND VELOCITY**
Albedo of a water surface, spectral variation, effects of atmospheric transmittance, sun angle and wind speed p 27 A85-42259
- WINTER**
Variation in the stratospheric aerosol associated with the North Cyclonic Polar Vortex as measured by the SAM II satellite sensor --- Stratospheric Aerosol Measurement p 45 A85-46424
Project Skywater, 1983-84 SCPP (Sierra Cooperative Pilot Project) data inventory [PB85-187052] p 49 N85-35565
- WORLD METEOROLOGICAL ORGANIZATION**
Commission for Marine Meteorology [WMO-640] p 33 N85-31735

Z

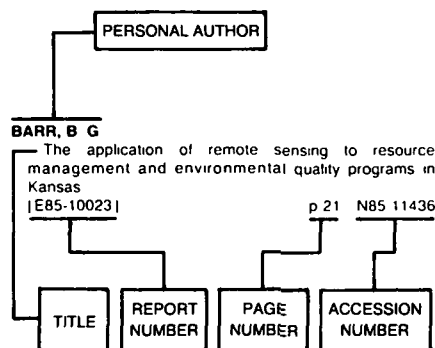
ZENITH

View azimuth and zenith, and solar angle effects on
wheat canopy reflectance p 2 A85-43120

ZINC

The Conterminous United States Mineral Assessment
Program p 24 N85-35458

Typical Personal Author Index Listing



Listings in this index are arranged alphabetically by personal author. The title of the document provides the user with a brief description of the subject matter. The report number helps to indicate the type of document listed (e.g., NASA report, translation, NASA contractor report). The page and accession numbers are located beneath and to the right of the title. Under any one author's name the accession numbers are arranged in sequence with the AIAA accession numbers appearing first.

A

- ABBOT, R. I.**
Establishment of three-dimensional geodetic control by interferometry with the global positioning system
p 9 A85-44102
- ABDEL-HADY, M. A.**
Remote sensing investigations on some fruit orchards in El Fayoum area, Egypt
p 1 A85-42581
- ABDEL-SAMIE, A. G.**
Remote sensing investigations on some fruit orchards in El Fayoum area, Egypt
p 1 A85-42581
- ABOUL-EID, H. Z.**
Remote sensing investigations on some fruit orchards in El Fayoum area, Egypt
p 1 A85-42581
- ABRAMOV, R. V.**
Repetition of dense cloud cover above Indian Ocean from generalized satellite data
p 41 N85-33165
- ACKLESON, S. G.**
A comparison of SPOT simulator data with Landsat MSS imagery for delineating water masses in Delaware Bay, Broadkill River, and adjacent wetlands
p 27 A85-45875
- ADAM, J.**
Preliminary results of Finnish-Hungarian Doppler Observation Campaign /FHDOP/
p 8 A85-41199
- AFANASEV, I. U. A.**
Program of experiments on the Cosmos-1500 satellite
p 28 A85-46251
- AHERN, F. J.**
Assessment of radiometric accuracy of Landsat-4 and Landsat-5 Thematic Mapper data products from Canadian production systems
p 39 A85-47812
- AIKIN, A. C.**
Comparison of mesospheric ozone measurements using the LRIR and UVMCS satellite instruments
p 46 A85-50022
- AKHMEDOV, S. A.**
Impact of fluctuations in optical properties of atmosphere on the ratio of spectral brightness from remote sensing of agricultural land
p 5 N85-33149
- AKHMETOV, R.**
Discovery in earthquake forecasting and seismic zoning recorded
p 16 N85-30426

- ALEKSANDROV, V. I. U.**
Quantitative interpretation of satellite radar images of sea ice using a priori data
p 28 A85-46255
- ALEKSEEV, V. I.**
The effect of the interface albedo of the underlying surface on the reflected radiation
p 10 A85-46131
- ALFORD, W. L.**
Landsat-4 and Landsat-5 MSS coherent noise - Characterization and removal
p 45 A85-47805
- ALLEY, R. E.**
Preliminary spectral and geologic analysis of Landsat-4 Thematic Mapper data, Wind River Basin area, Wyoming
p 15 A85-42476
- ANDERSON, G. P.**
Comparison of mesospheric ozone measurements using the LRIR and UVMCS satellite instruments
p 46 A85-50022
- ANDRAWIS, A. A.**
Geology and structures study of the Nuba Mountains, Sudan, using Landsat images
p 15 A85-42580
- ANUTA, P. E.**
Landsat-4 and Landsat-5 Thematic Mapper data quality analysis
p 39 A85-47818
- LANDSAT-4/5 image data quality analysis**
[E85-10105]
p 41 N85-35463
- ARCHWAMETY, C.**
Landsat Thematic Mapper image-derived MTF
p 39 A85-47817
- ASMUS, V. V.**
Digital processing of radar images obtained with the Cosmos-1500 satellite
p 29 A85-46266
- ATKINSON, P.**
Improving Thematic Mapper land cover classification using filtered data
p 37 A85-41664
- Effect of spatial filtering on scene noise and boundary detail in Thematic Mapper imagery**
p 40 A85-47825
- AUSTIN, G. L.**
Application of pattern-recognition and extrapolation techniques to forecasting
p 45 A85-47244

B

- BACHMANN, E.**
Satellite propagation in the South Pacific region
p 26 A85-42050
- BADHWAR, G. D.**
Inclusion of specular reflectance in vegetative canopy models
p 4 A85-49113
- BAKER, V. R.**
A new global geomorphology?
p 19 N85-32358
- BAKHAMATOV, A. Y.**
Determination of altitude of cloud cover top from Meteor satellite data
p 48 N85-33150
- BALMINO, G.**
Thermal isostasy in the South Atlantic Ocean from geoid anomalies
p 27 A85-44925
- BALSLEY, B. B.**
The effect of El Chichon on wind variability in the troposphere, stratosphere, and mesosphere over Alaska
p 31 A85-49933
- BANYAI, L.**
Calibration of Doppler receivers
p 8 A85-41195
- BARNETT, M. E.**
The generation and interpretation of false-colour composite principal component images
p 37 A85-41659
- BARSKIY, N.**
Cosmonauts participate in multilevel remote sensing experiment
p 48 N85-33130
- BARTOLUCCI, L. A.**
Landsat-4 and Landsat-5 Thematic Mapper data quality analysis
p 39 A85-47818
- LANDSAT-4/5 image data quality analysis**
[E85-10105]
p 41 N85-35463
- BARTON, I. J.**
Transmission model and ground-truth investigation of satellite-derived sea surface temperatures
p 25 A85-41994
- BARTSCH-WINKLER, S.**
The U S Geological Survey in Alaska Accomplishments during 1982
[US-GEOL-SURV-CIRC-939]
p 19 N85-31719
- The United States Geological Survey in Alaska Accomplishments during 1983**
[USGS-CIRC-945]
p 23 N85-34468
- BAUMER, G. M.**
Remote sensing of hydrologic transport processes using spot simulation data
[DE85-012412]
p 37 N85-35467
- BEAULIER, J. M.**
Selection of segment similarity measures for hierarchical picture segmentation
p 41 N85-34548
- BECKMAN, B.**
A water-vapor radiometer error model
p 8 A85-42464
- BEGNI, G.**
SPOT image quality and post-launch assessment
p 38 A85-45692
- Investigation of Landsat-4 Thematic Mapper line-to-line and band-to-band registration and relative detector calibration**
p 39 A85-47807
- BEHRENDT, J. C.**
Petroleum and mineral resources of Antarctica
[US-GEOL-SURV-CIRC-909]
p 18 N85-31605
- BELIAEVA, V. A.**
Reflections of possible oil- and gas-bearing structures of the pre-Jurassic complex in the present-day terrain of Western Siberia
p 16 A85-48387
- BELOV, D. G.**
The experimental oceanographic satellite Cosmos-1500
p 30 A85-46267
- BEN-YOSEF, N.**
Measurement and analysis of 2-D infrared natural background
p 37 A85-42511
- BENSON, A.**
Evaluation of Thematic Mapper data for mapping forest, agricultural and soil resources
p 2 A85-45690
- BENSON, A. S.**
Interpretation of Landsat-4 Thematic Mapper and Multispectral Scanner data for forest surveys
p 2 A85-47806
- BENTLEY, C. R.**
Continental magnetic anomaly constraints on continental reconstruction
p 12 N85-31599
- Regional magnetic anomaly constraints on continental rifting**
p 12 N85-31600
- BERNSTEIN, R. L.**
Large-scale sea surface temperature variability from satellite and shipboard measurements
[NASA-CR-176123]
p 34 N85-33651
- BESSETTE, R. P.**
Global geoid and gravity anomaly predictions using the collocation and point mass techniques
[AD-A154517]
p 13 N85-32387
- BIEHL, L. L.**
Specular, diffuse, and polarized light scattered by two wheat canopies
p 1 A85-42865
- BLAIR, R. W., JR.**
One application of mega-geomorphology in education
p 6 N85-32370
- BLOOM, A. L.**
Andean examples of mega-geomorphology themes
p 20 N85-32367
- BOCK, Y.**
Establishment of three-dimensional geodetic control by interferometry with the global positioning system
p 9 A85-44102
- BOISSIN, B.**
SPOT image quality and post-launch assessment
p 38 A85-45692
- Investigation of Landsat-4 Thematic Mapper line-to-line and band-to-band registration and relative detector calibration**
p 39 A85-47807
- BOND, R. E. L.**
Target observability for satellite-based sensors
[AD-A156139]
p 49 N85-35217
- BORENGASSER, M. X.**
Evaluation of SPOT simulator data for the detection of alteration in Goldfield/Cuprite, Nevada
p 15 A85-45873

BOSWORTH, J. M.

Space-age geodesy - The NASA Crustal Dynamics Project p 8 A85-42452

BOWKER, D. E.

Spectral reflectances of natural targets for use in remote sensing studies [NASA-RP-1139] p 41 N85-30450

BOWMAN, K. P.

A global climatology of total ozone from the Nimbus 7 total ozone mapping spectrometer p 44 A85-45235

BRAILE, L. W.

Improving the geological interpretation of magnetic and gravity satellite anomalies [E85-10103] p 11 N85-31585

MAGSAT scalar anomaly map of South America p 11 N85-31586

The south-central United States magnetic anomaly p 17 N85-31591

A comparative study of spherical and flat-Earth geopotential modeling at satellite elevations p 11 N85-31593

A comparative study of spherical and flat-Earth geopotential modeling at satellite elevations p 12 N85-31594

BRECKENRIDGE, K. S.

Secular variation, crustal contributions, and tectonic activity in California, 1976-1984 p 15 A85-47898

BROOKS, S. R.

The ERS-1 synthetic aperture radar and scatterometer p 45 A85-46849

BROWN, R. J.

Multiple sensor geocoded data p 38 A85-45695

BROWNING, K. A.

Conceptual models of precipitation systems p 45 A85-47245

BRUNET, Y.

Influence of spatial variability of hydraulic characteristics of soils on surface parameters obtained from remote sensing data in infrared and microwaves [NASA-TM-77902] p 5 N85-31604

BRYAN, W. B.

Deep sea mega-geomorphology Progress and problems p 33 N85-32369

BRYANT, N. A.

An analysis of Landsat Thematic Mapper P-Product internal geometry and conformity to earth surface geometry p 40 A85-47821

BRUYKHANOV, V. N.

Space methods for geological research p 16 N85-30429

BUCHHEIM, M. P.

Forest cover type mapping and spruce budworm defoliation detection using simulated SPOT imagery p 2 A85-45874

BUIS, J. S.

Evaluation of Thematic Mapper interband registration and noise characteristics p 46 A85-47819

BULOT, A.

Thermal isostasy in the South Atlantic Ocean from geoid anomalies p 27 A85-44925

BUNTZEN, R. R.

Using ship wake patterns to evaluate SAR (Synthetic Aperture Radar) ocean wave imaging mechanisms Joint US-Canadian Ocean Wave Investigation Project [AD-A154633] p 33 N85-32223

BURTSEV, A. I.

Radar maps of the Arctic and Antarctic compiled on the basis of Cosmos-1500 satellite data, and preliminary results of their analysis p 29 A85-46259

BUSH, V. A.

Space methods for geological research p 16 N85-30429

BUSHUEV, A. V.

Interpretation of sea ice on satellite radar images p 28 A85-46252

BUSHUEV, E. I.

The use of radar images obtained with the Cosmos-1500 satellite to study the distribution and dynamics of sea ice p 28 A85-46254

BUSHUEV, E. I.

The data acquisition system on the Cosmos-1500 satellite p 29 A85-46260

BYCHENKOV, I. U. D.

The use of radar images obtained with the Cosmos-1500 satellite to study the distribution and dynamics of sea ice p 28 A85-46254

C**CAMPBELL, D. L.**

Aeromagnetic and radiometric signatures of a possible porphyry system in the western Tushar Mountains, Utah p 23 N85-35437

CANAS, A. A. D.

The generation and interpretation of false-colour composite principal component images p 37 A85-41659

CAPSONI, C.

Profile statistics of rain in slant path as measured with a radar p 35 A85-40098

CARD, D. H.

Evaluation of Thematic Mapper interband registration and noise characteristics p 46 A85-47819

CARDER, K. L.

Solid-state spectral transmissometer and radiometer p 30 A85-48670

CARTER, W. E.

Polar motion measurements - Subdecimeter accuracy verified by intercomparison p 16 A85-48873

CATHCART, J. B.

Manne phosphonate deposits model for exploration, with emphasis on deposits in the US Atlantic coastal plain p 35 N85-35439

CHANG, H. C.

Wave-induced precipitation as a loss process for radiation belt particles p 25 A85-41961

CHAPUIS, E.

Results of the MIZEX preliminary campaign 29 June to 19 July 1983 [CNES-84/142/T/CT/DRT/TIT/R] p 32 N85-31609

CHARLOCK, T. P.

The albedo field and cloud radiative forcing produced by a general circulation model with internally generated cloud optics p 27 A85-43373

CHELTON, D. B.

Large-scale sea surface temperature variability from satellite and shipboard measurements [NASA-CR-176123] p 34 N85-33651

CHEMODANOV, V. P.

Investigation of the ocean with low-resolution multispectral scanners p 29 A85-46261

CHIN, R. T.

Restoration of multichannel microwave radiometric images p 42 A85-41089

CHOU, S.-H.

Lidar observations of vertically organized convection in the planetary boundary layer over the ocean p 30 A85-47921

CHRISTODOULIDIS, D.

Contemporary plate motions from LAGEOS p 19 N85-31689

CHRISTODOULIDIS, D. C.

Geodetic and geophysical results from Lageos p 7 A85-40003

COATES, R. J.

Space-age geodesy - The NASA Crustal Dynamics Project p 8 A85-42452

COHEN, S. C.

Geodynamics Branch research program [NASA-TM-86223] p 18 N85-31688

COLLINS, W. E.

Geophysical interpretation of satellite laser ranging measurements p 19 N85-31692

COLWELL, R. N.

SPOT simulation imagery for urban monitoring - A comparison with Landsat TM and MSS imagery and with high altitude color infrared photography p 6 A85-45871

CONEL, J. E.

Preliminary spectral and geologic analysis of Landsat-4 Thematic Mapper data, Wind River Basin area, Wyoming p 15 A85-42476

CONNORS, K. F.

Remote sensing of hydrologic transport processes using spot simulation data [DE85-012412] p 37 N85-35467

COOK, D. A.

Intraband radiometric performance of the Landsat Thematic Mappers p 39 A85-47810

COOPER, K. D.

A Monte Carlo reflectance model for soil surfaces with three-dimensional structure p 3 A85-49107

CORNEE, J. J.

A survey of the Rehamna Hercynian Range in western Morocco using Landsat color composite imagery p 15 A85-42582

COUNSELMAN, C. C., III

Establishment of three-dimensional geodetic control by interferometry with the global positioning system p 9 A85-44102

COX, D. P.

Some recent deposit modeling efforts p 23 N85-35453

CRAIN, I. K.

Applied computer graphics in a geographic information system Problems and successes p 6 N85-34563

CUNNINGHAM, C. G.

Aeromagnetic and radiometric signatures of a possible porphyry system in the western Tushar Mountains, Utah p 23 N85-35437

CUNNINGHAM, C. G.

The development of assessment techniques program p 24 N85-35457

CURRAN, P. J.

Principles of remote sensing p 49 A85-40793

CURRIE, N. C.

Techniques of radar reflectivity measurement p 44 A85-43944

CURTIN, G. C.

The Conterminous United States Mineral Assessment Program p 24 N85-35458

CUSHNIE, J. L.

Improving Thematic Mapper land cover classification using filtered data p 37 A85-41664

CZOBOR, A.

Effect of spatial filtering on scene noise and boundary detail in Thematic Mapper imagery p 40 A85-47825

CZOBOR, A.

Preliminary results of Finnish-Hungarian Doppler Observation Campaign /FHDOC/ p 8 A85-41199

D**DAVIS, R. E.**

Spectral reflectances of natural targets for use in remote sensing studies [NASA-RP-1139] p 41 N85-30450

DEEPAK, A.

Data analysis for lidar and quartz crystal microbalance systems [NASA-CR-172601] p 47 N85-32464

DEERING, D. W.

Evaluation of a canopy reflectance model for LAI estimation through its inversion p 3 A85-49108

DEGLORIA, S.

Evaluation of Thematic Mapper data for mapping forest, agricultural and soil resources p 2 A85-45690

DEGLORIA, S. D.

Evaluation of simulated SPOT imagery for the interpretation of agricultural resources in California p 2 A85-45872

DEGLORIA, S. D.

Interpretation of Landsat-4 Thematic Mapper and Multispectral Scanner data for forest surveys p 2 A85-47806

DESACHY, J.

Investigation of Landsat-4 Thematic Mapper line-to-line and band-to-band registration and relative detector calibration p 39 A85-47807

DESIATOVA, G. I.

Determination of the ice-cover characteristics of the Sea of Okhotsk in the winter of 1983-1984 on the basis of radar-sounding data p 28 A85-46253

DESIATOVA, G. I.

Combined analysis of radar and optical images of the northwest Pacific on December 6, 1983 p 29 A85-46258

DEVALU, J. E.

Albedo of a water surface, spectral variation, effects of atmospheric transmittance, sun angle and wind speed p 27 A85-42259

DEYOUNG, J. H., JR.

Applications of the mineral resources data system and the international strategic minerals inventory in mineral-resource assessments by region and commodity p 23 N85-35451

DIAMENT, M.

Thermal isostasy in the South Atlantic Ocean from geoid anomalies p 27 A85-44925

DIETRICH, R.

Interferometric analysis of Doppler measurements for differential receiver calibration p 8 A85-41203

DIETRICH, R.

The research work at the Central Institute for Physics of the Earth, Potsdam, GDR, in the field of Doppler satellite geodesy p 8 A85-41204

DOBSON, F.

Comment on 'Measurement of high-frequency waves using a wave follower' by S. Tang and O. H. Shemdin p 31 A85-49872

DONEAUD, A. A.

Rain volume estimation over areas using satellite and radar data [NASA-CR-176050] p 36 N85-32570

DOUGLAS, I.

Global geomorphology Report of Working Group Number 1 p 21 N85-32382

DOWMAN, I. J.

Application potential of SPOT imagery for topographic mapping p 9 A85-45694

DRANOVSKII, V. I.

The data acquisition system on the Cosmos-1500 satellite p 29 A85-46260

- DUFF, P. F.**
Assessment of radiometric accuracy of Landsat-4 and Landsat-5 Thematic Mapper data products from Canadian production systems p 39 A85-47812
- DUGAS, W. A.**
Relationships between measured and satellite-estimated solar irradiance in Texas p 46 A85-47917
- DUGGIN, M. J.**
Comments on the intercalibration of multisensor, multitemporal, multichannel digital radiance data p 38 A85-42853
Systematic and random variations in Thematic Mapper digital radiance data p 40 A85-47820
- DULOV, V. A.**
Identification of eddy formations in a radar image of the ocean surface p 28 A85-46256
- DUMMER, K.**
Evaluation of Thematic Mapper data for mapping forest, agricultural and soil resources p 2 A85-45690
- DURKEE, P. A.**
Properties of aerosol particles detected by satellites in coastal regions p 34 A85-36222
- DUVAL, J. S.**
Aeromagnetic and radiometric signatures of a possible porphyry system in the western Tushar Mountains, Utah p 23 A85-35437

E

- EANES, R. J.**
Polar motion measurements - Subdecimeter accuracy verified by intercomparison p 16 A85-48873
- EFIMOV, V. B.**
Investigation of ice cover from platforms in the air and in space using radar equipment p 25 A85-40644
The sidelooking radar on the Cosmos-1500 satellite p 29 A85-46262
Modeling of radio-wave scattering by ice cover p 30 A85-49477
- EHLERS, M.**
Comparative evaluations of the geodetic accuracy and cartographic potential of Landsat-4 and Landsat-5 Thematic Mapper image data p 10 A85-47804
- ELIASON, E. M.**
Intraband radiometric performance of the Landsat Thematic Mappers p 39 A85-47810
- ELIASON, J. R.**
Comparative study of fracture planes computed from topography and lineaments from imagery with structures and mineralization in the magnetic belt of Washington State [DE85-010972] p 18 A85-31608
- ELIASON, P. T.**
Intraband radiometric performance of the Landsat Thematic Mappers p 39 A85-47810
- ELIASON, V. L.**
Comparative study of fracture planes computed from topography and lineaments from imagery with structures and mineralization in the magnetic belt of Washington State [DE85-010972] p 18 A85-31608
- ELLROD, G. P.**
Surface cyclogenesis as indicated by satellite imagery [PB85-191815] p 42 A85-35566
- ELMAN, R. I.**
Interactive procedures for discriminating and restoring contour line networks p 41 A85-33158
- EMBLETON, C.**
Techniques, problems and uses of mega-geomorphological mapping p 21 A85-32378
- EOM, H. J.**
A comparison between active and passive sensing of soil moisture from vegetated terrains p 4 A85-49118
- ERAKER, J. H.**
Cryogenic magnetic gradiometers for space applications p 43 A85-42475
- ERMAKOV, V. B.**
Methods for the prediction of the attenuation statistics of radio waves in the 10-100 GHz range in rain - Inclined paths p 44 A85-44015
- EVANS, R. H.**
Small-scale cyclones on the periphery of a Gulf Stream warm-core ring p 30 A85-49855

F

- FAKHOURY, E.**
Evaluation of Thematic Mapper data for mapping forest, agricultural and soil resources p 2 A85-45690
- FARRUKH, U. O.**
Variation in the stratospheric aerosol associated with the North Cyclonic Polar Vortex as measured by the SAM II satellite sensor p 45 A85-46424

- FEIGIN, G.**
Measurement and analysis of 2-D infrared natural background p 37 A85-42511
- FETISOV, A. B.**
The sidelooking radar on the Cosmos-1500 satellite p 29 A85-46262
Informational potential of the sidelooking radar of the Cosmos-1500 satellite p 29 A85-46263
- FISCELLA, B.**
The impact of higher-order Bragg terms on radar sea return p 24 A85-40237
- FITZGERALD, A. J.**
Assessment of radiometric accuracy of Landsat-4 and Landsat-5 Thematic Mapper data products from Canadian production systems p 39 A85-47812
- FLOREN, E. E.**
Using ship wake patterns to evaluate SAR (Synthetic Aperture Radar) ocean wave imaging mechanisms Joint US-Canadian Ocean Wave Investigation Project [AD-A154633] p 33 A85-32223
- FLOUZAT, G.**
Modeling manual extraction of textural elements by mathematical morphology p 38 A85-42584
- FORD, J. P.**
Use of spaceborne imaging radar in regional geomorphic studies p 20 A85-32377
- FREI, U.**
Thematic Mapper - Operational activities and sensor performance at ESA/Earthnet p 46 A85-47808
- FREY, H.**
Space-age geodesy - The NASA Crustal Dynamics Project p 8 A85-42452
- FRIEDMANN, D.**
Multiple sensor geocoded data p 38 A85-45695
- FUNG, A. K.**
A comparison between active and passive sensing of soil moisture from vegetated terrains p 4 A85-49118
- FUSCO, L.**
Thematic Mapper - Operational activities and sensor performance at ESA/Earthnet p 46 A85-47808

G

- GARDASHOV, R. G.**
Model computations of light reflection from sea surface p 31 A85-30411
- GARDNER, T. W.**
Remote sensing of hydrologic transport processes using spot simulation data [DE85-012412] p 37 A85-35467
- GARELLO, R.**
The effect of El Chichon on wind variability in the troposphere, stratosphere, and mesosphere over Alaska p 31 A85-49933
- GAVERILOV, V. P.**
Highly important features of regional tectonics of Earth's Arctic sector p 17 A85-30449
- GEKTI, I. U. M.**
Investigation of the ocean with low-resolution multispectral scanners p 29 A85-46261
- GENDT, G.**
Further improvements of the orbital program system Potsdam-5 and their utilization in geodetic-geodynamic investigations p 7 A85-41189
- GERSTL, S. A. W.**
Remote sensing of angular characteristics of canopy reflectances p 3 A85-49105
- GILLE, J. C.**
Comparison of mesospheric ozone measurements using the LRIR and UVMCS satellite instruments p 46 A85-50022
- GIRARD, M. A.**
Microwave hydrology A trilogy [NASA-CR-176042] p 36 A85-31603
- GLADILIN, V. S.**
The experimental oceanographic satellite Cosmos-1500 p 30 A85-46267
- GLUSHKO, Y. V.**
Comprehensive mapping of and territories of Arizona using space photography p 14 A85-33164
- GOEL, N. S.**
Two-dimensional leaf orientation distributions p 2 A85-49104
Evaluation of a canopy reflectance model for LAI estimation through its inversion p 3 A85-49108
- GOKHMAN, B.**
An analysis of Landsat Thematic Mapper P-Product internal geometry and conformity to earth surface geometry p 40 A85-47821
- GOLDBERG, M.**
Selection of segment similarity measures for hierarchical picture segmentation p 41 A85-34548

- GONCHAROV, N. V.**
The variability of aerosol microstructure in continental and oceanic surface layers of the atmosphere in anticyclones p 34 A85-32660
- GOUREVITCH, S. A.**
Establishment of three-dimensional geodetic control by interferometry with the global positioning system p 9 A85-44102
- GOWARD, S. N.**
Shortwave infrared detection of vegetation p 2 A85-45691
- GOWER, J. F. R.**
A wind-induced mesoscale eddy over the Vancouver Island continental slope p 30 A85-49863
- GOYAL, H. K.**
Geologic analysis of averaged magnetic satellite anomalies p 17 A85-31588
Statistical magnetic anomalies from satellite measurements for geologic analysis p 17 A85-31589
Binning of satellite magnetic anomalies p 11 A85-31590
- GRANT, L.**
Specular, diffuse, and polarized light scattered by two wheat canopies p 1 A85-42865
Plant canopy specular reflectance model p 4 A85-49112
- GRAUCH, V. J. S.**
Aeromagnetic and gravity models of the pluton below the Lake City caldera, Colorado p 23 A85-35442
- GRIGGS, M.**
Satellite measurements of atmospheric aerosols [AD-A153807] p 32 A85-30556
- GRISHCHENKO, V. D.**
Interpretation of sea ice on satellite radar images p 28 A85-46252
- GRODY, N. C.**
Remote sensing of temperature profiles from a combination of observations from the satellite-based Microwave Sounding Unit and the ground-based Profiler p 43 A85-42292
- GRUSH, B.**
The scientific and technical issues in integrating remotely sensed imagery with geocoded data bases p 41 A85-34547
- GUERTIN, F. E.**
Multiple sensor geocoded data p 38 A85-45695
- GUGAN, D. J.**
Application potential of SPOT imagery for topographic mapping p 9 A85-45694
- GULKOV, V. N.**
Optical-physical methods for the study of the ocean p 26 A85-42134
- GUMETSKII, O. IA.**
Data acquisition and processing system based on a microprocessor set for the study of earth resources p 43 A85-43074
- GUYOT, L.**
The contribution of SPOT images to soil mapping - A SPOT simulation study on Lauragais (1981) p 1 A85-41350

H

- HACKER, J. M.**
Motor glider measurements during the Urban Atmosphere Energy Budget Experiment (EESA 1) p 7 A85-35553
- HADGIGEORGE, G.**
Global geoid and gravity anomaly predictions using the collocation and point mass techniques [AD-A154517] p 13 A85-32387
- HALL, D. W.**
To fly on the wings of the sun - A study of solar-powered aircraft p 44 A85-43691
- HALL, R. B.**
New silver resource map of the United States Potential for increased domestic silver production p 23 A85-35445
- HAMMOND, R. R.**
Using ship wake patterns to evaluate SAR (Synthetic Aperture Radar) ocean wave imaging mechanisms Joint US-Canadian Ocean Wave Investigation Project [AD-A154633] p 33 A85-32223
- HAMMOND, W. W., JR.**
Hydrogeology of the lower Glen Rose Aquifer, south-central Texas p 36 A85-35466
- HARLOW, C. A.**
Methods of obtaining offshore wind direction and sea-state data from X-band aircraft SAR imagery of coastal waters p 25 A85-41753
- HARRIS, R.**
Contextual classification post-processing of Landsat data using a probabilistic relaxation model p 37 A85-41658

HARRISON, A.

- HARRISON, A.**
Standardized principal components p 37 A85-41660
- HASTINGS, R.**
Cryogenic magnetic gradiometers for space applications p 43 A85-42475
- HAYDEN, R. S.**
Global Mega-Geomorphology [NASA-CP-2312] p 19 N85-32357
Geomorphological similarity and uniqueness p 19 N85-32361
- HEEL, F.**
Preliminary investigations concerning a 90 GHz radiometer satellite experiment [ESA-TT-860] p 46 N85-31225
- HELLIWEEL, R. A.**
Wave-induced precipitation as a loss process for radiation belt particles p 25 A85-41961
- HESS, P. G.**
The origin of temporal variance in long-lived trace constituents in the summer stratosphere p 6 A85-43375
- HEUER, M. L.**
Relationships between measured and satellite-estimated solar irradiance in Texas p 46 A85-47917
- HEYL, A. V.**
New silver resource map of the United States Potential for increased domestic silver production p 23 N85-35445
- HINDMAN, E. E.**
Properties of aerosol particles detected by satellites in coastal regions p 34 N85-32622
- HINKLEY, E. D.**
Lasers in space p 43 A85-42576
- HINZE, W. J.**
Improving the geological interpretation of magnetic and gravity satellite anomalies [E85-10103] p 11 N85-31585
MAGSAT scalar anomaly map of South America p 11 N85-31586
Geologic analysis of averaged magnetic satellite anomalies p 17 N85-31588
Statistical magnetic anomalies from satellite measurements for geologic analysis p 17 N85-31589
Binning of satellite magnetic anomalies p 11 N85-31590
The south-central United States magnetic anomaly p 17 N85-31591
A comparative study of spherical and flat-Earth geopotential modeling at satellite elevations p 11 N85-31593
A comparative study of spherical and flat-Earth geopotential modeling at satellite elevations p 12 N85-31594
Reduced to pole long-wavelength magnetic anomalies of Africa and Europe p 18 N85-31595
Euro-African MAGSAT anomaly-tectonic observations p 18 N85-31596
Long-wavelength magnetic and gravity anomaly correlations on Africa and Europe p 12 N85-31597
Continental and oceanic magnetic anomalies Enhancement through GRM p 32 N85-31598
Continental magnetic anomaly constraints on continental reconstruction p 12 N85-31599
Regional magnetic anomaly constraints on continental rifting p 12 N85-31600
- HLAVKA, C. A.**
Evaluation of Thematic Mapper interband registration and noise characteristics p 46 A85-47819
- HOLLANDER, J. P.**
Worldwide directory of national Earth-science agencies and related international organizations [GS-CIRC-934] p 50 N85-32386
- HOLTON, J. R.**
The origin of temporal variance in long-lived trace constituents in the summer stratosphere p 6 A85-43375
- HOVIS, W. A.**
Nimbus 7 Coastal Zone Color Scanner (CZCS) Level 2 data product users' guide [NASA-TM-86202] p 31 N85-30452
Nimbus 7 Coastal Zone Color Scanner (CZCS) Level 1 data product users' guide [NASA-TM-86203] p 31 N85-30453
- HSU, A.**
Thematic Mapper - Operational activities and sensor performance at ESA/Earthnet p 46 A85-47808
- HSU, S. A.**
Methods of obtaining offshore wind direction and sea-state data from X-band aircraft SAR imagery of coastal waters p 25 A85-41753
- HUDSON, W. D.**
Vegetation profiles from color-infrared airphotos p 1 A85-42650

- HUH, O. K.**
Methods of obtaining offshore wind direction and sea-state data from X-band aircraft SAR imagery of coastal waters p 25 A85-41753
Satellite observations of the circulation east of the Mississippi Delta - Cold-air outbreak conditions p 27 A85-43117
- HUTTER, M.**
Environmental-physical measurements and determination of atmospheric turbulence with the ASK-16 motor glider p 7 N85-35549
- IATSUN, I. A.**
Data acquisition and processing system based on a microprocessor set for the study of earth resources p 43 A85-43074
- IGDALOVA, I. S.**
The experimental oceanographic satellite Cosmos-1500 p 30 A85-46267
- IGOLKIN, V. V.**
The sidelooking radar on the Cosmos-1500 satellite p 29 A85-46262
- IMHOF, W. L.**
Wave-induced precipitation as a loss process for radiation belt particles p 25 A85-41961
- INAN, U. S.**
Wave-induced precipitation as a loss process for radiation belt particles p 25 A85-41961
- IOLETKHOVSKII, A. A.**
The effect of the interface albedo of the underlying surface on the reflected radiation p 10 A85-46131
The determination of the albedo of natural covers of the earth on the basis of remote measurement results p 10 A85-46132
- ISIORHO, S. A.**
The significance of lineaments mapped from remotely sensed images of the 1 250,000 Lau Sheet in Benue trough of Nigeria p 14 A85-41661
- ITO, T.**
On observation of middle atmosphere with LAS (limb-atmospheric infrared spectrometer) on board of satellite 'Ohzora' (EXOS-C) p 42 A85-41362
- IVANOV, A. V.**
Basic properties and interpretation of synthesized radar images of sea waves with long synthesize time p 34 N85-33384
- JACOBS, J. A.**
Geophysics 2001 p 10 A85-49660
- JAIN, A.**
Method and apparatus for Delta Kappa synthetic aperture radar measurement of ocean current [NASA-CASE-NPO-15704-1] p 35 N85-34327
- JIN, Y.-Q.**
Strong fluctuation theory for scattering, attenuation, and transmission of microwaves through snowfall p 36 A85-49116
- JOHNSON, R. M.**
High-latitude mesopause neutral winds and geomagnetic activity - A cross-correlation analysis p 16 A85-49227
- JOHNSTON, E. J.**
Microwave hydrology: A trilogy [NASA-CR-176042] p 36 N85-31603
- JOHNSTON, M. J. S.**
Secular variation, crustal contributions, and tectonic activity in California, 1976-1984 p 15 A85-47898
- JONES, O. D.**
Preliminary evaluation of the Landsat-4 Thematic Mapper data for mineral exploration p 15 A85-45688
A comparison of LANDSAT thematic mapper, multispectral scanner and airborne sensors for mapping the distribution of alteration minerals: Examples from the southwestern United States p 23 N85-35452
- JONES, W. T.**
Spectral reflectances of natural targets for use in remote sensing studies [NASA-RP-1139] p 41 N85-30450
- JORDAN, T. R.**
Comparative evaluations of the geodetic accuracy and cartographic potential of Landsat-4 and Landsat-5 Thematic Mapper image data p 10 A85-47804
- JOYCE, H.**
The ERS-1 synthetic aperture radar and scatterometer p 45 A85-46849
- JOYCE, T. M.**
Small-scale cyclones on the periphery of a Gulf Stream warm-core ring p 30 A85-49855

PERSONAL AUTHOR INDEX

K

- KACHINSKI, R.**
Interpretation of multiband photographs made during Telefoto-80 experiment for the purpose of discriminating agricultural crops p 5 N85-33152
- KAHN, W. D.**
Geodynamics Branch research program [NASA-TM-86223] p 18 N85-31688
Spaceborne gradiometer error analysis p 13 N85-31707
- KALMYKOV, A. I.**
Investigation of ice cover from platforms in the air and in space using radar equipment p 25 A85-40644
Ordered mesoscale structures on the ocean surface identified from satellite radar data p 28 A85-46257
The sidelooking radar on the Cosmos-1500 satellite p 29 A85-46262
Informational potential of the sidelooking radar of the Cosmos-1500 satellite p 29 A85-46263
- KATSAROS, K. B.**
Albedo of a water surface, spectral variation, effects of atmospheric transmittance, sun angle and wind speed p 27 A85-42259
- KATSURAKIS, J. P.**
Wave-induced precipitation as a loss process for radiation belt particles p 25 A85-41961
- KAUFMAN, Y. J.**
The atmospheric effect on the separability of field classes measured from satellites p 44 A85-43115
- KAVELIN, S. S.**
The data acquisition system on the Cosmos-1500 satellite p 29 A85-46260
The experimental oceanographic satellite Cosmos-1500 p 30 A85-46267
- KELNER, I. G.**
The USSR as viewed from space p 50 A85-48524
- KENNELLY, M. A.**
Small-scale cyclones on the periphery of a Gulf Stream warm-core ring p 30 A85-49855
- KENT, G. S.**
Variation in the stratospheric aerosol associated with the North Cyclonic Polar Vortex as measured by the SAM II satellite sensor p 45 A85-46424
Data analysis for lidar and quartz crystal microbalance systems [NASA-CR-172601] p 47 N85-32464
- KEUNING, W.**
Properties of aerosol particles detected by satellites in coastal regions p 34 N85-32622
- KEYDEL, W.**
Probabilities, problems, and perspectives of microwave long-range reconnaissance p 42 A85-41570
- KHARCHENKO, V. N.**
Distribution of the effective scattering area of the earth surface at low grazing angles p 10 A85-46079
- KHMYROV, B. E.**
Program of experiments on the Cosmos-1500 satellite p 28 A85-46251
- KHNYKIN, V. I.**
Using remote photographs in prospecting for hydrocarbons on the Kerch Peninsula p 22 N85-33154
- KIEFFER, H. H.**
Intraband radiometric performance of the Landsat Thematic Mappers p 39 A85-47810
- KIENKO, I. P.**
The USSR as viewed from space p 50 A85-48524
- KIETZMANN, H.**
Preliminary investigations concerning a 90 GHz radiometer satellite experiment [ESA-TT-860] p 46 N85-31225
- KIMES, D. S.**
Directional reflectance factor distributions for cover types of Northern Africa p 1 A85-43114
Modeling the radiant transfers of sparse vegetation canopies p 3 A85-49110
- KING, R. W.**
Establishment of three-dimensional geodetic control by interferometry with the global positioning system p 9 A85-44102
- KISHI, S.**
Eruption of Mount Ontake in 1979 - Detection of volcanic ash fall area from Landsat MSS CCT data p 15 A85-42583
- KLECKNER, R. L.**
Federal Mineral Land Information System p 7 N85-35459
- KLEMAS, V.**
A comparison of SPOT simulator data with Landsat MSS imagery for delineating water masses in Delaware Bay, Broadkill River, and adjacent wetlands p 27 A85-45875
- KLIMENKO, O. Y.**
Regression analysis of aircraft and ground measurement data on vegetation cover p 5 N85-33156

- KLOSKO, S. M.**
Geodetic and geophysical results from Lageos p 7 A85-40003
- KNOLL, J. S.**
Visible fluorescence from ultraviolet excited crude oil p 27 A85-42512
- KOBLINSKY, C. J.**
Ocean circulation studies p 32 N85-31712
- KOCHUBEI, A. N.**
Scattering in precipitation during microwave-beam power transmission p 45 A85-46297
- KOGAN, M. G.**
Thermal isotasy in the South Atlantic Ocean from geoid anomalies p 27 A85-44925
- KOLENKIEWICZ, R.**
Geodetic and geophysical results from Lageos
TOPEX error budget p 47 N85-31717
- KOLESHNIKOV, V. G.**
Specific effective scattering surfaces of certain terrains in the millimeter wave band p 10 A85-46081
- KOLODIY, N. V.**
Using remote photographs in prospecting for hydrocarbons on the Kerch Peninsula p 22 N85-33154
- KOLOSOV, M. A.**
Methods for the prediction of the attenuation statistics of radio waves in the 10-100 GHz range in rain - Inclined paths p 44 A85-44015
- KOMIAK, V. A.**
Investigation of ice cover from platforms in the air and in space using radar equipment p 25 A85-40644
- KOMISSAROVA, I. M.**
The USSR as viewed from space p 50 A85-48524
- KONDRATYEVA, T. I.**
Comprehensive mapping of and territories of Arizona using space photography p 14 N85-33164
- KONG, J. A.**
Theory of microwave remote sensing p 42 A85-40792
Strong fluctuation theory for scattering, attenuation, and transmission of microwaves through snowfall p 36 A85-49116
Active and passive remote sensing of ice [AD-A154406] p 31 N85-30459
- KONSTANTINOV, N.**
Spacecraft-aided research discussed at geology Congress p 22 N85-33147
- KOPROVA, L. I.**
Determination of altitude of cloud cover top from Meteor satellite data p 48 N85-33150
- KOPYL, I. V.**
Physico-geographical regionalization of Caspian lowland based on space survey materials p 14 N85-33162
- KOROTAEV, G. K.**
Identification of eddy formations in a radar image of the ocean surface p 28 A85-46256
- KOSLOW, M. H.**
A comparison of LANDSAT thematic mapper, multispectral scanner and airborne sensors for mapping the distribution of alteration minerals Examples from the southwestern United States p 23 N85-35452
- KOSTIUKOVICH, S. B.**
The determination of the albedo of natural covers of the earth on the basis of remote measurement results p 10 A85-46132
- KOVASIUK, V. V.**
Determination of the ice-cover characteristics of the Sea of Okhotsk in the winter of 1983-1984 on the basis of radar-sounding data p 28 A85-46253
Combined analysis of radar and optical images of the northwest Pacific on December 6, 1983 p 29 A85-46258
- KOZODEROV, V. V.**
Regression analysis of aircraft and ground measurement data on vegetation cover p 5 N85-33156
- KRAVTSOVA, V. I.**
Mapping of dynamics of deltas by space photography p 14 N85-33163
- KROPOTKIN, M. A.**
Optical-physical methods for the study of the ocean p 26 A85-42134
- KROVOTYNTSEV, V. A.**
Radar maps of the Arctic and Antarctic compiled on the basis of Cosmos-1500 satellite data, and preliminary results of their analysis p 29 A85-46259
- KRUEGER, A. J.**
A global climatology of total ozone from the Nimbus 7 total ozone mapping spectrometer p 44 A85-45235
- KUDRIAVTSEV, V. N.**
Identification of eddy formations in a radar image of the ocean surface p 28 A85-46256
- KULEMIN, G. P.**
Backscattering of centimeter and millimeter radio waves by the earth surface at low grazing angles (Review) p 9 A85-46078
- Distribution of the effective scattering area of the earth surface at low grazing angles p 10 A85-46079
- KUREKIN, A. S.**
Investigation of ice cover from platforms in the air and in space using radar equipment p 25 A85-40644
The sidelooking radar on the Cosmos-1500 satellite p 29 A85-46262
Informational potential of the sidelooking radar of the Cosmos-1500 satellite p 29 A85-46263
- KUZINA, A. M.**
Terrain illumination conditions when taking scanning photographs from space p 48 N85-33159
- ## L
- LANG, H. R.**
Preliminary spectral and geologic analysis of Landsat-4 Thematic Mapper data, Wind River Basin area, Wyoming p 15 A85-42476
- LANG, R. H.**
Microwave inversion of leaf area and inclination angle distributions from backscattered data p 3 A85-49109
- LANGEL, R. A.**
The magnetic field of the earth - Performance considerations for space-based observing systems p 9 A85-42474
- LANNELONGUE, N.**
Results of the MIZEX preliminary campaign 29 June to 19 July 1983 [CNES-84/142/T/CT/DRT/TIT/R] p 32 N85-31609
- LARSEN, P. F.**
Thermal satellite imagery applied to a littoral macrobenthos investigation in the Gulf of Maine p 25 A85-41662
- LATTMAN, L. H.**
Mega-geomorphology and neotectonics p 20 N85-32366
- LATTY, R. S.**
Performance comparisons between information extraction techniques using variable spatial resolution data p 40 A85-47823
- LEHMANN, K.**
Interferometric analysis of Doppler measurements for differential receiver calibration p 8 A85-41203
- LEICK, A.**
Application of GPS in a high precision engineering survey network [DE85-010556] p 10 N85-30539
- LEONARD, J. M.**
Handbook for obtaining and using aerial photography to map aquatic plant distribution [AD-A154584] p 33 N85-32388
- LESH, J. R.**
Lasers in space p 43 A85-42576
- LEVDA, A. S.**
Investigation of ice cover from platforms in the air and in space using radar equipment p 25 A85-40644
- LI, X.**
Geometric-optical modeling of a conifer forest canopy p 4 A85-49111
- LILLESAND, T. M.**
Forest cover type mapping and spruce budworm defoliation detection using simulated SPOT imagery p 2 A85-45874
- LIMABLANCO, W. R.**
Coastal erosion along Monterey Bay [AD-A155610] p 34 N85-32707
- LIND, R. J.**
Albedo of a water surface, spectral variation, effects of atmospheric transmittance, sun angle and wind speed p 27 A85-42259
- LINDSAY, J.**
Systematic and random variations in Thematic Mapper digital radiance data p 40 A85-47820
- LIPSKAYA, O. A.**
The variability of aerosol microstructure in continental and oceanic surface layers of the atmosphere in anticyclones p 34 N85-32660
- LIU, H. S.**
Satellite-determined stresses in the crust of Europe with particular consideration to the Liege earthquake of November 8, 1983 p 13 N85-31694
- LIU, W. T.**
Tropical Ocean and Global Atmosphere (TOGA) heat exchange project A summary report [NASA-CR-176038] p 33 N85-31738
- LOMBARDINI, P. P.**
The impact of higher-order Bragg terms on radar sea return p 24 A85-40237
- LOSHCHILOV, V. S.**
Quantitative interpretation of satellite radar images of sea ice using a priori data p 28 A85-46255
- LOZANO, D. F.**
Landsat-4 and Landsat-5 Thematic Mapper data quality analysis p 39 A85-47818
- LANDSAT-4/5 image data quality analysis [E85-10105] p 41 N85-35463
- LUCCHITTA, B. K.**
Use of the synoptic view: Examples from Earth and other planets p 20 N85-32371
- LUDWIG, H. R.**
Six mechanisms used on the SSM/1 radiometer p 49 N85-33534
- LUHMANN, J. G.**
High-latitude mesopause neutral winds and geomagnetic activity - A cross-correlation analysis p 16 A85-49227
- ## M
- MA, C.**
The global VLBI fiducial network p 12 N85-31690
- MACDONALD, C. L.**
Applied computer graphics in a geographic information system Problems and successes p 6 N85-34563
- MACK, P.**
Satellites and politics Weather, communications, and earth resources p 50 N85-35144
- MACKLIN, J. T.**
Inverse methods for ocean wave imaging by SAR p 30 A85-48970
- MACLEAN, A. L.**
Forest cover type mapping and spruce budworm defoliation detection using simulated SPOT imagery p 2 A85-45874
- MAHLER, R. P. S.**
Cryogenic magnetic gradiometers for space applications p 43 A85-42475
- MAKOVKIN, V. V.**
Automated processing of remote-sensing data obtained with the microwave radiometer of the Cosmos-1500 satellite p 29 A85-46265
- MALARET, E.**
Landsat-4 and Landsat-5 Thematic Mapper data quality analysis p 39 A85-47818
LANDSAT-4/5 image data quality analysis [E85-10105] p 41 N85-35463
- MALILA, W. A.**
Characterization and comparison of Landsat-4 and Landsat-5 Thematic Mapper data p 39 A85-47809
Comparison of the information contents of Landsat TM and MSS data p 40 A85-47822
Study of spectral/radiometric characteristics of the Thematic Mapper for land use applications [E85-10106] p 42 N85-35464
- MALTSEVA, I. G.**
Terrain illumination conditions when taking scanning photographs from space p 48 N85-33159
Calculating solar highlight and shadeless areas for scanning photographs from space and optimizing lighting conditions p 49 N85-33160
- MAPP, G. R.**
Wave refraction by warm core rings p 26 A85-42254
- MARCOS, F. A.**
Application of satellite accelerometer data to improve density models [AD-A154904] p 48 N85-32558
- MARKHAM, B.**
Performance comparisons between information extraction techniques using variable spatial resolution data p 40 A85-47823
- MARKHAM, B. L.**
Landsat-4 and Landsat-5 MSS coherent noise - Characterization and removal p 45 A85-47805
- MARKOV, V. F.**
The USSR as viewed from space p 50 A85-48524
- MARSH, J. G.**
Global mean sea surface based upon a combination of the GEOS-3 and SEASAT altimeter data p 32 N85-31710
- MARTIN, S.**
Dispersion of sea ice in the Bering Sea p 26 A85-42257
- MARUSSI, A.**
Intrinsic geodesy p 9 A85-43958
- MASANOV, A. D.**
Interpretation of sea ice on satellite radar images p 28 A85-46252
- MASLOV, V. D.**
Automated processing of remote-sensing data obtained with the microwave radiometer of the Cosmos-1500 satellite p 29 A85-46265
- MASTIN, G. A.**
Methods of obtaining offshore wind direction and sea-state data from X-band aircraft SAR imagery of coastal waters p 25 A85-41753
- MATRICCIANI, E.**
Profile statistics of rain in slant path as measured with a radar p 35 A85-40098

MATSON, M.

- Hydrologic and land sciences applications of NOAA polar-orbiting satellite data p 35 A85-41320

MATSUZAKI, A.

- On observation of middle atmosphere with LAS (limb-atmospheric infrared spectrometer) on board of satellite 'Ohzora' (EXOS-C) p 42 A85-41362

MAURI, M.

- Profile statistics of rain in slant path as measured with a radar p 35 A85-40098

MCCORMICK, M. P.

- Variation in the stratospheric aerosol associated with the North Cyclonic Polar Vortex as measured by the SAM II satellite sensor p 45 A85-46424

MCELROY, J. H.

- Space Station Polar Platform Integrating research and operational missions [PB85-195279] p 49 N85-35218

MCGILLEM, C. D.

- Landsat-4 and Landsat-5 Thematic Mapper data quality analysis p 39 A85-47818
LANDSAT-4/5 image data quality analysis [E85-10105] p 41 N85-35463

MCGREGOR, S. J.

- Microcomputer processing of LANDSAT Thematic Mapper data for the acquisition of military tactical terrain data [AD-A154781] p 47 N85-32389

MCKIM, H. L.

- Evaluation of SPOT HRV simulation data for Corps of Engineers applications p 36 A85-45693
A comparison of SPOT simulator data with Landsat MSS imagery for delineating water masses in Delaware Bay, Broadkill River, and adjacent wetlands p 27 A85-45875

MCMILLIN, L. M.

- Remote sensing of temperature profiles from a combination of observations from the satellite-based Microwave Sounding Unit and the ground-based Profiler p 43 A85-42292

MCMURDIE, L. A.

- Albedo of a water surface, spectral variation, effects of atmospheric transmittance, sun angle and wind speed p 27 A85-42259

MCNITT, J. A.

- Mesoscale features and atmospheric refraction conditions of the Arctic marginal ice zone [AD-A155139] p 33 N85-32584

MEAD, G. D.

- Space-age geodesy - The NASA Crustal Dynamics Project p 8 A85-42452

MEDLIN, A. L.

- Applications of the mineral resources data system and the international strategic minerals inventory in mineral-resource assessments by region and commodity p 23 N85-35451

MELFI, S. H.

- Lidar observations of vertically organized convection in the planetary boundary layer over the ocean p 30 A85-47921

MELHORN, W. N.

- Space imagery and some geomorphological problems of the Guana Shield, South America p 20 N85-32368

MENZIES, R. T.

- Lasers in space p 43 A85-42576

MERGHOUH, Y.

- Modeling manual extraction of textural elements by mathematical morphology p 38 A85-42584

MERRY, C. J.

- Evaluation of SPOT HRV simulation data for Corps of Engineers applications p 36 A85-45693
A comparison of SPOT simulator data with Landsat MSS imagery for delineating water masses in Delaware Bay, Broadkill River, and adjacent wetlands p 27 A85-45875

METZLER, M. D.

- Characterization and comparison of Landsat-4 and Landsat-5 Thematic Mapper data p 39 A85-47809
Study of spectral/radiometric characteristics of the Thematic Mapper for land use applications [E85-10106] p 42 N85-35464

MIHALY, SZ.

- Preliminary results of Finnish-Hungarian Doppler Observation Campaign /FHDOC/ p 8 A85-41199

MILLIER, F.

- Comparison of mesospheric ozone measurements using the LRIR and UVMCS satellite instruments p 46 A85-50022

MILLOT, C.

- Some features of the Algerian Current p 26 A85-42255

MIROSHNICHENKO, V. V.

- Automated processing of remote-sensing data obtained with the microwave radiometer of the Cosmos-1500 satellite p 29 A85-46265

MITNIK, L. M.

- Determination of the ice-cover characteristics of the Sea of Okhotsk in the winter of 1983-1984 on the basis of radar-sounding data p 28 A85-46253
Combined analysis of radar and optical images of the northwest Pacific on December 6, 1983 p 29 A85-46258

MOORE, R. K.

- Radar sensing of the ocean p 25 A85-41752
Sources of scattering from vegetation canopies at 10 GHz p 4 A85-49114

MORAIN, S. A.

- Commercialization of remote-sensing technology p 49 A85-41657

MORISAWA, M.

- Geomorphic analyses from space imagery p 20 N85-32374

MUELLER, R. J.

- Secular variation, crustal contributions, and tectonic activity in California, 1976-1984 p 15 A85-47898

MUESSIG, H.

- Evaluation Close-range photogrammetry for slope inventory and monitoring [PB85-192755] p 24 N85-35470

MULLER, J.

- A survey of the Rehanna Hercynian Range in western Morocco using Landsat color composite imagery p 15 A85-42582

MUNDAY, J. C.

- Wave refraction by warm core rings p 26 A85-42254

MURALIKRISHNA, I. V.

- Utility of proposed sensors for coastal engineering studies p 45 A85-45697

MURPHY, J. M.

- Assessment of radiometric accuracy of Landsat-4 and Landsat-5 Thematic Mapper data products from Canadian production systems p 39 A85-47812

MYRICK, D. L.

- Spectral reflectances of natural targets for use in remote sensing studies [NASA-RP-1139] p 41 N85-30450

N

NAESER, C. W.

- Aeromagnetic and radiometric signatures of a possible porphyry system in the western Tushar Mountains, Utah p 23 N85-35437

NAKAMURA, Y.

- On observation of middle atmosphere with LAS (limb-atmospheric infrared spectrometer) on board of satellite 'Ohzora' (EXOS-C) p 42 A85-41362

NARAEVA, M. K.

- Investigation of the ocean with low-resolution multispectral scanners p 29 A85-46261

NAZIROV, M.

- Ordered mesoscale structures on the ocean surface identified from satellite radar data p 28 A85-46257

- Radar maps of the Arctic and Antarctic compiled on the basis of Cosmos-1500 satellite data, and preliminary results of their analysis p 29 A85-46259

NEDOVESOV, A. N.

- Automated processing of remote-sensing data obtained with the microwave radiometer of the Cosmos-1500 satellite p 29 A85-46265

NELEPO, B. A.

- Program of experiments on the Cosmos-1500 satellite p 28 A85-46251

NELSON, R.

- Performance comparisons between information extraction techniques using variable spatial resolution data p 40 A85-47823

NELSON, R. F.

- Sensor-induced temporal variability of Landsat MSS data p 44 A85-43116

NEWCOMB, W. W.

- Directional reflectance factor distributions for cover types of Northern Africa p 1 A85-43114

NIELER, P. P.

- Tropical Ocean and Global Atmosphere (TOGA) heat exchange project A summary report [NASA-CR-176038] p 33 N85-31738

NIKITIN, P. A.

- Ordered mesoscale structures on the ocean surface identified from satellite radar data p 28 A85-46257

- Radar maps of the Arctic and Antarctic compiled on the basis of Cosmos-1500 satellite data, and preliminary results of their analysis p 29 A85-46259

- Digital processing of radar images obtained with the Cosmos-1500 satellite p 29 A85-46266

NIKOLAYEV, V. A.

- Physico-geographical regionalization of Caspian lowland based on space survey materials p 14 N85-33162

NORMAN, J. M.

- Contrasts among bidirectional reflectance of leaves, canopies, and soils p 3 A85-49106
Modeling the radiant transfers of sparse vegetation canopies p 3 A85-49110

NOVAKOVSKII, B. A.

- Cartographic-photogrammetric analysis and analytical correction of space scanner images p 38 A85-44864

O

OBRYADCHIKOV, O. S.

- Landscape interpretation capabilities using space photographs of regions of a multistage platform mantle structure p 22 N85-33151

OLDHAM, P. B.

- A microprocessor-controlled, multichannel fluorometer for analysis of sea water [AD-A154986] p 33 N85-32310

OLIVIER, R.

- Reduced to pole long-wavelength magnetic anomalies of Africa and Europe p 18 N85-31595
Euro-African MAGSAT anomaly-tectonic observations p 18 N85-31596

- Long-wavelength magnetic and gravity anomaly correlations on Africa and Europe p 12 N85-31597

- Continental magnetic anomaly constraints on continental reconstruction p 12 N85-31599

- Regional magnetic anomaly constraints on continental rifting p 12 N85-31600

OLSON, W. S.

- Restoration of multichannel microwave radiometric images p 42 A85-41089

P

PALM, S. P.

- Lidar observations of vertically organized convection in the planetary boundary layer over the ocean p 30 A85-47921

PALMER, J. M.

- Spectroradiometric calibration of the Thematic Mapper and Multispectral Scanner system [E85-10104] p 47 N85-31601

PANFILOV, A. S.

- Investigation of the ocean with low-resolution multispectral scanners p 29 A85-46261

PARKHOMOV, V. A.

- Fine structure of the preliminary impulse of a sudden storm commencement p 14 A85-40612

PARM, T.

- Preliminary results of Finnish-Hungarian Doppler Observation Campaign /FHDOC/ p 8 A85-41199

PARMENTER-HOLT, F.

- Hydrologic and land sciences applications of NOAA polar-orbiting satellite data p 35 A85-41320

PARROTT, M. H.

- A comparative study of spherical and flat-Earth geopotential modeling at satellite elevations p 11 N85-31593

- A comparative study of spherical and flat-Earth geopotential modeling at satellite elevations p 12 N85-31594

PASHCHENKO, E. G.

- Optical-physical methods for the study of the ocean p 26 A85-42134

PATONAY, G.

- A microprocessor-controlled, multichannel fluorometer for analysis of sea water [AD-A154986] p 33 N85-32310

PAYLOR, E. D.

- Preliminary spectral and geologic analysis of Landsat-4 Thematic Mapper data, Wind River Basin area, Wyoming p 15 A85-42476

PAYNE, P. R.

- Solid-state spectral transmissometer and radiometer p 30 A85-48670

PERBOS, J.

- SPOT image quality and post-launch assessment p 38 A85-45692

- Investigation of Landsat-4 Thematic Mapper line-to-line and band-to-band registration and relative detector calibration p 39 A85-47807

PETERSEN, G. W.

- Remote sensing of hydrologic transport processes using spot simulation data [DE85-012412] p 37 N85-35467

PETERSON, C. J.

- Methods for destriping Landsat Thematic Mapper images - A feasibility study for an online destriping process in the Thematic Mapper Image Processing System (TIPS) p 39 A85-47813

- PETERSON, U. K.**
Cataloging the spectral brightness coefficients of the forested region of the European territory of the USSR p 5 N85-33155
- PETROV, P. V.**
Cartographic-photogrammetric analysis and analytical correction of space scanner images p 38 A85-44864
- PETROV, S. Y.**
Landscape interpretation capabilities using space photographs of regions of a multistage platform mantle structure p 22 N85-33151
- PICHUGIN, A. P.**
Ordered mesoscale structures on the ocean surface identified from satellite radar data p 28 A85-46257
Informational potential of the sidelooking radar of the Cosmos-1500 satellite p 29 A85-46263
- PIKE, A. C.**
Geopotential heights and thicknesses as predictors of Atlantic tropical cyclone motion and intensity p 26 A85-42177
- PINTY, B.**
A new technique for inferring surface albedo from satellite observations p 46 A85-47916
- PISACANE, V. L.**
Geopotential Research Mission - Status report p 8 A85-42469
- PITKIN, J. A.**
Aeromagnetic and radiometric signatures of a possible porphyry system in the western Tushar Mountains, Utah p 23 N85-35437
- PLOKHENKO, Y. V.**
Enhancing precision of remote temperature sensing data from satellites under cloudy atmospheric conditions p 48 N85-33148
- PODWYSOCKI, M. H.**
Preliminary evaluation of the Landsat-4 Thematic Mapper data for mineral exploration p 15 A85-45688
A comparison of LANDSAT thematic mapper, multispectral scanner and airborne sensors for mapping the distribution of alteration minerals Examples from the southwestern United States p 23 N85-35452
- PONCE, D. A.**
Comparison of survey and photogrammetry methods to position gravity data, Yucca Mountain, Nevada [DE85-011685] p 13 N85-32316
- POPOV, A. E.**
Digital processing of radar images obtained with the Cosmos-1500 satellite p 29 A85-46266
- POPOV, V. I.**
Digital processing of radar images obtained with the Cosmos-1500 satellite p 29 A85-46266
- POROS, D. J.**
Methods for destriping Landsat Thematic Mapper images - A feasibility study for an online destriping process in the Thematic Mapper Image Processing System (TIPS) p 39 A85-47813
- POULTON, C. E.**
SPOT simulation imagery for urban monitoring - A comparison with Landsat TM and MSS imagery and with high altitude color infrared photography p 6 A85-45871
- POUPARD, J.-P.**
The contribution of SPOT images to soil mapping - A SPOT simulation study on Lauragais (1981) p 1 A85-41350
- POWER, M. S.**
Preliminary evaluation of the Landsat-4 Thematic Mapper data for mineral exploration p 15 A85-45688
A comparison of LANDSAT thematic mapper, multispectral scanner and airborne sensors for mapping the distribution of alteration minerals Examples from the southwestern United States p 23 N85-35452
- POZHIDAIEV, V. N.**
Methods for the prediction of the attenuation statistics of radio waves in the 10-100 GHz range in rain - Inclined paths p 44 A85-44015
- PRICE, J. C.**
On the analysis of thermal infrared imagery - The limited utility of apparent thermal inertia p 38 A85-43118
- PUSTOVOITENKO, V. V.**
The data acquisition system on the Cosmos-1500 satellite p 29 A85-46260
- PUTNEY, B. H.**
Geodyn systems development p 13 N85-31708
- R**
- RADOK, U.**
The Antarctic ice p 14 A85-42171
- RAIS ASSA, R.**
A survey of the Rehamna Hercynian Range in western Morocco using Landsat color composite imagery p 15 A85-42582
- RAKOV, V. I.**
Data acquisition and processing system based on a microprocessor set for the study of earth resources p 43 A85-43074
- RAMANATHAN, V.**
The albedo field and cloud radiative forcing produced by a general circulation model with internally generated cloud optics p 27 A85-43373
- RAMM, N. S.**
Terrain illumination conditions when taking scanning photographs from space p 48 N85-33159
- RANSON, K. J.**
Two-dimensional leaf orientation distributions p 2 A85-49104
- REED, K. M.**
The U.S. Geological Survey in Alaska Accomplishments during 1982 [US-GEOL-SURV-CIRC-939] p 19 N85-31719
The United States Geological Survey in Alaska Accomplishments during 1983 [USGS-CIRC-945] p 23 N85-34468
- REGUSTERS, H. A.**
Microwave hydrology A trilogy [NASA-CR-176042] p 36 N85-31603
- REYNA, E.**
Inclusion of specular reflectance in vegetative canopy models p 4 A85-49113
- RIDGWAY, J. R.**
MAGSAT scalar anomaly map of South America p 11 N85-31586
MAGSAT satellite magnetic anomaly map over South America p 11 N85-31587
Geologic analysis of averaged magnetic satellite anomalies p 17 N85-31588
- RITTER, D. F.**
Regional landform thresholds p 19 N85-32362
- ROBERTSON, D. S.**
Polar motion measurements - Subdecimeter accuracy verified by intercomparison p 16 A85-48873
- ROBINSON, B. F.**
Specular, diffuse, and polarized light scattered by two wheat canopies p 1 A85-42865
- ROBINSON, I. S.**
Satellite oceanography p 26 A85-42222
- ROSS, Y. K.**
Cataloging the spectral brightness coefficients of the forested region of the European territory of the USSR p 5 N85-33155
- ROSSBACHER, L. A.**
Planetary perspective Report of Working Group Number 4 p 22 N85-32385
- ROTHERAM, S.**
Inverse methods for ocean wave imaging by SAR p 30 A85-48970
- ROUSE, L. J., JR.**
Satellite observations of the circulation east of the Mississippi Delta - Cold-air outbreak conditions p 27 A85-43117
- ROZANOV, L. N.**
Discrimination of linear contour elements of space photographs based on visual perception model p 13 N85-33161
- RULAND, R.**
Application of GPS in a high precision engineering survey network [DE85-010556] p 10 N85-30539
- RYAN, J. W.**
First epoch measurements by Mark III VLBI of the San Andreas Fault experiment baseline p 12 N85-31691
- S**
- SABINS, F. F., JR.**
Geomorphology, tectonics, and exploration p 19 N85-32365
- SAKHAVAT, H.**
Systematic and random variations in Thematic Mapper digital radiance data p 40 A85-47820
- SALEH, H. A.**
Microwave inversion of leaf area and inclination angle distributions from backscattered data p 3 A85-49109
- SALOMONSON, V. V.**
Landsat image data quality studies p 38 A85-45687
- SALTIKOV, I. U. D.**
The data acquisition system on the Cosmos-1500 satellite p 29 A85-46260
- SANTEK, D. A.**
Measuring the global distribution of intense convection over land with passive microwave radiometry p 36 A85-47923
- SAWYER, F. G.**
The ERS-1 synthetic aperture radar and scatterometer p 45 A85-46849
- SCHGOUNN, C.**
Results of the MIZEX preliminary campaign 29 June to 19 July 1983 [CNES-84/142/T/CT/DRT/TIT/R] p 32 N85-31609
- SCHNEIDER, R., JR.**
Cryogenic magnetic gradiometers for space applications p 43 A85-42475
- SCHNEIDER, S. R.**
Space Station Polar Platform Integrating research and operational missions [PB85-195279] p 49 N85-35218
- SCHNETZLER, C. C.**
The magnetic field of the earth - Performance considerations for space-based observing systems p 9 A85-42474
- SCHOWENGERDT, R. A.**
Landsat Thematic Mapper image-derived MTF p 39 A85-47817
- SCHROEDER, W. W.**
Satellite observations of the circulation east of the Mississippi Delta - Cold-air outbreak conditions p 27 A85-43117
- SCHUELER, C. F.**
Landsat image data quality studies p 38 A85-45687
- SCHUTZ, B. E.**
Polar motion measurements - Subdecimeter accuracy verified by intercomparison p 16 A85-48873
- SELIVANOV, A. S.**
Program of experiments on the Cosmos-1500 satellite p 28 A85-46251
Investigation of the ocean with low-resolution multispectral scanners p 29 A85-46261
- SEMEV, V. S.**
Conditions for formation of parageneses containing kyanite-orthoclase in region of Mount Provender and Pratt Peak (Shackleton Range, Antarctica) p 16 N85-30447
- SHCHEVYAKOV, Y.**
Spacecraft-aided research discussed at geology Congress p 22 N85-33147
- SHESTOPALOV, V. P.**
Propagation and diffraction of radio waves in the millimeter and submillimeter ranges p 9 A85-46076
- SHIBAYAMA, M.**
View azimuth and zenith, and solar angle effects on wheat canopy reflectance p 2 A85-43120
- SHIFRIN, K. S.**
Model computations of light reflection from sea surface p 31 N85-30411
- SHIN, R. T.**
Theory of microwave remote sensing p 42 A85-40792
- SIDERIS, M. G.**
A fast Fourier transform method for computing terrain corrections p 37 A85-41396
- SILVERMAN, S. A.**
Secular variation, crustal contributions, and tectonic activity in California, 1976-1984 p 15 A85-47898
- SIMARD, R.**
Multiple sensor geocoded data p 38 A85-45695
- SIMHONY, S.**
Measurement and analysis of 2-D infrared natural background p 37 A85-42511
- SIMMER, C.**
Remote sensing of angular characteristics of canopy reflectances p 3 A85-49105
- SIMON, B.**
A survey of the Rehamna Hercynian Range in western Morocco using Landsat color composite imagery p 15 A85-42582
- SIMPSON, T. R.**
The Space Station An idea whose time has come p 50 A85-42223
- SINGER, D. A.**
Some recent deposit modeling efforts p 23 N85-35453
- SINGH, A.**
Standardized principal components p 37 A85-41660
- SINITSYN, I. U. A.**
Modeling of radio-wave scattering by ice cover p 30 A85-49477
- SKLAVIDIS, A. I.**
Coastal erosion along Monterey Bay [AD-A155610] p 34 N85-32707
- SLATER, P. N.**
Spectroradiometric calibration of the Thematic Mapper and Multispectral Scanner system [E85-10104] p 47 N85-31601
- SMIGIELSKI, F. J.**
Surface cyclogenesis as indicated by satellite imagery [PB85-191815] p 42 N85-35566
- SMIRNOV, M. V.**
Discrimination of linear contour elements of space photographs based on visual perception model p 13 N85-33161

SMIRNOV, V. V.

The variability of aerosol microstructure in continental and oceanic surface layers of the atmosphere in anticyclones p 34 N85-32660

SMITH, D. E.

Geodetic and geophysical results from Lageos p 7 A85-40003
Contemporary plate motions from LAGEOS p 19 N85-31689
Ocean tidal parameters from LAGEOS p 32 N85-31716

SMITH, D. J.

The ERS-1 synthetic aperture radar and scatterometer p 45 A85-46849

SMITH, F. L.

Engineering geology of selected areas, US army engineer division, lower Mississippi valley The American bottom area, MO-IL Volume 1 [AD-A154258] p 17 N85-30455

SMITH, J. A.

A Monte Carlo reflectance model for soil surfaces with three-dimensional structure p 3 A85-49107

SMITH, L. M.

Engineering geology of selected areas, US army engineer division, lower Mississippi valley The American bottom area, MO-IL Volume 1 [AD-A154258] p 17 N85-30455

SPENCER, R. W.

Measuring the global distribution of intense convection over land with passive microwave radiometry p 36 A85-47923

SPIELMAN, J. B.

Comparison of survey and photogrammetry methods to position gravity data, Yucca Mountain, Nevada [DE85-011685] p 13 N85-32316

SPINHIRNE, J. D.

Lidar observations of vertically organized convection in the planetary boundary layer over the ocean p 30 A85-47921

SPIRIDONOV, I. U. G.

Ordered mesoscale structures on the ocean surface identified from satellite radar data p 28 A85-46257
Radar maps of the Arctic and Antarctic compiled on the basis of Cosmos-1500 satellite data, and preliminary results of their analysis p 29 A85-46259
Digital processing of radar images obtained with the Cosmos-1500 satellite p 29 A85-46266

STACEY, J.

Microwave properties of a quiet sea [NASA-CR-176199] p 35 N85-35322

STACEY, J. M.

Microwave hydrology: A trilogy [NASA-CR-176042] p 36 N85-31603

STACY, K.

Spectral reflectances of natural targets for use in remote sensing studies [NASA-RP-1139] p 41 N85-30450

STARICH, P. J.

The south-central United States magnetic anomaly p 17 N85-31591
The south-central United States magnetic anomaly p 18 N85-31592

STERN, M.

Estimation of rural population in Kordofan, Sudan p 6 A85-42579

STEVEN, T. A.

Aeromagnetic and radiometric signatures of a possible porphyry system in the western Tushar Mountains, Utah p 23 N85-35437

STEWART, R. G.

Solid-state spectral transmissometer and radiometer p 30 A85-48670

STRAHLER, A. H.

Geometric-optical modeling of a conifer forest canopy p 4 A85-49111

STREBEL, D. E.

Two-dimensional leaf orientation distributions p 2 A85-49104

STROME, W. M.

The scientific and technical issues in integrating remotely sensed imagery with geocoded data bases p 41 N85-34547

SUESS, H.

Signature measurements using cooled microwave radiometers at frequencies from 90 GHz to 140 GHz p 43 A85-41571

SUETIN, V. S.

Identification of eddy formations in a radar image of the ocean surface p 28 A85-46256
Automated processing of remote-sensing data obtained with the microwave radiometer of the Cosmos-1500 satellite p 29 A85-46265

SUN, C.-L.

Message collision of data collection system and its computer simulation p 46 A85-48894

SUN, J. T.

USGS coastal research, studies and maps A source of information for coastal decision making [USGS-CIRC-883] p 35 N85-35465

SUSHKEVICH, T. A.

The determination of the albedo of natural covers of the earth on the basis of remote measurement results p 10 A85-46132

SUTPHIN, D. M.

Applications of the mineral resources data system and the international strategic minerals inventory in mineral-resource assessments by region and commodity p 23 N85-35451

SZAJNA, E. F.

Nimbus 7 Coastal Zone Color Scanner (CZCS) Level 2 data product users' guide [NASA-TM-86202] p 31 N85-30452

Nimbus 7 Coastal Zone Color Scanner (CZCS) Level 1 data product users' guide [NASA-TM-86203] p 31 N85-30453

SZEJWACH, G.

A new technique for inferring surface albedo from satellite observations p 46 A85-47916

T

TAMKOVICH, G. M.

Program of experiments on the Cosmos-1500 satellite p 28 A85-46251

TAPLEY, B. D.

Polar motion measurements - Subdecimeter accuracy verified by intercomparison p 16 A85-48873

TARANIK, J. V.

Evaluation of SPOT simulator data for the detection of alteration in Goldfield/Cuprite, Nevada p 15 A85-45873

TAYLOR, P. T.

The magnetic field of the earth - Performance considerations for space-based observing systems p 9 A85-42474

TEILLET, P. M.

Multiple sensor geocoded data p 38 A85-45695

TEREKHIN, I. U. V.

Identification of eddy formations in a radar image of the ocean surface p 28 A85-46256

THOMSON, R. E.

A wind-induced mesoscale eddy over the Vancouver Island continental slope p 30 A85-49863

THORNDIKE, A. S.

Dispersion of sea ice in the Bering Sea p 26 A85-42257

TIKHONOV, V. V.

Optical-physical methods for the study of the ocean p 26 A85-42134

TILTON, J. C.

Landsat-4 and Landsat-5 MSS coherent noise - Characterization and removal p 45 A85-47805

TIMCHENKO, A. I.

Modeling of radio-wave scattering by ice cover p 30 A85-49477

TINSLEY, E. J.

Worldwide directory of national Earth-science agencies and related international organizations [GS-CIRC-934] p 50 N85-32386

TOLL, D.

Performance comparisons between information extraction techniques using variable spatial resolution data p 40 A85-47823

TOLL, D. L.

Landsat-4 Thematic Mapper scene characteristics of a suburban and rural area p 40 A85-46424

TORRENCE, M. H.

Geodetic and geophysical results from Lageos p 7 A85-40003

TOWNSHEND, J. R. G.

Improving Thematic Mapper land cover classification using filtered data p 37 A85-41664

TREPTE, C. R.

Variation in the stratospheric aerosol associated with the North Cyclonic Polar Vortex as measured by the SAM II satellite sensor p 45 A85-46424

TRIVERO, P.

The impact of higher-order Bragg terms on radar sea return p 24 A85-40237

TSANG, L.

Theory of microwave remote sensing p 42 A85-40792

TSUCHIYA, K.

Verification studies of MOS-1 sensors p 44 A85-45696

TSYMBAL, V. N.

Informational potential of the sidelooking radar of the Cosmos-1500 satellite p 29 A85-46263

TUCKER, C. J.

Directional reflectance factor distributions for cover types of Northern Africa p 1 A85-43114

TWIDALE, C. R.

Landscape inheritance Report of Working Group Number 2 p 21 N85-32383

U

ULABY, F. T.

Microwave attenuation properties of vegetation canopies p 4 A85-49115

UNGAR, S. G.

The earth's surface studied from space, Proceedings of Workshop II of the COSPAR 25th Plenary Meeting, Graz, Austria, June 25-July 7, 1984 p 50 A85-45686

USIKOV, D. A.

Impact of fluctuations in optical properties of atmosphere on the ratio of spectral brightness from remote sensing of agricultural land p 5 N85-33149

USPENSKIY, A. B.

Enhancing precision of remote temperature sensing data from satellites under cloudy atmospheric conditions p 48 N85-33148

UVAROV, A. D.

The variability of aerosol microstructure in continental and oceanic surface layers of the atmosphere in anticyclones p 34 N85-32660

V

VAFIN, R. F.

Use of space photographs for analysis of structural and dynamic conditions of formation of ancient phlogopite and apatite deposits p 22 N85-33153

VAN WIJNGAARDEN, W.

Directional reflectance factor distributions for cover types of Northern Africa p 1 A85-43114

VANDERBILT, V. C.

Specular, diffuse, and polarized light scattered by two wheat canopies p 1 A85-42865
Plant canopy specular reflectance model p 4 A85-49112

VASILYEV, V.

Aerospace technology determines forest-fire danger p 5 N85-30427

VASS, T.

Preliminary results of Finnish-Hungarian Doppler Observation Campaign /FHDOC/ p 8 A85-41199

VAUCLIN, M.

Influence of spatial variability of hydraulic characteristics of soils on surface parameters obtained from remote sensing data in infrared and microwaves [NASA-TM-77902] p 5 N85-31604

VINOGRADOV, B. V.

Aerial and space-based remote sensing in ecological prognosis p 6 A85-46249

VONDERHAAR, T. H.

Rain volume estimation over areas using satellite and radar data [NASA-CR-176050] p 36 N85-32570

VONFRESE, R. R. B.

Improving the geological interpretation of magnetic and gravity satellite anomalies [E85-10103] p 11 N85-31585

Geologic analysis of averaged magnetic satellite anomalies p 17 N85-31588

Statistical magnetic anomalies from satellite measurements for geologic analysis p 17 N85-31589

Binning of satellite magnetic anomalies p 11 N85-31590

A comparative study of spherical and flat-Earth geopotential modeling at satellite elevations p 11 N85-31593

Reduced to pole long-wavelength magnetic anomalies of Africa and Europe p 18 N85-31595

Euro-African MAGSAT anomaly-tectonic observations p 18 N85-31596

Long-wavelength magnetic and gravity anomaly correlations on Africa and Europe p 12 N85-31597

Continental and oceanic magnetic anomalies Enhancement through GRM p 32 N85-31598

Continental magnetic anomaly constraints on continental reconstruction p 12 N85-31599

Regional magnetic anomaly constraints on continental rifting p 12 N85-31600

VOSTOKOVA, E. A.

The USSR as viewed from space p 50 A85-48524

W

WALKER, A. S.

Large format camera photographs A new tool for understanding and environments p 47 N85-32379

- WALKER, R. E.**
An analysis of Landsat Thematic Mapper P-Product internal geometry and conformity to earth surface geometry p 40 A85-47821
- WALTER, E. A.**
Contrasts among bidirectional reflectance of leaves, canopies, and soils p 3 A85-49106
- WALTER, L. S.**
Satellite geodynamics p 8 A85-42451
- WALTHALL, C. L.**
Modeling the radiant transfers of sparse vegetation canopies p 3 A85-49110
- WALTON, C.**
Satellite measurement of sea surface temperature in the presence of volcanic aerosols p 25 A85-41993
- WANG, C.-S.**
The selection of optimum spectral channels for multispectral remote sensing p 43 A85-42484
- WANG, Z.**
Remote sensing of temperature profiles from a combination of observations from the satellite-based Microwave Sounding Unit and the ground-based Profiler p 43 A85-42292
- WARNER, I. M.**
A microprocessor-controlled, multichannel fluorimeter for analysis of sea water [AD-A154986] p 33 N85-32310
- WEBSTER, W. J., JR.**
The magnetic field of the earth - Performance considerations for space-based observing systems p 9 A85-42474
- WELCH, C. S.**
Wave refraction by warm core rings p 26 A85-42254
- WELCH, R.**
Cartographic potential of SPOT image data p 9 A85-45870
Comparative evaluations of the geodetic accuracy and cartographic potential of Landsat-4 and Landsat-5 Thematic Mapper image data p 10 A85-47804
- WELKER, J. E.**
SEASAT altimetry for surface height of inland seas p 32 N85-31714
- WELLES, J. M.**
Contrasts among bidirectional reflectance of leaves, canopies, and soils p 3 A85-49106
- WESTWATER, E. R.**
Remote sensing of temperature profiles from a combination of observations from the satellite-based Microwave Sounding Unit and the ground-based Profiler p 43 A85-42292
- WIEGAND, C. L.**
View azimuth and zenith, and solar angle effects on wheat canopy reflectance p 2 A85-43120
- WILLIAMS, D.**
Performance comparisons between information extraction techniques using variable spatial resolution data p 40 A85-47823
- WILLIAMS, R. S., JR.**
Geomorphic classification of Icelandic and Martian volcanoes Limitations of comparative planetology research from LANDSAT and Viking orbiter images p 20 N85-32372
Quantitative analysis of geomorphic processes using satellite image data at different scales p 21 N85-32380
Quantitative geomorphologic studies from spaceborne platforms p 21 N85-32381
Process thresholds Report of Working Group Number 3 p 21 N85-32384
- WILLIAMS, S. P.**
Nimbus 7 Coastal Zone Color Scanner (CZCS) Level 2 data product users' guide [NASA-TM-86202] p 31 N85-30452
Nimbus 7 Coastal Zone Color Scanner (CZCS) Level 1 data product users' guide [NASA-TM-86203] p 31 N85-30453
- WILNER, K.**
Measurement and analysis of 2-D infrared natural background p 37 A85-42511
- WILSON, A.**
Improving Thematic Mapper land cover classification using filtered data p 37 A85-41664
- WILSON, E. A.**
Microwave attenuation properties of vegetation canopies p 4 A85-49115
- WILSON, F. H.**
Processing of LANDSAT imagery to map surface mineral alteration on the Alaska Peninsula, Alaska p 23 N85-35455
- WINDLEY, B. F.**
The evolving continents /2nd revised and enlarged edition/ p 50 A85-42220
- WINKLER, G. R.**
The Alaska Mineral Resources Assessment Program p 24 N85-35460
- WISEMAN, W. J., JR.**
Satellite observations of the circulation east of the Mississippi Delta - Cold-air outbreak conditions p 27 A85-43117
- WRIGLEY, R. C.**
Landsat Thematic Mapper image-derived MTF p 39 A85-47817
Evaluation of Thematic Mapper interband registration and noise characteristics p 46 A85-47819
- WU, L.-K.**
Sources of scattering from vegetation canopies at 10 GHz p 4 A85-49114
- WU, S. S. C.**
Comparison of survey and photogrammetry methods to position gravity data, Yucca Mountain, Nevada [DE85-011685] p 13 N85-32316

Y

- YAZAKI, S.**
Eruption of Mount Ontake in 1979 - Detection of volcanic ash fall area from Landsat MSS CCT data p 15 A85-42583
- YEFREMOVA, O. N.**
Mapping of dynamics of deltas by space photography p 14 N85-33163
- YEH, C.-L.**
Restoration of multichannel microwave radiometric images p 42 A85-41089
- YIÖNOULIS, S. M.**
Geopotential Research Mission - Status report p 8 A85-42469
- YORK, J. E.**
Processing of LANDSAT imagery to map surface mineral alteration on the Alaska Peninsula, Alaska p 23 N85-35455

Z

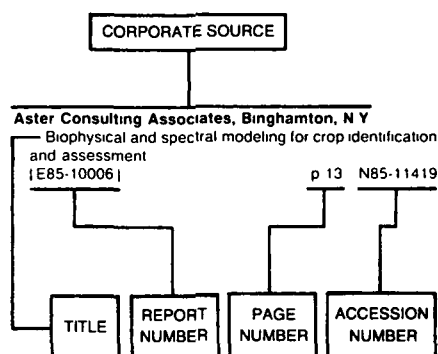
- ZAITSSEV, V. A.**
Optical-physical methods for the study of the ocean p 26 A85-42134
- ZAMARAEV, B. D.**
Specific effective scattering surfaces of certain terrains in the millimeter wave band p 10 A85-46081
- ZAPIVALOV, N. P.**
Reflections of possible oil- and gas-bearing structures of the pre-Jurassic complex in the present-day terrain of Western Siberia p 16 A85-48387
- ZINATOV, K. G.**
Use of space photographs for analysis of structural and dynamic conditions of formation of ancient phlogopite and apatite deposits p 22 N85-33153
- ZOBRIST, A. L.**
An analysis of Landsat Thematic Mapper P-Product internal geometry and conformity to earth surface geometry p 40 A85-47821
- ZONNEVELD, I. S.**
Directional reflectance factor distributions for cover types of Northern Africa p 1 A85-43114
- ZOUGH, R.**
Sources of scattering from vegetation canopies at 10 GHz p 4 A85-49114
- ZUBENKO, V. F.**
The experimental oceanographic satellite Cosmos-1500 p 30 A85-46267

CORPORATE SOURCE INDEX

EARTH RESOURCES / A Continuing Bibliography (Issue 48)

JANUARY 1986

Typical Corporate Source Index Listing



Listings in this index are arranged alphabetically by corporate source. The title of the document is used to provide a brief description of the subject matter. The page number and the accession number are included in each entry to assist the user in locating the abstract in the abstract section. If applicable, a report number is also included as an aid in identifying the document.

A

Air Force Geophysics Lab., Hanscom AFB, Mass.

Comparison of mesospheric ozone measurements using the LRIR and UVMCS satellite instruments p 46 A85-50022

Global geoid and gravity anomaly predictions using the collocation and point mass techniques [AD-A154517] p 13 N85-32387

Application of satellite accelerometer data to improve density models [AD-A154904] p 48 N85-32558

Arizona Univ., Tucson.

Landsat Thematic Mapper image-derived MTF p 39 A85-47817

Spectroradiometric calibration of the Thematic Mapper and Multispectral Scanner system [E85-10104] p 47 N85-31601

A new global geomorphology? p 19 N85-32358

Army Engineer Waterways Experiment Station, Vicksburg, Miss.

Engineering geology of selected areas, US army engineer division, lower Mississippi valley The American bottom area, MO-IL Volume 1 [AD-A154258] p 17 N85-30455

Handbook for obtaining and using aerial photography to map aquatic plant distribution [AD-A154584] p 33 N85-32388

Army Military Personnel Center, Alexandria, Va.

Microcomputer processing of LANDSAT Thematic Mapper data for the acquisition of military tactical terrain data [AD-A154781] p 47 N85-32389

Atmospheric and Environmental Research, Inc., Cambridge, Mass.

Strong fluctuation theory for scattering, attenuation, and transmission of microwaves through snowfall p 36 A85-49116

B

Bonn Univ. (West Germany).

Motor glider measurements during the Urban Atmosphere Energy Budget Experiment (EESA 1) p 7 N85-35553

Bureau of Reclamation, Denver, Colo.

Project Skywater, 1983-84 SCPP (Sierra Cooperative Pilot Project) data inventory [PB85-187052] p 49 N85-35565

C

California Univ., Berkeley.

Evaluation of Thematic Mapper data for mapping forest, agricultural and soil resources p 2 A85-45690
Interpretation of Landsat-4 Thematic Mapper and Multispectral Scanner data for forest surveys p 2 A85-47806

California Univ., Davis.

Evaluation of Thematic Mapper data for mapping forest, agricultural and soil resources p 2 A85-45690

Canada Land Data Systems, Ottawa (Ontario).

Applied computer graphics in a geographic information system Problems and successes p 6 N85-34563

Centre National d'Etudes Spatiales, Toulouse (France).

Results of the MIZEX preliminary campaign 29 June to 19 July 1983 [CNES-84/142/T/CT/DRT/TIT/R] p 32 N85-31609

The French space program p 50 N85-33127

Centre National de la Recherche Scientifique, Verrieres-Le Buisson (France).

Comparison of mesospheric ozone measurements using the LRIR and UVMCS satellite instruments p 46 A85-50022

Chevron Oil Field Research Co., La Habra, Calif.

Geomorphology, tectonics, and exploration p 19 N85-32365

Colorado State Univ., Fort Collins.

A Monte Carlo reflectance model for soil surfaces with three-dimensional structure p 3 A85-49107
Rain volume estimation over areas using satellite and radar data [NASA-CR-176050] p 36 N85-32570
Properties of aerosol particles detected by satellites in coastal regions p 34 N85-32622

Committee on Commerce, Science, and Transportation (U. S. Senate).

Antarctica [S-HRG-98-1181] p 50 N85-31584

Computer Sciences Corp., Hampton, Va.

Spectral reflectances of natural targets for use in remote sensing studies [NASA-RP-1139] p 41 N85-30450

Cornell Univ., Ithaca, N.Y.

Andean examples of mega-geomorphology themes p 20 N85-32367

D

Dennett, Muessing, Ryan and Associates Ltd., Iowa City, Iowa

Evaluation Close-range photogrammetry for slope inventory and monitoring [PB85-192755] p 24 N85-35470

Department of Energy, Morgantown, W. Va.

Arctic and offshore research [DE85-001995] p 34 N85-33653

Deutsche Forschungs- und Versuchsanstalt fuer Luft- und Raumfahrt, Oberpfaffenhofen (West Germany).

Proceedings of Meteorological Motor Glider (MEMO) Workshop '84 [DFVLR-MITT-85-04] p 7 N85-35542

E

Eastman Kodak Co., Rochester, N. Y.

Restoration of multichannel microwave radiometric images p 42 A85-41089

EG and G Energy Measurements, Inc., Las Vegas, Nev

Remote Sensing Technology Symposium Proceedings [DE85-010212] p 47 N85-31606

EG & G Washington Analytical Services Center, Inc., Riverdale, Md.

Geodetic and geophysical results from Lageos p 7 A85-40003

Eidgenossisches Inst. fuer Reaktorforschung, Wuerenlingen (Switzerland).

Environmental-physical measurements and determination of atmospheric turbulence with the ASK-16 motor glider p 7 N85-35549

Emory Univ., Atlanta, Ga.

A microprocessor-controlled, multichannel fluorometer for analysis of sea water [AD-A154986] p 33 N85-32310

Environmental Research Inst. of Michigan, Ann Arbor.

Characterization and comparison of Landsat-4 and Landsat-5 Thematic Mapper data p 39 A85-47809
Comparison of the information contents of Landsat TM and MSS data p 40 A85-47822
Study of spectral/radiometric characteristics of the Thematic Mapper for land use applications [E85-10106] p 42 N85-35464

European Space Agency, Paris (France).

Preliminary investigations concerning a 90 GHz radiometer satellite experiment [ESA-TT-860] p 46 N85-31225

F

Farran Research Associates, Farnham (Ireland).

Millimetre wave pulse technology [ESA-CR(P)-2004] p 47 N85-31611

Fort Lewis A&M Coll., Durango, Colo.

One application of mega-geomorphology in education p 6 N85-32370

G

General Electric Co., Lanham, Md.

Methods for destriping Landsat Thematic Mapper images - A feasibility study for an online destriping process in the Thematic Mapper Image Processing System (TIPS) p 39 A85-47813

Geological Survey, Alexandria, Va.

Aeromagnetic and radiometric signatures of a possible porphyry system in the western Tushar Mountains, Utah p 23 N85-35437

Marine phosphonate deposits model for exploration, with emphasis on deposits in the US Atlantic coastal plain p 35 N85-35439

Aeromagnetic and gravity models of the pluton below the Lake City caldera, Colorado p 23 N85-35442
New silver resource map of the United States Potential for increased domestic silver production p 23 N85-35445

Applications of the mineral resources data system and the international strategic minerals inventory in mineral-resource assessments by region and commodity p 23 N85-35451

A comparison of LANDSAT thematic mapper, multispectral scanner and airborne sensors for mapping the distribution of alteration minerals Examples from the southwestern United States p 23 N85-35452
Some recent deposit modeling efforts p 23 N85-35453

Processing of LANDSAT imagery to map surface mineral alteration on the Alaska Peninsula, Alaska p 23 N85-35455

Mineral resources programs p 24 N85-35456

The development of assessment techniques program p 24 N85-35457

The Conterminous United States Mineral Assessment Program p 24 N85-35458

Federal Mineral Land Information System p 7 N85-35459

The Alaska Mineral Resources Assessment Program p 24 N85-35460

Geological Survey, Flagstaff, Ariz.

Geological Survey, Flagstaff, Ariz.

Use of the synoptic view Examples from Earth and other planets p 20 N85-32371

Geological Survey, Menlo Park, Calif.

Comparison of survey and photogrammetry methods to position gravity data, Yucca Mountain, Nevada [DE85-011685] p 13 N85-32316

Geological Survey, Reston, Va.

Geomorphic classification of Icelandic and Martian volcanoes Limitations of comparative planetology research from LANDSAT and Viking orbiter images p 20 N85-32372

Large format camera photographs A new tool for understanding and environments p 47 N85-32379

Quantitative analysis of geomorphic processes using satellite image data at different scales p 21 N85-32380

Quantitative geomorphologic studies from spaceborne platforms p 21 N85-32381

Geological Survey, Washington, D.C.

Petroleum and mineral resources of Antarctica [US-GEOL-SURV-CIRC-909] p 18 N85-31605

The U.S. Geological Survey in Alaska Accomplishments during 1982 [US-GEOL-SURV-CIRC-939] p 19 N85-31719

Worldwide directory of national Earth-science agencies and related international organizations [GS-CIRC-934] p 50 N85-32386

The United States Geological Survey in Alaska. Accomplishments during 1983 [USGS-CIRC-945] p 23 N85-34468

USGS coastal research, studies and maps A source of information for coastal decision making [USGS-CIRC-883] p 35 N85-35465

George Mason Univ., Fairfax, Va.

Geomorphological similarity and uniqueness p 19 N85-32361

George Washington Univ., Washington, D.C.

Microwave inversion of leaf area and inclination angle distributions from backscattered data p 3 A85-49109

Georgia Univ., Athens.

Cartographic potential of SPOT image data p 9 A85-45870

Comparative evaluations of the geodetic accuracy and cartographic potential of Landsat-4 and Landsat-5 Thematic Mapper image data p 10 A85-47804

H

Hughes Aircraft Co., El Segundo, Calif.

Six mechanisms used on the SSM/1 radiometer p 49 N85-33534

Hunter Coll., New York.

Geometric-optical modeling of a conifer forest canopy p 4 A85-49111

I

Illinois Univ., Chicago.

A comparison between active and passive sensing of soil moisture from vegetated terrains p 4 A85-49118

Institute for Atmospheric Optics and Remote Sensing, Hampton, Va.

Variation in the stratospheric aerosol associated with the North Cyclonic Polar Vortex as measured by the SAM II satellite sensor p 45 A85-46424

Data analysis for lidar and quartz crystal microbalance systems [NASA-CR-172601] p 47 N85-32464

Institute of Experimental Meteorology (USSR).

The variability of aerosol microstructure in continental and oceanic surface layers of the atmosphere in anticyclones p 34 N85-32660

International Inst. for Aerial Survey and Earth Sciences, Enschede (Netherlands).

Directional reflectance factor distributions for cover types of Northern Africa p 1 A85-43114

J

Jet Propulsion Lab., California Inst. of Tech., Pasadena.

A water-vapor radiometer error model p 8 A85-42464

Preliminary spectral and geologic analysis of Landsat-4 Thematic Mapper data, Wind River Basin area, Wyoming p 15 A85-42476

Lasers in space An analysis of Landsat Thematic Mapper P-Product internal geometry and conformity to earth surface geometry p 40 A85-47821

Microwave hydrology A trilogy [NASA-CR-176042] p 36 N85-31603

Tropical Ocean and Global Atmosphere (TOGA) heat exchange project A summary report [NASA-CR-176038] p 33 N85-31738

Use of spaceborne imaging radar in regional geomorphic studies p 20 N85-32377

Large-scale sea surface temperature variability from satellite and shipboard measurements [NASA-CR-176123] p 34 N85-33651

Method and apparatus for Delta Kappa synthetic aperture radar measurement of ocean current [NASA-CASE-NPO-15704-1] p 35 N85-34327

Microwave properties of a quiet sea [NASA-CR-176199] p 35 N85-35322

Model computations of light reflection from sea surface p 31 N85-30411

Discovery in earthquake forecasting and seismic zoning recorded p 16 N85-30426

Aerospace technology determines forest-fire danger p 5 N85-30427

Space methods for geological research p 16 N85-30429

Conditions for formation of parageneses containing kyanite-orthoclase in region of Mount Proveder and Pratt Peak (Shackleton Range, Antarctica) p 16 N85-30447

Highly important features of regional tectonics of Earth's Arctic sector p 17 N85-30449

Cosmonauts participate in multilevel remote sensing experiment p 48 N85-33130

Spacecraft-aided research discussed at geology Congress p 22 N85-33147

Enhancing precision of remote temperature sensing data from satellites under cloudy atmospheric conditions p 48 N85-33148

Impact of fluctuations in optical properties of atmosphere on the ratio of spectral brightness from remote sensing of agricultural land p 5 N85-33149

Determination of altitude of cloud cover top from Meteor satellite data p 48 N85-33150

Landscape interpretation capabilities using space photographs of regions of a multistage platform mantle structure p 22 N85-33151

Interpretation of multiband photographs made during Telefoto-80 experiment for the purpose of discriminating agricultural crops p 5 N85-33152

Use of space photographs for analysis of structural and dynamic conditions of formation of ancient phlogopite and apatite deposits p 22 N85-33153

Using remote photographs in prospecting for hydrocarbons on the Kerch Peninsula p 22 N85-33154

Cataloging the spectral brightness coefficients of the forested region of the European territory of the USSR p 5 N85-33155

Regression analysis of aircraft and ground measurement data on vegetation cover p 5 N85-33156

Interactive procedures for discriminating and restoring contour line networks p 41 N85-33158

Terrain illumination conditions when taking scanning photographs from space p 48 N85-33159

Calculating solar highlight and shadeless areas for scanning photographs from space and optimizing lighting conditions p 49 N85-33160

Discrimination of linear contour elements of space photographs based on visual perception model p 13 N85-33161

Physico-geographical regionalization of Caspian lowland based on space survey materials p 14 N85-33162

Mapping of dynamics of deltas by space photography p 14 N85-33163

Comprehensive mapping of and territories of Arizona using space photography p 14 N85-33164

Repetition of dense cloud cover above Indian Ocean from generalized satellite data p 41 N85-33165

Basic properties and interpretation of synthesized radar images of sea waves with long synthesis time p 34 N85-33384

K

Kansas Univ. Center for Research, Inc., Lawrence.

Sources of scattering from vegetation canopies at 10 GHz p 4 A85-49114

L

Lockheed Engineering and Management Services Co., Inc., Houston, Tex.

Inclusion of specular reflectance in vegetative canopy models p 4 A85-49113

London Univ. (England).

Techniques, problems and uses of mega-geomorphological mapping p 21 N85-32378

CORPORATE SOURCE

M

Maryland Univ., Baltimore.

The atmospheric effect on the separability of field classes measured from satellites p 44 A85-43115

Maryland Univ., College Park.

Shortwave infrared detection of vegetation p 2 A85-45691

Massachusetts Inst. of Tech., Cambridge.

Theory of microwave remote sensing p 42 A85-40792

Strong fluctuation theory for scattering, attenuation, and transmission of microwaves through snowfall p 36 A85-49116

Active and passive remote sensing of ice [AD-A154406] p 31 N85-30459

Miami Univ., Fla.

Small-scale cyclones on the periphery of a Gulf Stream warm-core ring p 30 A85-49855

N

National Aeronautics and Space Administration,

Washington, D. C.

Influence of spatial variability of hydraulic characteristics of soils on surface parameters obtained from remote sensing data in infrared and microwaves [NASA-TM-77902] p 5 N85-31604

National Aeronautics and Space Administration, Ames

Research Center, Moffett Field, Calif. Landsat Thematic Mapper image-derived MTF p 39 A85-47817

Evaluation of Thematic Mapper interband registration and noise characteristics p 46 A85-47819

National Aeronautics and Space Administration,

Goddard Inst. for Space Studies, New York.

The earth's surface studied from space, Proceedings of Workshop II of the COSPAR 25th Plenary Meeting, Graz, Austria, June 25-July 7, 1984 p 50 A85-45686

National Aeronautics and Space Administration,

Goddard Space Flight Center, Greenbelt, Md.

Geodetic and geophysical results from Lageos p 7 A85-40003

Satellite geodynamics p 8 A85-42451

Space-age geodesy - The NASA Crustal Dynamics Project p 8 A85-42452

The magnetic field of the earth - Performance considerations for space-based observing systems p 9 A85-42474

Directional reflectance factor distributions for cover types of Northern Africa p 1 A85-43114

The atmospheric effect on the separability of field classes measured from satellites p 44 A85-43115

Sensor-induced temporal variability of Landsat MSS data p 44 A85-43116

A global climatology of total ozone from the Nimbus 7 total ozone mapping spectrometer p 44 A85-45235

Landsat image data quality studies p 38 A85-45687

Landsat-4 and Landsat-5 MSS coherent noise - Characterization and removal p 45 A85-47805

Performance comparisons between information extraction techniques using variable spatial resolution data p 40 A85-47823

Landsat-4 Thematic Mapper scene characteristics of a suburban and rural area p 40 A85-47824

Lidar observations of vertically organized convection in the planetary boundary layer over the ocean p 30 A85-47921

Evaluation of a canopy reflectance model for LAI estimation through its inversion p 3 A85-49108

Modeling the radiant transfers of sparse vegetation canopies p 3 A85-49110

Comparison of mesospheric ozone measurements using the LRIR and UVMCS satellite instruments p 46 A85-50022

MIZEX, 1984, NASA CV-990 flight report [NASA-TM-86216] p 31 N85-30451

Nimbus 7 Coastal Zone Color Scanner (CZCS) Level 2 data product users' guide [NASA-TM-86202] p 31 N85-30452

Nimbus 7 Coastal Zone Color Scanner (CZCS) Level 1 data product users' guide [NASA-TM-86203] p 31 N85-30453

Geodynamics Branch research program [NASA-TM-86223] p 18 N85-31688

Contemporary plate motions from LAGEOS p 19 N85-31689

The global VLBI fiducial network p 12 N85-31690

First epoch measurements by Mark III VLBI of the San Andreas Fault experiment baseline p 12 N85-31691

Geophysical interpretation of satellite laser ranging measurements p 19 N85-31692

Satellite-determined stresses in the crust of Europe with particular consideration to the Liege earthquake of November 8, 1983 p 13 N85-31694

- Spaceborne gradiometer error analysis p 13 N85-31707
- Geodyn systems development p 13 N85-31708
- Global mean sea surface based upon a combination of the GEOS-3 and SEASAT altimeter data p 32 N85-31710
- Ocean circulation studies p 32 N85-31712
- SEASAT altimetry for surface height of inland seas p 32 N85-31714
- Ocean tidal parameters from LAGEOS p 32 N85-31716
- TOPEX error budget p 47 N85-31717
- Global Mega-Geomorphology [NASA-CP-2312] p 19 N85-32357
- Global geomorphology Report of Working Group Number 1 p 21 N85-32382
- Landscape inheritance Report of Working Group Number 2 p 21 N85-32383
- Process thresholds Report of Working Group Number 3 p 21 N85-32384
- Planetary perspective Report of Working Group Number 4 p 22 N85-32385
- Crustal Dynamics Project Catalogue of site information [NASA-TM-86218] p 14 N85-33552
- National Aeronautics and Space Administration.**
- Johnson (Lyndon B.) Space Center,**
- Inclusion of specular reflectance in vegetative canopy models p 4 A85-49113
- National Aeronautics and Space Administration.**
- Langley Research Center, Hampton, Va.**
- The albedo field and cloud radiative forcing produced by a general circulation model with internally generated cloud optics p 27 A85-43373
- Variation in the stratospheric aerosol associated with the North Cyclonic Polar Vortex as measured by the SAM II satellite sensor p 45 A85-46424
- Spectral reflectances of natural targets for use in remote sensing studies [NASA-RP-1139] p 41 N85-30450
- National Aeronautics and Space Administration.**
- Pasadena Office, Calif.**
- Method and apparatus for Delta Kappa synthetic aperture radar measurement of ocean current [NASA-CASE-NPO-15704-1] p 35 N85-34327
- National Center for Atmospheric Research, Boulder, Colo.**
- Comparison of mesospheric ozone measurements using the LRIR and UVMCS satellite instruments p 46 A85-50022
- National Environmental Satellite Service, Washington, D. C.**
- Space Station Polar Platform Integrating research and operational missions [PB85-195279] p 49 N85-35218
- National Oceanic and Atmospheric Administration, Washington, D. C.**
- Surface cyclogenesis as indicated by satellite imagery [PB85-191815] p 42 N85-35566
- National Research Council of Canada, Ottawa (Ontario).**
- Selection of segment similarity measures for hierarchical picture segmentation p 41 N85-34548
- Naval Ocean Systems Center, San Diego, Calif.**
- Using ship wake patterns to evaluate SAR (Synthetic Aperture Radar) ocean wave imaging mechanisms Joint US-Canadian Ocean Wave Investigation Project [AD-A154633] p 33 N85-32223
- Naval Postgraduate School, Monterey, Calif.**
- Mesoscale features and atmospheric refraction conditions of the Arctic marginal ice zone [AD-A155139] p 33 N85-32584
- Coastal erosion along Monterey Bay [AD-A155610] p 34 N85-32707
- Target observability for satellite-based sensors [AD-A156139] p 49 N85-35217
- Nebraska Univ., Lincoln.**
- Contrasts among bidirectional reflectance of leaves, canopies, and soils p 3 A85-49106
- Modeling the radiant transfers of sparse vegetation canopies p 3 A85-49110
- New Mexico Inst. of Mining and Technology, Socorro.**
- Mega-geomorphology and neotectonics p 20 N85-32366
- New York State Univ., Syracuse.**
- Comments on the intercalibration of multisensor, multitemporal, multichannel digital radiance data p 38 A85-42853

O

- Statistical magnetic anomalies from satellite measurements for geologic analysis p 17 N85-31589
- Binning of satellite magnetic anomalies p 11 N85-31590
- Long-wavelength magnetic and gravity anomaly correlations on Africa and Europe p 12 N85-31597
- Continental and oceanic magnetic anomalies Enhancement through GRM p 32 N85-31598
- Continental magnetic anomaly constraints on continental reconstruction p 12 N85-31599
- Regional magnetic anomaly constraints on continental rifting p 12 N85-31600

P

- Pacific Northwest Lab., Richland, Wash**
- Comparative study of fracture planes computed from topography and lineaments from imagery with structures and mineralization in the magnetic belt of Washington State [DE85-010972] p 18 N85-31608
- Pennsylvania State Univ., University Park.**
- Remote sensing of hydrologic transport processes using spot simulation data [DE85-012412] p 37 N85-35467
- Pennsylvania Univ., Philadelphia.**
- Satellites and politics Weather, communications, and earth resources p 50 N85-35144
- Perception Computing, Inc., Downsview (Ontario).**
- The scientific and technical issues in integrating remotely sensed imagery with geocoded data bases p 41 N85-34547
- Purdue Univ., West Lafayette, Ind.**
- Specular, diffuse, and polarized light scattered by two wheat canopies p 1 A85-42865
- Two-dimensional leaf orientation distributions p 2 A85-49104
- Plant canopy specular reflectance model p 4 A85-49112
- Improving the geological interpretation of magnetic and gravity satellite anomalies [E85-10103] p 11 N85-31585
- MAGSAT scalar anomaly map of South America p 11 N85-31586
- MAGSAT satellite magnetic anomaly map over South America p 11 N85-31587
- The south-central United States magnetic anomaly p 17 N85-31591
- The south-central United States magnetic anomaly p 18 N85-31592
- A comparative study of spherical and flat-Earth geopotential modeling at satellite elevations p 11 N85-31593
- A comparative study of spherical and flat-Earth geopotential modeling at satellite elevations p 12 N85-31594
- Reduced to pole long-wavelength magnetic anomalies of Africa and Europe p 18 N85-31595
- Euro-African MAGSAT anomaly-tectonic observations p 18 N85-31596
- Space imagery and some geomorphological problems of the Guiana Shield, South America p 20 N85-32368
- LANDSAT-4/5 image data quality analysis [E85-10105] p 41 N85-35463

S

- Santa Barbara Research Center, Goleta, Calif**
- Landsat image data quality studies p 38 A85-45687
- Science Applications International Corp., La Jolla, Calif.**
- Satellite measurements of atmospheric aerosols [AD-A153807] p 32 N85-30556
- SeaSpace, San Diego, Calif.**
- Large-scale sea surface temperature variability from satellite and shipboard measurements [NASA-CR-176123] p 34 N85-33651
- South Dakota School of Mines and Technology, Rapid City.**
- Rain volume estimation over areas using satellite and radar data [NASA-CR-176050] p 36 N85-32570
- Stanford Linear Accelerator Center, Calif.**
- Application of GPS in a high precision engineering survey network [DE85-010556] p 10 N85-30539
- State Univ. of New York, Binghamton.**
- Two-dimensional leaf orientation distributions p 2 A85-49104
- Evaluation of a canopy reflectance model for LAI estimation through its inversion p 3 A85-49108
- Geomorphic analyses from space imagery p 20 N85-32374

- State Univ. of New York, Syracuse.**
- Systematic and random variations in Thematic Mapper digital radiance data p 40 A85-47820
- Systems and Applied Sciences Corp., Vienna, Va.**
- Systematic and random variations in Thematic Mapper digital radiance data p 40 A85-47820

T

- Technicolor Government Services, Inc., Moffett Field, Calif**
- Evaluation of Thematic Mapper interband registration and noise characteristics p 46 A85-47819
- Texas Univ., Arlington.**
- A comparison between active and passive sensing of soil moisture from vegetated terrains p 4 A85-49118
- Texas Univ., Austin.**
- Hydrogeology of the lower Glen Rose Aquifer, south-central Texas p 36 N85-35466

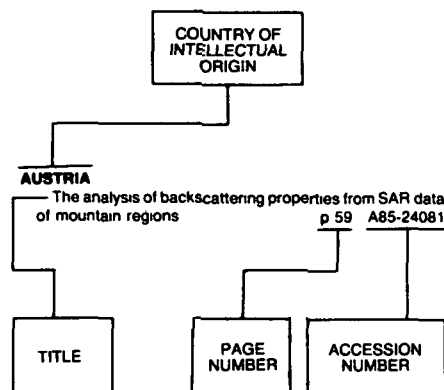
U

- University of South Florida, St. Petersburg**
- Solid-state spectral transmissometer and radiometer p 30 A85-48670
- University of Southern Illinois, Carbondale**
- Regional landform thresholds p 19 N85-32362

W

- Wageningen Agricultural Univ (Netherlands).**
- Directional reflectance factor distributions for cover types of Northern Africa p 1 A85-43114
- Washington Univ., Seattle**
- Theory of microwave remote sensing p 42 A85-40792
- The origin of temporal variance in long-lived trace constituents in the summer stratosphere p 6 A85-43375
- Small-scale cyclones on the periphery of a Gulf Stream warm-core ring p 30 A85-49855
- Wisconsin Univ., Madison.**
- Restoration of multichannel microwave radiometric images p 42 A85-41089
- Measuring the global distribution of intense convection over land with passive microwave radiometry p 36 A85-47923
- Woods Hole Oceanographic Institution, Mass.**
- Small-scale cyclones on the periphery of a Gulf Stream warm-core ring p 30 A85-49855
- Deep sea mega-geomorphology Progress and problems p 33 N85-32369
- World Meteorological Organization, Geneva (Switzerland).**
- Commission for Marine Meteorology [WMO-640] p 33 N85-31735

Typical Foreign Technology Index Listing



Listings in this index are arranged alphabetically by country of intellectual origin. The title of the document is used to provide a brief description of the subject matter. The page number and the accession number are included in each entry to assist the user in locating the citation in the abstract section.

F

FRANCE

- The contribution of SPOT images to soil mapping - A SPOT simulation study on Lauragais (1981) p 1 A85-41350
- Some features of the Algerian Current p 26 A85-42255
- A survey of the Rehamna Hercynian Range in western Morocco using Landsat color composite imagery p 15 A85-42582
- Modeling manual extraction of textural elements by mathematical morphology p 38 A85-42584
- SPOT image quality and post-launch assessment p 38 A85-45692
- Investigation of Landsat-4 Thematic Mapper line-to-line and band-to-band registration and relative detector calibration p 39 A85-47807
- A new technique for inferring surface albedo from satellite observations p 46 A85-47916
- Comparison of mesospheric ozone measurements using the LRIR and UVMCS satellite instruments p 46 A85-50022
- Influence of spatial variability of hydraulic characteristics of soils on surface parameters obtained from remote sensing data in infrared and microwaves [NASA-TM-77902] p 5 N85-31604
- Results of the MIZEX preliminary campaign 29 June to 19 July 1983 [CNES-84/142/T/CT/DRT/TIT/R] p 32 N85-31609
- The French space program p 50 N85-33127

G

GERMANY, FEDERAL REPUBLIC OF

- Probabilities, problems, and perspectives of microwave long-range reconnaissance p 42 A85-41570
- Signature measurements using cooled microwave radiometers at frequencies from 90 GHz to 140 GHz p 43 A85-41571
- Intrinsic geodesy p 9 A85-43958
- Preliminary investigations concerning a 90 GHz radiometer satellite experiment [ESA-TT-860] p 46 N85-31225
- Proceedings of Meteorological Motor Glider (MEMO) Workshop '84 [DFVLR-MITT-85-04] p 7 N85-35542
- Environmental-physical measurements and determination of atmospheric turbulence with the ASK-16 motor glider p 7 N85-35549
- Motor glider measurements during the Urban Atmosphere Energy Budget Experiment (EESA 1) p 7 N85-35553

GERMANY, PEOPLES DEMOCRATIC REPUBLIC OF

- Further improvements of the orbital program system Potsdam-5 and their utilization in geodetic-geodynamic investigations p 7 A85-41189
- Interferometric analysis of Doppler measurements for differential receiver calibration p 8 A85-41203
- The research work at the Central Institute for Physics of the Earth, Potsdam, GDR, in the field of Doppler satellite geodesy p 8 A85-41204

H

HUNGARY

- Calibration of Doppler receivers p 8 A85-41195
- Preliminary results of Finnish-Hungarian Doppler Observation Campaign /FHDOP/ p 8 A85-41199

I

INDIA

- Utility of proposed sensors for coastal engineering studies p 45 A85-45697

INTERNATIONAL ORGANIZATION

- Thematic Mapper - Operational activities and sensor performance at ESA/Earthnet p 46 A85-47808

ISRAEL

- Measurement and analysis of 2-D infrared natural background p 37 A85-42511

ITALY

- Profile statistics of rain in slant path as measured with a radar p 35 A85-40098
- The impact of higher-order Bragg terms on radar sea return p 24 A85-40237

J

JAPAN

- On observation of middle atmosphere with LAS (limb-atmospheric infrared spectrometer) on board of satellite 'Ohzora' (EXOS-C) p 42 A85-41362
- Eruption of Mount Ontake in 1979 - Detection of volcanic ash fall area from Landsat MSS CCT data p 15 A85-42583
- Verification studies of MOS-1 sensors p 44 A85-45696

S

SWEDEN

- Estimation of rural population in Kordofan, Sudan p 6 A85-42579

SWITZERLAND

- Commission for Marine Meteorology [WMO-640] p 33 N85-31735

U

U.S.S.R.

- Fine structure of the preliminary impulse of a sudden storm commencement p 14 A85-40612
- Investigation of ice cover from platforms in the air and in space using radar equipment p 25 A85-40644
- Optical-physical methods for the study of the ocean p 26 A85-42134
- Data acquisition and processing system based on a microprocessor set for the study of earth resources p 43 A85-43074
- Methods for the prediction of the attenuation statistics of radio waves in the 10-100 GHz range in rain - Inclined paths p 44 A85-44015
- Cartographic-photogrammetric analysis and analytical correction of space scanner images p 38 A85-44864
- Thermal isotasy in the South Atlantic Ocean from geoid anomalies p 27 A85-44925
- Propagation and diffraction of radio waves in the millimeter and submillimeter ranges p 9 A85-46078
- Backscattering of centimeter and millimeter radio waves by the earth surface at low grazing angles (Review) p 9 A85-46078
- Distribution of the effective scattering area of the earth surface at low grazing angles p 10 A85-46079
- Specific effective scattering surfaces of certain terrains in the millimeter wave band p 10 A85-46081
- The effect of the interface albedo of the underlying surface on the reflected radiation p 10 A85-46131
- The determination of the albedo of natural covers of the earth on the basis of remote measurement results p 10 A85-46132
- Aerial and space-based remote sensing in ecological prognosis p 6 A85-46249
- Program of experiments on the Cosmos-1500 satellite p 28 A85-46251
- Interpretation of sea ice on satellite radar images p 28 A85-46252
- Determination of the ice-cover characteristics of the Sea of Okhotsk in the winter of 1983-1984 on the basis of radar-sounding data p 28 A85-46253
- The use of radar images obtained with the Cosmos-1500 satellite to study the distribution and dynamics of sea ice p 28 A85-46254
- Quantitative interpretation of satellite radar images of sea ice using a priori data p 28 A85-46255
- Identification of eddy formations in a radar image of the ocean surface p 28 A85-46256

Ordered mesoscale structures on the ocean surface identified from satellite radar data p 28 A85-46257
 Combined analysis of radar and optical images of the northwest Pacific on December 6, 1983 p 29 A85-46258

Radar maps of the Arctic and Antarctic compiled on the basis of Cosmos-1500 satellite data, and preliminary results of their analysis p 29 A85-46259

The data acquisition system on the Cosmos-1500 satellite p 29 A85-46260

Investigation of the ocean with low-resolution multispectral scanners p 29 A85-46261

The sidelooking radar on the Cosmos-1500 satellite p 29 A85-46262

Informational potential of the sidelooking radar of the Cosmos-1500 satellite p 29 A85-46263

Automated processing of remote-sensing data obtained with the microwave radiometer of the Cosmos-1500 satellite p 29 A85-46265

Digital processing of radar images obtained with the Cosmos-1500 satellite p 29 A85-46266

The experimental oceanographic satellite Cosmos-1500 p 30 A85-46267

Scattering in precipitation during microwave-beam power transmission p 45 A85-46297

Reflections of possible oil- and gas-bearing structures of the pre-Jurassic complex in the present-day terrain of Western Siberia p 16 A85-48387

The USSR as viewed from space p 50 A85-48524

Modeling of radio-wave scattering by ice cover p 30 A85-49477

Model computations of light reflection from sea surface p 31 N85-30411

Discovery in earthquake forecasting and seismic zoning recorded p 16 N85-30426

Aerospace technology determines forest-fire danger p 5 N85-30427

Space methods for geological research p 16 N85-30429

Conditions for formation of parageneses containing kyanite-orthoclase in region of Mount Provender and Pratt Peak (Shackleton Range, Antarctica) p 16 N85-30447

Highly important features of regional tectonics of Earth's Arctic sector p 17 N85-30449

The variability of aerosol microstructure in continental and oceanic surface layers of the atmosphere in anticyclones p 34 N85-32660

Cosmonauts participate in multilevel remote sensing experiment p 48 N85-33130

Spacecraft-aided research discussed at geology Congress p 22 N85-33147

Enhancing precision of remote temperature sensing data from satellites under cloudy atmospheric conditions p 48 N85-33148

Impact of fluctuations in optical properties of atmosphere on the ratio of spectral brightness from remote sensing of agricultural land p 5 N85-33149

Determination of altitude of cloud cover top from Meteor satellite data p 48 N85-33150

Landscape interpretation capabilities using space photographs of regions of a multistage platform mantle structure p 22 N85-33151

Interpretation of multiband photographs made during Telefoto-80 experiment for the purpose of discriminating agricultural crops p 5 N85-33152

Use of space photographs for analysis of structural and dynamic conditions of formation of ancient phlogopite and apatite deposits p 22 N85-33153

Using remote photographs in prospecting for hydrocarbons on the Kerch Peninsula p 22 N85-33154

Cataloging the spectral brightness coefficients of the forested region of the European territory of the USSR p 5 N85-33155

Regression analysis of aircraft and ground measurement data on vegetation cover p 5 N85-33156

Interactive procedures for discriminating and restoring contour line networks p 41 N85-33158

Terrain illumination conditions when taking scanning photographs from space p 48 N85-33159

Calculating solar highlight and shadeless areas for scanning photographs from space and optimizing lighting conditions p 49 N85-33160

Discrimination of linear contour elements of space photographs based on visual perception model p 13 N85-33161

Physico-geographical regionalization of Caspian lowland based on space survey materials p 14 N85-33162

Mapping of dynamics of deltas by space photography p 14 N85-33163

Comprehensive mapping of and terrones of Arizona using space photography p 14 N85-33164

Repetition of dense cloud cover above Indian Ocean from generalized satellite data p 41 N85-33165

Basic properties and interpretation of synthesized radar images of sea waves with long synthesize time p 34 N85-33384

UNITED ARAB REPUBLIC

Remote sensing investigations on some fruit orchards in El Fayoum area, Egypt p 1 A85-42581

UNITED KINGDOM

Contextual classification post-processing of Landsat data using a probabilistic relaxation model p 37 A85-41658

The generation and interpretation of false-colour composite principal component images p 37 A85-41659

Standardized principal components p 37 A85-41660

Improving Thematic Mapper land cover classification using filtered data p 37 A85-41664

The evolving continents /2nd revised and enlarged edition/ p 50 A85-42220

Satellite oceanography p 26 A85-42222

Application potential of SPOT imagery for topographic mapping p 9 A85-45694

The ERS-1 synthetic aperture radar and scatterometer p 45 A85-46849

Conceptual models of precipitation systems p 45 A85-47245

Effect of spatial filtering on scene noise and boundary detail in Thematic Mapper imagery p 40 A85-47825

Inverse methods for ocean wave imaging by SAR p 30 A85-48970

Geophysics 2001 p 10 A85-49660

Millimetre wave pulse technology [ESA-CR(P)-2004] p 47 N85-31611

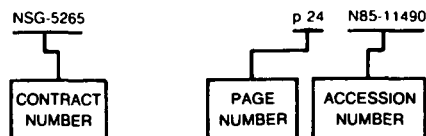
Techniques, problems and uses of mega-geomorphological mapping p 21 N85-32378

CONTRACT NUMBER INDEX

EARTH RESOURCES / A Continuing Bibliography (Issue 48)

JANUARY 1986

Typical Contract Number Index Listing



Listings in this index are arranged alpha-numerically by contract number. Under each contract number, the accession numbers denoting documents that have been produced as a result of research done under that contract are arranged in ascending order with the AIAA accession numbers appearing first. The accession number denotes the number by which the citation is identified in the abstract section. Preceding the accession number is the page number on which the citation may be found.

NCC5-26	p 2	A85-45691
NERC-F60/G6/03	p 37	A85-41664
	p 40	A85-47825
NGT-28-004-801	p 3	A85-49106
NOAA-NA-79SAC00775	p 26	A85-42254
NOAA-NA-80FAC0008	p 25	A85-41662
NOAA-NA-83SAC00650	p 35	A85-41320
NR PROJ ZR0-0001	p 33	N85-32223
NR PROJ ZR0-3103	p 33	N85-32223
NR PROJECT 083-012	p 26	A85-42257
NSF ATM-83-12199	p 16	A85-49227
NSF ATM-83-14111	p 6	A85-43375
NSF DPP-82-17594	p 26	A85-42257
NSF ECS-82-03390	p 36	A85-49116
NSF OCE-80-16983	p 30	A85-49855
NSF OCE-80-169919	p 30	A85-49855
N00014-75-C-0502-P00015	p 27	A85-42259
N00014-77-C-0489	p 32	N85-30556
N00014-79-C-0793	p 34	N85-32622
N00014-79-C-0824	p 25	A85-41961
N00014-80-C-0252-P00015	p 27	A85-42259
N00014-82-K-0489	p 25	A85-41961
N00014-83-K-0026	p 33	N85-32310
N00014-83-K-0258	p 31	N85-30459
N00014-83-K-0528	p 36	A85-49116
N00014-84-C-0111	p 26	A85-42257
USDA-58-319T-40238X	p 38	A85-42853
619-12-30-03	p 41	N85-30450
636	p 31	N85-30452
	p 31	N85-30453

AF PROJ 6690	p 48	N85-32558
DE-AC02-83ER-60182	p 37	N85-35467
DE-AC03-76SF-00515	p 10	N85-30539
DE-AC06-76RL-01830	p 18	N85-31608
DE-AC08-83NV-10282	p 47	N85-31606
DE-AI08-78ET-44802	p 13	N85-32316
ESTEC-5264/82/NL-GM	p 47	N85-31611
F19628-82-K-0002	p 9	A85-44102
F19628-83-C-0097	p 9	A85-44102
NAGW-272	p 30	A85-49855
NAGW-273	p 30	A85-49855
NAGW-380	p 42	A85-41089
NAGW-465	p 30	A85-48670
NAGW-662	p 6	A85-43375
NAG5-265	p 3	A85-49109
NAG5-268	p 4	A85-49118
NAG5-269	p 1	A85-42865
	p 4	A85-49112
NAG5-270	p 3	A85-49107
	p 36	A85-49116
NAG5-271	p 4	A85-49114
NAG5-273	p 4	A85-49111
NAG5-2777	p 3	A85-49106
NAG5-304	p 11	N85-31585
NAG5-386	p 36	N85-32570
NAG5-391	p 36	A85-47923
NASA ORDER S-19583-D	p 3	A85-49106
NASW-4006	p 5	N85-31604
NAS1-16253	p 47	N85-32464
NAS1-17032	p 45	A85-46424
NAS1-17165	p 45	A85-46424
NAS13-190	p 9	A85-45870
NAS5-25300	p 39	A85-47813
NAS5-26859	p 41	N85-35463
NAS5-27346	p 39	A85-47809
	p 40	A85-47822
	p 42	N85-35464
NAS5-27377	p 2	A85-45690
	p 2	A85-47806
NAS5-27383	p 10	A85-47804
NAS5-27595	p 38	A85-42853
	p 40	A85-47820
NAS5-27832	p 47	N85-31601
NAS7-918	p 36	N85-31603
	p 33	N85-31738
	p 35	N85-35322
NAS9-14970	p 1	A85-42865
NAS9-16528	p 2	A85-49104
NCC2-205	p 2	A85-45690
NCC2-234	p 39	A85-47817
NCC5-20	p 2	A85-45691

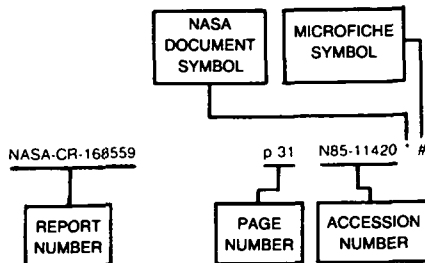
CONTRACT

REPORT NUMBER INDEX

EARTH RESOURCES / A Continuing Bibliography (Issue 48)

JANUARY 1986

Typical Report Number Index Listing



Listings in this index are arranged alphabetically by report number. The page number indicates the page on which the citation is located. The accession number denotes the number by which the citation is identified. An asterisk (*) indicates that the item is a NASA report. A pound sign (#) indicates that the item is available on microfiche.

AD-A153807 p 32 N85-30556 #
AD-A154258 p 17 N85-30455 #
AD-A154406 p 31 N85-30459 #
AD-A154517 p 13 N85-32387 #
AD-A154584 p 33 N85-32388 #
AD-A154633 p 33 N85-32223 #
AD-A154781 p 47 N85-32389 #
AD-A154904 p 48 N85-32558 #
AD-A154986 p 33 N85-32310 #
AD-A155139 p 33 N85-32584 #
AD-A155610 p 34 N85-32707 #
AD-A156139 p 49 N85-35217 #

AD-F630645 p 33 N85-32584 #

AFGL-AFSG-446 p 13 N85-32387 #

AFGL-ERP-887 p 48 N85-32558 #

AFGL-TR-84-0211 p 48 N85-32558 #
AFGL-TR-84-0236 p 13 N85-32387 #

AR-3 p 18 N85-31688 * #

CNES-84/142/T/CT/DRT/TIT/RL p 32 N85-31609 #

CONF-830286 p 47 N85-31606 #
CONF-8504111-1 p 10 N85-30539 #
CONF-850413-1 p 18 N85-31608 #

DE85-001995 p 34 N85-33653 #
DE85-010212 p 47 N85-31606 #
DE85-010556 p 10 N85-30539 #
DE85-010972 p 18 N85-31608 #
DE85-011685 p 13 N85-32316 #
DE85-012412 p 37 N85-35467 #

DFVLR-FB-84-02 p 46 N85-31225 #

DFVLR-MITT-85-04 p 7 N85-35542 #

DOE/ER-60182/1 p 37 N85-35467 #

DOE/METC/85-0219 p 34 N85-33653 #

EGG-10282-1057 p 47 N85-31606 #

EMORY/DC/TR/6 p 33 N85-32310 #

ERIM-164000-18-P p 42 N85-35464 * #

ESA-CR(P)-2004 p 47 N85-31611 #

ESA-TT-860 p 46 N85-31225 #

E85-10103
E85-10104
E85-10105
E85-10106

FHWA/PA-84-012

GPO-40-553

GS-CIRC-934

ISBN-92-63-10640-1

ISSN-0176-7739

JPL-PUB-85-21
JPL-PUB-85-33
JPL-PUB-85-49

JPL-9950-1142

L-15920

LARS-CR-060185

LC-76-608093
LC-84-600161

NAS 1 15 77902
NAS 1 15 86202
NAS 1 15 86203
NAS 1 15 86216
NAS 1 15 86218
NAS 1 15 86223
NAS 1 26 172601
NAS 1 26 175317
NAS 1 26 175614
NAS 1 26 176008
NAS 1 26 176038
NAS 1 26 176042
NAS 1 26 176050
NAS 1 26 176123
NAS 1 26 176199
NAS 1 26 176264
NAS 1 55 2312
NAS 1 61 1139

NASA-CASE-NPO-15704-1

NASA-CP-2312

NASA-CR-172601
NASA-CR-175317
NASA-CR-175614
NASA-CR-176008
NASA-CR-176038
NASA-CR-176042
NASA-CR-176050
NASA-CR-176123
NASA-CR-176199
NASA-CR-176264

NASA-RP-1139

NASA-TM-77902
NASA-TM-86202
NASA-TM-86203
NASA-TM-86216
NASA-TM-86218
NASA-TM-86223

NOAA-TR-NESDIS-19

NOAA/TM-NESDIS-9

NOSC/TR-978

PB85-187052
PB85-191815
PB85-192755
PB85-195279

PNL-SA-12666

p 11 N85-31585 * #
p 47 N85-31601 * #
p 41 N85-35463 * #
p 42 N85-35464 * #

p 24 N85-35470 #

p 50 N85-31584 #
p 50 N85-32386 #
p 33 N85-31735
p 7 N85-35542 #
p 36 N85-31603 * #
p 35 N85-35322 * #
p 33 N85-31738 * #

p 34 N85-33651 * #
p 41 N85-30450 * #
p 41 N85-35463 * #
p 19 N85-31719 #
p 50 N85-32386 #
p 5 N85-31604 * #
p 31 N85-30452 * #
p 31 N85-30453 * #
p 31 N85-30451 * #
p 14 N85-33552 * #
p 18 N85-31688 * #
p 47 N85-32464 * #
p 42 N85-35464 * #
p 11 N85-31585 * #
p 47 N85-31601 * #
p 33 N85-31738 * #
p 36 N85-31603 * #
p 36 N85-32570 * #
p 34 N85-33651 * #
p 35 N85-35322 * #
p 41 N85-35463 * #
p 19 N85-32357 * #
p 41 N85-30450 * #
p 35 N85-34327 * #
p 19 N85-32357 * #
p 47 N85-32464 * #
p 42 N85-35464 * #
p 11 N85-31585 * #
p 47 N85-31601 * #
p 33 N85-31738 * #
p 36 N85-31603 * #
p 36 N85-32570 * #
p 34 N85-33651 * #
p 35 N85-35322 * #
p 41 N85-35463 * #
p 41 N85-30450 * #
p 5 N85-31604 * #
p 31 N85-30452 * #
p 31 N85-30453 * #
p 31 N85-30451 * #
p 14 N85-33552 * #
p 18 N85-31688 * #
p 49 N85-35218 #
p 42 N85-35566 #
p 33 N85-32223 #
p 49 N85-35565 #
p 42 N85-35566 #
p 24 N85-35470 #
p 49 N85-35218 #
p 18 N85-31608 #

QR-10 p 47 N85-31601 * #

REPT-85B0302 p 31 N85-30452 * #
REPT-85B0358 p 31 N85-30453 * #
REPT-85B0413 p 14 N85-33552 * #
REPT-85B0472 p 19 N85-32357 * #

S-HRG-98-1181 p 50 N85-31584 #

SAIC-85/1606 p 32 N85-30556 #

SU-SLAC-PUB-3620 p 10 N85-30539 #

US-GEOL-SURV-CIRC-909 p 18 N85-31605 #
US-GEOL-SURV-CIRC-939 p 19 N85-31719 #

US-PATENT-APPL-SN-359382 p 35 N85-34327 * #

US-PATENT-CLASS-343-17 2-P p 35 N85-34327 * #
US-PATENT-CLASS-343-5-CM p 35 N85-34327 * #
US-PATENT-CLASS-343-5-W p 35 N85-34327 * #

US-PATENT-4,509,048 p 35 N85-34327 * #

USGS-CIRC-883 p 35 N85-35465 #
USGS-CIRC-945 p 23 N85-34468 #

USGS-OFR-85-36 p 13 N85-32316 #

WES-IR-A-84-2 p 33 N85-32388 #

WES/TR/GL-84-14-VOL-1 p 17 N85-30455 #

WMO-640 p 33 N85-31735

X-601-85-6 p 14 N85-33552 * #

REPORT

JANUARY 1986

AVAILABILITY OF CITED PUBLICATIONS

IAA ENTRIES (A85-10000 Series)

Publications announced in *IAA* are available from the AIAA Technical Information Service as follows: Paper copies of accessions are available at \$10.00 per document (up to 50 pages), additional pages \$0.25 each. Microfiche⁽¹⁾ of documents announced in *IAA* are available at the rate of \$4.00 per microfiche on demand. Standing order microfiche are available at the rate of \$1.45 per microfiche for *IAA* source documents and \$1.75 per microfiche for AIAA meeting papers.

Minimum air-mail postage to foreign countries is \$2.50. All foreign orders are shipped on payment of pro-forma invoices.

All inquiries and requests should be addressed to: Technical Information Service, American Institute of Aeronautics and Astronautics, 555 West 57th Street, New York, NY 10019. Please refer to the accession number when requesting publications.

STAR ENTRIES (N85-10000 Series)

One or more sources from which a document announced in *STAR* is available to the public is ordinarily given on the last line of the citation. The most commonly indicated sources and their acronyms or abbreviations are listed below. If the publication is available from a source other than those listed, the publisher and his address will be displayed on the availability line or in combination with the corporate source line.

Avail: NTIS. Sold by the National Technical Information Service. Prices for hard copy (HC) and microfiche (MF) are indicated by a price code preceded by the letters HC or MF in the *STAR* citation. Current values for the price codes are given in the tables on NTIS PRICE SCHEDULES.

Documents on microfiche are designated by a pound sign (#) following the accession number. The pound sign is used without regard to the source or quality of the microfiche.

Initially distributed microfiche under the NTIS SRIM (Selected Research in Microfiche) is available at greatly reduced unit prices. For this service and for information concerning subscription to NASA printed reports, consult the NTIS Subscription Section, Springfield, Va. 22161.

NOTE ON ORDERING DOCUMENTS When ordering NASA publications (those followed by the * symbol), use the N accession number. NASA patent applications (only the specifications are offered) should be ordered by the US-Patent-Appl-SN number. Non-NASA publications (no asterisk) should be ordered by the AD, PB, or other *report* number shown on the last line of the citation, not by the N accession number. It is also advisable to cite the title and other bibliographic identification.

Avail: SOD (or GPO). Sold by the Superintendent of Documents, U.S. Government Printing Office, in hard copy. The current price and order number are given following the availability line (NTIS will fill microfiche requests, as indicated above, for those documents identified by a # symbol)

Avail: NASA Public Document Rooms. Documents so indicated may be examined at or purchased from the National Aeronautics and Space Administration, Public Document Room (Room 126), 600 Independence Ave., S.W., Washington, D.C. 20546, or public document rooms located at each of the NASA research centers, the NASA Space Technology Laboratories, and the NASA Pasadena Office at the Jet Propulsion Laboratory.

(1) A microfiche is a transparent sheet of film, 105 by 148 mm in size containing as many as 60 to 98 pages of information reduced to micro images (not to exceed 26:1 reduction)

- Avail: DOE Depository Libraries. Organizations in U.S. cities and abroad that maintain collections of Department of Energy reports, usually in microfiche form, are listed in *Energy Research Abstracts*. Services available from the DOE and its depositories are described in a booklet, *DOE Technical Information Center - Its Functions and Services* (TID-4660), which may be obtained without charge from the DOE Technical Information Center.
- Avail: Univ. Microfilms. Documents so indicated are dissertations selected from *Dissertation Abstracts* and are sold by University Microfilms as xerographic copy (HC) and microfilm. All requests should cite the author and the Order Number as they appear in the citation.
- Avail: USGS. Originals of many reports from the U.S. Geological Survey, which may contain color illustrations, or otherwise may not have the quality of illustrations preserved in the microfiche or facsimile reproduction, may be examined by the public at the libraries of the USGS field offices whose addresses are listed in this introduction. The libraries may be queried concerning the availability of specific documents and the possible utilization of local copying services, such as color reproduction.
- Avail: HMSO. Publications of Her Majesty's Stationery Office are sold in the U.S. by Pendragon House, Inc. (PHI), Redwood City, California. The U.S. price (including a service and mailing charge) is given, or a conversion table may be obtained from PHI.
- Avail: BLL (formerly NLL): British Library Lending Division, Boston Spa, Wetherby, Yorkshire, England. Photocopies available from this organization at the price shown. (If none is given, inquiry should be addressed to the BLL.)
- Avail: Fachinformationszentrum, Karlsruhe. Sold by the Fachinformationszentrum Energie, Physik, Mathematik GMBH, Eggenstein Leopoldshafen, Federal Republic of Germany, at the price shown in deutschmarks (DM)
- Avail: Issuing Activity, or Corporate Author, or no indication of availability. Inquiries as to the availability of these documents should be addressed to the organization shown in the citation as the corporate author of the document.
- Avail: U.S. Patent and Trademark Office. Sold by Commissioner of Patents and Trademarks, U.S. Patent and Trademark Office, at the standard price of 50 cents each, postage free.
- Avail: ESDU. Pricing information on specific data, computer programs, and details on ESDU topic categories can be obtained from ESDU International Ltd. Requesters in North America should use the Virginia address while all other requesters should use the London address, both of which are on page vii.
- Other availilities: If the publication is available from a source other than the above, the publisher and his address will be displayed entirely on the availability line or in combination with the corporate author line.

PUBLIC COLLECTIONS OF NASA DOCUMENTS

DOMESTIC: NASA and NASA-sponsored documents and a large number of aerospace publications are available to the public for reference purposes at the library maintained by the American Institute of Aeronautics and Astronautics, Technical Information Service, 555 West 57th Street, 12th Floor, New York, New York 10019.

EUROPEAN: An extensive collection of NASA and NASA-sponsored publications is maintained by the British Library Lending Division, Boston Spa, Wetherby, Yorkshire, England for public access. The British Library Lending Division also has available many of the non-NASA publications cited in *STAR*. European requesters may purchase facsimile copy or microfiche of NASA and NASA-sponsored documents, those identified by both the symbols # and * from ESA — Information Retrieval Service European Space Agency, 8-10 rue Mario-Nikis, 75738 CEDEX 15, France.

FEDERAL DEPOSITORY LIBRARY PROGRAM

In order to provide the general public with greater access to U.S. Government publications, Congress established the Federal Depository Library Program under the Government Printing Office (GPO), with 50 regional depositories responsible for permanent retention of material, inter-library loan, and reference services. Over 1,300 other depositories also exists. A list of the regional GPO libraries appears on the inside back cover.

ADDRESSES OF ORGANIZATIONS

American Institute of Aeronautics and
Astronautics
Technical Information Service
555 West 57th Street, 12th Floor
New York, New York 10019

British Library Lending Division,
Boston Spa, Wetherby, Yorkshire,
England

Commissioner of Patents and
Trademarks
U.S. Patent and Trademark Office
Washington, D.C. 20231

Department of Energy
Technical Information Center
P.O. Box 62
Oak Ridge, Tennessee 37830

ESA-Information Retrieval Service
ESRIN
Via Galileo Galilei
00044 Frascati (Rome) Italy

ESDU International, Ltd
1495 Chain Bridge Road
McLean, Virginia 22101

ESDU International, Ltd.
251-259 Regent Street
London, W1R 7AD, England

Fachinformationszentrum Energie, Physik,
Mathematik GMBH
7514 Eggenstein Leopoldshafen
Federal Republic of Germany

Her Majesty's Stationery Office
P.O. Box 569, S.E. 1
London, England

NASA Scientific and Technical Information
Facility
P.O. Box 8757
B.W.I. Airport, Maryland 21240

National Aeronautics and Space
Administration
Scientific and Technical Information
Branch (NIT-1)
Washington, D.C. 20546

National Technical Information Service
5285 Port Royal Road
Springfield, Virginia 22161

Pendragon House, Inc.
899 Broadway Avenue
Redwood City, California 94063

Superintendent of Documents
U.S. Government Printing Office
Washington, D.C. 20402

University Microfilms
A Xerox Company
300 North Zeeb Road
Ann Arbor, Michigan 48106

University Microfilms, Ltd.
Tylers Green
London, England

U.S. Geological Survey Library
National Center – MS 950
12201 Sunrise Valley Drive
Reston, Virginia 22092

U.S. Geological Survey Library
2255 North Gemini Drive
Flagstaff, Arizona 86001

U.S. Geological Survey
345 Middlefield Road
Menlo Park, California 94025

U.S. Geological Survey Library
Box 25046
Denver Federal Center, MS 914
Denver, Colorado 80225

NTIS PRICE SCHEDULES

(Effective October 1, 1985)

Schedule A STANDARD PRICE DOCUMENTS AND MICROFICHE

PRICE CODE	PAGE RANGE	NORTH AMERICAN PRICE	FOREIGN PRICE
A01	Microfiche	\$ 5 95	\$11 90
A02-A03	001-050	9 95	19 90
A04-A05	051-100	11 95	23.90
A06-A09	101-200	16 95	33.90
A10-A13	201-300	22 95	45 90
A14-A17	301-400	28 95	57.90
A18-A21	401-500	34 95	69 90
A22-A25	501-600	40 95	81.90
A99	601-up	*	*
NO1		\$40.00	70 00
NO2		40 00	70 00

Schedule E EXCEPTION PRICE DOCUMENTS AND MICROFICHE

PRICE CODE	NORTH AMERICAN PRICE	FOREIGN PRICE
E01	\$ 7 50	15 00
E02	10 00	20 00
E03	11 00	22 00
E04	13 50	27.00
E05	15 50	31 00
E06	18 00	36 00
E07	20 50	41.00
E08	23 00	46 00
E09	25 50	51 00
E10	28 00	56.00
E11	30 50	61.00
E12	33.00	66 00
E13	35 50	71 00
E14	38 50	77 00
E15	42 00	84 00
E16	46 00	92 00
E17	50 00	100 00
E18	54.00	108.00
E19	60.00	120 00
E20	70 00	140 00
E99	*	*

*Contact NTIS for price quote.

IMPORTANT NOTICE

NTIS Shipping and Handling Charges (effective June 1, 1985)

U.S., Canada, Mexico — ADD \$3 00 per TOTAL ORDER

All Other Countries — ADD \$4.00 per TOTAL ORDER

Exceptions — Does NOT apply to:

ORDERS REQUESTING NTIS RUSH HANDLING
ORDERS FOR SUBSCRIPTION OR STANDING ORDER PRODUCTS ONLY

NOTE: Each additional delivery address on an order
requires a separate shipping and handling charge.

TYPICAL CITATION AND ABSTRACT FROM STAR

NASA SPONSORED DOCUMENT → **N85-15248*** # Utah Univ., Salt Lake City Center for Remote Sensing and Cartography. → **AVAILABLE ON MICROFICHE**

NASA ACCESSION NUMBER → **AN INTEGRATED LANDSAT/ANCILLARY DATA CLASSIFICATION OF DESERT RANGELAND** → **CORPORATE SOURCE**

TITLE → **K. P. PRICE, M. K. RIDD, and J. A. MEROLA 1984 8 p** → **PUBLICATION DATE**

AUTHORS → **Sponsored in part by Utah Dept. of Agriculture ERTS (Contract NAGW-95)** → **AVAILABILITY SOURCE**

CONTRACT OR GRANT → **(E85-10046, NASA-CR-174222; NAS 1.26.174222) Avail: NTIS HC A02/MF A01 CSCL 08B** → **COSATI CODE**

REPORT NUMBER → **Range inventorying methods using LANDSAT MSS data, coupled with ancillary data were examined. The study area encompassed nearly 20,000 acres in Rush Valley, Utah. The vegetation is predominately desert shrub and annual grasses, with some annual forbs. Three LANDSAT scenes were evaluated using a Kauth-Thomas brightness/greenness data transformation (May, June, and August dates). The data was classified using a four-band maximum-likelihood classifier. A print map was taken into the field to determine the relationship between print symbols and vegetation. It was determined that classification confusion could be greatly reduced by incorporating geomorphic units and soil texture (coarse vs fine) into the classification. Spectral data, geomorphic units, and soil texture were combined in a GIS format to produce a final vegetation map identifying 12 vegetation types.** Author

TYPICAL CITATION AND ABSTRACT FROM IAA

NASA SPONSORED DOCUMENT → **A85-17493*** National Aeronautics and Space Administration Lyndon B. Johnson Space Center, Houston, Tex. → **TITLE**

AIAA ACCESSION NUMBER → **EVALUATION OF PROCEDURES TO CORRECT FOR VARIABLE VIEWING AND ILLUMINATION GEOMETRY WHEN OBSERVING A NON-LAMBERTIAN SURFACE THROUGH THE ATMOSPHERE** → **AUTHOR'S AFFILIATION**

AUTHORS → **V. S. WHITEHEAD (NASA, Johnson Space Center, Houston, TX), W. R. JOHNSON, M. L. MATHEWS, and N. C. HORVATH (Lockheed Engineering and Management Services Co., Inc., Houston, TX)** → **MEETING DATE**

MEETING → **IN: 1983 International Geoscience and Remote Sensing Symposium (IGARSS '83), San Francisco, CA, August 31-September 2, 1983, Digest. Volume 1. New York, Institute of Electrical and Electronics Engineers, Inc., 1983, 6 p refs**

Abstract: Data from the Advanced Very High Resolution Radiometer aboard the NOAA polar orbiting satellite are being operationally applied to provide estimates of vegetation cover and/or condition over a large part of the earth by the USDA. The wide scan angle (+ or - 54 deg) of this system permits daily views of the earth when used to its limits. Five-day repetitive coverage is acquired, assuming cloud-free conditions, in current operations which limit the use of the scan to the center + or - 14 deg of swath. While use of the full scan width would provide clear acquisitions frequent enough to monitor crop development and condition even with normal cloudiness, these off-nadir data are made difficult to interpret due to the non-Lambertian nature of the surface, enhanced effect of the atmosphere, inclusion of subpixel and thin invisible clouds in the scene, and differences in illumination across the scene; all of which contribute to variations in observed reflected radiation. Some approaches to provide corrections for these effects are discussed here. Author

1. Report No. NASA SP-7041 (48)		2. Government Accession No.		3. Recipient's Catalog No.	
4. Title and Subtitle EARTH RESOURCES A Continuing Bibliography (Issue 48)				5. Report Date January 1986	
				6. Performing Organization Code	
7. Author(s)				8. Performing Organization Report No.	
9. Performing Organization Name and Address National Aeronautics and Space Administration Washington, D. C. 20546				10. Work Unit No.	
				11. Contract or Grant No.	
12. Sponsoring Agency Name and Address				13. Type of Report and Period Covered	
				14. Sponsoring Agency Code	
15. Supplementary Notes					
16. Abstract <p>This bibliography lists 326 reports, articles and other documents introduced into the NASA Scientific and Technical Information System between October 1 and December 31, 1985. Emphasis is placed on the use of remote sensing and geophysical instrumentation in spacecraft and aircraft to survey and inventory natural resources and urban areas. Subject matter is grouped according to agriculture and forestry, environmental changes and cultural resources, geodesy and cartography, geology and mineral resources, hydrology and water management, data processing and distribution systems, instrumentation and sensors, and economic analysis.</p>					
17. Key Words (Suggested by Author(s)) Bibliographies Earth Resources Remote Sensors			18. Distribution Statement Unclassified - Unlimited		
19. Security Classif. (of this report) Unclassified		20. Security Classif. (of this page) Unclassified		21. No. of Pages 106	
				22. Price* \$14.50 HC	

FEDERAL DEPOSITORY LIBRARY PROGRAM

The Federal Depository Library Program provides Government publications to designated libraries throughout the United States. The Regional Depository Libraries listed below receive and retain at least one copy of nearly every Federal Government publication, either in printed or microfilm form, for use by the general public. These libraries provide reference services and inter-library loans; however, they are *not* sales outlets. You may wish to ask your local library to contact a Regional Depository to help you locate specific publications, or you may contact the Regional Depository yourself.

ARKANSAS STATE LIBRARY
One Capitol Mall
Little Rock, AR 72201
(501) 371-2326

AUBURN UNIV. AT MONTGOMERY LIBRARY
Documents Department
Montgomery, AL 36193
(205) 279-9110, ext. 253

UNIV. OF ALABAMA LIBRARY
Documents Dept.—Box S
University, AL 35486
(205) 348-7369

DEPT. OF LIBRARY, ARCHIVES AND PUBLIC RECORDS
Third Floor—State Cap
1700 West Washington
Phoenix, AZ 85007
(602) 255-4121

UNIVERSITY OF ARIZONA LIB
Government Documents Dept
Tucson, AZ 85721
(602) 626-5233

CALIFORNIA STATE LIBRARY
Govt. Publications Section
P O Box 2037
Sacramento, CA 95809
(916) 322-4572

UNIV. OF COLORADO LIB
Government Pub. Division
Campus Box 184
Boulder, CO 80309
(303) 492-8834

DENVER PUBLIC LIBRARY
Govt. Pub. Department
1357 Broadway
Denver, CO 80203
(303) 571-2131

CONNECTICUT STATE LIBRARY
Government Documents Unit
231 Capitol Avenue
Hartford, CT 06106
(203) 566-4971

UNIV. OF FLORIDA LIBRARIES
Library West
Documents Department
Gainesville, FL 32611
(904) 392-0367

UNIV. OF GEORGIA LIBRARIES
Government Reference Dept
Athens, GA 30602
(404) 542-8951

UNIV. OF HAWAII LIBRARY
Govt. Documents Collection
2550 The Mall
Honolulu, HI 96822
(808) 948-8230

UNIV. OF IDAHO LIBRARY
Documents Section
Moscow, ID 83843
(208) 885-6344

ILLINOIS STATE LIBRARY
Information Services Branch
Centennial Building
Springfield, IL 62706
(217) 782-5185

INDIANA STATE LIBRARY
Serials Documents Section
140 North Senate Avenue
Indianapolis, IN 46204
(317) 232-3686

UNIV. OF IOWA LIBRARIES
Govt. Documents Department
Iowa City, IA 52242
(319) 353-3318

UNIVERSITY OF KANSAS
Doc. Collect.—Spencer Lib
Lawrence, KS 66045
(913) 864-4662

UNIV. OF KENTUCKY LIBRARIES
Govt. Pub. Department
Lexington, KY 40506
(606) 257-3139

LOUISIANA STATE UNIVERSITY
Middleton Library
Govt. Docs. Dept.
Baton Rouge, LA 70803
(504) 388-2570

LOUISIANA TECHNICAL UNIV. LIBRARY
Documents Department
Ruston, LA 71272
(318) 257-4962

UNIVERSITY OF MAINE
Raymond H. Fogler Library
Tri-State Regional Documents
Depository
Orono, ME 04469
(207) 581-1680

UNIVERSITY OF MARYLAND
McKeldin Lib.—Doc. Div.
College Park, MD 20742
(301) 454-3034

BOSTON PUBLIC LIBRARY
Government Docs. Dept.
Boston, MA 02117
(617) 536-5400 ext. 226

DETROIT PUBLIC LIBRARY
Sociology Department
5201 Woodward Avenue
Detroit, MI 48202
(313) 833-1409

MICHIGAN STATE LIBRARY
P O Box 30007
Lansing, MI 48909
(517) 373-0640

UNIVERSITY OF MINNESOTA
Government Pubs. Division
409 Wilson Library
309 19th Avenue South
Minneapolis, MN 55455
(612) 373-7813

UNIV. OF MISSISSIPPI LIB.
Documents Department
University, MS 38677
(601) 232-5857

UNIV. OF MONTANA
Mansfield Library
Documents Division
Missoula, MT 59812
(406) 243-6700

NEBRASKA LIBRARY COMM.
Federal Documents
1420 P Street
Lincoln, NE 68508
(402) 471-2045
In cooperation with University of
Nebraska-Lincoln

UNIVERSITY OF NEVADA LIB.
Govt. Pub. Department
Reno, NV 89557
(702) 784-6579

NEWARK PUBLIC LIBRARY
5 Washington Street
Newark, NJ 07101
(201) 733-7812

UNIVERSITY OF NEW MEXICO
Zimmerman Library
Government Pub. Dept.
Albuquerque, NM 87131
(505) 277-5441

NEW MEXICO STATE LIBRARY
Reference Department
325 Don Gaspar Avenue
Santa Fe, NM 87501
(505) 827-2033, ext. 22

NEW YORK STATE LIBRARY
Empire State Plaza
Albany, NY 12230
(518) 474-5563

UNIVERSITY OF NORTH CAROLINA AT CHAPEL HILL
Wilson Library
BA/SS Documents Division
Chapel Hill, NC 27515
(919) 962-1321

UNIVERSITY OF NORTH DAKOTA
Chester Fritz Library
Documents Department
Grand Forks, ND 58202
(701) 777-2617, ext. 27
(In cooperation with North
Dakota State Univ. Library)

STATE LIBRARY OF OHIO
Documents Department
65 South Front Street
Columbus, OH 43215
(614) 462-7051

OKLAHOMA DEPT. OF LIB.
Government Documents
200 NE 18th Street
Oklahoma City, OK 73105
(405) 521-2502

OKLAHOMA STATE UNIV. LIB
Documents Department
Stillwater, OK 74078
(405) 624-6546

PORTLAND STATE UNIV. LIB
Documents Department
P O Box 1151
Portland, OR 97207
(503) 229-3673

STATE LIBRARY OF PENN.
Government Pub. Section
P O Box 1601
Harrisburg, PA 17105
(717) 787-3752

TEXAS STATE LIBRARY
Public Services Department
P O Box 12927—Cap. Sta.
Austin, TX 78753
(512) 471-2996

TEXAS TECH UNIV. LIBRARY
Govt. Documents Department
Lubbock, TX 79409
(806) 742-2268

UTAH STATE UNIVERSITY
Merrill Library, U M C 30
Logan, UT 84322
(801) 750-2682

UNIVERSITY OF VIRGINIA
Alderman Lib.—Public Doc.
Charlottesville, VA 22901
(804) 924-3133

WASHINGTON STATE LIBRARY
Documents Section
Olympia, WA 98504
(206) 753-4027

WEST VIRGINIA UNIV. LIB.
Documents Department
Morgantown, WV 26506
(304) 293-3640

MILWAUKEE PUBLIC LIBRARY
814 West Wisconsin Avenue
Milwaukee, WI 53233
(414) 278-3000

ST. HIST. LIB. OF WISCONSIN
Government Pub. Section
816 State Street
Madison, WI 53706
(608) 262-4347

WYOMING STATE LIBRARY
Supreme Ct. & Library Bld.
Cheyenne, WY 82002
(307) 777-6344

National Aeronautics and
Space Administration
Code NIT-4

Washington, D.C.
20546-0001

Official Business
Penalty for Private Use, \$300

BULK RATE
POSTAGE & FEES PAID
NASA
Permit No G-27

NASA

POSTMASTER: If Undeliverable (Section 158
Postal Manual) Do Not Return
